Alma Mater Studiorum – Università di Bologna

DOTTORATO DI RICERCA IN
INGEGNERIA ENERGETICA, NUCLEARE E DEL
CONTROLLO AMBIENTALE

Ciclo XXVIII

Settore Concorsuale di afferenza: 09/C2

Settore Scientifico disciplinare: ING-IND/10

Development and applications of simulation codes for air-to-water and ground-coupled heat pump systems

Presentata da: **CLAUDIA NALDI**

Coordinatore Dottorato   **Relatore**

Prof. Vincenzo Parenti Castelli   **Prof. Enzo Zanchini**

                                                Correlatore

                                        Prof. Gian Luca Morini

Esame finale anno 2016

To Doriano, Maria and Bruno

ABSTRACT

In this Thesis, new simulation codes for the evaluation of the seasonal performance of heat pump systems are presented. The codes apply to electric air-to-water and ground-coupled heat pump systems based on a vapor compression cycle, coupled with buildings.

Heat pumps are a very efficient technology for building heating, cooling and domestic hot water (DHW) production, which reached an important development during the last decades and have been widely studied in the literature.

This work is composed of three main parts. In the first part, numerical models are developed to simulate different kinds of air-to-water heat pumps by means of the bin-method. The latter, which is derived from the European standard EN 14825 and the Italian standard UNI/TS 11300-4, is here extended in order to consider the different operating modes of mono-compressor on-off heat pumps (ON-OFF HPs), multi-compressor heat pumps (MCHPs) and inverter-driven heat pumps (IDHPs). A code for heating and DHW production mode during winter and a code for cooling and DHW production mode during summer are developed. By applying the codes, the heat pump system seasonal performance is analyzed in relation to the thermal characteristics of the building, the climate of the location and the kind of heat pump control system. The results show that the best seasonal performance in winter is obtained with IDHPs by adopting as bivalent temperature the design temperature. For reversible heat pumps used in summer for cooling and DHW production through condensation heat recovery, the primary energy saving can be higher than 30 % with respect to traditional solutions in which the heat pump supplies only cooling and DHW is produced by a gas boiler.

In the second part of this Thesis, numerical codes for the hourly simulation of air-to-water heat pump systems are developed. The dynamic codes are implemented in the software MATLAB and apply to ON-OFF HPs and to IDHPs for building heating, cooling and DHW production, coupled with storage tanks and integrated by a gas boiler or electric heaters. The codes are used, in particular, to evaluate the seasonal performance and the primary energy consumption of the multi-function inverter-driven air-to-water heat pump employed in the retrofit of a residential building in Bologna (Italy). The retrofit intervention is expected to yield a primary energy saving of more than 85 % with respect to the pre-retrofit scenario. The codes are validated by comparing the results obtained with those yielded by the dynamic software TRNSYS (maximum discrepancy 0.80 %).

The predictions of the bin-method have been proved to be in agreement with those of the dynamic simulation only in particular conditions, varying with the climate data and with the considered heat pump type. The discrepancies in the Seasonal Coefficient Of Performance (*SCOP*) can be higher than 20 % (ON-OFF HPs with high bivalent temperature).

In the third part of this Thesis, a code for the hourly simulation of Ground-Coupled Heat Pump (GCHP) systems is developed. The code, which employs the *g-functions* obtained by Zanchini and Lazzari (E. Zanchini, S. Lazzari, Energy, 59, 2013, 570-80), is implemented in MATLAB and applies to on-off and inverter-driven GCHPs, used for building heating and/or cooling. The whole system, composed by the heat pump and the coupled Borehole Heat Exchanger (BHE) field, can be simulated for several years. The code is applied to analyze the effects of the inverter and of the total length of the BHE field on the mean seasonal performance of a GCHP system designed for a residential house with dominant heating loads. The results show that 40 % increase of the BHE length can yield a *SCOP* enhancement of about 7 % in winter, while in summer the Seasonal Energy Efficiency Ratio (*SEER*) remains nearly unchanged. The replacement of the ON-OFF HP by an IDHP yields a *SCOP* enhancement of about 30 % and a *SEER* enhancement of about 52 %. The dynamic code is validated by comparing the mean monthly temperatures of the BHE fluid obtained by the proposed model with those evaluated through the software Earth Energy Designer (maximum discrepancy 2.18 %).

SOMMARIO

In questa Tesi vengono presentati nuovi codici di simulazione per la valutazione delle prestazioni stagionali di sistemi a pompa di calore. Tali codici sono riferiti a sistemi con pompe di calore elettriche aria-acqua o accoppiate al terreno, basate su un ciclo a compressione di vapore e accoppiate ad edifici.

Le pompe di calore rappresentano un'efficiente tecnologia per riscaldamento, raffrescamento e produzione di acqua calda sanitaria (ACS) negli edifici, che durante gli ultimi decenni ha raggiunto un importante sviluppo e che è stata ampiamente studiata in letteratura.

Nella prima parte di questo lavoro sono sviluppati modelli di simulazione numerica per diverse tipologie di pompe di calore aria-acqua, basati sul metodo bin. Quest'ultimo, derivato dalla norma europea EN 14825 e dalla norma italiana UNI/TS 11300-4, è qui esteso allo scopo di considerare le diverse modalità di funzionamento di pompe di calore mono-compressore on-off (ON-OFF HP), multi-compressore (MCHP) e dotate di inverter (IDHP). È sviluppato un codice per la modalità invernale di riscaldamento e produzione di ACS e un codice per la modalità estiva di raffrescamento e produzione di ACS. Impiegando i codici, le prestazioni stagionali di sistemi a pompa di calore sono analizzate in relazione alle caratteristiche termiche dell'edificio, del clima locale e del tipo di sistema di regolazione della pompa di calore. I risultati mostrano come le migliori prestazioni stagionali in inverno siano ottenute con le IDHP adottando come temperatura bivalente la temperatura esterna di progetto. Per le pompe di calore reversibili usate in estate per raffrescamento e produzione di ACS tramite recupero del calore di condensazione, il risparmio di energia primaria può superare il 30 % rispetto a soluzioni tradizionali in cui la pompa di calore provvede al solo raffrescamento e l'ACS è fornita da una caldaia a gas.

Nella seconda parte di questa Tesi sono sviluppati codici numeri per la simulazione oraria di sistemi a pompa di calore aria-acqua. I codici dinamici sono implementati sul software MATLAB e si applicano alle ON-OFF HP e IDHP per riscaldamento, raffrescamento e produzione di ACS in edifici, accoppiate a serbatoi di accumulo e integrate da una caldaia a gas o da resistenze elettriche. I codici sono utilizzati, in particolare, per valutare le prestazioni stagionali e il consumo di energia primaria della pompa di calore aria-acqua multifunzione con inverter impiegata nel retrofit di un edificio residenziale a Bologna (Italia). L'intervento di retrofit dovrebbe produrre un risparmio di energia primaria superiore all'80 % rispetto allo

scenario pre-retrofit. I codici sono validati confrontando i risultati ottenuti con quelli prodotti dal software dinamico TRNSYS (massima differenza: 0.80 %).

Le previsioni del metodo bin si sono dimostrate in accordo con quelle della simulazione dinamica solo in particolari condizioni, al variare dei dati climatici e della tipologia di pompa di calore considerata. Le differenze nel Coefficiente di Prestazione Stagionale (*SCOP*) possono risultare maggiori del 20 % (ON-OFF HP con alte temperature bivalenti).

Nella terza parte di questa Tesi è sviluppato un codice di simulazione oraria per sistemi a pompa di calore accoppiata al terreno (GCHP). Il codice, che impiega le *g-function* ottenute da Zanchini e Lazzari (E. Zanchini, S. Lazzari, Energy, 59, 2013, 570-80), è implementato su MATLAB e si applica a GCHP on-off e con inverter, usate per riscaldamento e/o raffrescamento di edifici. L'intero sistema, composto da pompa di calore e campo di sonde geotermiche accoppiato, può essere simulato per diversi anni. Il codice è impiegato per analizzare gli effetti dell'inverter e della lunghezza totale del campo sonde sulle prestazioni stagionali medie di un sistema GCHP progettato per un edificio residenziale con carichi dominanti per riscaldamento. I risultati mostrano che un aumento della lunghezza delle sonde del 40 % può produrre in inverno un incremento di *SCOP* del 7 % circa, mentre in estate l'Indice di Efficienza Energetica Stagionale (*SEER*) rimane quasi invariato. Sostituire la ON-OFF HP con una IDHP produce un aumento di *SCOP* del 30 % circa e un aumento di *SEER* del 52 % circa. Il codice dinamico è validato confrontando le temperature medie mensili del fluido nelle sonde ottenute col modello proposto con quelle calcolate dal software Earth Energy Designer.

CONTENTS

LIST OF FIGURES

LIST OF TABLES

NOMENCLATURE

ROMAN LETTERS

A	Dimensionless load amplitude
b_u	Temperature reduction factor
C_c	Degradation coefficient
c_p	Specific heat capacity at constant pressure
D	Diameter
E	Energy
F_{sc}	Short Circuit Factor
Fo	Fourier number
G	*G* factor
g	*g-function*
H	Solar radiation
i	*i*-th bin or hour
k	Thermal conductivity
L	Borehole length
M	Number of inverter frequencies
$\dot{m}$	Mass flow rate
N	Number of compressors
n	Number of activated compressors
P	Power
p_d	Load coefficient for domestic hot water
Q	Thermal energy
q	Thermal load per unit length
R	Thermal resistance per unit length
r	Radial coordinate
S	Floor area
T	Temperature
t	Time
U	Heat loss (or transfer) coefficient

V	Volume
$\dot{V}$	Volumetric flow rate
z	Vertical coordinate

GREEK LETTERS

α	Thermal diffusivity
η	Efficiency
ρ	Density
σ	Standard deviation
Φ	Inverter frequency

SUPERSCRIPTS, SUBSCRIPTS

$*$	Dimensionless quantity
$avail$	Available
b	Building
bin	Bin
biv	Bivalent
bk	Back-up
c	Cooling
$compr$	Compressor
$cond$	Condenser
$corr$	Correction
d	Domestic hot water
des	Design
$despr$	Desuperheater
dis	Distribution
dly	Daily
eff	Effective
el	Electric
em	Emission

evap	Evaporator
ext	External air
f	Fluid
g	Ground
h	Heating
HP	Heat pump
in	Inlet
int	Internal
m	Mean
max	Maximum
min	Minimum
mly	Monthly
net	Of the heat pump
on	Of the heat pump and back-up system
out	Outlet
p	Penalty
prim	Primary
r	Condensation heat recovery
res	Residual
s	Storage
tot	Total
uncov	Uncovered
us	Used
virt	Virtual
w	Water
yly	Annual
zl	Zero-load

ACRONYMS

BES	Building Energy Signature
BHE	Borehole Heat Exchanger
COP	Coefficient Of Performance
CR	Capacity Ratio

DHW	Domestic Hot Water
DST	Duct STorage
EER	Energy Efficiency Ratio
FCS	Finite Cylindrical Source
FLS	Finite Line Source
FUE	Fuel Utilization Efficiency
GCHP	Ground-Coupled Heat Pump
ICS	Infinite Cylindrical Source
IDHP	Inverter-Driven Heat Pump
ILS	Infinite Line Source
MCHP	Multi-Compressor Heat Pump
ON-OFF HP	Mono-compressor ON-OFF Heat Pump
PLF	Partial Load Factor
SCOP	Seasonal Coefficient Of Performance
SEER	Seasonal Energy Efficiency Ratio
SPF	Seasonal Performance Factor
TMY	Typical Meteorological Year
TOL	Temperature Operative Limit
TRY	Test Reference Year

1

INTRODUCTION AND AIM OF THE WORK

The economic growth of the 20th century has been based on a progressive increase of the world annual use of fossil fuels. The world annual use of primary energy is still increasing and fossil fuels represent even now the most important source of primary energy, as shown in Figure 1.1. The figure illustrates the world annual use of primary energy by source from 1980 to 2012, according to EIA [1] (US Energy Information Administration).
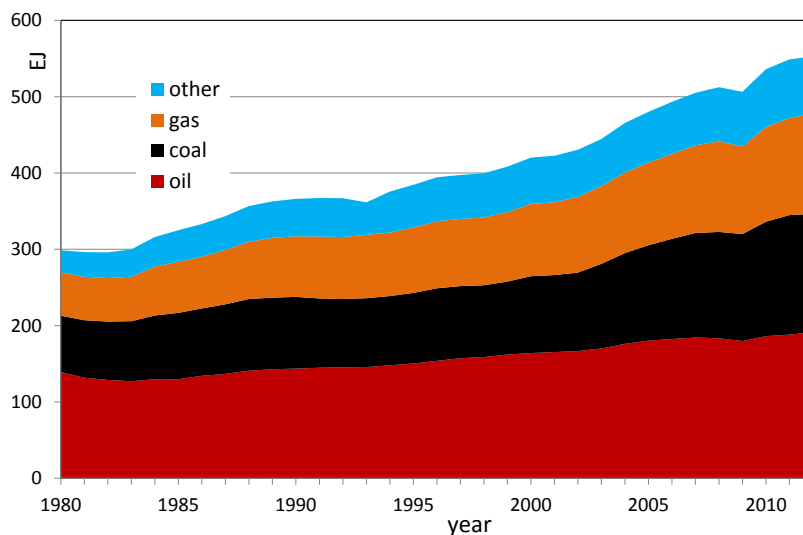
Figure 1.1: World annual use of primary energy by source from 1980 to 2012, data according to EIA [1].

As evidenced by Figure 1.1, 86 % of the world primary energy use in 2012 is due to oil, carbon and gas. The fossil-fuel-based development has caused two important problems: the

reserves of oil and natural gas are decreasing and the emission of carbon dioxide and of other greenhouse gases is causing a climate change (see Ref. [2]). As a consequence, all the industrialized and developing countries and, most of all, the European Union, are struggling to shift the economic growth towards a sustainable development, based on two main pillars: the increase of energy efficiency and the use of renewable energy sources.

The energy policy of the European Union already obtained some success: the annual use of primary energy of the Union is slightly decreasing from 2006, as shown in Figure 1.2, which illustrates the use of primary energy of the European Union by sector from 1990 to 2014, according to Eurostat [3] (European Commission portal for statistics).
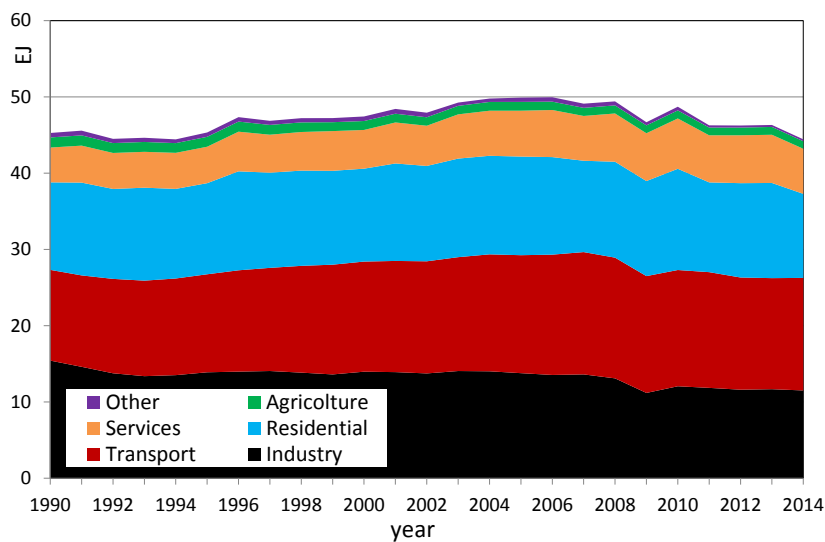
Figure 1.2: Annual use of primary energy by sector in Europe, from 1990 to 2014, data according to Eurostat [3].

Figure 1.2 reveals that the fractions of energy use in the residential sector and in the service sector are quite relevant. The fractions of primary energy use in sectors for 2014 are better evidenced by Figure 1.3, where it is shown that the sum of the fractions which refer to the residential sector and to the service sector (i.e., the total fraction due mainly to building operation) is 38.1 %.

2
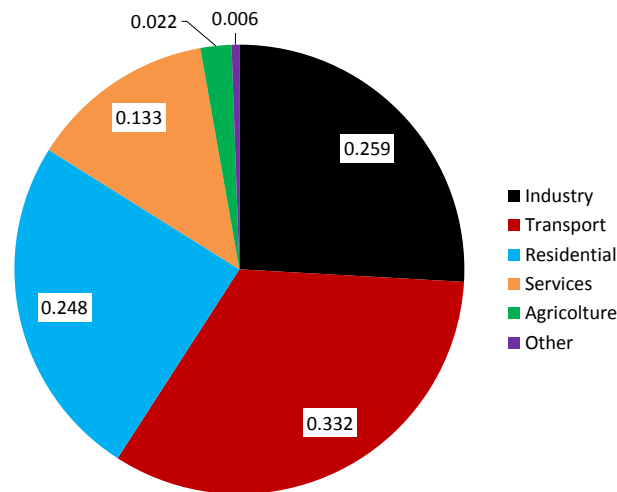
Figure 1.3: Fractions of primary energy use in main sectors in Europe, in 2012, data according to Eurostat [3].

According to an official document of the European Commission [4], buildings use 40 % of the total European energy consumption and generate 36 % of greenhouse gases in Europe.

As a consequence, important steps towards the reduction of the use of fossil fuels in Europe would be the enhancement of the energy efficiency of buildings and the use of renewable energy sources in building plants. In particular, the European Commission has enacted the EPBD Recast Directive [5], which promotes in the Member States a transition to Nearly Zero Energy Buildings (namely buildings with very low energy needs) within 2020. In the Directive [5], the improvement of the thermal performance of the building envelope and the improvement of the heating, cooling and ventilating systems are recommended.

Heat pump systems represent useful solutions for building air-conditioning and Domestic Hot Water (DHW) production, which reached an important development during the last decades ([6], [7]). Heat pumps can contribute to achieve the mentioned European objectives, since aero-thermal, geothermal and hydrothermal energy are recognized as renewable energy sources by the European RES Directive [8].

Thanks to the relative cheapness of the plant, air-source heat pumps are good candidates for the replacement or integration of gas boilers in retrofits of existing buildings. Ground-Coupled Heat Pumps (GCHPs) achieve better performance, but require higher investment costs and soil drilling. Consequently, they are at present less widely used.

A heat pump performance is strongly influenced by the variable heat load of the building, kind of control system and source temperature. Therefore, the calculation of the seasonal performance is not an easy task. In this Thesis, new simulation codes are developed for the

evaluation of the seasonal performance of air-to-water and ground-coupled heat pump systems for building heating, cooling and DHW production.

The evaluation of a heat pump seasonal efficiency has been widely investigated in the literature; Chapter 2 of this Thesis provides a classification of the available methods, and stresses the differences between those methods and the new simulation models proposed.

Chapter 3 presents new mathematical codes for the simulation of air-to-water heat pumps through the bin-method. Different calculation methods are employed for mono-compressor on-off heat pumps (ON-OFF HPs), multi-compressor heat pumps (MCHPs) and inverter-driven heat pumps (IDHPs). By applying the codes, the seasonal efficiency of heat pump systems is analyzed in relation to the characteristics of the building, local climate and kind of heat pump control system.

In Chapter 4, new codes for the hourly simulation of air-to-water heat pump systems are presented. The dynamic code developed for winter operation is used to analyze the seasonal performance of heat pump heating systems as a function of the bivalent temperature and of the volume of the thermal storage tank. Moreover, the dynamic codes are used to calculate the primary energy consumption of the IDHP used in the retrofit of a residential building in Bologna (North-Center Italy).

Chapter 5 presents a new code for the hourly simulation of ground-coupled heat pump systems. The code employs the *g-functions* obtained by Zanchini and Lazzari [9] and is applied to analyze the effects of the inverter and of the total length of the BHE field on the seasonal efficiency of a GCHP system designed for heating and cooling a residential house with dominant heating loads.

Chapter 6 reports the conclusions of this Thesis and some opportunities for future work.

The developed codes are shown in the Appendix, while the publications and a software application derived from the work of this Thesis appear in Chapters 8 and 9, respectively.

2

HEAT PUMP SIMULATION MODELS IN THE LITERATURE

In this chapter, a classification of the methods for the simulation of heat pump systems is presented. Design models, temperature class approaches and dynamic simulation methods are described and compared to each other. In particular, the heat pump simulation methods indicated by the European standard EN 14825 [10] and the Italian standard UNI/TS 11300-4 [11] are analyzed. The dynamic simulation of air-to-water heat pumps by means of the software TRNSYS is also described.

Some design methods of borehole heat exchanger fields for ground-coupled heat pump systems are studied too. The ASHRAE method, models based on the *g-functions* and the software Earth Energy Designer are particularly analyzed.

2.1 HEAT PUMP DESIGN MODELS

Several approaches for a heat pump simulation are available in the literature. As noticed by Afjei and Dott [12], the different models can be classified on the basis of the level of detail of the calculations, aim of the model and computational time required to run it.

There exist models for a heat pump design, whose aim is to optimize the heat pump unit on the level of the refrigerant cycle. These models require high computational time and represent each heat pump component individually, in order to optimize the interaction between the evaporator, the compressor, the condenser and the expansion valve.

Most of these models are empirical and rely both on physical equations and on numerical correlations derived from experimental results ([13]-[15]); fewer models are based on CFD simulations.

2.2 TEMPERATURE CLASS MODELS

Other simulation models focus on the whole heat pump system. With this approach the heat pump is a black box with given performance (at fixed source and sink temperatures), coupled to a building in a specific climate, and possibly provided with a thermal storage tank and a back-up system. In this case, the aim is to simulate the entire system and to optimize its seasonal performance.

Some of these models are based on a temperature class approach, like the methods indicated by the European standard EN 14825 [10] and by the Italian standard UNI/TS 11300-4 [11], which simulate a heat pump behavior with the bin-method. As will be explained in detail in Subsection 2.2.1, a bin represents the number of hours, in a selected time period, with approximately the same value of external air temperature. A selected climate is thus schematized by means of a bin trend, which gives the local distribution of outdoor temperature.

Frequently, comparisons between different commercial heat pumps refers to the Coefficient Of Performance, *COP* (ratio between the thermal power released and the corresponding electric power used, in heating or DHW production mode) or to the Energy Efficiency Ratio, *EER* (ratio between the cooling power released and the corresponding electric power used, in cooling mode) of single operating conditions. In this case, the *COP* or *EER* is measured at specific temperatures of the heat pump source and sink, according to the European standards EN 14511-2 [16] and EN 14511-3 [17]. With this method, however, only approximate comparisons for selected conditions can be made, but no estimations of a heat pump seasonal efficiency can be performed. The models indicated by the standards [10], [11], on the contrary, are able to give predictions about a heat pump seasonal performance (Seasonal Coefficient Of Performance, *SCOP*, and Seasonal Energy Efficiency Ratio, *SEER*), by weighting the *COP* or *EER* obtained in each bin on the basis of its duration.

Cecchinato et al. [18], for instance, evaluated the performance of vapor compression heat pumps by means of a simplified numerical method, based on performance data at nominal conditions and on refrigerant circuit information. By solving a system of equations, the method estimates the heat pump cooling or heating capacity and power consumption at part load conditions for mono-compressor on-off, bi-compressor and inverter-driven heat pumps. The authors applied the method to evaluate, in four test conditions, the *EER* at full load and at part load of two reversible air-to-water heat pumps (a mono-compressor on-off heat pump and an inverter-driven heat pump). Hence, they evaluated the *SEER* of the systems through a simple temperature class approach, by employing the weighted average of the *EER* values

obtained in the four test conditions. This method refers to a preliminary version of the standard EN 14825 [10], where weighting coefficients representing conventional operating times were provided for each of the four test conditions, as functions of the heat pump typology. The so-obtained seasonal performance coefficient can be used as a reference for energy comparisons between different heat pumps, or for a first approximate evaluation of the system energy consumption when detailed information about the building energy demand is not available. The authors obtained a good agreement between the predicted *SEER* values and the experimental results.

Kinab et al. [15] employed a similar method to evaluate the seasonal performance of an air-to-water heat pump in heating mode and in cooling mode. The authors developed a model able to evaluate the heat pump performance for several system configurations by means of detailed sub-models for each heat pump component (heat pump design model). The heat pump model was coupled to a model for building energy simulation, in order to calculate the system seasonal performance parameters, *SCOP* and *SEER*. The heat pump model provides the values of *COP* or *EER* for different conditions of part load and outdoor temperature, while the building model provides the corresponding weighting coefficients. In this case, the weighting coefficient is evaluated as the fraction of energy which the system delivers in a specific condition of part load and outdoor temperature over the total energy delivered to the building.

Francisco et al. [19] adopted a different simulation strategy, by employing computer modeling in which the bin-method described by ASHRAE [20] is implemented in order to investigate the influence of the climate on the seasonal efficiency of air-to-air heat pumps in heating mode. The authors evaluated the system performance in each bin through a simulation model which includes the effects of the back-up system (electric heaters) and of the duct losses. The energy consumption of the heat pump obtained in each bin was multiplied by the number of hours of the bin and then summed to get seasonal results. The authors considered two climates of the Northwest United States and found that a heat pump seasonal energy consumption is strongly affected by the climate, by the heat pump control strategy and by the duct losses. Some common control strategies that employ great use of back-up heat, in particular, can seriously compromise the expected heat pump seasonal performance, especially if combined with important duct losses.

Sarbu et al. [21] developed a computational model for the calculation of the seasonal energy performance of air-to-water heat pumps employed to provide building heating and domestic hot water production. The model is based on the bin-method defined in the European standard EN 15316-4-2 [22] and allows the evaluation of a heat pump *SCOP* (called in the

standard [22] *SPF*, namely Seasonal Performance Factor). The authors performed a comparative analysis of different building heating solutions, investigating the economic, energy and environmental advantages of employing heat pumps as heating generation systems.

The models based on a temperature class approach have a medium level of detail (e.g. they cannot consider the charge and discharge of a thermal storage tank coupled to a heat pump), but they are easy to use, do not require long computational time and can yield accurate predictions about the seasonal behavior of a heat pump system. In addition, they can be used for fast comparisons, in terms of seasonal efficiency, between different heat pump devices or between different heat generation technologies.

2.2.1   Heat pump seasonal performance evaluation according to European and Italian standards

The European standard EN 14825 [10] and the Italian standard UNI/TS 11300-4 [11] present calculation methods for the evaluation of the seasonal performance of heat pumps in heating, cooling and DHW production mode. The standards [10], [11] suggest to model the outdoor climate by means of the bin-method. A bin represents the number of hours, during a selected time period, in which the external air has a value of temperature within a fixed interval, centered on an integer value of temperature and 1 K wide. For instance, a bin duration of 20 hours in correspondence of an outdoor temperature T_{ext} equal to 15 °C means that for 20 hours during a certain time period the external air temperature had a value between 14.5 °C and 15.5 °C.

The standard EN 14825 [10] gives indication to calculate the reference Seasonal Coefficient Of Performance (*SCOP*) of heat pumps in heating mode and the reference Seasonal Energy Efficiency Ratio (*SEER*) of heat pumps in cooling mode.

The standard [10] splits Europe in three winter climates (Colder, Average and Warmer) and directly assigns the bin trends for the reference heating season of each climate. The duration of each bin is rounded to a whole number and is derived from weather data collected over the 1982 – 1999 period for the locations of Helsinki, Strasbourg and Athens, selected as representative of the Colder, Average and Warmer climate, respectively.

Figures 2.1-2.3 show the bin profiles of the Colder, Average and Warmer heating seasons derived from Ref. [10].

For selected heat pump and building, one can calculate a value of Seasonal Coefficient Of Performance for each of the three reference climate and compare different heat pump models under the same reference conditions.
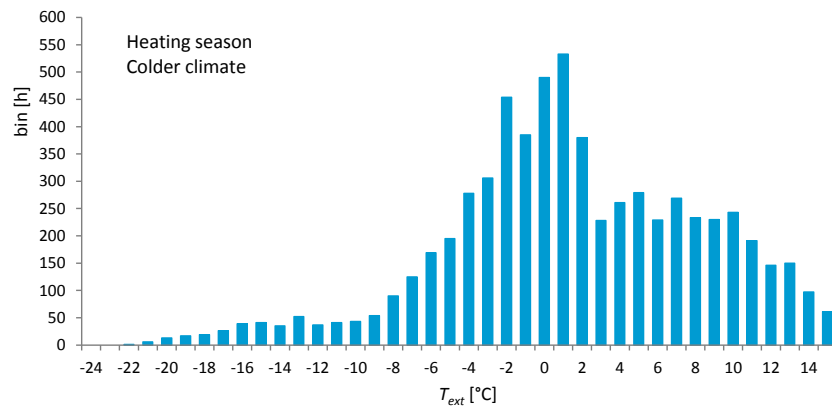
Figure 2.1: Bin distribution for the heating season in the Colder climate from standard EN 14825.
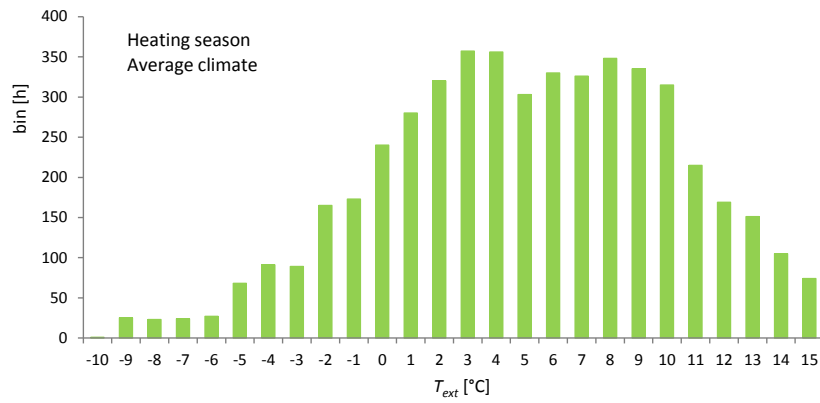
Figure 2.2: Bin distribution for the heating season in the Average climate from standard EN 14825.
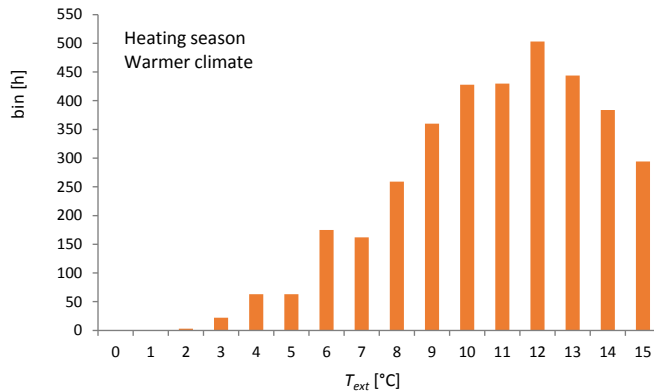
Figure 2.3: Bin distribution for the heating season in the Warmer climate from standard EN 14825.

Regarding the cooling season, the standard [10] suggest a single bin profile for whole Europe, illustrated in Figure 2.4.
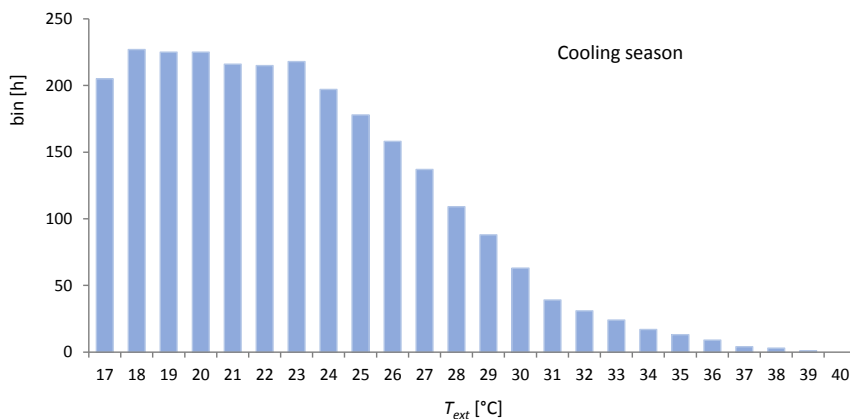
Figure 2.4: Bin distribution for the cooling season from standard EN 14825.

It can be noticed from Figures 2.1-2.4 that the bin trends of the standard [10] are stopped in correspondence of an outdoor temperature equal to 16 °C for all climates in cooling and heating mode. In the standard [10], in fact, the heat pump is considered coupled to a building whose loads are expressed as a linear function of the external air temperature, T_{ext}. The method for the determination of this function, called Building Energy Signature (BES), is described in the European standard EN 15603 [23]. The standard EN 14825 [10] considers BES lines which vanishes for T_{ext} equal to 16 °C (in this Thesis called zero-load external air temperature, T_{zl}). In Figure 2.5, examples of linear BES lines for heating and for cooling are shown.
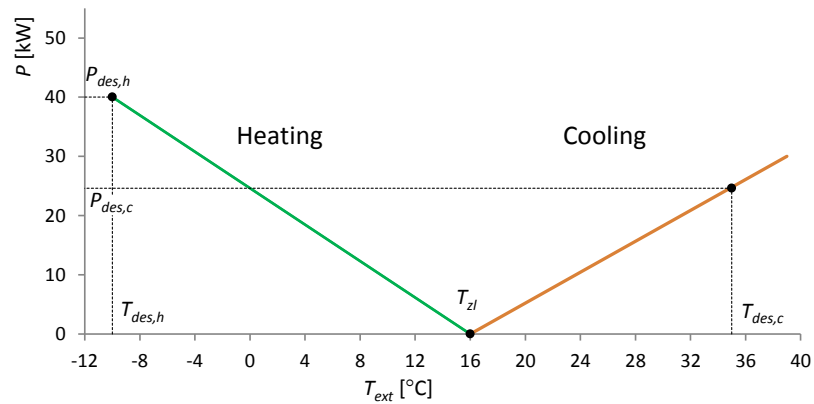
Figure 2.5: Examples of Building Energy Signatures for heating (left) and for cooling (right).

In Figure 2.5, P_{des} is the design load, namely the building load in correspondence of the outdoor design temperature, T_{des}. With reference to the heating mode, the standard [10] sets the outdoor design temperature, $T_{des,h}$, equal to -22 °C for the Colder climate, -10 °C for the Average climate and 2 °C for the Warmer climate; the outdoor design temperature for cooling, $T_{des,c}$, is 35 °C. It can be noticed that, while the values of $T_{des,h}$ for the winter climates coincide with the minimum outdoor temperature obtainable from the bin trends, the summer bin profile presents values of T_{ext} greater than the summer outdoor design temperature.

The standard [10] sets the part load conditions at which the heat pump *COP* or *EER* must be evaluated by the manufacturer, in order to be used as input data for the calculation of the reference seasonal performance coefficients. Indications are given for testing the heat pumps at part load conditions and for measuring their performance, with reference to the European standards EN 14511-2 [16] and EN 14511-3 [17].

Ref. [10] differentiates the part load conditions on the basis of the heat pump typology (air-to-air, air-to-water etc.) and, referring to the heating mode, also on the basis of the indoor heat exchanger temperature (low, medium, high and very high) and on the climate (Colder, Average, Warmer). Table 2.1 reports the part load conditions A–G at which an air-to-water heat pump for low temperature applications must be tested in order to determine the reference *SCOP* in the Colder climate.

Table 2.1: Part load conditions for reference *SCOP*, air-to-water units for low temperature applications, reference heating season Colder.

Part load condition	Part load ratio	T_{ext} [°C]	Indoor heat exchanger inlet/outlet temperatures [°C] for fixed outlet units	Indoor heat exchanger inlet/outlet temperatures [°C] for variable outlet units
A	$(-7 - 16) / (T_{des,h} - 16) \approx 61\%$	-7	30 / 35	25 / 30
B	$(2 - 16) / (T_{des,h} - 16) \approx 37\%$	2	30 / 35	22 / 27
C	$(7 - 16) / (T_{des,h} - 16) \approx 24\%$	7	30 / 35	20 / 25
D	$(12 - 16) / (T_{des,h} - 16) \approx 11\%$	12	30 / 35	19 / 24
E	$(TOL - 16) / (T_{des,h} - 16)$	TOL	30 / 35	interpolation or extrapolation from the temperatures closest to TOL
F	$(T_{biv} - 16) / (T_{des,h} - 16)$	T_{biv}	30 / 35	Interpolation between the upper and lower temperatures closest to T_{biv}
G	$(-15 - 16) / (T_{des,h} - 16) \approx 82\%$	-15	30 / 35	27 / 32

In Table 2.1, the part load ratio gives, for each of the A–G conditions, the percentage of the building design load at which the heat pump must be tested. It is possible to calculate the seasonal performance coefficients of a heat pump for more than one P_{des} value.

In Table 2.1, *TOL* is the Temperature Operative Limit, namely the minimum value of T_{ext}, given by the heat pump manufacturer, at which the heat pump is able to deliver heating capacity. T_{biv} is the bivalent temperature, namely the outdoor temperature at which the heat pump capacity equals the building load. These temperature values vary from case to case; the European standard [10], however, indicates to use bivalent temperatures equal to or lower than -7 °C for the Colder climate, equal to or lower than 2 °C for the Average climate and equal to or lower than 7 °C for the Warmer climate.

The part load condition G is applied in case of Colder climate if the *TOL* is lower than -20 °C. For each part load condition, the inlet and outlet temperatures of the indoor heat exchanger are differentiated between fixed and variable outlet heat pumps. The second heat pump typology, which will not be analyzed in this Thesis, allows a variation of the indoor heat exchanger outlet temperature as a function of the external air temperature.

Table 2.2 shows the part load conditions A–F at which an air-to-water heat pump for high temperature applications must be tested in order to determine the reference *SCOP* in the Average climate according to the standard [10].

Table 2.2: Part load conditions for reference *SCOP*, air-to-water units for high temperature applications, reference heating season Average.

Part load condition	Part load ratio	T_{ext} [°C]	Indoor heat exchanger inlet/outlet temperatures [°C] for fixed outlet units	Indoor heat exchanger inlet/outlet temperatures [°C] for variable outlet units
A	$(-7 - 16) / (T_{des,h} - 16) \approx 88\ \%$	-7	47 / 55	44 / 52
B	$(2 - 16) / (T_{des,h} - 16) \approx 54\ \%$	2	47 / 55	34 / 42
C	$(7 - 16) / (T_{des,h} - 16) \approx 35\ \%$	7	47 / 55	28 / 36
D	$(12 - 16) / (T_{des,h} - 16) \approx 15\ \%$	12	47 / 55	22 / 30
E	$(TOL - 16) / (T_{des,h} - 16)$	*TOL*	47 / 55	interpolation or extrapolation from the temperatures closest to *TOL*
F	$(T_{biv} - 16) / (T_{des,h} - 16)$	T_{biv}	47 / 55	Interpolation between the upper and lower temperatures closest to T_{biv}

From Table 2.2 one can note that the part load condition G, which refers to T_{ext} equal to -15 °C, does not apply to the case of Average climate, whose minimum outdoor temperature is $T_{des,h}$ = -10 °C. In addition, if the *TOL* declared by the manufacturer is lower than $T_{des,h}$ of the considered climate, it may be assumed equal to $T_{des,h}$.

Table 2.3 reports the part load conditions for a water-to-water heat pump, or a brine-to-water heat pump, for medium temperature heating applications in the Warmer climate.

Table 2.3: Part load conditions for reference *SCOP*, water-to-water or brine-to-water units for medium temperature applications, reference heating season Warmer.

Part load condition	Part load ratio	Ground water inlet temperature [°C]	Brine inlet temperature [°C]	Indoor heat exchanger inlet/outlet temperatures [°C] for fixed outlet units	Indoor heat exchanger inlet/outlet temperatures [°C] for variable outlet units
B	$(2 - 16) / (T_{des,h} - 16) = 100\%$	10	0	40 / 45	40 / 45
C	$(7 - 16) / (T_{des,h} - 16) \approx 64\%$	10	0	40 / 45	34 / 39
D	$(12 - 16) / (T_{des,h} - 16) \approx 29\%$	10	0	40 / 45	26 / 31
F	$(T_{biv} - 16) / (T_{des,h} - 16)$	10	0	40 / 45	Interpolation between upper and lower temperatures closest to T_{biv}

From Table 2.3 one can note that the part load condition A (which refers to T_{ext} = -7 °C) does not apply to the case of Warmer climate, whose minimum outdoor temperature is $T_{des,h}$ = 2 °C. The part load condition E refers to T_{ext} = $T_{des,h}$ in the cases of water-to-water or brine-to-water heat pumps, therefore in the Warmer climate the condition E equals the condition B. Tables 2.4, 2.5 show the part load conditions for the determination of the reference *SEER* of air-to-water heat pumps and water-to-water (or brine-to-water) heat pumps, respectively. In part load condition A (full load), the heat pump power is considered equal to the building cooling load, which means that the bivalent temperature for the cooling mode is 35 °C.

Table 2.4: Part load conditions for reference *SEER*, air-to-water units.

Part load condition	Part load ratio	T_{ext} [°C]	Indoor heat exchanger inlet/outlet temperatures [°C] for fixed outlet fan coil	Indoor heat exchanger inlet/outlet temperatures [°C] for variable outlet fan coil	Indoor heat exchanger inlet/outlet temperatures [°C] for cooling floor
A	$(35 - 16) / (T_{des,c} - 16) =$ 100 %	35	12 / 7	12 / 7	23 / 18
B	$(30 - 16) / (T_{des,c} - 16) \approx$ 74 %	30	12 / 7	13.5 / 8.5	23 / 18
C	$(25 - 16) / (T_{des,c} - 16) \approx$ 47 %	25	12 / 7	15 / 10	23 / 18
D	$(20 - 16) / (T_{des,c} - 16) \approx$ 21 %	20	12 / 7	16.5 / 11.5	23 / 18

Table 2.5: Part load conditions for reference *SEER*, water-to-water or brine-to-water units.

Part load condition	Part load ratio	Outdoor heat exchanger inlet/outlet temperatures [°C]			Indoor heat exchanger inlet/outlet temperatures [°C]		
		Cooling tower	Ground coupled application	Dry cooler	Fixed outlet fan coil	Variable outlet fan coil	Cooling floor
A	$(35 - 16) / (T_{des,c} - 16)$ = 100 %	30 / 35	10 / 15	50 / 55	12 / 7	12 / 7	23 / 18
B	$(30 - 16) / (T_{des,c} - 16)$ ≈ 74 %	26 / 31	10 / 15	45 / 50	12 / 7	13.5 / 8.5	23 / 18
C	$(25 - 16) / (T_{des,c} - 16)$ ≈ 47 %	22 / 27	10 / 15	40 / 45	12 / 7	15 / 10	23 / 18
D	$(20 - 16) / (T_{des,c} - 16)$ ≈ 21 %	18 / 23	10 / 15	35 / 40	12 / 7	16.5 / 11.5	23 / 18

The standard [10] requires the determination of a heat pump power, *COP* and *EER* in correspondence of the bins representative of the predefined part load conditions. If for a condition the heat pump power at full load is equal to or lower than the required building load, the corresponding power, *COP* and *EER* values at full load must be used. If the heat pump power at full load is higher than the required building load, the heat pump performance must be calculated depending on the capacity control of the unit. In particular, mono-compressor on-off heat pumps employ on-off cycles to match the building needs. As evidenced by Henderson et al. [24], on-off cycles cause an efficiency loss of the heat pump, since the electric energy consumption of the unit does not vanish during the off-cycle and, when the heat pump restarts, its compressor has to re-establish the pressure.

The efficiency loss due to on-off cycles is taken into account by Ref. [10] through the correction factor, f_{corr}. The factor f_{corr}, evaluated for air-to-water, water-to-water and brine-to-water heat pumps according to Eq. (2.1), multiplies the heat pump *COP* or *EER* at full load in order to derive the corresponding part load value.

$$f_{corr}(i) = \frac{CR(i)}{C_c\ CR(i) + \left(1 - C_c\right)} \ .$$

(2.1)

In Eq. (2.1), the letter *i* indicates the *i*-th predefined part load condition, *CR* is the capacity ratio and C_c is the degradation coefficient. The capacity ratio *CR* is the ratio between the building load and the heat pump power at the same temperature conditions. If the heat pump power equals the building demand, *CR* is equal to 1 and the correction factor for on-off condition turns out equal to 1. The degradation coefficient C_c measures the specific heat pump efficiency decrease for on-off cycles and should be determined for each specific unit by means of laboratory tests. If C_c is not determined by tests, then the default value of 0.9 shall be used.

Multi-compressor and inverter-driven heat pumps, on the contrary, are able to adapt the power released in order to follow the building load and delay the on-off cycles activation. In these cases, the standard [10] indicates to determine the heat pump power, *COP* and *EER* at the step of the heat pump capacity closest to the required building load. If this step does not allow to reach the building load within ±10 % (e.g. between 8.1 kW and 9.9 kW for a required building load of 9 kW), then the heat pump performance must be evaluated at the steps on either side of the required building load. The part load heat pump power, *COP* and *EER* are then determined by linear interpolation between the results obtained from these two steps. If the smallest control step of the unit is higher than the required building load, the procedure for mono-compressor on-off heat pumps shall apply.

The European standard [10] evaluates the heat pump power and *COP* (or *EER*) in each bin through linear interpolations between the values of the two closest part load conditions. Regarding the heating mode, the heat pump performance for values of T_{ext} above the part load condition D is extrapolated from the values at the part load conditions C and D. Regarding the cooling mode, for values of T_{ext} above the part load condition A or below the part load condition D, the same heat pump performance in correspondence of the condition A or of the condition D is used, respectively.

Figure 2.6 shows an example of winter BES and of characteristic curve of an air-to-water ON-OFF HP for high temperature application in the Average climate, where the heat pump power has been obtained by interpolating the values at the part load conditions A–F, according to Ref. [10].
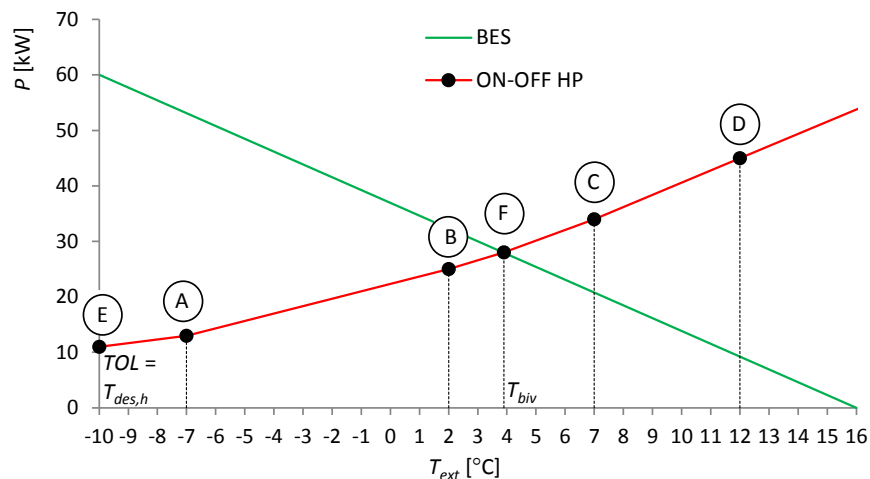
Figure 2.6: Examples of Building Energy Signature and of characteristic curve of an air-to-water ON-OFF HP in heating mode, high temperature application, Average climate.

In Figure 2.6 one can note the balance point, which is the intersection between the BES and the heat pump characteristic curve at full load. The outdoor temperature corresponding to the balance point is called bivalent temperature, T_{biv}. As previously mentioned, at T_{biv} the heat pump power equals the building load. Considering the heating mode, for values of T_{ext} between the *TOL* and T_{biv} the heat pump power is lower than the building need and an additional back-up system is necessary to fulfil the full heating load. The standard [10] considers as back-up system only electric heaters, whereas the codes developed in this Thesis for the evaluation of a heat pump seasonal efficiency distinguish between electric heaters and gas boiler. For values of T_{ext} higher than T_{biv}, the heat pump power at full load is higher

than the heating demand and the heat pump *COP* must be corrected as previously described. For values of T_{ext} lower than the *TOL*, the heat pump is not running and only the back-up system is activated.

Considering the cooling mode, the heat pump power at full load is higher than the building demand for values of T_{ext} below T_{biv}, whereas for outdoor temperatures above T_{biv} the heat pump is not able to completely satisfy the cooling load, but no back-up systems are employed. The European standard [10] takes into account the real *COP* (or *EER*) values of a heat pump only for a limited number of predefined conditions, among which linear interpolations are employed. With this method, however, considerable approximations are introduced, especially for multi-compressor heat pumps (MCHPs) and inverter-driven heat pumps (IDHPs), in correspondence of the bins intermediate between two part load conditions. The codes developed in this Thesis, on the contrary, calculate the *COP* (or *EER*) values for each bin, by using for MCHPs and IDHPs a number of characteristic curves corresponding to different heat pump capacity (see Chapter 3).

Different reference seasonal coefficients are defined by the standard EN 14825 [10]. The Seasonal Coefficient Of Performance of the heat pump, $SCOP_{net}$, is the ratio between the thermal energy delivered by the heat pump during the heating season and the corresponding electric energy used. $SCOP_{net}$ is evaluated by Ref. [10] as:

$$SCOP_{net} = \frac{\sum_{i=1}^{n} t_{bin}(i)\left[P_{b,h}(i) - P_{bk}(i) \right]}{\sum_{i=1}^{n} t_{bin}(i)\ \dfrac{P_{b,h}(i) - P_{bk}(i)}{COP(i)}}\ . \tag{2.2}$$

In Eq. (2.2), i indicates the i-th bin, n is the total amount of bins for the selected winter climate, $t_{bin}(i)$ is the time duration of the i-th bin, $P_{b,h}(i)$ is the thermal power required by the building in the i-th bin (obtainable from the BES multiplying $P_{des,h}$ by the part load ratio of the i-th bin), $P_{bk}(i)$ is the power released by the electric back-up system in the i-th bin and $COP(i)$ is the value of Coefficient Of Performance obtained for the i-th bin.

Obviously, the difference between $P_{b,h}$ and P_{bk}, employed by Ref. [10] to evaluate the $SCOP_{net}$ value, is equal to the thermal power delivered by the heat pump. The energy supplied and used by the back-up system, in fact, does not apply for the calculation of $SCOP_{net}$, which refers only to the heat pump.

Another performance coefficient for the heating season is the Seasonal Coefficient Of Performance of the whole system (composed of heat pump and back-up system), $SCOP_{on}$, evaluated as the total energy required by the building during the heating season (covered by

the heat pump and, if needed, by the back-up system) and the total electric energy used by the system:

$$SCOP_{on} = \frac{\sum_{i=1}^{n} t_{bin}(i)\, P_{b,h}(i)}{\sum_{i=1}^{n} t_{bin}(i) \left[\dfrac{P_{b,h}(i) - P_{bk}(i)}{COP(i)} + P_{bk}(i) \right]} \ . \tag{2.3}$$

The thermal power that the back-up electric heaters give is obviously equal to the electric power that they use and both these quantities are indicated as P_{bk} in Eq. (2.3).

No back-up systems are present for the heat pump cooling mode and only the seasonal coefficient $SEER_{on}$ is defined:

$$SEER_{on} = \frac{\sum_{i=1}^{n} t_{bin}(i)\, P_{b,c}(i)}{\sum_{i=1}^{n} t_{bin}(i)\, \dfrac{P_{b,c}(i)}{EER(i)}} \ , \tag{2.4}$$

where $P_{b,c}(i)$ is the cooling power required by the building in the i-th bin (obtainable from the BES multiplying $P_{des,c}$ by the part load ratio of the i-th bin) and $EER(i)$ is the value of Energy Efficiency Ratio obtained for the i-th bin.

In Eq. (2.4), using $P_{b,c}$ instead of the heat pump power yields a small approximation due to the bins with temperature higher than T_{biv} (35 °C), where the whole building demand is not covered by the heat pump.

Both $SCOP_{net}$, $SCOP_{on}$ and $SEER_{on}$ refer to the active mode of a heat pump, namely to the hours in which the building load is present and the heating or cooling function of the heat pump is thus activated. Energy consumptions can occur also when the heat pump is not used to fulfil the building demand, such as the energy consumption of the crankcase heater or of the standby mode of the unit (mode wherein the unit is partially switched off and can be reactivated by a control device or timer). These consumptions, which are considered by the standard [10] with the definition of other seasonal coefficients, are not studied in the present Thesis.

The Italian standard UNI/TS 11300-4 [11] defines a calculation method to evaluate the primary energy consumption of a heat pump system for building heating and/or domestic hot water production. According to the standard [11], the calculation for heat pumps linked to stable thermal reservoirs (i.e. water or ground) is performed with time steps of one month. For air-source heat pumps, on the contrary, the bin-method is recommended in order to take into account the variability of the outside temperature.

Unlike the standard EN 14825 [10], which directly gives three winter bin trends, the standard UNI/TS 11300-4 [11] provides a bin calculation method, based on a normal external air temperature distribution. The method allows to evaluate the monthly bin profile of a specific location in Italy and the bin trend for the whole heating season can be obtained by summing the corresponding monthly bin profiles.

The method of the Italian standard employs as input data: the monthly average outdoor temperature ($T_{m,month}$), according to the standard UNI 10349 [25]; the winter outdoor design temperature ($T_{des,h}$), according to the national annex A of the standard EN 12831 [26] and the monthly average daily solar radiation on a horizontal plane ($H_{m,month}$), according to Ref. [25]. The mean value of the normal distribution is assumed equal to $T_{m,month}$ and the standard deviation, σ_{month}, is evaluated as:

$$\sigma_{month} = 1.8 + 0.16\ H_{m,month} + \Delta\sigma_{month}\ , \tag{2.5}$$

where σ_{month} is expressed in °C, $H_{m,month}$ in MJ/m^2 and $\Delta\sigma_{month}$ is the standard deviation correction:

$$\Delta\sigma_{month} = \Delta\sigma_{max}\ k_{\sigma,month}\ . \tag{2.6}$$

The factor $k_{\sigma,month}$ of Eq. (2.6) is given by the following Table:

Table 2.6: Values of the factor $k_{\sigma,month}$.

Month	$k_{\sigma,month}$
January	1
February	0.5
December	0.5
Other months	0

In Eq. (2.6), $\Delta\sigma_{max}$ is calculated as:

$$\Delta\sigma_{max} = -0.502 - 0.15825\ (T_{m,month,1} - T_{des,h}) + 0.06375\ (T_{m,month,1} - T_{des,h})^2 - 0.16\ H_{m,month,1}\ , \tag{2.7}$$

where the subscript *1* indicates the month of January, assumed as the coldest month of the year.

The bin density factor of the *i*-th bin of the month, $K_{bin,month}(i)$, is evaluated as:

$$K_{bin,month}(i) = \frac{1}{\sigma_{month}\sqrt{2\pi}}\ e^{-\frac{1}{2}\left(\frac{T_{ext}(i)-T_{m,month}}{\sigma_{month}}\right)^2}\ , \tag{2.8}$$

where $T_{ext}(i)$ is the external air temperature value corresponding to the i-th bin.

The theoretical duration of the i-th bin of the month, $t'_{bin,month}(i)$, is given by:

$$t'_{bin,month}(i) = K_{bin,month}(i)\, t_{month} \quad , \tag{2.9}$$

where t_{month} is the time duration of the considered month.

Since the theoretical normal distribution would extend to infinity, it is shortened by setting to 0 the bin durations lower than 1.5 % t_{month}. The effective duration of the i-th bin, $t_{bin,month}(i)$, is finally calculated as:

$$t_{bin,month}(i) = t_{month}\, \frac{t'_{bin,month}(i)}{\sum_i t'_{bin,month}(i)} \quad . \tag{2.10}$$

For the performance evaluation of an electric heat pump, the standard [11] requires manufacturer data of heat pump power and *COP* at full load at the source and sink temperatures reported in Tables 2.7, 2.8:

Table 2.7: Reference conditions for performance data provided by the manufacturer. Heat pumps for heating-only or heating and DHW production.

Source	Source temperature [°C]				Sink temperature [°C] – Air space heating	Sink temperature [°C] – Water space heating		Sink temperature [°C] – DHW production		
Air	-7	2	7	12	20	35	45	55	45	55
Water	--	5	10	15	20	35	45	55	45	55
Ground	-5	0	5	10	20	35	45	55	45	55

Table 2.8: Reference conditions for performance data provided by the manufacturer. Heat pumps for DHW production only.

Source	Source temperature [°C]				Sink temperature [°C] – DHW production		
Air	7	15	20	35	(45)	55	(65)

Also performance data at part load ratios different from 1 are needed, for the same source and sink temperatures of Tables 2.7, 2.8, according to the reference climates Colder, Average and Warmer defined by the standard EN 14825 [10].

Unlike Ref. [10], the standard [11] indicates to evaluate the *COP* at full load, for conditions different from those tabulated in Tables 2.7, 2.8, through linear interpolation of the second law efficiency, η_{II}:

$$\eta_{II} = \frac{COP(T_{cold}, T_{hot})}{COP_{max}(T_{cold}, T_{hot})} = \frac{COP(T_{cold}, T_{hot})}{\frac{T_{hot} + 273.15}{T_{hot} - T_{cold}}} \quad , \tag{2.11}$$

where T_{cold} is the heat pump source temperature and T_{hot} is the heat pump sink temperature ([°C]). As example, to obtain the *COP* value for a sink temperature $T_{hot,x}$ intermediate between the two tabulated temperatures $T_{hot,1}$ and $T_{hot,2}$, at the same source temperature T_{cold}, the following procedure is employed by Ref. [11]:

$$\eta_{II,1} = \frac{COP(T_{cold}, T_{hot,1})}{\frac{T_{hot,1} + 273.15}{T_{hot,1} - T_{cold}}} \quad , \tag{2.12}$$

$$\eta_{II,2} = \frac{COP(T_{cold}, T_{hot,2})}{\frac{T_{hot,2} + 273.15}{T_{hot,2} - T_{cold}}} \quad , \tag{2.13}$$

$$\eta_{II,x} = \eta_{II,1} + \left(\eta_{II,2} - \eta_{II,1}\right)\frac{T_{hot,x} - T_{hot,1}}{T_{hot,2} - T_{hot,1}} \quad , \tag{2.14}$$

$$COP(T_{cold}, T_{hot,x}) = \eta_{II,x} \frac{T_{hot,x} + 273.15}{T_{hot,x} - T_{cold}} \quad . \tag{2.15}$$

In particular, the linear interpolation of η_{II} is employed to obtain *COP* values for intermediate source or sink temperatures within the manufacturer data field. For temperatures outside the data field (with 5 °C of maximum deviation), η_{II} is assumed equal to that of the closer temperature provided by the manufacturer.

To evaluate the heat pump power for conditions within the manufacturer data field, but intermediate between those of Tables 2.7, 2.8, a linear interpolation between the tabulated power values is adopted. The heat pump power for values of T_{hot} outside the manufacturer data field (with 5 °C of maximum deviation) is assumed equal to that of the closer temperature provided by the manufacturer. The heat pump power for values of T_{cold} outside the manufacturer data field (with 5 °C of maximum deviation) is obtained by multiplying the corresponding *COP* value (calculated as just described) by the electric power used at the closer temperature provided by the manufacturer.

To correct a heat pump performance in the case on on-off cycles, the standard [11] employs the *COP* correction factor defined by Ref. [10].

The standard [11] divides the heat pump systems into monovalent plants, where all the building thermal demand is covered by the heat pump, and bivalent plants, where the building thermal demand is covered by the heat pump and by an auxiliary back-up system. Unlike the standard [10], Ref. [11] takes into account both mono-energetic bivalent plants (where the back-up system utilizes the same energy source of the heat pump; e.g. electric heaters considering electric heat pumps) and bi-energetic bivalent plants (where the back-up system utilizes a different energy source; e.g. gas boilers considering electric heat pumps).

Starting from the manufacturer data of heat pump power and *COP*, the thermal energy delivered by the heat pump and, if needed, by the back-up system and the corresponding primary energy use are evaluated for each bin (or month, for water-source and ground-source heat pumps) of the considered period.

Ref. [11] is applicable to heat pumps which provide only heating, only DHW or both heating and DHW, either with separate circuits for the two functions (not studied in the present Thesis), or with one circuit for combined service. In this latter case, the standard [11] considers priority of satisfaction of the DHW demand and calculates for each bin (or month) the residual time available for the heating function.

Unlike Ref. [10], the Italian standard [11] considers that a heat pump can be switched off for values of T_{cold} below the bivalent temperature T_{biv} (alternate operation), below the heat pump Temperature Operative Limit *TOL* (parallel operation) or below the cut-off temperature $T_{cut\text{-}off}$ (partial parallel operation). $T_{cut\text{-}off}$ is the value of T_{cold}, possibly higher than the *TOL*, at which the heat pump control system switches the heat pump off due to, for instance, economic evaluations. See as example Figure 2.7, where an air-source heat pump characteristic curve and a building energy signature are drawn as functions of the outdoor temperature, T_{ext}.
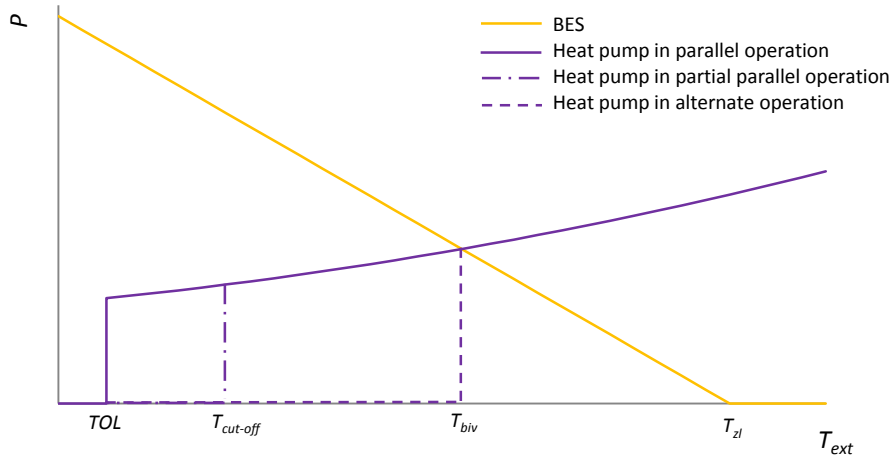
Figure 2.7: Examples of building energy signature and air-source heat pump characteristic curve in different operations.

In the alternate operation, for values of T_{cold} lower than T_{biv}, only the back-up system supplies the thermal energy required by the building. In the parallel operation, below T_{biv} the heat pump is not switched off and the back-up system provides only the missing energy. In the partial parallel operation, if T_{cold} is lower than T_{biv}, the back-up system provides to the building thermal need which the heat pump cannot cover, until $T_{cut-off}$; below $T_{cut-off}$ only the back-up system is switched on. In the present Thesis, the parallel and partial parallel operations are analyzed.

While the European standard [10] adopts a value of zero-load external air temperature, T_{zl}, equal to 16 °C, Ref. [11] suggests a default T_{zl} value of 20 °C.

The codes developed for the simulation of air-to-water heat pumps described in Chapter 3 of this Thesis are built starting from the standards [10], [11]. Unlike the standards, however, the codes consider in detail the specific operating modes of different heat pump typologies (mono-compressor on-off heat pumps, multi-compressor heat pumps and inverter-driven heat pumps) and they can take into account the heat recovery mode for DHW production.

2.3   DYNAMIC SIMULATION MODELS

A more detailed method to evaluate the mean seasonal performance of a whole heat pump system is the dynamic simulation, which is able to take into account the dynamic variation of the building load, of the heat pump source temperature and, consequently, of the heat pump performance. It can also consider the presence of a thermal storage tank coupled to a heat pump.

Normally, in these models the calculations are carried out at quasi-steady-state conditions, namely at steady-state conditions for each time interval, which is equal to the time step of the calculation method of the building thermal load (usually 1 hour).

Performance map based models are employed in most dynamic simulation software (e.g. TRNSYS), which means that the thermodynamic properties of the heat pump working fluid are not modeled physically, but interpolations among a number of heat pump characteristic points, given by the user, are employed in order to model the heat pump behavior. The dynamic software TRNSYS uses the temperatures of the heat pump source and sink to evaluate the thermal power delivered and the electric power needed by the heat pump in each time step (see Subsection 2.3.1). To simulate the whole heating (or cooling) generation system, the TRNSYS user has to couple the model of the heat pump with models of the other components of the system (e.g. thermal storage, building, borehole heat exchangers). No direct calculations of a heat pump efficiency at part loads is performed by the software.

Bettanini et al. [14] proposed a mathematical model for the evaluation of a heat pump behavior at part load, observing that the seasonal performance of a heat pump is strongly influenced by its capacity to maintain high values of efficiency at part loads. The authors applied the model to evaluate dynamically the seasonal performance of several heat pump systems in heating and cooling mode. The building energy requirements, obtained from an hourly simulation, were used to identify the heat pump part load conditions, on the basis of the reference working curves of the heat pump at full load. Consequently, the hourly mean *COP* or *EER* was calculated and corrected by using the proposed model for part loads. Dividing the mean hourly capacity of the heat pump by this value of *COP* or *EER*, the mean hourly electric consumption was calculated and the seasonal parameters, *SCOP* and *SEER*, were obtained as the ratio between the satisfied building energy requirement, integrated in the season period, and the total electric consumption of the heat pump. The authors found a relative discrepancy always less than 1 % between the seasonal performance parameters calculated and the real parameters measured from monitoring of the machines.

Klein et al. [27] investigated, by means of dynamic numerical simulations, the performance of a hybrid system, composed of an electric mono-compressor on-off air-to-water heat pump for building heating, coupled to a condensing gas boiler. A thermal storage was included in the study in order to increase the thermal inertia of the system and to reduce the number of operating cycles of the heat generators (heat pump and gas boiler). The heat generators were connected in series, with the heat pump located upstream of the gas boiler. The study was conducted by using Modelica (an equation-based modeling language for complex physical systems simulation) in the software environment Dymola 2012. The weather was modeled

by using the Test Reference Year created by the German national meteorological service for the Western Germany region. The building thermal needs were taken into account by evaluating the building energy signature. The heat pump was simulated by means of a performance map based model, in which a two-dimensional tabulated performance map returned the heat pump thermal capacity and electric power consumption as functions of the source and sink temperatures. Also the boiler model was table-based, by employing experimental data. The thermal storage, assumed as a stratified cylindrical tank, was discretized in six water volumes, each with uniform temperature; the heat flow between adjacent layers was modeled by thermal connections. A partial parallel operation strategy was chosen to operate the heat pump and the gas boiler (see Subsection 2.2.1). The building insulation, the nominal heat pump capacity and the volume of the thermal storage tank were varied, in order to analyze their impact on the system performance. The authors attained the highest seasonal performance with mid-range heat pump capacities and well insulated buildings. The volume of the storage tank, on the other hand, had a very limited impact on the system performance.

Madonna and Bazzocchi [28] developed a mathematical model for hourly simulation of a small size air-to-water inverter-driven heat pump in heating and cooling mode. The proposed model used a linear relationship between the performance of the real refrigeration cycle and that of the Carnot refrigeration cycle (ideal cycle), operating at the same temperatures. To take into account the heat pump efficiency decrease due to on-off cycles, the authors employed Eq. (2.1) from the standard EN 14825 [10], with the heat pump capacity ratio *CR* evaluated as the ratio between the thermal energy supplied by the heat pump in one hour and the thermal energy which could be supplied with the compressor continuously running at the minimum inverter frequency. This second quantity actually depends on the heat pump condensation and evaporation temperatures. The model [28], however, neglects this dependency and approximates the denominator of *CR* with the energy delivered by the heat pump in one hour by running the compressor at one third of its maximum capacity. On the contrary, the heat pump simulation codes presented in the next chapters of this Thesis evaluate the minimum energy that an inverter-driven heat pump can supply in given conditions, by taking into account the temperature values of the heat pump source and sink. The calculation of the building thermal energy needs was performed in Ref. [28] through the simplified "three-node" dynamic method described in the international standard ISO 13790 [29] and the IWEC climate files were used to simulate the weather. No thermal storage tanks or back-up systems were considered in the study. The model was calibrated by means of experimental data, collected in a field trial monitoring campaign, and it was used

to evaluate the heat pump performance in different residential buildings and Italian locations. The authors noticed that a heat pump seasonal performance is strongly affected by the climate and also the ratio between heating and cooling loads plays an important role. Heat pumps which are sized for the most severe season, in particular, can result oversized during the other season, causing excessive on-off cycles and a consequent reduction of the heat pump efficiency, despite the use of an inverter.

Al-Zahrani et al [30] analyzed, through the dynamic software TRNSYS, a case study about the integration of a water-to-water heat pump with a hot water and a cold water storage tank, for simultaneous cooling and DHW production in residential and office buildings in a tropical climate. The authors evaluated the system performance at different operation modes and storage tank sizes. Day-time operation, night-time operation and whole-day operation of the heat pump were considered. Since all the waste heat rejected by the heat pump is stored in the hot tank, the authors studied the influence of the tank volumes and of the heat transfer balancing between the storages in maintaining suitable temperatures in the storage tanks. On the contrary, in the codes developed in this Thesis for the simulation of heat pumps in simultaneous cooling and DHW production, the heat pump can also reject heat to the external air, working in cooling-only mode, when all the building energy demand for DHW production is satisfied. Al-Zahrani et al. [30] found that the day-time operation mode requires the smallest size of both storages, but is unable to provide domestic hot water sufficiently hot during early morning, unlike the other two operation modes, which can supply hot water at the required temperature.

Dynamic simulation models are more detailed than the previous methods and require greater effort to be developed; nevertheless, they can be easy to use and can require short computational time. Moreover, these models allow comparisons between different heat pump systems in more realistic conditions and they are able to evaluate the system behavior over long-term periods (like the long-term sustainability of heat pumps coupled to borehole heat exchangers).

Chapter 4 presents the codes developed in this Thesis for the dynamic simulation of air-to-water heat pumps systems, whereas Chapter 5 presents the codes developed for the dynamic simulation of systems based on ground-coupled heat pumps.

2.3.1 Dynamic simulation of air-to-water heat pumps with the software TRNSYS

TRNSYS (TRaNsient SYstems Simulation) is a simulation program that uses built-in subroutines to model the transient operation of a variety of systems, including heat pumps.

TRNSYS is made up of an engine, that reads and processes the input file and iteratively solves the system, of a graphical interface (Simulation Studio) and of a library of components, called Types, each of which models one part of the system (Ref. [31]). A Type is a pre-defined mathematical subroutines which represents a physical component of the simulated system. The Types selected from the library are dragged and dropped into the TRNSYS workspace and linked to each other: the outputs of one component are graphically connected to the inputs of another, while the parameters of a Type can be set by the user. When a simulation is run, for each time step (defined by the user) the software iteratively solves the equations of all the components and provides the achieved results in an output file.

Air-to-water heat pumps can be modelled in TRNSYS by means of Type 917 or Type 941, which are not directly available from the standard component library, but from the TESS component library.

Type 917 computes the change in humidity across the air side of the heat pump, while in Type 917 the humidity effects are ignored. In this work the heat pump defrost cycles are not taken into account (see Section 6.2) and this subsection is focused on the TRNSYS Type 941 (Ref. [32]). Figure 2.8 shows the Type 941 general information from the component proforma file, that is the standard method for documenting a component model.

Figure 2.8: TRNSYS Type 941 characteristics from the component proforma.

Type 941 is based on user supplied files containing manufacturer data of the heat pump power delivered and used, as functions of the temperature of the external air and of the

water stream entering the heat pump. A file contains the cooling performance data and another file contains the heating performance data. The required data can be obtained from the catalog performance data files typically provided by manufacturers in tabular form. In both performance files, the values of power delivered and used by the heat pump are normalized to the rated condition (set by the user). This implies that, for given outdoor air and water stream temperatures, the provided value of heat pump power is dimensionless, because it is divided by the power of the device at its rated condition. By normalizing the data, the process of creating the performance files is time consuming, but saves time when the simulated heat pump is changed with a different sized unit, as only the rated parameters must usually be adjusted (on a normalized basis, a heat pump performance is not heavily dependent upon its size).

The rated power used by the device and the corresponding normalized values in the data files must contain the compressor power and the outdoor blower fan power but must not contain the auxiliary heater power.

In the performance files, the tabulated values of entering water temperature (in °C) must appear on the first row and the tabulated values of external air temperature (in °C) must appear on the second line. The normalized values of heat pump performance must then appear on the following lines for each combination of provided air and water temperatures. Any text following an exclamation point (!) on a line is interpreted as a comment and is ignored by TRNSYS. Figure 2.9 shows an example of input file provided by the software for a heat pump in heating mode.

```
25      30      35      40      45      50              !T_water_in
2.2     7.2     12.2    15      20                      !T_air_in
0.759   0.787                                           !Fraction capacity and power at T_air = 2.2    deg. C and T_water_in = 25
1.080   0.868                                           !Fraction capacity and power at T_air = 7.2    deg. C and T_water_in = 25
1.137   0.843                                           !Fraction capacity and power at T_air = 12.2   deg. C and T_water_in = 25
1.233   0.843                                           !Fraction capacity and power at T_air = 15     deg. C and T_water_in = 25
1.403   0.844                                           !Fraction capacity and power at T_air = 20     deg. C and T_water_in = 25
0.737   0.860                                           !Fraction capacity and power at T_air = 2.2    deg. C and T_water_in = 30
1.048   0.938                                           !Fraction capacity and power at T_air = 7.2    deg. C and T_water_in = 30
1.106   0.923                                           !Fraction capacity and power at T_air = 12.2   deg. C and T_water_in = 30
1.199   0.924                                           !Fraction capacity and power at T_air = 15     deg. C and T_water_in = 30
1.359   0.924                                           !Fraction capacity and power at T_air = 20     deg. C and T_water_in = 30
0.714   0.944                                           !Fraction capacity and power at T_air = 2.2    deg. C and T_water_in = 35
1.017   1.044                                           !Fraction capacity and power at T_air = 7.2    deg. C and T_water_in = 35
1.075   1.016                                           !Fraction capacity and power at T_air = 12.2   deg. C and T_water_in = 35
1.165   1.017                                           !Fraction capacity and power at T_air = 15     deg. C and T_water_in = 35
1.314   1.018                                           !Fraction capacity and power at T_air = 20     deg. C and T_water_in = 35
0.692   1.027                                           !Fraction capacity and power at T_air = 2.2    deg. C and T_water_in = 40
0.986   1.136                                           !Fraction capacity and power at T_air = 7.2    deg. C and T_water_in = 40
1.043   1.108                                           !Fraction capacity and power at T_air = 12.2   deg. C and T_water_in = 40
1.131   1.109                                           !Fraction capacity and power at T_air = 15     deg. C and T_water_in = 40
1.269   1.112                                           !Fraction capacity and power at T_air = 20     deg. C and T_water_in = 40
0.670   1.132                                           !Fraction capacity and power at T_air = 2.2    deg. C and T_water_in = 45
0.955   1.255                                           !Fraction capacity and power at T_air = 7.2    deg. C and T_water_in = 45
1.012   1.224                                           !Fraction capacity and power at T_air = 12.2   deg. C and T_water_in = 45
1.097   1.226                                           !Fraction capacity and power at T_air = 15     deg. C and T_water_in = 45
1.224   1.229                                           !Fraction capacity and power at T_air = 20     deg. C and T_water_in = 45
0.648   1.249                                           !Fraction capacity and power at T_air = 2.2    deg. C and T_water_in = 50
0.923   1.385                                           !Fraction capacity and power at T_air = 7.2    deg. C and T_water_in = 50
0.981   1.352                                           !Fraction capacity and power at T_air = 12.2   deg. C and T_water_in = 50
1.062   1.355                                           !Fraction capacity and power at T_air = 15     deg. C and T_water_in = 50
1.180   1.359                                           !Fraction capacity and power at T_air = 20     deg. C and T_water_in = 50
```

Figure 2.9: Example of heating performance file for Type 941.

The number (minimum 2 and maximum 10) of specified values of external air and water inlet temperature in the data files must coincide with the corresponding parameter in the component's proforma.

Type 941 linearly interpolates among the performance points as function of the hourly values of outdoor air and inlet water temperature. The component does not extrapolate beyond the data range provided, so, if values outside the data range are provided, the maximum or minimum heat pump performance values are returned.

The heat pump conditions the primary water stream, by absorbing energy from (heating mode) or rejecting energy to (cooling mode) an air-to-refrigerant heat exchanger. The heat pump can be equipped with an optional desuperheater, that can be used to heat a secondary water stream such as a domestic hot water service. To disable the desuperheater, it suffices to set to zero its inlet flow rate (an input of Type 941). To use it, the TRNSYS user has to provide the conditions of the water stream entering the desuperheater and must specify a heat transfer coefficient between the refrigerant and the water stream, both for heating mode ($U_{despr,h}$) and cooling mode ($U_{despr,c}$).

In cooling mode, the desuperheater recovers a part of the rejected energy. In heating mode, it causes the heat pump to absorb the electric energy required both for space heating and for domestic hot water production at the same time.

If the heating control signal of Type 941 is on (equal to or greater than 0.5), then the component calls the TRNSYS data interpolation routine to determine the power supplied and used by the heat pump in heating mode as functions of the external air temperature and of the water inlet temperature, by reading the data of the heating performance file. Next, the model calculates the amount $P_{HP,d}$ of the total capacity P_{HP} used to heat the secondary water stream (DHW stream) and the resulting DHW outlet temperature, $T_{w,out,DHW}$:

$$P_{HP,d} = U_{despr,h} \left(T_{despr} - T_{w,in,DHW} \right) , \qquad (2.16)$$

$$T_{w,out,DHW} = T_{w,in,DHW} + \frac{P_{HP,d}}{\dot{m}_{DHW} c_{p,w}} . \qquad (2.17)$$

T_{despr} is the temperature of the refrigerant entering the desuperheater, $T_{w,in,DHW}$ and $\dot{m}_{DHW}$ are the DHW stream inlet temperature and mass flow rate and $c_{p,w}$ is the water specific heat capacity at constant pressure.

The electric power used by the compressor, P_{compr}, is computed by Type 941 as the power read from the data file, $P_{HP,us}$, minus the blower power (which is entered as a model parameter).

The power released to the condenser, P_{cond}, and the power absorbed by the evaporator, P_{evap}, are then:

$$P_{cond} = P_{HP} - P_{HP,d} \ , \tag{2.18}$$

$$P_{evap} = P_{HP} - P_{compr} \ . \tag{2.19}$$

If the heating capacity of the heat pump is insufficient at some time during the simulation, it is possible to specify in Type 941 an additional heating capacity, which is handled by the Type as an electric heater. The auxiliary heating capacity, P_{bk}, is a parameter of Type 941 and its control signal is an input.

If the auxiliary heating control signal is on (its input is equal to or greater than 0.5), the entire capacity of the auxiliary heater is applied to the primary water stream. The primary water stream outlet temperature, $T_{w,out}$, is then:

$$T_{w,out} = T_{w,in} + \frac{P_{cond} + P_{bk}}{\dot{m}_w c_{p,w}} \ , \tag{2.20}$$

where $T_{w,in}$ and $\dot{m}_w$ are the primary water stream inlet temperature and mass flow rate, respectively.

The *COP* of the device, consisting of heat pump and auxiliary heater, is evaluated by Type 941 as:

$$COP = \frac{P_{cond} + P_{bk}}{P_{HP,us} + P_{bk}} \ . \tag{2.21}$$

If the cooling control signal of Type 941 is on, the procedure to determine the heat pump cooling performance is the same as the procedure for the heating performance. The heat pump is able to use a desuperheater to heat a secondary water stream (typically for domestic hot water production) while cooling the primary water stream (heat recovery mode). The values of the heat transfer coefficient between the refrigerant and the water stream and the temperature of the refrigerant entering the desuperheater can be different from the values used in heating mode.

The energy rejected by the condenser and the energy absorbed by the evaporator in cooling mode are:

$$P_{cond} = P_{HP} + P_{compr} - P_{HP,d} \ , \tag{2.22}$$

$$P_{evap} = P_{HP} \ . \tag{2.23}$$

31

The outlet temperature of the primary water stream is:

$$T_{w,out} = T_{w,in} - \frac{P_{evap}}{\dot{m}_w c_{p,w}}$$

(2.24)

and the *EER* of the heat pump is:

$$EER = \frac{P_{evap}}{P_{HP,us}} \quad .$$

(2.25)

In conclusion, the TRNSYS Type 941 can be used to simulate the dynamic behavior of air-to-water heat pumps, but it has some limitations.

First of all, TRNSYS is not able to simulate directly inverter-driven heat pumps or multi-function heat pumps. The codes presented in this work, on the contrary, employ a specific mathematical procedure for each heat pump typology.

Type 941, moreover, does not accept the building energy need as a direct input: for each time step it evaluates the values of heat pump power and *COP*, or *EER*, as functions of the external air temperature. Instead, the codes developed in this Thesis check automatically the building energy demand and can consequently evaluate the energy delivered and used by the heat pump.

In Type 941 a desuperheater is used to produce domestic hot water, simply assuming that a part of the heat pump capacity (in winter) or of the condensation heat (in summer) is used to heat a secondary DHW stream. TRNSYS has not the possibility of modeling, directly into the pre-defined Type 941, a heat pump performance in DHW mode (or heat recovery mode) different from that in heating mode (or cooling-only mode). It would be possible to implement heat pump performance values specific for DHW production into the performance data file, read by Type 941, in correspondence of a different water inlet temperature. In this way, however, during each hour of the simulation, the heat pump would be able to work only in DHW mode (heat recovery mode) or only in heating mode (cooling-only mode), without taking into account hours with building energy needs both for DHW production and for heating (cooling), which are usually the majority. On the contrary, the codes described in the following chapters can take into account, for each time step, different simultaneous energy needs of the building, such as heating and DHW production or cooling and DHW production; the corresponding values of heat pump power and *COP*, or *EER*, are then returned by the codes.

If the auxiliary heating control signal of the TRNSYS Type 941 is on, then the entire capacity of the auxiliary heater is indiscriminately applied to the primary water stream, yielding a

variation of the primary water stream outlet temperature. In the simulation codes subject of this work the outlet temperature of the water heated by the heat pump is fixed and the building energy need not covered by the heat pump is evaluated and supplied by the back-up system. In the codes presented in this work, moreover, the auxiliary heater capacity can be used not only for heating, but also for DHW production; furthermore, the auxiliary device can be either electric heaters or a gas boiler.

Finally, no *COP* (or *EER*) corrections for on-off cycles are considered by Type 941. In the codes developed in this Thesis the correction factors indicated by the standards [10], [11] are employed.

The TRNSYS Type 941 will be used to validate in some simple cases the dynamic codes developed in this Thesis for the simulation of air-to-water heat pumps (see Section 4.4).

2.4 DESIGN AND SIMULATION OF GROUND-COUPLED HEAT PUMP SYSTEMS

The design of Ground-Coupled Heat Pump (GCHP) systems is usually divided in two parts: the design of the Borehole Heat Exchanger (BHE) field; the choice of the heat pump and the evaluation of its seasonal performance.

Most design methods of BHE fields in the literature are based on the evaluation of the temperature distribution in the borehole field, as a function of time. In these studies, groundwater movement is usually neglected and the ground is considered as an infinite solid medium with constant thermo-physical properties. The problem to be studied is that of conduction in the ground, which is a problem of transient three dimensional conduction, for which approximate solutions, either analytical or numerical, are usually employed.

Analytical solutions are normally available with reference to the following classification: Infinite Line Source (ILS) models, Infinite Cylindrical Source (ICS) models, Finite Line Source (FLS) models. In these models, a borehole heat exchanger is considered either as an infinitely long line, as an infinitely long cylinder or as a line with finite length, respectively.

Solutions of the temperature distribution are often presented in dimensionless form. Let us introduce the following dimensionless form of the radial coordinate *r*, vertical coordinate *z*, time *t*, and temperature *T*:

$$r^* = \frac{r}{D} \ , \tag{2.26}$$

$$z^* = \frac{z}{D} \ , \tag{2.27}$$

$$t^* = \frac{\alpha_g t}{D^2} \ , \tag{2.28}$$

$$T^* = k_g \frac{T - T_g}{q_0} \ , \tag{2.29}$$

where D is the BHE diameter, α_g, k_g and T_g are the ground thermal diffusivity, thermal conductivity and undisturbed temperature, respectively, and q_0 is a reference heat flux per unit length.

As mentioned e.g. by Do and Haberl [33], Philippe et al. [34] and Yang et al. [35], the ILS model is known also as "Kelvin's line source theory", since the earliest application of this approach was developed by Lord Kelvin. The ILS solution for a BHE subjected to a constant heat transfer rate per unit length (q) was deduced by Carslaw and Jaeger [36] and is reported e.g. by Fossa [37], Philippe et al. [34] and Yang et al. [35]. With reference to the dimensionless quantities of Eqs. (2.26)-(2.29), the solution has the expression:

$$T^*(r^*, t^*) = \frac{q}{4\pi q_0} \int_{\frac{r^{*2}}{4t^*}}^{\infty} \frac{e^{-u}}{u} \, du \ . \tag{2.30}$$

Approximate solutions of Eq. (2.30), which contains an exponential integral, are employed in thermal response tests to evaluate the ground thermo-physical properties.

The ICS solution was obtained by Carslaw and Jaeger [36] and is reported, for instance, by Zanchini and Pulvirenti [38]. In dimensionless form, with reference to Eqs. (2.26)-(2.29), it is:

$$T^*(r^*, t^*) = \frac{1}{\pi^2} \int_0^{+\infty} \left[\frac{Y_0(2r^* u) J_1(u) - J_0(2r^* u) Y_1(u)}{J_1^2(u) + Y_1^2(u)} \ \frac{1 - e^{-4t^* u^2}}{u^2} \right] du \ , \tag{2.31}$$

where J_n is the Bessel function of the first kind with order n and Y_n is the Bessel function of the second kind with order n.

The ICS solution by Carslaw and Jaeger [36] is employed by Kavanaugh and Rafferty [39] in the design method for BHE fields recommended by ASHRAE [40] (see Subsection 2.4.1).

The analytical solution of the FLS model was determined by Claesson and Eskilson [41], [42] and is reported e.g. by Zanchini and Lazzari [9] in dimensionless form, with the dimensionless quantities defined in Eqs. (2.26)-(2.29):

$$T^*(r^*, z^*, t^*) = \frac{1}{4\pi} \int_0^{L^*} \left\{ \frac{erfc\left[0.5\sqrt{r^{*2} + \left(z^* - u\right)^2} / \sqrt{t^*} \right]}{\sqrt{r^{*2} + \left(z^* - u\right)^2}} - \frac{erfc\left[0.5\sqrt{r^{*2} + \left(z^* + u\right)^2} / \sqrt{t^*} \right]}{\sqrt{r^{*2} + \left(z^* + u\right)^2}} \right\} du \ , \tag{2.32}$$

where $L^* = L/D$ is the dimensionless BHE length and *erfc* is the complementary error function. Zeng et al. [43] pointed out that Eq. (2.32) evaluated at the middle of the length of the BHE yields an overestimation (up to 5 %) of the mean temperature field at the BHE surface. The authors recommended to use the value given by that expression when averaged along the BHE length, which is called *g-function*. The *g-functions* are time-dependent expressions of the dimensionless temperature, averaged along the BHE length, due to a uniform and constant heat load which starts at the time instant $t = 0$. The *g-function* expression based on the FLS model, i.e. on Eq. (2.32), is given by:

$$g_{FLS}(r^*,t^*) = \frac{1}{4\pi L^*} \int_0^{L^*} \int_0^{L^*} \left\{ \frac{erfc\left[0.5\sqrt{r^{*2} + (z^* - u)^2} / \sqrt{t^*}\right]}{\sqrt{r^{*2} + (z^* - u)^2}} - \frac{erfc\left[0.5\sqrt{r^{*2} + (z^* + u)^2} / \sqrt{t^*}\right]}{\sqrt{r^{*2} + (z^* + u)^2}} \right\} du\, dz^* \quad ,(2.33)$$

A simplified form of Eq. (2.33) was proposed by Bandos et al. [44]. By employing the dimensionless quantities of Eqs. (2.26)-(2.29), the solution of Bandos et al. [44] is:

$$g_{FLS}(r^*,t^*) = \frac{1}{4\pi} \int_{\frac{r^*}{2\sqrt{t^*}}}^{\infty} \left[4erf(2L^*u) - 2erf(4L^*u) - \frac{3 + e^{-16L^{*2}u^2} - 4e^{-4L^{*2}u^2}}{2\sqrt{\pi}L^*u} \right] \frac{e^{-u^2}}{u}\, du \quad , \quad (2.34)$$

where *erf* is the error function. Bandos et al. [44], moreover, analyzed the effects of the geothermal gradient and of the surface temperature oscillations.

Another simplified form of Eq. (2.33) was proposed by Lamarche and Beauchamp [45].

By employing the results obtained by Bandos et al. [44], Fossa [37], [46] proposed simple approximate expressions for g_{FLS}, which require low computational time and use empirical coefficients, determined through the analysis of different BHE fields.

Accurate analytical expressions of the *g-functions* were determined by Zanchini and Lazzari [9] for fields of BHEs with different values of length and diameter (see Subsection 2.4.2). These *g-functions* are based on the Finite Cylindrical Source (FCS) model and are expressed in the form of polynomial functions of the logarithm of the dimensionless time.

Numerical simulations of BHE fields can be performed by means of software like Earth Energy Designer (EED), which is entirely dedicated to borehole heat exchangers (see Subsection 2.4.3), or software like EnergyPlus or TRNSYS, which can perform energy analysis of the whole building-plant system.

EnergyPlus simulates BHE fields by employing the *g-function* model developed by Eskilson [41] by means of an enhanced algorithm by Yavuzturk and Spitler [47]. As reported

by Yang et al. [35], this algorithm is based on two-dimensional, fully implicit finite volume calculations and the numerical results are expressed in terms of short time-step response factors (*g-functions*).

In order to simulate BHE fields, the software TRNSYS employs the Duct STorage (DST) model developed by Hellström [48], which was adapted to be run on TRNSYS by Hellstrom et al. [49]. As reported by Fossa and Minchio [50], the DST model employs spatial superposition of three basic solutions of the conduction equation: the global temperature difference between the heat store volume and the undisturbed ground temperature, calculated numerically; the local temperature response inside the heat store volume, calculated numerically; the additional temperature difference which accounts for the local steady heat flux, calculated analytically.

Despite its complicated structure, the DST model is computationally efficient, but it is developed for compact and regular dispositions of BHEs and does not provide precise results for in line boreholes and unbalanced heat loads, as evidenced by Fossa and Minchio [50].

In order to simulate the whole GCHP system, the TRNSYS user has to couple the Type of the BHE field with that of the heat pump, which, however, is not able to take into account inverter-driven heat pumps.

2.4.1 The ASHRAE method

The American Society of Heating, Refrigerating and Air-Conditioning Engineers, ASHRAE, recommends a simple design method for BHE fields (Ref. [40]). The method was developed by Kavanaugh and Rafferty [39] and is based on the solution of the equation for the heat transfer from an infinitely long cylinder placed in a homogeneous solid medium, determined by Carlslaw and Jaeger [36].

By analogy with the stationary case, one has:

$$T_g - T_{f,m} = R\, q = R\, \frac{Q}{L_{tot}} \quad . \tag{2.35}$$

In Eq. (2.35), T_g is the undisturbed ground temperature, $T_{f,m}$ is the BHE fluid mean temperature, R is the thermal resistance per unit BHE length and q is the thermal load per unit BHE length, given by the ratio between the thermal load (Q) and the total length of the boreholes (L_{tot}).

From Eq. (2.35), one can find:

$$L_{tot} = \frac{Q\, R}{T_g - T_{f,m}} \quad . \tag{2.36}$$

The thermal resistance R must take into account both the BHE internal resistance and the (equivalent) ground thermal resistance, which depends on the duration of the considered thermal load. The method considers the superposition of the effects of three heat pulses, each with a constant power, which account for seasonal heat imbalances, monthly average heat load during the design month, and peak heat pulse during the design day, respectively. Two different expressions are suggested to determine the value of L_{tot}, one valid if the design is based on the building heating loads (Eq. (2.37)) and one valid if the design is based on the building cooling loads (Eq. (2.38)):

$$L_{tot,h} = \frac{P_{yly}R_{g,yly} + \left(P_{des,h} - P_{us,h}\right)\left(R_{BHE} + PLF_{mly}R_{g,mly} + R_{g,dly}F_{sc}\right)}{T_g - T_{f,m} - T_p} \ , \tag{2.37}$$

$$L_{tot,c} = \frac{P_{yly}R_{g,yly} + \left(P_{des,c} - P_{us,c}\right)\left(R_{BHE} + PLF_{mly}R_{g,mly} + R_{g,dly}F_{sc}\right)}{T_g - T_{f,m} - T_p} \ . \tag{2.38}$$

In Eqs. (2.37), (2.38), P_{yly} is the mean yearly value of the thermal power exchanged between BHEs and ground (obtained by considering as positive the energy drawn from the ground for heating and as negative the energy released to the ground for cooling); P_{des} is the building design load (positive for heating, $P_{des,h}$, negative for cooling, $P_{des,c}$); P_{us} is the electric power used by the heat pump and the circulation pumps at P_{des}; R_{BHE} is the BHE thermal resistance; $R_{g,yly}$ is the ground thermal resistance for (pluri-)annual heat pulses; $R_{g,mly}$ is the ground thermal resistance for monthly heat pulses; $R_{g,dly}$ is the ground thermal resistance for daily (actually of 6 hours) heat pulses; PLF_{mly} is the partial load factor of the design month; F_{sc} is the short circuit factor (due to the non-perfect thermal insulation between a BHE supply and return) and T_p is the temperature penalty for thermal interference between BHEs (positive for heating and negative for cooling).

From Eqs. (2.37), (2.38) one can note that, the higher the difference between T_g and $T_{f,m}$, the lower the resultant total BHE length.

The total length of the boreholes should be the greater between $L_{tot,h}$ and $L_{tot,c}$; if $L_{tot,c}$ is greater than $L_{tot,h}$, however, it is possible to install a total BHE length equal to $L_{tot,h}$ and couple a cooling tower, thus obtaining a balance of the seasonal loads.

To evaluate $R_{g,yly}$, $R_{g,mly}$ and $R_{g,dly}$, three heat pulses are considered, one of 10 years (3650 days), one of 1 month (30 days) and one of 6 hours (0.25 days). Three corresponding time instants, t, are defined as:

$$t_{dly} = 6 \text{ hours} = 0.25 \text{ days}$$
$$t_{mly} = 1 \text{ month} + 6 \text{ hours} = 30.25 \text{ days} \tag{2.39}$$
$$t_{yly} = 10 \text{ years} + 1 \text{ month} + 6 \text{ hours} = 3680.25 \text{ days}$$

Time (t) is non-dimensionalized by means of the Fourier number, Fo:

$$Fo = \frac{4\alpha_g t}{D_{BHE}^2} \ , \tag{2.40}$$

where α_g is the ground thermal diffusivity and D_{BHE} is the borehole diameter.

The three Fourier numbers corresponding to the three time instants of Eq. (2.39) are:

$$Fo_{dly} = \frac{4\alpha_g t_{dly}}{D_{BHE}^2} ; \qquad Fo_{mly} = \frac{4\alpha_g t_{mly}}{D_{BHE}^2} ; \qquad Fo_{yly} = \frac{4\alpha_g t_{yly}}{D_{BHE}^2} \ . \tag{2.41}$$

For each Fourier number, the corresponding value of the G factor is evaluated. The G factor is the dimensionless temperature at the BHE-ground interface due to a constant heat load per unit length q_0, defined as:

$$G = \frac{\left(T_{BHE-g} - T_g\right)k_g}{q_0} \ , \tag{2.42}$$

where T_{BHE-g} is the temperature at the BHE-ground interface and k_g is the ground thermal conductivity.

ASHRAE gives the correspondence between Fo and G through a table and a semi-logarithmic diagram, reported in Figure 2.10.
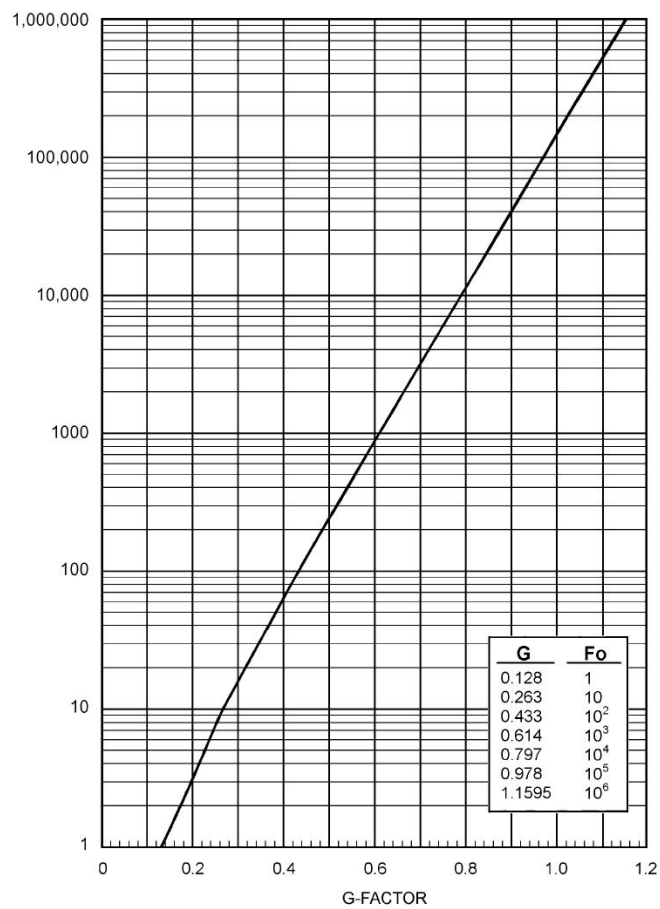
Figure 2.10: Fourier – G factor graph from Ref. [39].

By interpolating the values of the table it is possible to find a polynomial expression of *G* as a function of the logarithm with base 10 of *Fo*, which is given by:

$$G = 0.000339\left[\log(Fo)\right]^4 - 0.005388\left[\log(Fo)\right]^3 + 0.030407\left[\log(Fo)\right]^2 + 0.110234\log(Fo) + 0.127886 \quad . \quad (2.43)$$

A plot of Eq. (2.43) is reported in Figure 2.11.
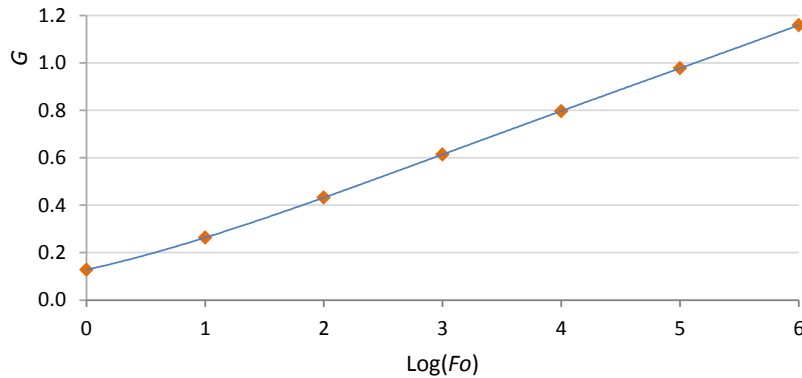
Figure 2.11: *G* factor values and fourth order polynomial interpolating function.

Once obtained the three values of the *G* factor (G_{yly}, G_{mly}, G_{dly}) corresponding to the three Fourier numbers (Fo_{yly}, Fo_{mly}, Fo_{dly}, respectively), the ground thermal resistances $R_{g,yly}$, $R_{g,mly}$ and $R_{g,dly}$ are evaluated as:

$$R_{g,yly} = \frac{G_{yly} - G_m}{k_g}; \qquad R_{g,mly} = \frac{G_{mly} - G_{dly}}{k_g}; \qquad R_{g,dly} = \frac{G_{dly}}{k_g} \ . \qquad (2.44)$$

The decrease in borehole performance due to short-circuiting heat exchange between the upward and downward flowing legs of the U-tube is taken into account in Eqs. (2.37), (2.38) by means of the short-circuiting factor, F_{sc}. The values of F_{sc} are given in Table 2.9 as functions of the fluid flow rate and of the number of BHE in series.

Table 2.9: Short circuit factor values.

BHE in series	Fluid flow rate [cm^3/(s kW)]	
	36	54
1	1.06	1.04
2	1.03	1.02
3	1.02	1.01

Usually U-tubes are piped in parallel, but in the case of two or three loops piped in series the short-circuiting heat exchange is reduced and the corresponding values of F_{sc} in Table 2.9 are smaller.

The values of temperature penalty for thermal interference between BHEs (T_p) are given by ASHRAE as functions of the distance between adjacent BHEs and of the equivalent full load hours for heating/cooling (see Tables 2.10, 2.11).

Table 2.10: Temperature penalty T_p for 10 × 10 BHE field after 10 years.

Equivalent full load hours heating/cooling	Distance between adjacent BHEs [m]	T_p [°C]
1000/500	4.6	Negligible
1000/1000	4.6	2.6
	6.1	1.3
500/1000	4.6	4.2
	6.1	2.2
	4.6	7.1
500/1500	6.1	3.7
	7.6	1.9
	4.6	Not advisable
0/2000	6.1	5.8
	7.6	3.1

Table 2.11: T_p correction factors for other BHE grid patterns.

1 × 10 grid	2 × 10 grid	5 × 5 grid	20 × 20 grid
0.36	0.45	0.75	1.14

Typical distances between adjacent BHEs are from 6 to 10 m. The farther the BHEs, the lower the thermal interferences (but the bigger the occupied area). Under equal boreholes separation, an inline grid has less interference than a square or rectangular grid.

The values of T_p provided by ASHRAE are not completely reliable: for instance, considering the temperature penalty as negligible in the first row of Table 2.10 seems optimistic. More reliable values of T_p after 10 years are given by Bernier et al. [51] in dimensionless form (T_p^*, defined in Eq. (2.45)), for several BHE field geometries and ground properties (see Table 2.12).

$$T_p^* = \frac{T_p 2\pi k_g}{q} \quad .$$
(2.45)

Table 2.12: Dimensionless temperature penalty $T_p{}^*$ after 10 years from Ref [51].

Grid	Distance between adjacent BHEs [m]	α_g [m²/s]	
		1.03×10^{-6}	6.481×10^{-7}
1 × 8	5	5.1	4.2
	6	4.4	3.6
	7	3.8	3.0
3 × 8	5	14.9	12.3
	6	12.8	10.4
	7	10.9	8.7
5 × 5	5	16.7	13.7
	6	14.3	11.6
	7	12.1	9.7
10 × 10	5	30.3	23.3
	6	25.2	19.1
	7	20.7	15.5

The partial load factor of the design month, PLF_{mly}, appearing in Eqs. (2.37), (2.38), is defined as:

$$PLF_{mly} = \frac{P_{b,m,dly}}{P_{b,max,dly}} \frac{\text{days of occupancy}}{\text{days of the month}} \; , \qquad (2.46)$$

where $P_{b,m,dly}$ is the mean building load during a typical day of the design month (for the heating or cooling season) and $P_{b,max,dly}$ is the corresponding peak load. To evaluate PLF_{mly}, the building load profile during a typical day of the design month must be known. Figure 2.12 shows an example of load profile for a residential building from Ref. [52], where the peak load is almost twice the mean daily load.
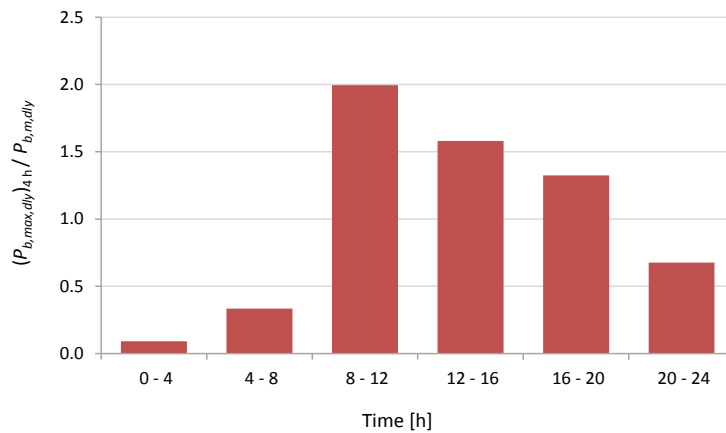
Figure 2.12: Ratio between the building thermal load averaged over 4 hours and the mean daily load, during the day with maximum heating load, for a residential building in Bologna (Italy), with indoor temperature 20 °C by day and 18 °C by night (figure from Ref. [52]).

The ASHRAE method is limited to 10 years of operation and, thus, does not guarantee the long-term sustainability for several decades of borehole fields with unbalanced seasonal thermal loads.

2.4.2   A recent study for ground-coupled heat pump systems design through the *g-functions*

Recently, Zanchini and Lazzari [9] presented a method, based on the *g-functions*, to evaluate the long-term temperature distribution in a field of long borehole heat exchangers subjected to a monthly averaged heat flux, under the assumption that the effects of the groundwater flow are negligible. In Ref. [9] each BHE is considered as a finite cylindrical heat source (FCS model), with diameter D and length L, subjected to a uniform heat load per unit length, q, which is constant during each month but varies during the year. The heat load q is considered negative during winter (heat extracted from the ground) and positive during summer (heat released to the ground).

In a broad range of values of the dimensionless time, a *g-function* is determined for each dimensionless BHE length, $L^* = L/D$, and each dimensionless radial distance from the BHE axis, $r^* = r/D$, by means of finite element simulations, and is written in polynomial form by means of accurate interpolations.

The authors assumed that the ground is a semi-infinite solid medium with constant thermo-physical properties (undisturbed temperature T_g, thermal diffusivity α_g, thermal conductivity k_g), without groundwater movement.

On account of the axial symmetry, the temperature field in the ground is a function of the radial coordinate *r*, the vertical coordinate *z*, and time *t*. The authors adopted a cylindrical reference frame centered in the BHE axis and a cylindrical computational domain around the BHE, with an external dimensionless radius equal to 2500 and a dimensionless depth equal to L^* + 2000 (sizes that ensured results independent of the domain extension).

At the initial time instant, *t* = 0, the temperature *T* is uniform and equal to T_g. For *t* > 0, a uniform heat flux per unit area, *q'*, is applied to the boundary surface between BHE and ground,

$$q' = \frac{q_0}{\pi D} F(t) \; , \tag{2.47}$$

where q_0 is the magnitude of the highest (lowest if negative) heat flux per unit length applied to the BHE-ground interface and $F(t)$ is a dimensionless function of time, with values between -1 and 1. Negative values of $F(t)$ correspond to winter operation, positive values to summer operation.

The differential equation to be solved is

$$\frac{\partial T}{\partial t} = \alpha_g \nabla^2 T \; . \tag{2.48}$$

The lateral and bottom boundaries of the computational domain are considered as adiabatic. The upper boundary (ground surface, *z* = 0) is assumed to be isothermal, with constant temperature equal to T_g,

$$T(r,0,t) = T_g \; . \tag{2.49}$$

The effects of the external air temperature changes are neglected, because long BHEs are considered.

The boundary condition at the BHE-ground interface is:

$$-k_g \left(\nabla T \cdot \mathbf{n} \right) \Big|_{r=D/2} = \frac{q_0}{\pi D} F(t) \; , \tag{2.50}$$

where **n** is the outward unit normal.

By considering the dimensionless operator $\nabla^* = D \nabla$ and the dimensionless quantities of Eqs. (2.26)-(2.29), one can rewrite Eqs. (2.48)-(2.50) in the following dimensionless form:

$$\frac{\partial T^*}{\partial t^*} = \nabla^{*2} T^* \; , \tag{2.51}$$

$$T^*(r^*,0,t^*)=0 \ , \tag{2.52}$$

$$-\left(\nabla^*T^*\cdot\mathbf{n}\right)\Big|_{r^*=1/2}=\frac{1}{\pi}F(t^*) \ . \tag{2.53}$$

The dimensionless initial condition is $T^* = 0$ for the whole computational domain.

$F(t^*)$ is a periodic function of the dimensionless time, with period one year, constant during each month and stepwise variable. The authors assumed that all months have the same duration (730 hours) and denoted by t_1^* the dimensionless duration of each month (which depends on D and α_g). Considering a period of n months, $F(t^*)$ can thus be expressed as:

$$F(t^*)=\sum_{i=0}^{n-1}A_i\left\{H\left[t^*-it_1^*\right]-H\left[t^*-(i+1)t_1^*\right]\right\} \ , \tag{2.54}$$

where H is the Heaviside unit step function, A_i is the ratio between the i-th value of q and q_0, and the following recursive relation holds:

$$A_{i+12}=A_i \ . \tag{2.55}$$

Since Eqs. (2.51)-(2.53) represent a system of linear equations, the dimensionless temperature T_m^*, averaged along the BHE length, produced at r^* by a BHE subjected to the dimensionless heat load given by Eq. (2.54), can be expressed as:

$$T_m^*(r^*,t^*)=\sum_{i=0}^{n-1}A_i\left\{g\left[r^*,t^*-it_1^*\right]-g\left[r^*,t^*-(i+1)t_1^*\right]\right\} \tag{2.56}$$

where $g(r^*,t^*)$ is the *g-function* at the dimensionless distance r^* and dimensionless time instant t^*.

The average dimensionless temperature at the surface of any borehole of the field can be evaluated as the sum of the average dimensionless temperature produced by the BHE itself on its surface, and of those produced by the other BHEs of the field at their dimensionless distances from its axis (superposition of effects in space).

The dimensionless governing equations (2.51)-(2.53), with the initial condition $T^* = 0$, were solved by the authors by means of finite element simulations with the software COMSOL Multiphysics. An unstructured mesh of triangular elements was adopted, with finer size near the BHE and coarser size towards the boundaries. A direct linear system solver was employed, based on the Unsymmetric MultiFrontal method (UMFPACK) and a backward differentiation formula with an interpolating polynomial of the fifth order.

The authors plotted each *g-function* versus $x = \log_{10}(t^*)$. The numerical results were interpolated in a very broad range of values of the dimensionless time by means of two

polynomial functions of x, the first valid for low values of x, and the second for high values of x, as reported in the following equation:

$$
\begin{aligned}
g(x) &= 0 && if \;\; -4 \le x < x_0 \\
g(x) &= a_6\, x^6 + a_5\, x^5 + a_4\, x^4 + a_3\, x^3 + a_2\, x^2 + a_1\, x + a_0 && if \;\; x_0 \le x < x_1 \\
g(x) &= b_6\, x^6 + b_5\, x^5 + b_4\, x^4 + b_3\, x^3 + b_2\, x^2 + b_1\, x + b_0 && if \;\; x_1 \le x < 6
\end{aligned} \qquad (2.57)
$$

For $D = 10$ cm and $\alpha_g = 10^{-6}$ m^2/s, the considered interval of time ranges from 1 s to 10^{10} s (about 317 years).

The authors evaluated the values of the constants $a_0,\dots, a_6$; $b_0,\dots, b_6$; x_0; x_1 in correspondence of several values of L^* (2000, 1400, 1000, 700 and, in Ref. [53], 500) and of r^* (0.5, 30, 40, 60, 80, 120, 170, 230, 300, 400, 600).

Table 2.13 reports the *g-function* constants for the case of $L^* = 1000$ and Figure 2.13 shows the plots of the *g-functions* at the BHE surface ($r^* = 0.5$) for $L^* = 2000, 1400, 1000$ and 700.

Table 2.13: Values of the constants x_0, a_6, a_5, a_4, a_3, a_2, a_1, a_0, and x_1, b_6, b_5, b_4, b_3, b_2, b_1, b_0, for $L^* = 1000$.

r^*	x_0	a_6	a_5	a_4	a_3	a_2	a_1	a_0
0.5	-3.72	0.000072	0.000495	-0.000492	-0.006093	0.021673	0.148764	0.195869
30	1.406	0.022977	-0.311470	1.715928	-4.894902	7.639513	-6.204900	2.055385
40	1.732	0.012103	-0.187776	1.177887	-3.808313	6.712151	-6.139983	2.286260
60	2.1	0.012134	-0.213351	1.526737	-5.677042	11.585585	-12.334074	5.364861
80	2.408	0.013381	-0.250674	1.919240	-7.669695	16.877065	-19.409867	9.124934
120	2.812	---	---	-0.028220	0.398616	-2.045276	4.560451	-3.750200
170	3.088	---	---	-0.02873	0.437099	-2.431959	5.904104	-5.299886
230	3.37	---	---	-0.027941	0.451622	-2.681060	6.964124	-6.701557
300	3.588	---	---	-0.028345	0.480094	-2.998636	8.217026	-8.357324
400	3.83	---	---	-0.029194	0.518305	-3.406821	9.851624	-10.594886
600	4.184	---	---	-0.020485	0.389076	-2.739891	8.496694	-9.805977

r^*	x_1	b_6	b_5	b_4	b_3	b_2	b_1	b_0
0.5	1.4	0.0002093	-0.0044515	0.03708526	-0.158007	0.3625348	0.2443693	0.37623
30	3.0	---	0.001317	-0.027382	0.213648	-0.791010	1.546621	-1.304216
40	3.62	---	0.002860	-0.063489	0.547974	-2.320022	4.995565	-4.412737
60	3.92	---	---	0.008711	-0.178599	1.323852	-4.114005	4.614348
80	4.0	---	---	0.009565	-0.196992	1.472420	-4.647859	5.2934296
120	4.17	---	---	0.010329	-0.215061	1.632139	-5.273427	6.15343
170	4.4	---	---	0.010620	-0.224153	1.730175	-5.720348	6.84812
230	4.8	---	---	0.013842	-0.297518	2.356776	-8.100110	10.203761
300	4.92	---	---	0.022198	-0.483624	3.911578	-13.875862	18.227086
400	5.02	---	---	0.026129	-0.574998	4.709802	-16.981824	22.742842
600	5.13	---	---	0.025927	-0.580556	4.849463	-17.884039	24.560770
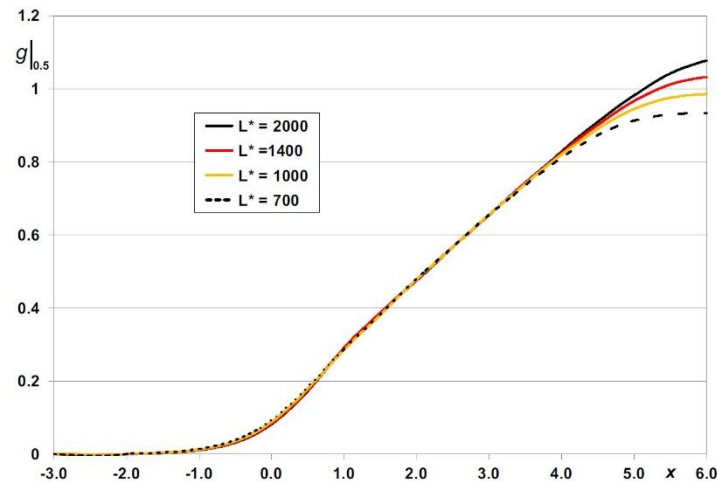
Figure 2.13: Plots of the *g-functions* at $r^* = 0.5$, for $L^* = 2000, 1400, 1000, 700$, figure from Ref. [9].

The discrepancy between the interpolated and the numerical values of the *g-functions* is very low, as shown by Figure 2.14.
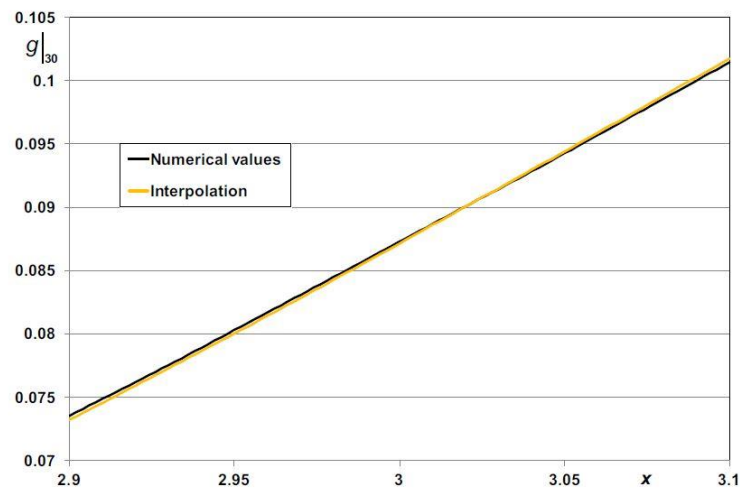
Figure 2.14: Discrepancy between the interpolated and the numerical values of the *g-function* for $L^* = 1000$ and $r^* = 30$, in the neighborhood of $x_1 = 3.0$, from Ref. [9].

With respect to the methods of Refs. [42], [44], [45], the method of Zanchini and Lazzari [9] is much faster in computations, because it is based on *g-functions* expressed in polynomial form. On the other hand, it has the disadvantage of requiring interpolations to obtain *g-functions* for values of r^* and L^* not tabulated (however, the interpolations are fast and precise).

The code for the hourly simulation of GCHP systems presented in Chapter 5 of this Thesis employs the *g-functions* obtained in Ref. [9]. These *g-functions*, as well as those presented in Refs. [37], [41], [44], [45], allow to determine the time evolution at the interface BHE-ground, for each BHE. The time evolution of the working fluid is then obtained by assuming that the heat transfer within the BHE is stationary, and thus employing the BHE thermal resistance R_{BHE}.

New *g-functions*, which consider also the internal structure of the BHE and allow to determine with higher accuracy the time evolution of the working fluid have been presented in a more recent work by Zanchini and Lazzari [53]. The new *g-functions*, however, apply only to double U-tube BHEs with given ratios between tube external diameter and BHE diameter and between tube spacing and BHE diameter.

2.4.3   The software Earth Energy Designer (EED)

Earth Energy Designer (EED) is a commercial software for borehole heat exchanger design (see Figure 2.15), developed by Hellström, Sanner et al. [54], which is able to perform long-term calculations of the temperature profile of the BHE fluid, as a function of the field configuration, ground properties and building thermal loads.
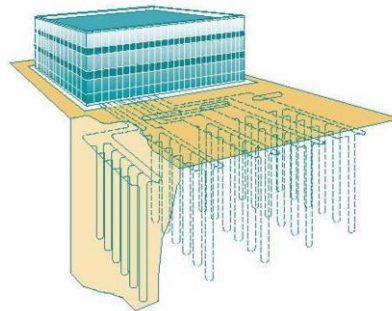
Figure 2.15: Earth Energy Design (EED) desktop.

EED performs simulations on a monthly basis, by employing *g-functions* and the superposition of the effects in space. EED algorithms are derived from modelling and parameter studies performed by Hellström et al. (Refs. [55], [56]). The *g-functions*, which depend on the borehole field geometry and derive from two-dimensional finite-difference numerical simulations, are stored in a data file, which is accessed by the software.

The EED user has to provide input data about: ground parameters, properties of pipe materials and heat carrier fluid, simulation time, monthly average heating and cooling loads (called "base loads"). In addition, an extra pulse for peak heating or cooling loads over several hours can be considered at the end of each month. Databases for some materials properties are directly provided by the software.

The inputs about the ground include the ground thermal conductivity, for which a database according to the type of rock or soil is provided, if no measured data from the site (e.g. from a thermal response test) are available. A recommended value of thermal conductivity and the minimum and maximum values found in the literature are given. The volumetric heat capacity of the ground, the annual average ground surface temperature and the geothermal heat flux are also required. The undisturbed ground temperature for half of the borehole depth is then calculated by the software.

The user has to select the type of borehole heat exchanger among coaxial, single-U pipe, double-U pipe and triple-U pipe. The EED input menu for a double-U pipe borehole heat exchanger is shown in Figure 2.16.

Figure 2.16: EED input data for a double-U pipe borehole heat exchanger.

The borehole grid geometry (e.g. single BHE, in line, rectangular) is chosen from a list of possible configurations, in order to select the adequate *g-functions*. The borehole depth, spacing and diameter are asked and the software checks if the diameter is large enough to house the pipes. The thermal contact resistance between pipe and borehole fill and the grout thermal conductivity are also required, as well as the volumetric flow rate through the pipes, the pipe outer diameter, wall thickness and thermal conductivity and the shank spacing (distance between the centers of the up and down pipes in each "U", see Figure 2.16). The borehole thermal resistance can be either calculated by EED or stated, if it is known e.g. from a thermal response test; the user can choose whether to take into account the internal heat transfer between the up and down flows of individual pipes.

Regarding the heat carrier fluid, thermal conductivity, specific heat capacity, density, viscosity and freezing point are input data.

The inputs for building heating and cooling loads are divided into base load and peak load. As for the base load, EED accepts two input methods: the first one requires the whole annual heating and cooling loads (in MWh), which are distributed to each month by means of a given load profile; the second method requires the heating and cooling load for each month. A separate input value can be entered for the annual building energy need for domestic hot water, which is spread out equally for the whole year by the software.

To switch from the building base loads to the loads required to the BHE field, the software needs a mean value of the Seasonal Performance Factor, *SPF*. The Seasonal Performance Factor is equal to the *SCOP* in the case of heating and DHW production mode, while it is equal to the *SEER* in the case of cooling mode; one *SPF* value for heating, one for DHW production and one for cooling can be provided by the user. The thermal load Q exchanged between BHE and ground is then evaluated by EED for the i-th month as:

$$Q(i) = P_b(i) \frac{SPF \pm 1}{SPF} \; , \tag{2.58}$$

where P_b is the building load, the sign - is used for heating and DHW production mode, while the sign + is used for cooling mode. An example of annual profile of P_b and Q is shown in Figure 2.17, where cooling loads are assumed as negative.
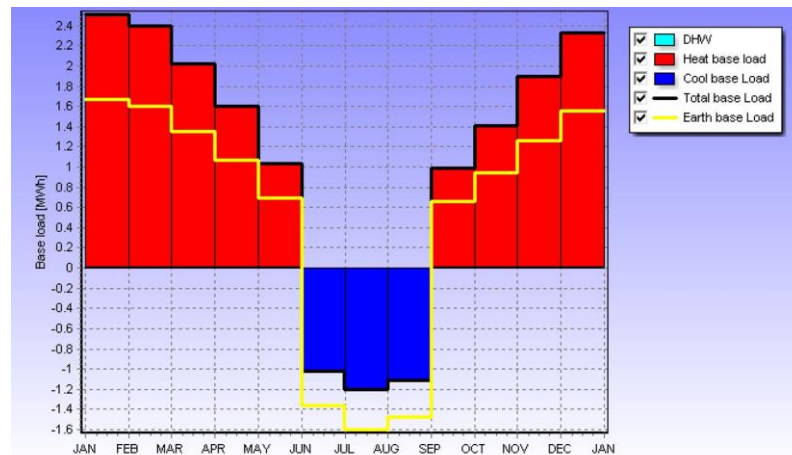
Figure 2.17: Annual trend of building heating and cooling base loads and corresponding thermal load exchanged between BHE and ground (earth base load).

For each month, the heating or cooling peak power and its duration are provided as separated input data. Peak loads are used by the software to estimate the maximum fluid temperature variations. The heat extraction from, or rejection to, the ground due to the peak load is added to the base load at the end of each month (which is usually the worst scenario). The resulting fluid temperatures are calculated and stored to show the minimum, or maximum, temperature values reached by the BHE fluid.

The base load is employed to determine the time evolution of the mean temperature of the fluid and of the BHE surface in response to the heat extraction and injection, whereas the peak load gives the maximum temperature variations. Since EED performs monthly calculations, temperature values are given only at the end of each month (or at the beginning of each following month, which is the same).

The number of years of simulation and the starting month are also stated. Simple cost data (e.g. fix cost per borehole, fix cost per borehole for soil drilling) can be specified to evaluate the economic impact of the simulated BHE field.

The simulations can be performed in two different ways: calculation of the mean fluid temperature at given loads and BHE field layout, or calculation of the required borehole length at given loads and fluid temperature limits. The optimization option, moreover, gives the minimum total borehole length (or cost) for a given set of parameters (land area, number of boreholes…).

Once the software has completed the calculation, a window showing the input and output data is displayed (see an example in Figure 2.18).

```
        C A L C U L A T E D   V A L U E S
        ========================================

 Total borehole length                  110 m

THERMAL RESISTANCES

 Borehole therm. res. internal          0.62 (m·K)/W

 Reynolds number                        1.981E4
 Thermal resistance fluid/pipe          0.00305 (m·K)/W
 Thermal resistance pipe material       0.07868 (m·K)/W
 Contact resistance pipe/filling        0 (m·K)/W

 Borehole therm. res. fluid/ground      0.1465 (m·K)/W

 Effective borehole thermal res.        0.1466 (m·K)/W

SPECIFIC HEAT EXTRACTION RATE [W/m]

 Month          Base load    Peak heat    Peak cool
  JAN            20.85           0            0
  FEB            19.91           0            0
  MAR            16.81           0            0
  APR            13.32           0            0
  MAY             8.61           0            0
  JUN           -16.94           0            0
  JUL           -19.93           0            0
  AUG           -18.43           0            0
  SEP             8.2            0            0
  OCT            11.7            0            0
  NOV            15.74           0            0
  DEC            19.37           0            0

BASE LOAD: MEAN FLUID TEMPERATURES (at end of month) [°C]
```

```
BASE LOAD: MEAN FLUID TEMPERATURES (at end of month) [°C]

 Year      1        2        5       10       25
 JAN      8.94     1.51     1.38     1.29     1.2
 FEB      8.94     1.69     1.56     1.47     1.38
 MAR      8.94     2.63     2.5      2.41     2.32
 APR      8.94     3.76     3.63     3.55     3.46
 MAY      8.94     5.34     5.21     5.13     5.04
 JUN      8.94    13.84    13.71    13.63    13.55
 JUL      8.94    15.26    15.13    15.04    14.96
 AUG      8.94    15.05    14.93    14.84    14.76
 SEP      6.24     6.44     6.31     6.23     6.15
 OCT      4.95     5        4.88     4.8      4.72
 NOV      3.5      3.49     3.37     3.29     3.21
 DEC      2.15     2.12     2        1.93     1.85

 BASE LOAD: YEAR  25
 Minimum mean fluid temperature  1.2 °C at end of JAN
 Maximum mean fluid temperature  14.96 °C at end of JUL

PEAK HEAT LOAD: MEAN FLUID TEMPERATURES (at end of month) [°C]

 Year      1        2        5       10       25
 JAN      8.94     1.51     1.38     1.29     1.2
 FEB      8.94     1.69     1.56     1.47     1.38
 MAR      8.94     2.63     2.5      2.41     2.32
 APR      8.94     3.76     3.63     3.55     3.46
 MAY      8.94     5.34     5.21     5.13     5.04
 JUN      8.94    13.84    13.71    13.63    13.55
 JUL      8.94    15.26    15.13    15.04    14.96
 AUG      8.94    15.05    14.93    14.84    14.76
 SEP      6.24     6.44     6.31     6.23     6.15
 OCT      4.95     5        4.88     4.8      4.72
 NOV      3.5      3.49     3.37     3.29     3.21
 DEC      2.15     2.12     2        1.93     1.85
```

Figure 2.18: Some sections of the EED output text report.

Outputs are also provided in graphic form: examples of the fluid temperature profile over the months of the last year of simulation and of the evolution of the highest and lowest fluid temperatures for each year of the simulation period are plotted in Figure 2.19 and Figure 2.20, respectively.
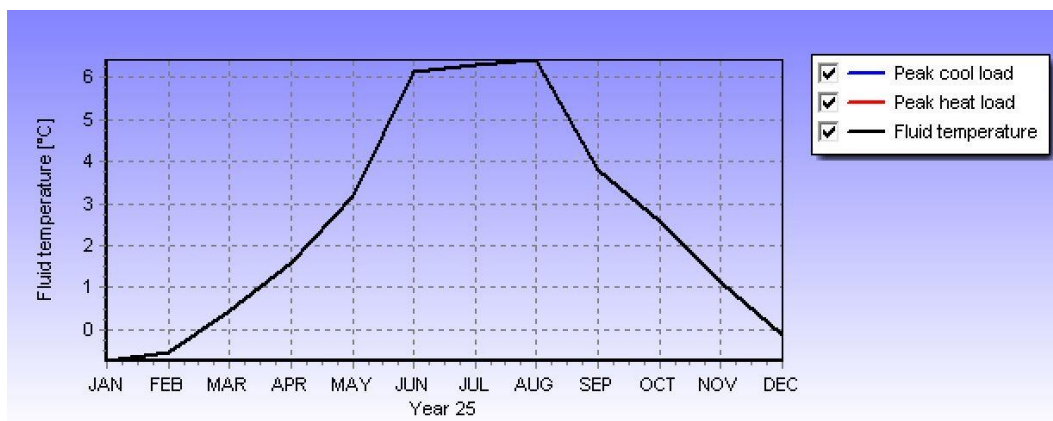
Figure 2.19: Fluid temperature profile for the last year of simulation.
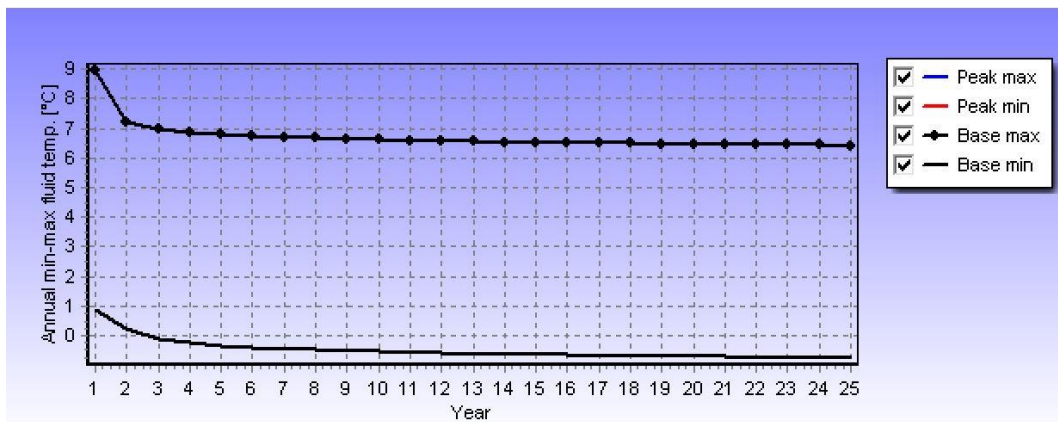
Figure 2.20: Maximum and minimum fluid temperature over the simulation period.

As usual, the effects of the groundwater flow are not taken into account by the software.

As highlighted by Sarbu and Sebarchievici [57], for cases with borehole lengths or distances between boreholes not considered in the stored *g-functions*, EED interpolates between the available *g-functions*, with consequent computing errors.

EED cannot perform hourly simulations; it evaluates the fluid temperature monthly, by placing the effect of hourly peak loads at the end of each month. Moreover, EED does not simulate the heat pump, but only the borehole field and, in order to calculate the BHE fluid temperature, it employs a mean value of the heat pump Seasonal Performance Factor. On the contrary, the real hourly *COP* or *EER* depends on the BHE fluid temperature, to be evaluated, so that a hourly simulation of the whole system would be necessary.

In Chapter 5 a dynamic code for the hourly simulation of both the borehole field and the coupled heat pump (with or without inverter) is presented.

The code is based on the *g-functions* obtained by Zanchini and Lazzari [9] and can evaluate, for the *i*-th hour of the simulated period (several years), the heat pump performance, the thermal energy exchanged between BHE and ground, the temperature at the surface BHE-ground and the updated value of the fluid temperature. For borehole lengths and distances intermediate between the tabulated values, the code does not interpolate between the *g-function* coefficients, but between the corresponding dimensionless BHE temperatures.

Earth Energy Designer will be used to validate the code presented in this Thesis for the simulation of GCHPs (see Section 5.3).

3

SIMULATION CODES FOR AIR-TO-WATER HEAT PUMPS THROUGH THE BIN-METHOD

This chapter presents numerical models for the evaluation of the seasonal performance of different kinds of electric air-to-water heat pumps based on a vapor compression cycle, coupled with buildings. The model is based on the bin-method derived from the European standard EN 14825 [10] and Italian standard UNI/TS 11300-4 [11], but takes into account also the different operating modes of mono-compressor on-off heat pumps, multi-compressor heat pumps and inverter-driven heat pumps.

First, the code developed for heating and DHW production during winter is described, then the code developed for cooling and DHW production during summer is presented, giving particular attention to the possibility of DHW production through condensation heat recovery, which is not taken into account by the standards [10], [11].

Results, derived by applying the proposed simulation codes, are finally discussed. The system seasonal performance is analyzed in relation to the thermal characteristics of the building, the climate profile of the location and the kind of heat pump control system.

3.1 MATHEMATICAL MODEL FOR WINTER OPERATION

By applying the bin-method, a numerical code has been developed to evaluate the seasonal performance of heating and DHW production systems based on electric air-to-water heat pumps, possibly integrated by a back-up system. The topic of this section is discussed in Ref. [58].

3.1.1 Bin distribution

The winter bin distribution for a European location is directly provided by the European standard UNI EN 14825 [10] on the basis of the climate zone (i.e. Colder, Average or Warmer). The Italian standard UNI/TS 11300-4 [11], on the other hand, suggests a bin calculation method based on a normal outdoor temperature distribution, obtainable, as described in the previous chapter, starting from the local data of monthly average outdoor temperature, outdoor design temperature and monthly average daily solar radiation on a horizontal plane. On the other hand, it is possible to derive the bin distribution of a specific location by using the hourly values of the external air temperature T_{ext} of the Test Reference Year for the selected location.

Figure 3.1 shows the bin distribution of the city of Bologna (North-Center Italy; 44.29 °N, 11.20 °E) obtained by applying the method of Ref. [11] for the conventional heating season, which starts on October 15th and ends on April 15th of each year. By observing the distribution of Figure 3.1, it is possible to note that the minimum outdoor temperature which occurs in Bologna is equal to -4 °C (while the outdoor design temperature, $T_{des,h}$, for Bologna is -5 °C) and that the mode of the distribution is equal to 6 °C.
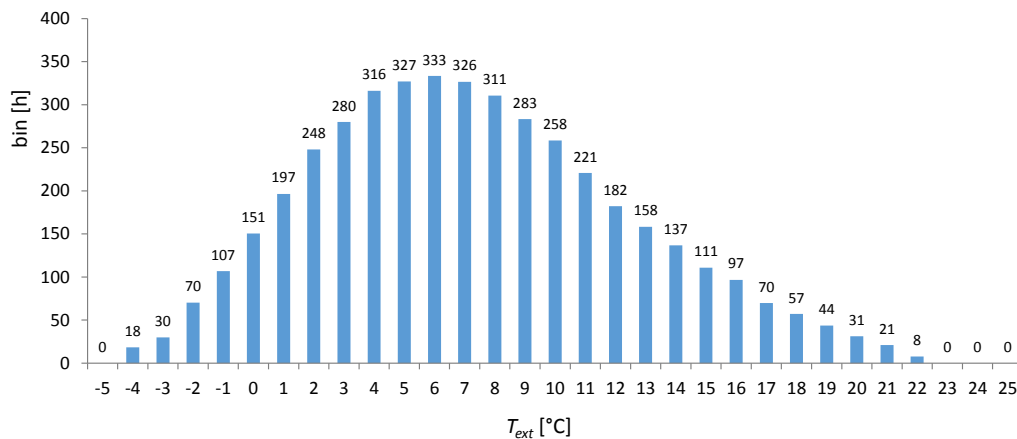
Figure 3.1: Bin distribution for the heating season in Bologna (Italy).

3.1.2 Building energy signature

Regarding the heating mode, for the analysis of the energy interaction between a building and the coupled heat pump, Refs. [10], [11] indicate to use the Building Energy Signature (BES), defined, as seen in Subsection 2.2.1, as the thermal power required by the building at

55

the outlet of the generation subsystem (heat pump) as a function of the outdoor temperature T_{ext}.

When a building can be characterized by means of a linear BES curve, in order to draw the BES it is sufficient to know the values of T_{zl} (outdoor temperature in correspondence of which the building heating demand vanishes) and of the design load, $P_{des,h}$, in correspondence of the outdoor design temperature, $T_{des,h}$.

In Figure 3.2, a linear BES is represented with a dashed red line, drawn by considering a design thermal load of the building equal to 40 kW in correspondence of a design temperature equal to -5 °C, and a value of T_{zl} equal to 16 °C.
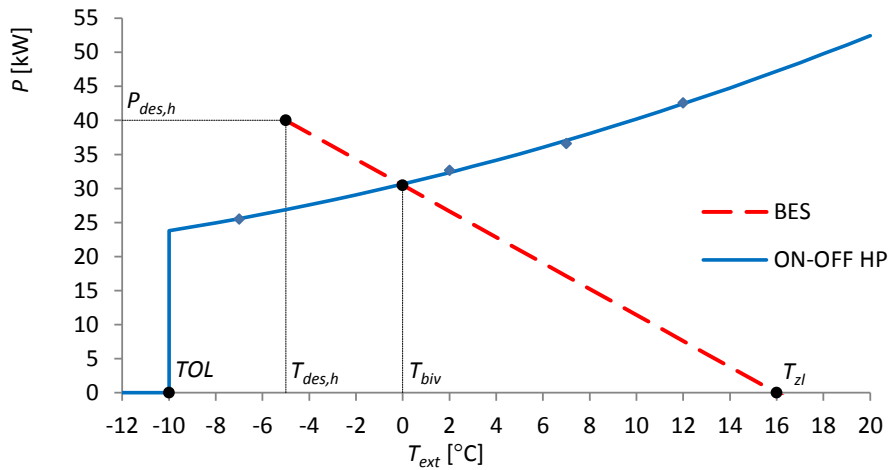
Figure 3.2: Examples of trend of the winter building energy signature and characteristic curve of a mono-compressor on-off air-source heat pump.

The heating power required by the building ($P_{b,h}$) as a function of the outdoor temperature can thus be written as:

$$P_{b,h}(i) = P_{des} \left[\frac{T_{zl} - T_{ext}(i)}{T_{zl} - T_{des}} \right] ,$$

(3.1)

where the notation $P_{b,h}(i)$ indicates the thermal power required by the building in the i-th bin. Obviously, if $P_{b,h}(i)$ turns out lower than 0, it is set equal to 0.

The building thermal energy demand $E_{b,h}$ is evaluated in correspondence of each bin as:

$$E_{b,h}(i) = P_{b,h}(i) \, t_{bin}(i) ,$$

(3.2)

where $t_{bin}(i)$ is the time duration of the i-th bin.

3.1.3 Building domestic hot water demand

The domestic hot water volume daily needed by a residential building, V_w, is evaluated according to the standard UNI/TS 11300-2 [59] as:

$$V_w = a_w S_b + b_w \ , \tag{3.3}$$

where S_b is the building floor area and the coefficients a_w and b_w are obtained from Table 3.1:

Table 3.1: Values of the coefficients a_w and b_w.

S_b [m^2]	$S_b \leq 35$	$35 < S_b \leq 50$	$50 < S_b \leq 200$	$S_b > 200$
a_w [l/(m^2 day)]	0	2.667	1.067	0
b_w [l/day]	50	-43.33	36.67	250

The building daily energy demand for DHW production, $E_{b,d,day}$, is thus evaluated according to the standard [59] as:

$$E_{b,d,day} = \rho_w c_{p,w} V_w (T_{w,out,DHW} - T_{w,in,DHW}) \ , \tag{3.4}$$

In Eq. (3.4) ρ_w is the water density, set by the standard [59] equal to 1000 kg/m^3; $c_{p,w}$ is the water specific heat capacity at constant pressure, set by Ref. [59] equal to 1.162×10^{-3} kWh/(kg K); $T_{w,out,DHW}$ is the DHW supply temperature, set by the standard [59] equal to 40 °C and $T_{w,in,DHW}$ is the cold water inlet temperature, set by Ref. [59] equal to the local annual mean outdoor temperature from the standard UNI 10349 [25].

The energy needed by the building in correspondence of each bin ($E_{b,d}(i)$ in Eq. (3.5)) can be obtained allocating, on the basis of the duration of the i-th bin, the daily energy need at the outlet of the generation subsystem (heat pump):

$$E_{b,d}(i) = \frac{t_{bin}(i)}{24} \frac{E_{b,d,day}}{\eta_{em,d} \ \eta_{dis,d}} \ . \tag{3.5}$$

In Eq. (3.5), $\eta_{em,d}$ and $\eta_{dis,d}$ are the emission and distribution efficiencies for DHW, respectively.

3.1.4 Heat pump characterization

In the same (T_{ext}, P) chart reported in Figure 3.2 it is possible to draw the characteristic curve of an air-source heat pump, by considering that the thermal power delivered by the heat pump (P_{HP}) depends on the outdoor temperature, for a fixed value of the temperature T_w of the hot water produced by the heat pump.

The heat pump characteristic curve can be obtained from the technical datasheets given by the heat pump manufacturer. Different kinds of electric air-to-water heat pumps, like mono-compressor ON-OFF Heat Pumps (ON-OFF HPs), Multi-Compressor Heat Pumps (MCHPs) and Inverter-Driven Heat Pumps (IDHPs), have different characteristic curves. In fact, for an ON-OFF HP the thermal power delivered by the heat pump is only a function of the temperature of the two sources (air: T_{ext}; water: T_w) between which the heat pump works ($P_{HP} = f(T_{ext}, T_w)$). On the contrary, for MCHPs the thermal power delivered by the heat pump depends also on the number n of compressors switched on ($P_{HP} = f(T_{ext}, T_w, n)$), while for IDHPs it is a function of the inverter frequency Φ ($P_{HP} = f(T_{ext}, T_w, \Phi)$).

The model presented in this work considers a fixed value of T_w, hence ON-OFF HPs are represented by a single curve in the chart (T_{ext}, P); MCHPs are represented by N curves (with N equal to the number of the heat pump compressors) and IDHPs are represented by a family of curves, obtained by varying the inverter frequency between the maximum (Φ_{max}) and minimum (Φ_{min}) value.

A typical characteristic curve of a mono-compressor on-off heat pump working in heating mode is shown in Figure 3.2 together with the BES previously defined. The heat pump characteristic curve is stopped in correspondence of the Temperature Operative Limit (TOL), that is the minimum value of T_{ext}, generally given by the heat pump manufacturer, at which the heat pump is able to deliver heating capacity.

In the case of an ON-OFF HP, the BES and the heat pump characteristic curve in heating mode have only one common point, called balance point, in correspondence of which the heating power delivered by the heat pump equals the heating demand of the building. As seen in Subsection 2.2.1, the outdoor temperature corresponding to the balance point is called bivalent temperature (T_{biv}). When the outdoor temperature is lower than T_{biv}, the building heating demand cannot be completely satisfied by the heat pump and, if present, an integration system (back-up system) must be activated (e.g. electric heaters, gas boiler). On the contrary, when the outdoor temperature is higher than T_{biv}, the heat pump heating power exceeds the building thermal request and on-off cycles need to start in order to match the energy demand.

In Figure 3.3, the same graph is drawn for MCHPs and IDHPs: the two characteristic curves correspond to the maximum (blue line) and minimum (black line) heating power deliverable by:

- a MCHP, with all the compressors switched on (N/N), or with only one compressor switched on ($1/N$);

- an IDHP, with the inverter set at the maximum frequency (Φ_{max}) or at the minimum frequency (Φ_{min}).
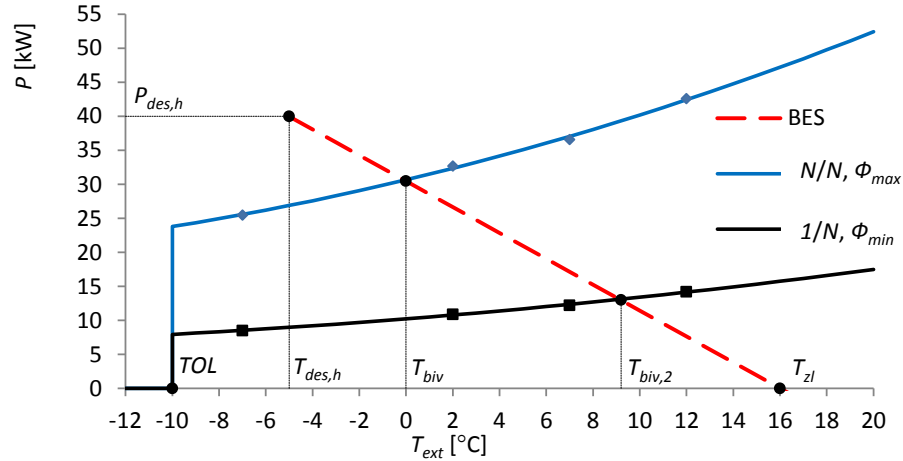
Figure 3.3: Typical trend of the winter building energy signature and characteristic curves of a multi-compressor or an inverter-driven air-source heat pump.

In the cases of MCHPs and IDHPs, Figure 3.3 shows that it is possible to define, in addition to the bivalent temperature T_{biv}, a secondary bivalent temperature ($T_{biv,2}$), which is the maximum outdoor temperature that the heat pump can manage without starting on-off cycles.

In addition to the knowledge of the heat pump characteristic curve, for a complete characterization of a heat pump working in heating or DHW production mode it is mandatory to know the value of the heat pump *COP* in correspondence of given values of the external air temperature and of the water temperature T_w. Similarly to the heat pump characteristic curves, *COP* curves as functions of the outdoor temperature are defined.

The model developed in this Thesis requires as input for the heat pump characterization: values (given by the manufacturer) of the heat pump power and *COP*, in heating and in DHW production mode, for a fixed value of T_w and for different external air temperatures, in correspondence of the activation of each compressor (MCHPs) or in correspondence of the maximum, minimum and at least an additional intermediate inverter frequency (IDHPs). The model can thus derive the heat pump power and *COP* curves by interpolating the input data as functions of the outdoor temperature, using second-order polynomial functions.

For mono-compressor on-off heat pumps, it is possible to write:

$$P_{HP}(i) = a_1\left(T_w\right) T_{ext}^2(i) + b_1\left(T_w\right) T_{ext}(i) + c_1\left(T_w\right)$$
$$COP(i) = a_2\left(T_w\right) T_{ext}^2(i) + b_2\left(T_w\right) T_{ext}(i) + c_2\left(T_w\right)$$

(3.6)

In this way, P_{HP} and COP become functions of the i-th bin considered. The six coefficients a_1, a_2, b_1, b_2, c_1, c_2 are functions of the hot water temperature T_w for a mono-compressor on-off heat pump.

For a multi-compressor heat pump, the heat pump thermal power and COP change if the number n of activated compressors changes; this means that the six coefficients a_1, a_2, b_1, b_2, c_1, c_2 depend also on the number of compressors switched on:

$$P_{HP,n/N}(i) = a_{1,n/N}\left(T_w\right) T_{ext}^2(i) + b_{1,n/N}\left(T_w\right) T_{ext}(i) + c_{1,n/N}\left(T_w\right)$$
$$COP_{n/N}(i) = a_{2,n/N}\left(T_w\right) T_{ext}^2(i) + b_{2,n/N}\left(T_w\right) T_{ext}(i) + c_{2,n/N}\left(T_w\right)$$

with $n = 1, ..., N$.   (3.7)

The notation n/N means that the corresponding quantity is evaluated by considering n compressors switched on among the N compressors of the heat pump. In this way, a MCHP with N compressors can be completely characterized by means of 6xN coefficients.

The situation is similar for the characterization of an inverter-driven heat pump; in this case the heat pump power and COP change with the inverter frequency, as well as with the hot water temperature. By fixing M values of frequency from Φ_{min} to Φ_{max}, declared by the manufacturer, the values of the heat pump thermal power and COP can be evaluated by knowing 6xM coefficients:

$$P_{HP,\Phi_j}(i) = a_{1,\Phi_j}\left(T_w\right) T_{ext}^2(i) + b_{1,\Phi_j}\left(T_w\right) T_{ext}(i) + c_{1,\Phi_j}\left(T_w\right)$$
$$COP_{\Phi_j}(i) = a_{2,\Phi_j}\left(T_w\right) T_{ext}^2(i) + b_{2,\Phi_j}\left(T_w\right) T_{ext}(i) + c_{2,\Phi_j}\left(T_w\right)$$

with $j = 1, ..., M$.   (3.8)

The values of the coefficients recalled in Eqs. (3.6)-(3.8) are obtained by interpolating the input data given by the heat pump manufacturer.

3.1.5   Energy calculation for winter operation

Once selected the building and the heat pump, the program evaluates the energy delivered and used by the heat pump in each bin, considering priority of satisfaction of the building demand for DHW production, and, secondly, of the building demand for heating. The heating-only mode, or DHW-only mode, can be simulated by setting equal to zero the building DHW demand, or the heating demand, respectively.

Firstly, the time $t_d(i)$ taken by the heat pump in the i-th bin to deliver the energy needed by the building for DHW production is evaluated. Considering as an example the case of a MCHP with two compressors:

$$t_d(i) = E_{b,d}(i) / P_{HP,d,2/2}(i) \; , \qquad (3.9)$$

where the subscript d indicates the DHW mode and the notation n/N indicates n activated compressors out of N. In Eq. (3.9) it has been considered that the heat pump works at its maximum capacity to satisfy the building DHW demand, leaving in the i-th bin as much time as possible to satisfy the building heating demand and, consequently, avoiding if possible the back-up activation. Obviously, if $t_d(i)$ turns out greater than the bin duration $t_{bin}(i)$, $t_d(i)$ is set equal to $t_{bin}(i)$; this situation means that in the i-th bin the heat pump is not able to completely satisfy the DHW demand and the activation of the back-up system is required.

The energy $E_{HP,d}(i)$ delivered by the heat pump for DHW is obtained multiplying the heat pump capacity by $t_d(i)$ and the corresponding electric energy used by the heat pump, $E_{HP,d,us}(i)$, is evaluated dividing $E_{HP,d}(i)$ by the COP at maximum capacity.

If a back-up system is present, the thermal energy $E_{bk,d}(i)$ it delivers for DHW, if needed, is obtained by subtracting $E_{HP,d}(i)$ to $E_{b,d}(i)$ and the corresponding energy used, $E_{bk,d,us}(i)$, is equal to the ratio between $E_{bk,d}(i)$ and the efficiency η_{bk} of the back-up system. $E_{bk,d,us}$ is an electric consumption if the back-up system is composed by electric heaters, while it is a primary energy consumption in the case of a gas boiler.

The residual time $t_{res}(i)$, available in the i-th bin for heating mode, is given by the difference between $t_{bin}(i)$ and $t_d(i)$.

If $E_{b,h}(i)$ is higher than the product between the maximum heat pump capacity in heating mode and $t_{res}(i)$, the thermal energy delivered by the heat pump for heating, $E_{HP,h}(i)$, is equal to the product between the maximum heat pump capacity and $t_{res}(i)$, otherwise, $E_{HP,h}(i)$ is equal to $E_{b,h}(i)$.

The heat pump COP in heating mode, COP_h, (in correspondence of each active compressor, for MCHPs, or in correspondence of each of the M inverter frequencies considered, for IDHPs) is evaluated for each bin by means of Eqs. (3.6)-(3.8). The actual COP value, $COP_{h,eff}$, which takes into account the losses linked to the on-off cycles, is obtained as:

$$COP_{h,eff}(i) = COP_h(i) \, f_{corr}(i) \; , \qquad (3.10)$$

where f_{corr} is the COP correction factor for on-off condition, evaluated according to the standards [10], [11] (see Subsection 2.2.1).

For MCHPs and IDHPs, $COP_{h,eff}$ is evaluated by using the value of COP in correspondence of the activation of only one compressor, or in correspondence of the minimum inverter frequency, and by using the value of f_{corr} obtained with the capacity ratio evaluated as:

$$CR(i) = \frac{E_{b,h}(i)}{P_{HP,h,1/2}(i)\, t_{res}(i)} \ ,$$ (3.11)

for MCHPs, or with the capacity ratio evaluated through Eq. (3.11) replacing $P_{HP,h,1/2}$ with $P_{HP,h,\Phi_{min}}$, for IDHPs. If $CR(i)$ turns out greater than 1, it is set equal to 1.

In fact, for a MCHP or IDHP, the on-off cycles start when the energy needed by the building becomes lower than the energy that the heat pump would deliver with only one compressor activated, or at the minimum inverter frequency (situation corresponding to $T_{ext} > T_{biv,2}$, considering the heating-only mode).

For an ON-OFF HP, the electric energy $E_{HP,h,us}(i)$, used by the heat pump for heating in the i-th bin, is:

$$E_{HP,h,us}(i) = E_{HP,h}(i)\,/\,COP_{h,eff}(i) \ .$$ (3.12)

For a MCHP, in order to evaluate $E_{HP,h,us}(i)$, for each bin it is mandatory to know how many compressors are activated and how long. In fact, if the heating power required by the building is higher than the heat pump capacity corresponding to the activation of n compressors, but it is lower than the heat pump capacity corresponding to the activation of $n+1$ compressors, then $n+1$ compressors are activated for a certain period of time and n compressors for the remaining time, so as the total energy delivered by the heat pump equals the building energy demand.

As an example, if in the i-th bin a MCHP with two compressors has to provide an amount of energy intermediate between the energy which would be delivered with one compressor and with two compressors working for the time $t_{res}(i)$, then the time period with two working compressors ($t_{res,2/2}(i)$) can be estimated as:

$$t_{res,2/2}(i) = \frac{E_{b,h}(i) - P_{HP,h,1/2}(i)\, t_{res}(i)}{P_{HP,h,2/2}(i) - P_{HP,h,1/2}(i)} \ .$$ (3.13)

Consequently, the time period in which the MCHP works with only one compressor switched on ($t_{res,1/2}(i)$) is equal to:

$$t_{res,1/2}(i) = t_{res}(i) - t_{res,2/2}(i) \ .$$ (3.14)

The electric energy consumption of the MCHP is:

$$E_{HP,h,us}(i) = \begin{cases} \dfrac{E_{HP,h}(i)}{COP_{h,eff}(i)} & \text{if } E_{b,h}(i) < P_{HP,h,1/2}(i)\, t_{res}(i) \\[2ex] \dfrac{P_{HP,h,2/2}(i)\, t_{res,2/2}(i)}{COP_{h,2/2}(i)} + \dfrac{P_{HP,h,1/2}(i)\, t_{res,1/2}(i)}{COP_{h,1/2}(i)} & \text{if } P_{HP,h,1/2}(i)\, t_{res}(i) \leq E_{b,h}(i) < P_{HP,h,2/2}(i)\, t_{res}(i) \\[2ex] \dfrac{E_{HP,h}(i)}{COP_{h,2/2}(i)} & \text{if } E_{b,h}(i) \geq P_{HP,h,2/2}(i)\, t_{res}(i) \end{cases} \quad (3.15)$$

As an IDHP is able to change the inverter frequency in order to follow the building demand, to evaluate the electric energy used by the heat pump for heating it is mandatory to know the actual values of power ($P_{HP,h,\Phi_{eff}}$) and COP ($COP_{h,\Phi_{eff}}$) at which the heat pump is working. Once evaluated $P_{HP,h,\Phi_{eff}}(i)$ as the ratio between $E_{HP,h}(i)$ and $t_{res}(i)$ (if $P_{HP,h,\Phi_{eff}}(i)$ turns out lower than $P_{HP,h,\Phi_{min}}(i)$, it is set equal to $P_{HP,h,\Phi_{min}}(i)$), $COP_{h,\Phi_{eff}}$ is obtained through interpolations between the M values of the heat pump power and COP derived from Eq. (3.8).

The electric energy consumption of the IDHP is therefore:

$$E_{HP,h,us}(i) = \begin{cases} \dfrac{E_{HP,h}(i)}{COP_{h,eff}(i)} & \text{if } E_{b,h}(i) < P_{HP,h,\Phi_{min}}(i)\, t_{res}(i) \\[2ex] \dfrac{E_{HP,h}(i)}{COP_{h,\Phi_{eff}}(i)} & \text{if } P_{HP,h,\Phi_{min}}(i)\, t_{res}(i) \leq E_{b,h}(i) < P_{HP,h,\Phi_{max}}(i)\, t_{res}(i) \\[2ex] \dfrac{E_{HP,h}(i)}{COP_{h,\Phi_{max}}(i)} & \text{if } E_{b,h}(i) \geq P_{HP,h,\Phi_{max}}(i)\, t_{res}(i) \end{cases} \quad (3.16)$$

For each kind of heat pump, if the heat pump capacity in the i-th bin is lower than the building thermal demand ($T_{ext} < T_{biv}$, considering the heating-only mode), the missing energy $E_{bk,h}(i)$ is delivered by the back-up system, if present. The corresponding energy used by the back-up for heating, $E_{bk,h,us}(i)$ is equal to the ratio between $E_{bk,h}(i)$ and η_{bk}.

The seasonal values of energy delivered and used by the heat pump and the back-up system are obtained by summing the corresponding values of each bin. The mean seasonal COP of the heat pump, $SCOP_{net}$, and of the whole system, consisting of electric air-to-water heat pump and electric heaters as back-up system, $SCOP_{on}$, are evaluated according to the standards [10], [11]:

$$SCOP_{net} = \dfrac{\sum_i E_{HP,h}(i) + \sum_i E_{HP,d}(i)}{\sum_i E_{HP,h,us}(i) + \sum_i E_{HP,d,us}(i)}, \quad (3.17)$$

$$SCOP_{on} = \frac{\left[\sum_i E_{HP,h}(i) + \sum_i E_{HP,d}(i)\right] + \left[\sum_i E_{bk,h}(i) + \sum_i E_{bk,d}(i)\right]}{\left[\sum_i E_{HP,h,us}(i) + \sum_i E_{HP,d,us}(i)\right] + \left[\sum_i E_{bk,h,us}(i) + \sum_i E_{bk,d,us}(i)\right]} \ . \qquad (3.18)$$

Obviously, if the back-up system is represented by a gas boiler, only the coefficient $SCOP_{net}$ can be defined.

Another seasonal performance parameter evaluated by the code is the Fuel Utilization Efficiency, *FUE*, which is the ratio between the total thermal energy provided by the system and the corresponding primary energy used:

$$FUE = \frac{\left[\sum_i E_{HP,h}(i) + \sum_i E_{HP,d}(i)\right] + \left[\sum_i E_{bk,h}(i) + \sum_i E_{bk,d}(i)\right]}{\left[\dfrac{\sum_i E_{HP,h,us}(i) + \sum_i E_{HP,d,us}(i)}{\eta_{el}}\right] + \left[\sum_i E_{bk,h,prim}(i) + \sum_i E_{bk,d,prim}(i)\right]} \ . \qquad (3.19)$$

In Eq. (3.19), η_{el} is the thermodynamic efficiency of the electricity system of the country (for Italy equal to 0.46, according to the Italian Regulatory Authority for Electricity, Gas and Water) and $E_{bk,h,prim}$ and $E_{bk,d,prim}$ are the values of primary energy used by the back-up system, for heating and DHW production, respectively. $E_{bk,h,prim}$ ($E_{bk,d,prim}$) is equal to $E_{bk,h,us}$ ($E_{bk,d,us}$) if the back-up system is composed by a gas boiler, while it is equal to the ratio between $E_{bk,h,us}$ ($E_{bk,d,us}$) and η_{el} in the case electric heaters are used as back-up system.

The draft standard prUNI/TS 11300-5 [60], not yet published at the moment of writing this Thesis, is about to change the evaluation of a system primary energy use, by considering a renewable primary energy factor and a non-renewable primary energy factor for each energy carrier.

3.2 MATHEMATICAL MODEL FOR SUMMER OPERATION

By applying the bin-method, a numerical code is developed to evaluate the seasonal performance of cooling and DHW production systems based on electric reversible air-to-water heat pumps, possibly integrated by a back-up system for DHW production. The code takes into account the possibility of simultaneous production of cooling energy for air-conditioning and thermal energy for DHW through the condensation heat recovery. The topic of this section is treated in Ref. [61].

3.2.1 Bin distribution, building energy need and heat pump characterization

The standard EN 14825 [10] directly provides a single European bin profile for the cooling season, whereas the standard UNI/TS 11300-4 [11] derives the bin distribution of a selected time period starting from the local data of temperature and radiation. The model presented in this Thesis applies the bin calculation method proposed by standard [11] to evaluate the local hourly bin distribution during the cooling season.

The histogram of Figure 3.4 represents the bin profile obtained for the Italian city of Bologna, considering a cooling season from May 15th to September 15th
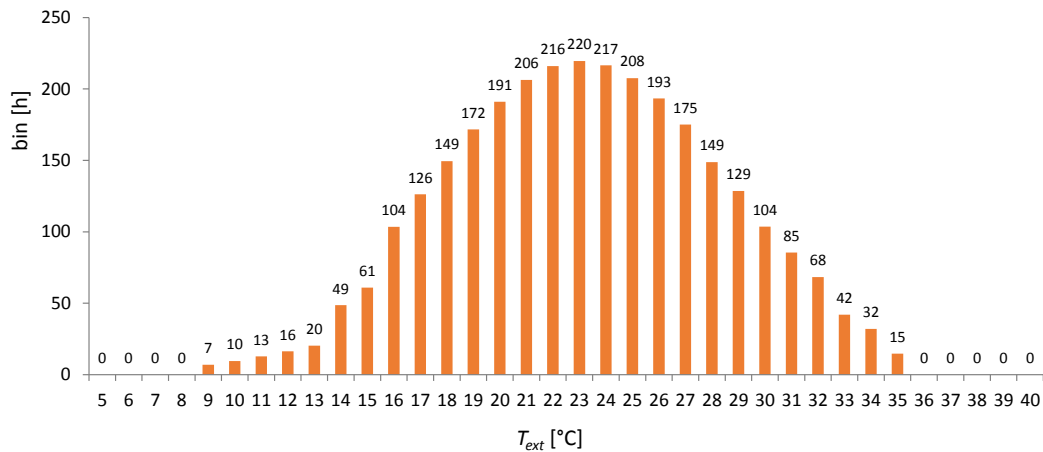
Figure 3.4: Bin distribution for the cooling season in Bologna (Italy).

From Figure 3.4 one can notice that the outdoor temperature in Bologna during summer runs from a minimum value of 9 °C to a maximum one of 35 °C, with a mode of the distribution equal to 23 °C.

For the characterization of the building cooling loads, the summer building energy signature is used, according to Ref. [10]. In the case of a straight BES curve, like the red line drawn in Figure 3.5 as an example, the cooling power required by the building in correspondence of each bin, $P_{b,c}(i)$, can be obtained through Eq. (3.1), knowing the values of the zero-load outdoor temperature and of the cooling power required by the building in correspondence of the summer outdoor design temperature.
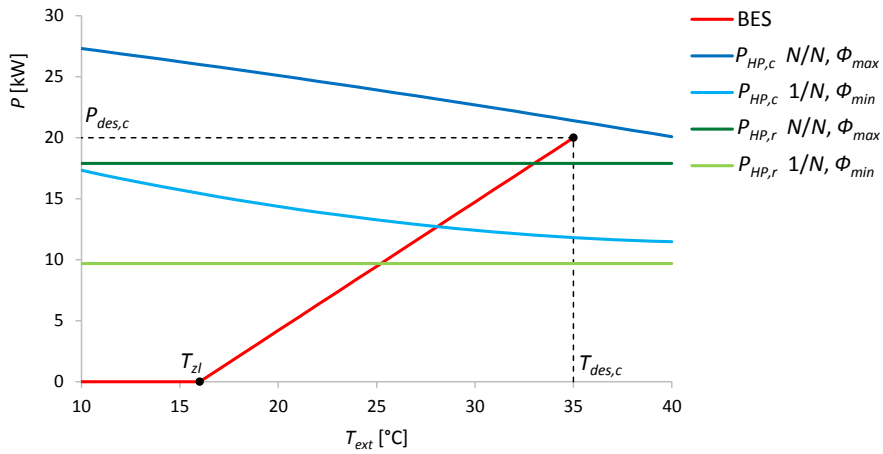
Figure 3.5: Typical trend of the summer building energy signature and characteristic curves of a multi-compressor or inverter-driven air-source heat pump.

The corresponding cooling energy required by the building is:

$$E_{b,c}(i) = P_{b,c}(i) \, t_{bin}(i) \; . \tag{3.20}$$

The energy needed by the building in each bin for DHW production ($E_{b,d}(i)$) is obtained as described in Subsection 3.1.3.

The cooling power $P_{HP,c}$ delivered by a reversible air-source mono-compressor on-off heat pump depends on the outdoor temperature T_{ext}, for a fixed temperature $T_{w,c}$ of the cold water produced. As explained in Subsection 3.1.4, the heat pump characteristic curve can be obtained by interpolation of the manufacturer data of power as functions of the outdoor temperature, by using second-order polynomial functions. For MCHPs and IDHPs, the heat pump characteristic curve is actually a number of curves equal to the number N of compressors (MCHPs), or it is represented by a family of curves obtained by varying the inverter frequency between the maximum and minimum value (IDHPs). Blue lines in Figure 3.5 are examples of characteristic curves at maximum capacity (all the compressors activated, or maximum inverter frequency) and minimum capacity (only one compressor activated, or minimum inverter frequency).

Similarly, the curves of the heat pump Energy Efficiency Ratio, EER_c, are obtained through interpolations of the manufacturer technical data (see Subsection 3.1.4).

$P_{HP,c}$ and EER_c are thus functions of the i-th bin.

The heat pumps considered in the model are able to recover the thermal energy released at the condenser during the cooling function in order to produce at the same time domestic hot

water (condensation heat recovery). In this way, it is possible to avoid or reduce the activation of a back-up system for DHW.

The cooling-only mode, or DHW-only mode, can be simulated by setting equal to zero the building DHW demand, or the cooling demand, respectively.

It is important to observe that the heat pump operates like an air-to-water heat pump only when DHW production is absent. On the contrary, during the heat recovery mode, the heat pump does not release the condensation heat to the outdoor air, but to a storage tank for DHW production, working as a water-to-water heat pump. As a consequence, in this mode the heat pump cooling power ($P_{HP,r}$) and *EER* (EER_r) depend only on the temperatures of the cold water ($T_{w,c}$) and hot water ($T_{w,d}$) produced, and they are not influenced by the bin considered (see green lines in Figure 3.5).

3.2.2 Energy calculation for summer operation

Once selected the building and the heat pump, the program evaluates the energy delivered and used by the heat pump, considering that in the generic *i*-th bin the building can require at the same time cooling energy for air-conditioning ($E_{b,c}$) and thermal energy for DHW production ($E_{b,d}$).

For each bin, the time in which the heat pump works in heat recovery mode, releasing at the same time cooling energy and thermal energy for DHW, must be evaluated.

By considering the case of a MCHP with two compressors, the heat pump virtual activation times in heat recovery mode, with both compressors on ($t_{r,2/2,virt}$) and with only one compressor on ($t_{r,1/2,virt}$), can be evaluated according to Eq. (3.21) and Eq. (3.22), respectively:

$$t_{r,2/2,virt}(i) = \begin{cases} t_{bin}(i) & \text{if } E_{b,c}(i) > P_{HP,r,2/2}(i)\, t_{bin}(i) \\ 0 & \text{if } E_{b,c}(i) < P_{HP,r,1/2}(i)\, t_{bin}(i) \\ \dfrac{E_{b,c}(i) - P_{HP,r,1/2}(i)\, t_{bin}(i)}{P_{HP,r,2/2}(i) - P_{HP,r,1/2}(i)} & \text{if } P_{HP,r,1/2}(i)\, t_{bin}(i) < E_{b,c}(i) < P_{HP,r,2/2}(i)\, t_{bin}(i) \end{cases} \quad , \quad (3.21)$$

$$t_{r,1/2,virt}(i) = \begin{cases} 0 & \text{if } E_{b,c}(i) > P_{HP,r,2/2}(i)\, t_{bin}(i) \\ \dfrac{E_{b,c}(i)}{P_{HP,r,1/2}(i)} & \text{if } E_{b,c}(i) < P_{HP,r,1/2}(i)\, t_{bin}(i) \\ t_{bin}(i) - t_{r,2/2,virt}(i) & \text{if } P_{HP,r,1/2}(i)\, t_{bin}(i) < E_{b,c}(i) < P_{HP,r,2/2}(i)\, t_{bin}(i) \end{cases} \quad . \quad (3.22)$$

The consequent thermal energy available at the heat pump condenser for DHW production, $E_{avail,cond}$, can be calculated:

$$E_{avail,cond}(i) = t_{r,2/2,virt}\left[P_{HP,r,2/2}(i) + \frac{P_{HP,r,2/2}(i)}{EER_{r,2/2}(i)}\right] + t_{r,1/2,virt}\left[P_{HP,r,1/2}(i) + \frac{P_{HP,r,1/2}(i)}{EER_{r,1/2}(i)}\right] . \quad (3.23)$$

If in the i-th bin $E_{b,d}$ is equal to – or higher than – $E_{avail,cond}$, the heat pump effective activation times in heat recovery mode, with two compressors activated ($t_{r,2/2,eff}$) and with one compressor activated ($t_{r,1/2,eff}$), are equal to the corresponding virtual activation times. Otherwise, the heat pump provides cooling energy to the building in heat recovery mode only until the DHW thermal demand is satisfied; $t_{r,2/2,eff}$ and $t_{r,1/2,eff}$ are then evaluable through Eq. (3.24) and Eq. (3.25), respectively:

$$t_{r,2/2,eff}(i) = \begin{cases} \dfrac{E_{b,d}(i)}{P_{HP,r,2/2}(i) + \dfrac{P_{HP,r,2/2}(i)}{EER_{r,2/2}(i)}} & \text{if } E_{b,c}(i) > P_{HP,r,2/2}(i)\, t_{bin}(i) \\[2em] 0 & \text{if } E_{b,c}(i) < P_{HP,r,1/2}(i)\, t_{bin}(i) \\[2em] \dfrac{E_{b,d}(i)}{P_{HP,r,2/2}(i) + \dfrac{P_{HP,r,2/2}(i)}{EER_{r,2/2}(i)} + \dfrac{t_{r,1/2,virt}(i)}{t_{r,2/2,virt}(i)}\left[P_{HP,r,1/2}(i) + \dfrac{P_{HP,r,1/2}(i)}{EER_{r,1/2}(i)}\right]} & \text{else} \end{cases} \quad (3.24)$$

$$t_{r,1/2,eff}(i) = \begin{cases} 0 & \text{if } E_{b,c}(i) > P_{HP,r,2/2}(i)\, t_{bin}(i) \\[2em] \dfrac{E_{b,d}(i)}{P_{HP,r,1/2}(i) + \dfrac{P_{HP,r,1/2}(i)}{EER_{r,1/2}(i)}} & \text{if } E_{b,c}(i) < P_{HP,r,1/2}(i)\, t_{bin}(i) \\[2em] t_{r,2/2,eff}(i)\dfrac{t_{r,1/2,virt}(i)}{t_{r,2/2,virt}(i)} & \text{if } P_{HP,r,1/2}(i)\, t_{bin}(i) < E_{b,c}(i) < P_{HP,r,2/2}(i)\, t_{bin}(i) \end{cases} \quad (3.25)$$

The cooling energy $E_{HP,r}$ supplied by the heat pump in heat recovery mode is given by:

$$E_{HP,r}(i) = P_{HP,r,2/2}(i)\, t_{r,2/2,eff} + P_{HP,r,1/2}(i)\, t_{r,1/2,eff} , \quad (3.26)$$

while the thermal energy $E_{HP,d}$ recovered at the heat pump condenser for DHW production is:

$$E_{HP,d}(i) = \min\left[E_{avail,cond}(i);\ E_{b,d}(i)\right] . \quad (3.27)$$

If $E_{HP,r}$ is lower than $E_{b,c}$, that is if in heat recovery mode the heat pump has not completely satisfied the building cooling demand, during the residual time of the bin the heat pump delivers cooling energy releasing the condensation heat to the external air. The residual time,

t_{res}, is evaluated by means of Eq. (3.28), which takes also into account the time lost in the case of heat pump on-off cycles:

$$t_{res}(i) = \frac{t_{bin}(i)}{t_{r,2/2,virt} + t_{r,1/2,virt}} \left[\left(t_{r,2/2,virt} + t_{r,1/2,virt} \right) - \left(t_{r,2/2,eff} + t_{r,1/2,eff} \right) \right] \ . \tag{3.28}$$

The heat pump activation times in cooling-only mode, with two compressors activated ($t_{c,2/2}$) and with one compressor activated ($t_{c,1/2}$), are obviously equal to 0 if $E_{b,d}$ is higher than $E_{avail,cond}$, else can be evaluated through Eq. (3.29) and Eq. (3.30), respectively:

$$t_{c,2/2}(i) = \begin{cases} t_{res}(i) & \text{if } E_{b,c}(i) - E_{HP,r}(i) > P_{HP,c,2/2}(i) \, t_{res}(i) \\ 0 & \text{if } E_{b,c}(i) - E_{HP,r}(i) < P_{HP,c,1/2}(i) \, t_{res}(i) \\ \dfrac{E_{b,c}(i) - E_{HP,r}(i) - P_{HP,c,1/2}(i) \, t_{res}(i)}{P_{HP,c,2/2}(i) - P_{HP,c,1/2}(i)} & \text{if } P_{HP,c,1/2}(i) \, t_{res}(i) < E_{b,c}(i) - E_{HP,r}(i) < P_{HP,c,2/2}(i) \, t_{res}(i) \end{cases} \tag{3.29}$$

$$t_{c,1/2}(i) = \begin{cases} 0 & \text{if } E_{b,c}(i) - E_{HP,r}(i) > P_{HP,c,2/2}(i) \, t_{res}(i) \\ \dfrac{E_{b,c}(i) - E_{HP,r}(i)}{P_{HP,c,1/2}(i)} & \text{if } E_{b,c}(i) - E_{HP,r}(i) < P_{HP,c,1/2}(i) \, t_{res}(i) \\ t_{res}(i) - t_{c,2/2}(i) & \text{if } P_{HP,c,1/2}(i) \, t_{res}(i) < E_{b,c}(i) - E_{HP,r}(i) < P_{HP,c,2/2}(i) \, t_{res}(i) \end{cases} \tag{3.30}$$

The energy $E_{HP,c}$ that the heat pump delivers to the building for air-conditioning in cooling-only mode is:

$$E_{HP,c}(i) = P_{HP,c,2/2}(i) \, t_{c,2/2}(i) + P_{HP,c,1/2}(i) \, t_{c,1/2}(i) \ . \tag{3.31}$$

The electric energy used by the heat pump in heat recovery mode ($E_{HP,r,us}$) and in cooling-only mode ($E_{HP,c,us}$) are calculated by means of Eq. (3.32) and Eq. (3.33), respectively:

$$E_{HP,r,us}(i) = \left[\frac{P_{HP,r,2/2}(i)}{EER_{r,2/2}(i)} t_{r,2/2,eff}(i) + \frac{P_{HP,r,1/2}(i)}{EER_{r,1/2}(i) \, f_{corr,r}(i)} t_{r,1/2,eff}(i) \right] , \tag{3.32}$$

$$E_{HP,c,us}(i) = \left[\frac{P_{HP,c,2/2}(i)}{EER_{c,2/2}(i)} t_{c,2/2}(i) + \frac{P_{HP,c,1/2}(i)}{EER_{c,1/2}(i) \, f_{corr,c}(i)} t_{c,1/2}(i) \right] , \tag{3.33}$$

where $f_{corr,r}$ and $f_{corr,c}$ are the *EER* correction factors for on-off cycles, in heat recovery mode and cooling-only mode, respectively. $f_{corr,r}$ and $f_{corr,c}$ are evaluated according to Ref. [10], using the values of the capacity ratio *CR* obtained through Eq. (3.34) and Eq. (3.35), respectively:

$$CR_r(i) = \frac{P_{b,c}(i)}{P_{HP,r,1/2}(i)} \quad, \tag{3.34}$$

$$CR_c(i) = \frac{E_{b,c}(i) - E_{HP,r}(i)}{P_{HP,c,1/2}(i)\, t_{res}(i)} \quad. \tag{3.35}$$

If the capacity ratio turns out greater than 1, it is set equal to 1.

A similar procedure can be adopted in order to model an IDHP.

If in the i-th bin $E_{b,d}$ is higher than $E_{HP,d}$, the back-up system for DHW (if present) must be activated in order to supply the missing thermal energy, E_{bk}. The corresponding energy used by the back-up system, $E_{bk,us}$, is equal to the ratio between E_{bk} and the efficiency η_{bk} of the back-up system.

Finally, the seasonal energy values are obtained by summing the corresponding values of each bin, and the seasonal performance coefficients of the system can be evaluated. The Seasonal Energy Efficiency Ratio, $SEER$ (Eq. (3.36), from Ref. [10]), is the ratio between the total cooling energy provided by the heat pump and the corresponding electric energy used. The Fuel Utilization Efficiency, FUE (Eq. (3.37)), for summer operation is the ratio between the total energy delivered to the building by the heat pump and the back-up system (for air-conditioning and DHW production) and the corresponding primary energy used.

$$SEER = \frac{\sum_i E_{HP,r}(i) + \sum_i E_{HP,c}(i)}{\sum_i E_{HP,r,us}(i) + \sum_i E_{HP,c,us}(i)} \quad, \tag{3.36}$$

$$FUE = \frac{\sum_i E_{HP,r}(i) + \sum_i E_{HP,c}(i) + \sum_i E_{HP,d}(i) + \sum_i E_{bk}(i)}{\dfrac{\sum_i E_{HP,r,us}(i) + \sum_i E_{HP,c,us}(i)}{\eta_{el}} + \sum_i E_{bk,prim}(i)} \quad. \tag{3.37}$$

In Eq. (3.37), $E_{bk,prim}$ is the primary energy used by the back-up system for DHW production, equal to $E_{bk,us}$ in the case of a gas boiler, or equal to the ratio between $E_{bk,us}$ and η_{el} in the case of electric heaters.

3.3 CASE STUDIES

The topics of this section are discussed in Refs. [61]-[64].

3.3.1 Seasonal performance of air-to-water heat pumps for heating

The mathematical model for winter operation presented in Section 3.1 is here applied to evaluate the seasonal efficiency of mono-compressor on-off, multi-compressor and inverter-driven heat pumps, integrated by electric heaters as back-up system, and used to provide heating to several buildings, located in different Italian climates. The influence of the outside climate on the seasonal performance of different kinds of heat pumps is investigated. Figure 3.6 shows the bin distribution for the heating season of three different Italian cities: Brescia (45.32 °N, 10.12 °E), Florence (43.41 °N, 11.15 °E) and Trapani (38.01 °N, 12.32 °E). The conventional heating season is from October 15th to April 15th for Brescia, from November 1st to April 15th for Florence and from December 1st to March 31st for Trapani.
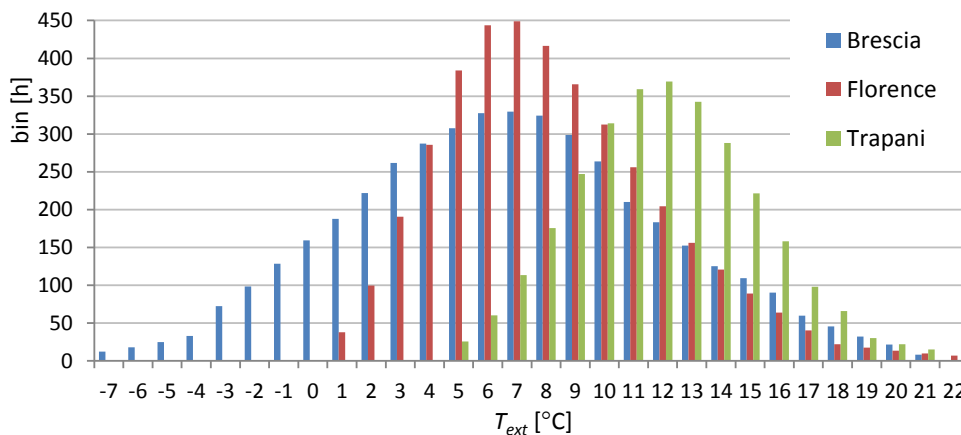
Figure 3.6: Bin distribution for the heating season in Brescia, Florence and Trapani (Italy).

By observing the charts of Figure 3.6, the difference in terms of weather among the selected localities is clear: Brescia, in the North of Italy, is characterized by the lowest external temperature, with a minimum, equal to $T_{des,h}$, at -7 °C, and a mode of the bin distribution equal to 7 °C; Florence, North-Center Italy, is characterized by a value of $T_{des,h}$ equal to 0 °C, with a minimum external air temperature of 1 °C, and a mode of the distribution equal to 7 °C; Trapani, Southern Italy, is characterized by a minimum outdoor temperature, equal to $T_{des,h}$, at 5 °C, and a mode of the distribution equal to 12 °C.

In order to take into account the effects of the building heating loads on the heat pump seasonal performance, several linear building energy signatures are considered, by setting T_{zl}

equal to 16 °C (according to Ref. [10]), and by varying the value of $P_{des,h}$. In Figure 3.7, the dashed line is an example of BES, drawn by considering a building with a design load $P_{des,h}$ equal to 43.13 kW ($T_{des,h}$ = -7 °C), while the dotted line represents a building having a design load equal to 71.88 kW ($P'_{des,h}$).
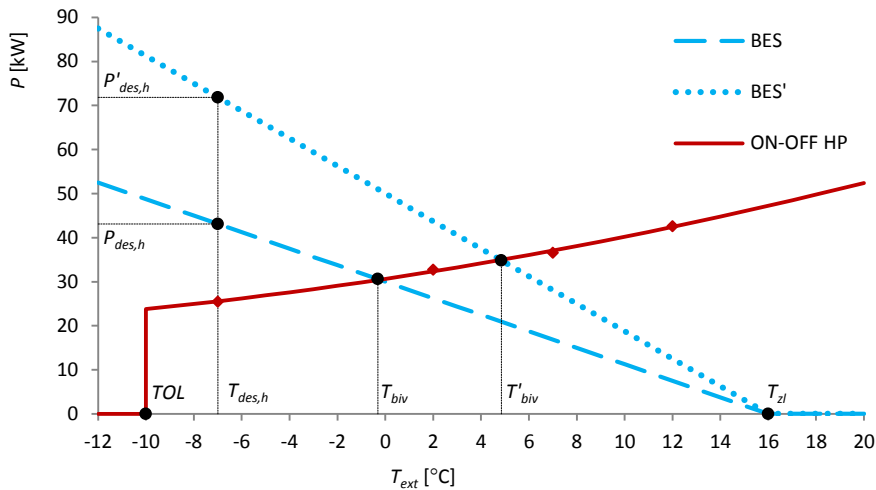
Figure 3.7: BES and characteristic curve of the ON-OFF HP.

The red line in Figure 3.7 represents the characteristic curve of the considered electric air-source mono-compressor on-off heat pump, obtained for a value equal to 35 °C of the temperature $T_{w,h}$ of the hot water produced for heating. The curve is stopped in correspondence of a value of Temperature Operative Limit, given by the heat pump manufacturer, equal to -10 °C, and the intersection between the heat pump characteristic curve and the building energy signature yields a bivalent temperature equal to -0.3 °C, considering the dashed BES, and equal to 4.8 °C, considering the dotted BES.

Tables 3.2, 3.3 show the manufacturer data for the considered ON-OFF HP, MCHP and IDHP.

Table 3.2: Heat pumps technical data.

Heat pump typology	ON-OFF HP	MCHP	IDHP
TOL [°C]	-10	-10	-18
N	1	2	1
Φ range [Hz]	50	50	30-120

Table 3.3: Heat pumps thermal power and *COP* at maximum and minimum capacity.

T_{ext} [°C]	$T_{w,h}$ [°C]	ON-OFF HP power [kW] and (*COP*)	MCHP power [kW] and (*COP*)		IDHP power [kW] and (*COP*)	
			$n = 1$	$n = 2$	Φ_{min}	Φ_{max}
TOL	35	23.30 (2.75)	12.30 (2.76)	23.10 (2.70)	5.58 (2.48)	19.90 (1.86)
-7	35	25.50 (3.07)	13.20 (2.95)	25.00 (2.90)	6.87 (3.05)	26.10 (2.85)
2	35	32.70 (3.83)	16.70 (3.71)	31.20 (3.59)	8.68 (3.86)	32.40 (3.49)
7	35	36.60 (4.23)	19.30 (4.26)	34.80 (3.98)	10.00 (4.48)	36.40 (3.91)
12	35	42.60 (4.86)	22.30 (4.89)	40.80 (4.65)	11.60 (5.25)	41.70 (4.45)

By comparing the data shown in Table 3.3, it is evident that, with the same temperature of the two sources (air: T_{ext}, water: $T_{w,h}$), the heat pumps selected are characterized by very similar values of the maximum thermal power delivered.

The seasonal performance of the system is evaluated by means of the model of Section 3.1 in different conditions, by varying the combinations of heat pump (ON-OFF HP, MCHP, or IDHP) – building (different building energy signatures) – location (Brescia, Florence, or Trapani). Some significant numerical results are reported in Table 3.4.

The values of T_{biv}, and, for the MCHP and the IDHP, also of the secondary bivalent temperature, $T_{biv,2}$, are reported in Table 3.4 together with the seasonal energy values and the obtained $SCOP_{net}$ and $SCOP_{on}$.

The values of $E_{HP,h,us}$ highlight as the ON-OFF HP uses more electric energy than the MCHP and IDHP, in similar conditions, while the value of $E_{bk,h}$ (equal to $E_{bk,h,us}$) is an indication of the level of under-sizing of the heat pump with respect to the building thermal needs. Obviously, if $E_{bk,h}$ is equal to 0 (no back-up activation needed), the value of $SCOP_{on}$ equals that of $SCOP_{net}$.

Table 3.4: Numerical results of some case studies.

$T_{des,h}$ [°C]	$P_{des,h}$ [kW]	Heat pump typology	T_{biv} [°C]	$T_{biv,2}$ [°C]	$E_{b,h}$ [MWh]	$E_{HP,h}$ [MWh]	$E_{HP,h,us}$ [MWh]	$E_{bk,h}$ [MWh]	$SCOP_{net}$	$SCOP_{on}$
-7	28.75	ON-OFF HP	-5.3	/	51.21	51.15	17.82	0.066	2.87	2.86
-7	115.00	ON-OFF HP	8.3	/	204.86	126.17	36.41	78.68	3.47	1.78
-7	28.75	MCHP	-4.8	2.5	51.21	51.12	13.96	0.0939	3.66	3.65
-7	115.00	MCHP	8.6	11.6	204.86	121.83	31.31	83.02	3.89	1.79
-7	28.75	IDHP	-5.5	7.8	51.21	51.16	12.49	0.051	4.10	4.08
-7	115.00	IDHP	8.4	13.6	204.86	125.84	32.05	79.01	3.93	1.84
0	30	ON-OFF HP	-0.3	/	58.55	58.55	18.41	0	3.18	3.18
0	110	ON-OFF HP	10.1	/	214.67	129.37	35.16	85.30	3.68	1.78
0	30	MCHP	0.3	6.0	58.55	58.55	14.57	0	4.02	4.02
0	110	MCHP	10.4	12.7	214.67	124.25	30.32	90.42	4.10	1.78
0	30	IDHP	-0.3	10.1	58.55	58.55	13.07	0	4.48	4.48
0	110	IDHP	10.2	14.2	214.67	128.32	31.40	86.35	4.09	1.82
5	34.38	ON-OFF HP	4.8	/	37.54	37.54	10.91	0	3.44	3.44
5	75.63	ON-OFF HP	10.1	/	82.59	71.29	18.26	11.30	3.90	2.79
5	34.38	MCHP	5.2	9.4	37.54	37.52	8.63	0.02	4.35	4.34
5	75.63	MCHP	10.4	12.7	82.59	69.62	15.63	12.97	4.45	2.89
5	34.38	IDHP	4.9	12.3	37.54	37.54	7.66	0	4.90	4.90
5	75.63	IDHP	10.2	14.2	82.59	70.78	15.52	11.81	4.56	3.02

In Figures 3.8-3.13 the $SCOP_{net}$ and $SCOP_{on}$ trends as functions of the bivalent temperature are shown with continuous lines for each building location and type of heat pump considered. As pointed out by Figures 3.8-3.13, the best $SCOP$ values are almost always obtained with the inverter-driven heat pump, while the ON-OFF HP gives the lowest results.
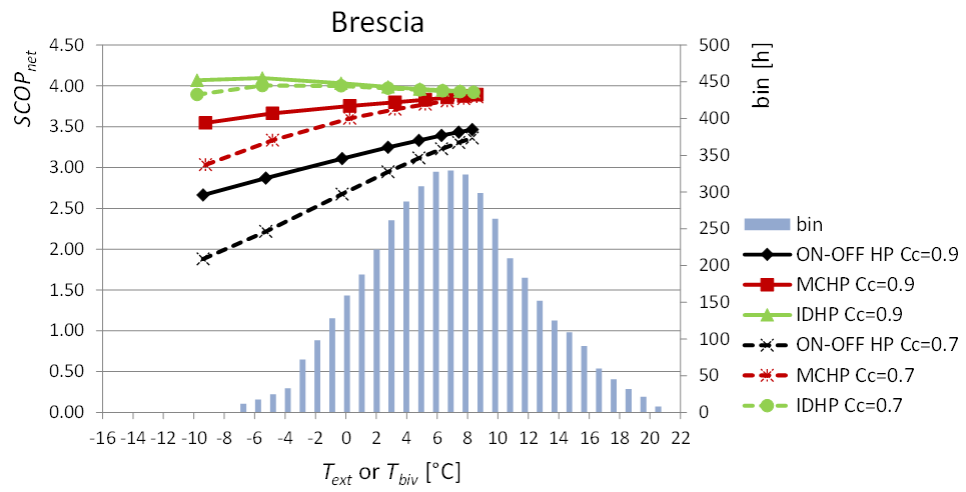
Figure 3.8: $SCOP_{net}$ and bin distribution for Brescia.
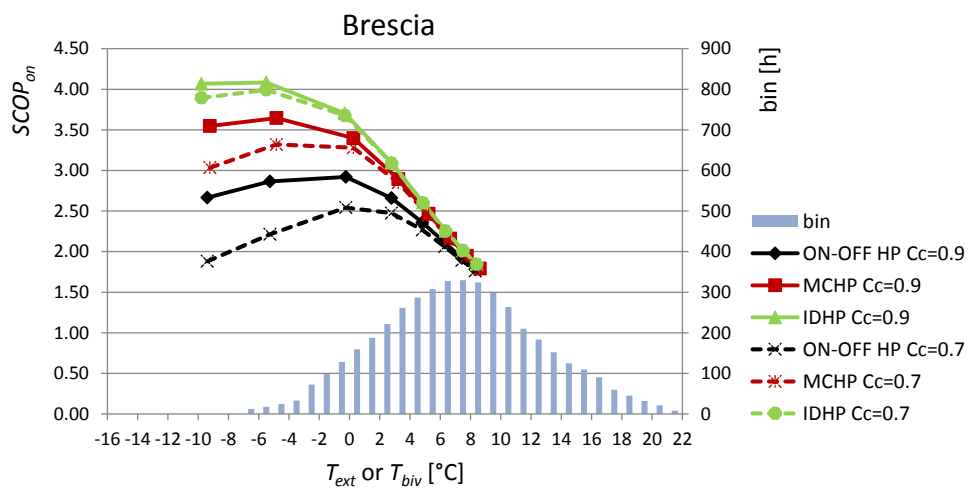
Figure 3.9: $SCOP_{on}$ and bin distribution for Brescia.
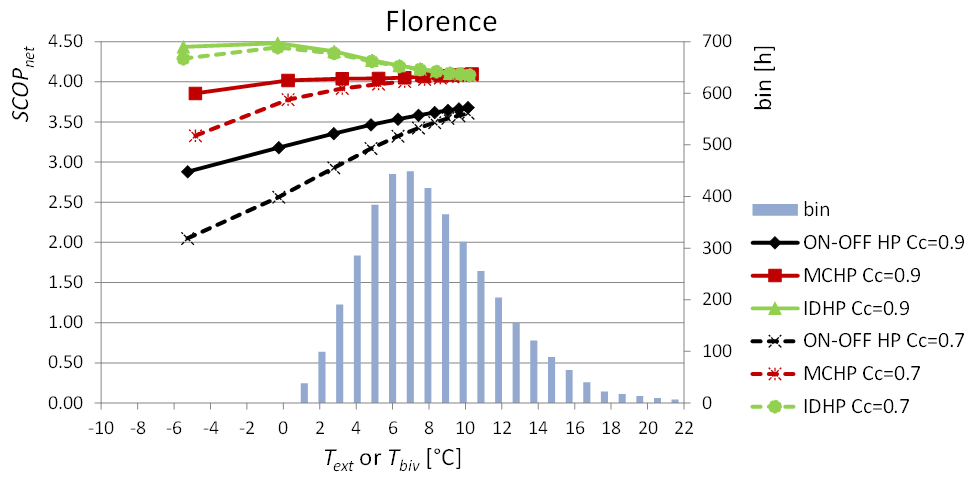
Figure 3.10: $SCOP_{net}$ and bin distribution for Florence.
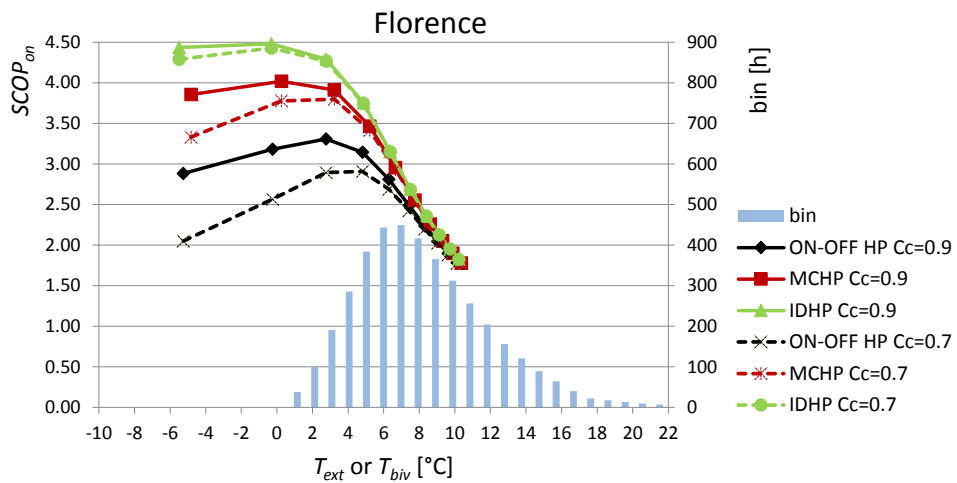
Figure 3.11: $SCOP_{on}$ and bin distribution for Florence.
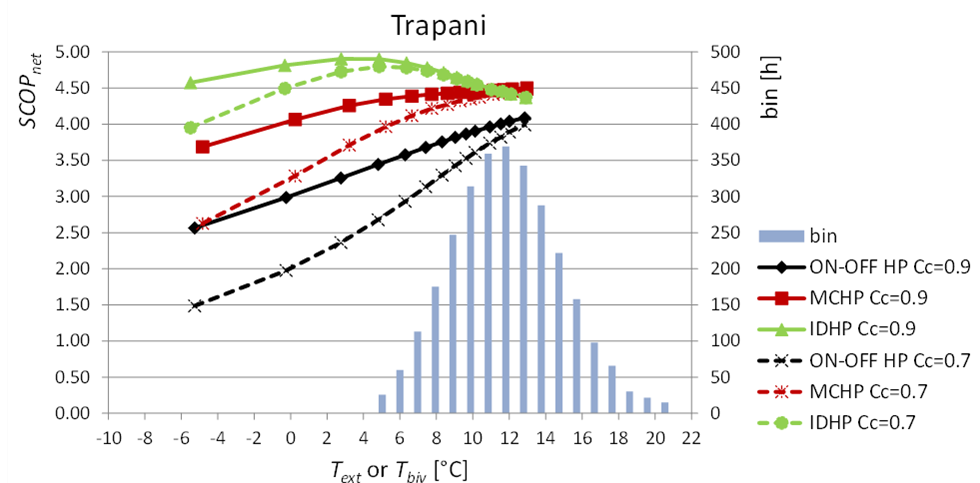
Figure 3.12: *SCOP_net* and bin distribution for Trapani.
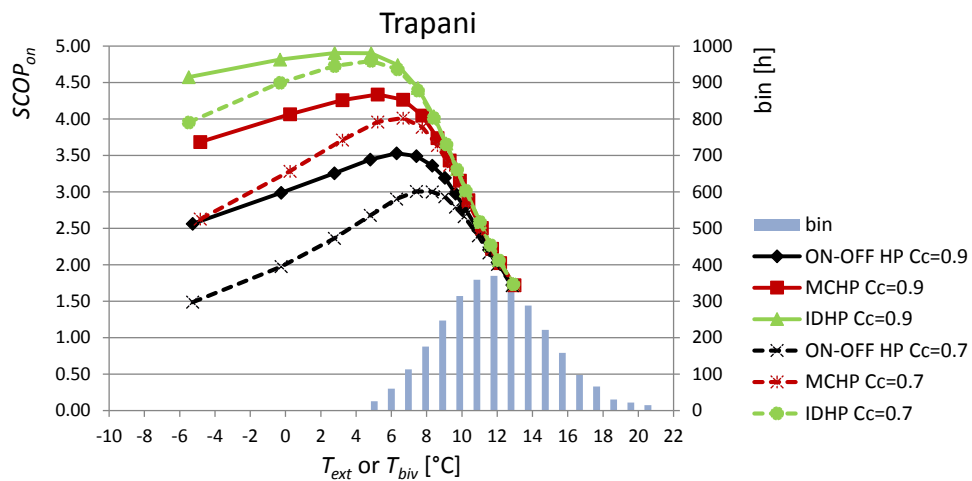
Figure 3.13: *SCOP_on* and bin distribution for Trapani.

As highlighted by Figures 3.9, 3.11, 3.13, there is a value of bivalent temperature which maximizes the *SCOP_on*, which means that there exists an optimal choice of the heat pump size, for a fixed building and location.

The highest values of *SCOP_net* and *SCOP_on* are achievable in the hottest climate (Trapani) by selecting an IDHP having a bivalent temperature equal to the design temperature ($T_{des,h}$ = 5 °C). This result is confirmed also for Brescia and Florence (Figures 3.8-3.11). Therefore, it is possible to conclude that the best seasonal performance of an IDHP can be generally obtained by adopting as bivalent temperature the design temperature.

This conclusion is not valid for MCHPs and especially for ON-OFF HPs; in these cases, the results of Figures 3.9, 3.11, 3.13 demonstrate that, in order to maximize the $SCOP_{on}$, there exists an optimal bivalent temperature, but this value is always larger than the design temperature.

In terms of $SCOP_{net}$, the trend is monotonically increasing with the value of T_{biv}, apart from the case of IDHP, for which the $SCOP_{net}$ trend in each climate has a peak in correspondence of a value of T_{biv} equal to the design temperature, $T_{des,h}$.

The $SCOP_{on}$ trend, which always shows a maximum point in proximity of $T_{des,h}$ for the IDHP, and towards larger values of the bivalent temperature for the MCHP and ON-OFF HP, is maximized with a value of T_{biv} higher for hotter climates.

The difference in both the $SCOP_{net}$ and $SCOP_{on}$ values caused by the different types of heat pumps becomes more and more negligible with the increasing of T_{biv}.

The $SCOP$ values of the dashed lines in Figures 3.8-3.13 have been obtained, in comparison with the $SCOP$ values of the continuous lines, by adopting a different value of the degradation coefficient, C_c, used in the evaluation of the COP correction factor for on-off cycles (see Eq. (2.1)).

The numerical value of the degradation coefficient must be experimentally quantified by the manufacturer, but, in absence of indications, the standards [10], [11] suggest to use a value of C_c equal to 0.9: this value of C_c has been used for the evaluation of the $SCOP$ shown in Figures 3.8-3.13 with continuous lines.

However, as demonstrated in [28], the value of C_c suggested by the standards has proved to be too optimistic in order to take into account the real losses linked to the impact of the on-off cycles on the COP of a real heat pump. As a consequence, the same calculation has been repeated by considering a value of C_c equal to 0.7 (similar to that found in Ref. [28]) and the obtained $SCOP$ values are shown by using dashed curves in Figures 3.8-3.13. In this way, it is possible to highlight the impact of the degradation coefficient on the evaluation of the seasonal performance of the air-source heat pumps with different sizing conditions.

Obviously, the degradation coefficient value is more influent on the value of the $SCOP$ for ON-OFF HPs, with respect to MCHPs or IDHPs, since, for external air temperatures higher than T_{biv}, mono-compressor on-off heat pumps must start the on-off cycles in order to follow the building demand, while, for MCHPs and IDHPs, the on-off condition is avoided until T_{ext} is higher than $T_{biv,2}$.

The difference between the $SCOP_{on}$ values obtained with C_c equal to 0.9, with respect to the ones calculated in the same conditions with C_c equal to 0.7, ranges from 0 %, (IDHP in Trapani with T_{biv} = 12.9 °C), up to 42 % (ON-OFF HP in Trapani with T_{biv} = -5.3 °C).

The role of the degradation coefficient becomes more significant for lower values of the bivalent temperature T_{biv}, which means that C_c is more important when heat pumps over-sized with respect to the building needs are adopted. A lower value of T_{biv}, in fact, corresponds to a lower value of $T_{biv,2}$ (which represents the maximum external air temperature at which the on-off cycles can be avoided). Obviously, $T_{biv,2}$ coincides with T_{biv} for an ON-OFF HP.

The difference between the results obtained with the different C_c values is also enhanced at hotter climates (compare Figures 3.8, 3.9 with Figures 3.12, 3.13, respectively): the bin distribution is shifted to higher temperatures, with a consequent increase of the number of the seasonal on-off cycles.

3.3.2 Summer performance of reversible air-to-water heat pumps with heat recovery for domestic hot water production

The mathematical model for summer operation presented in Section 3.2 is here applied to evaluate the seasonal performance of two commercial air-to-water reversible heat pumps, with similar full-load capacity: a MCHP with two compressors and an IDHP with frequency range 30 - 88 Hz. The heat pumps are placed at the service of several buildings in Palermo (Southern Italy, 38 ° 06 ' N, 13 ° 21 ' E) and are integrated by electric heaters as back-up system for DHW.

Figure 3.14 shows the bin distribution obtained for Palermo, considering a cooling season from May 15th to September 15th. It can be noticed from Figure 3.14 that the outdoor temperature in Palermo during summer runs from a minimum value of 9 °C to a maximum one of 35 °C, with a mode of the distribution equal to 23 °C.
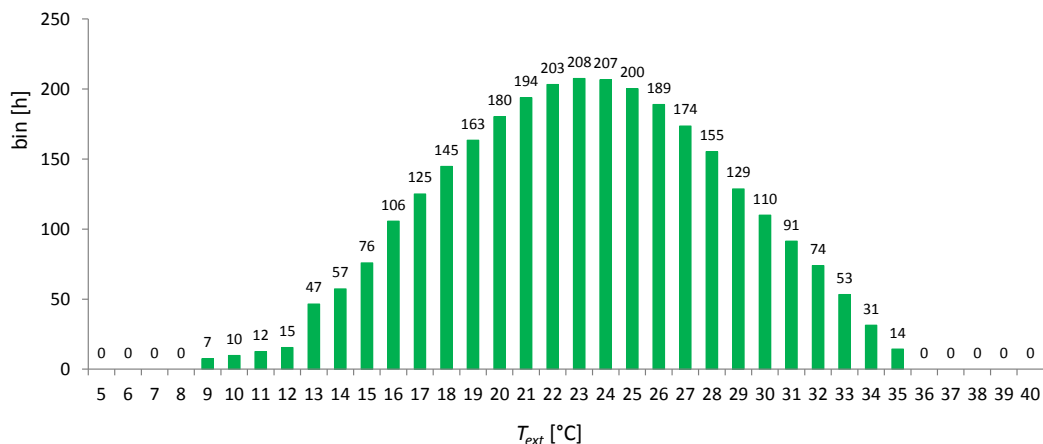
Figure 3.14: Bin distribution for the cooling season in Palermo (Italy).

Table 3.5 shows the heat pumps technical data declared by the manufacturer, for the maximum and minimum capacity, in cooling-only mode ($T_{w,c}$ = 7 °C) and in heat recovery mode for DHW production ($T_{w,d}$ = 55 °C).

Table 3.5: Heat pumps cooling power and *EER* at maximum and minimum capacity ($T_{w,c}$ = 7 °C).

	MCHP power [kW] and (*EER*)		IDHP power [kW] and (*EER*)	
T_{ext} [°C]	n = 2	n = 1	Φ_{max}	Φ_{min}
20	25.10 (4.49)	14.40 (4.81)	26.80 (4.41)	10.3 (4.88)
25	23.90 (4.06)	13.20 (4.19)	25.80 (3.88)	9.89 (4.31)
30	22.70 (3.55)	12.50 (3.69)	24.60 (3.38)	9.49 (3.83)
35	21.40 (3.04)	11.80 (3.17)	23.30 (2.93)	9.04 (3.37)
$T_{w,d}$ = 55 °C	17.90 (2.10)	9.70 (2.37)	20.40 (2.22)	7.51 (2.60)

The effect of the building cooling load on the seasonal efficiency is analyzed by taking into account different building energy signatures, in which T_{zl} is set equal to 16 °C (according to Ref. [10]) and $P_{des,c}$ in correspondence of $T_{des,c}$ (35 °C) is varied. As no back-up system for air-conditioning is present, the choice of the building – heat pump combinations has been made in order to have the building cooling demand fully covered at the highest outdoor temperature.

Different building loads for DHW production are also considered, by varying the ratio between the building total DHW demand, $E_{b,d,tot}$, and total cooling demand, $E_{b,c,tot}$.

Figure 3.15 shows the *SEER*, as a function of the ratio between $E_{b,d,tot}$ and $E_{b,c,tot}$, obtained with the selected heat pumps, with several building cooling loads.
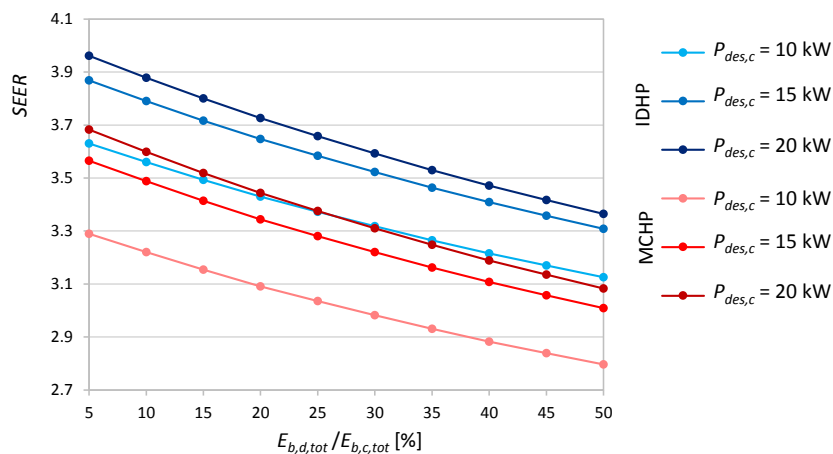
Figure 3.15: *SEER* with different building loads.

The obtained *SEER* ranges from 2.80 (MCHP, $P_{des,c}$ = 10 kW, $E_{b,d,tot}$ = 50 % $E_{b,c,tot}$) to 3.96 (IDHP, $P_{des,c}$ = 20 kW, $E_{b,d,tot}$ = 5 % $E_{b,c,tot}$) and it decreases with the increase of the building DHW demand, because of the increase of time in heat recovery mode, where the heat pump releases the condensation heat at higher temperature ($T_{w,d}$ = 55 °C versus $T_{des,c}$ = 35 °C).

In addition, for a selected heat pump and fraction of DHW building demand, worse seasonal efficiency is obtained with lower $P_{des,c}$: in this case, the heat pump is oversized with respect to the building cooling demand, with consequent increase of the heat pump on-off cycles.

On the same conditions, the IDHP (blue curves in Figure 3.15) reaches better *SEER* with respect to the MCHP (red curves in Figure 3.15), thanks to higher *EER* values at part load and to a lower number of on-off cycles (the IDHP is able to reach a minimum capacity lower than that of the MCHP).

This result is confirmed by Figure 3.16, where the correction factors for on-off cycles $f_{corr,r}$ and $f_{corr,c}$ are reported as functions of the outdoor temperature for $P_{des,c}$ = 20 kW and $E_{b,d,tot}$ / $E_{b,c,tot}$ = 15 %.
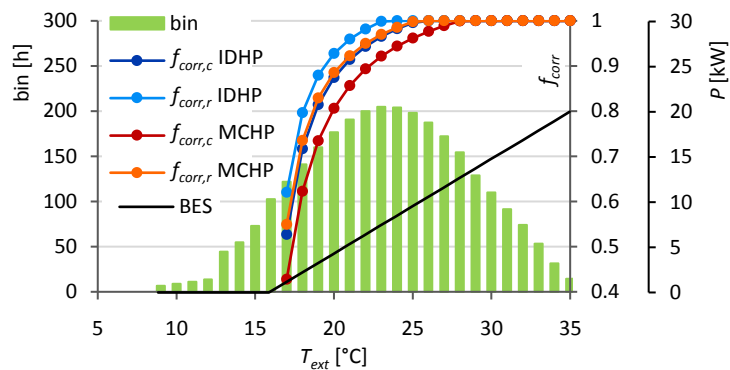
Figure 3.16: f_{corr} in cooling-only and heat recovery mode ($P_{des,c}$ = 20 kW; $E_{b,d,tot}$ / $E_{b,c,tot}$ = 15 %), BES, bin trend.

The correction factors are equal to 1 (no on-off cycles) for high values of T_{ext}, while they decrease when T_{ext} decreases. This result is due to the increase of the number of on-off cycles, owing to the decrease of both the building cooling demand (low BES values) and the DHW demand (low number of bin hours).

The curves shown in Figure 3.16 highlight that the IDHP is characterized by values of f_{corr} higher than those of the MCHP, both in cooling-only mode and in heat recovery mode.

Figure 3.17 shows the trend of the *FUE* as a function of the building cooling and DHW demand, obtained with the selected IDHP integrated by electric back-up, and with a traditional system, in which the reversible heat pump only provides air-conditioning and the domestic hot water

is entirely produced by a gas boiler. The comparison has been made by using for the traditional system the same IDHP (without heat recovery mode) and a gas boiler with an efficiency of 0.98.
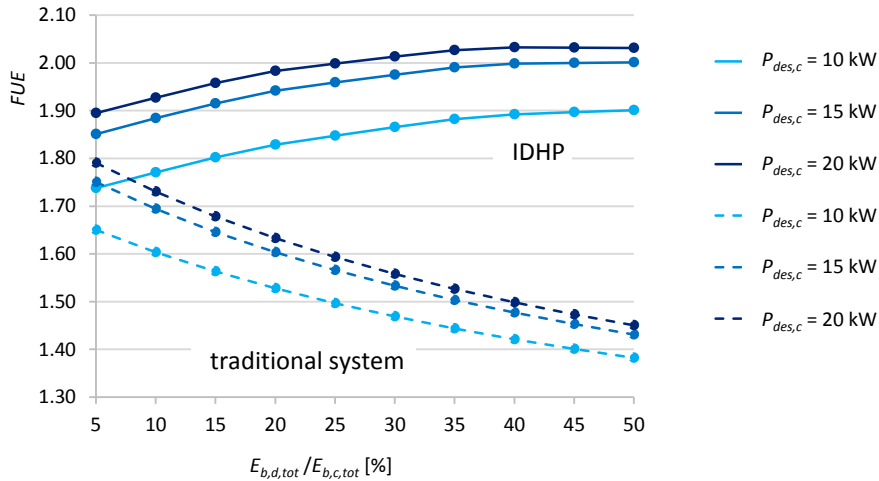
Figure 3.17: *FUE* of IDHP and traditional system with different building loads.

On the same conditions, the *FUE* of the studied system is higher than that of the traditional system and this gap is enhanced for high DHW demand (*FUE* = 2.03 versus *FUE* = 1.45 for $P_{des,c}$ = 20 kW, $E_{b,d,tot}$ = 50 % $E_{b,c,tot}$). In fact, even if the primary energy used for cooling by the traditional system is lower (heat released to the outdoor air, i.e. at lower temperatures, with consequent better *EER* values), the primary energy used by the gas boiler (which provides to all the DHW demand) is higher than that used by the electric back-up (which only supplies the energy for DHW which the chiller cannot provide in heat recovery mode).

Figure 3.18 shows the primary energy saving obtainable by using the studied system with respect to the traditional solution, with different building cooling and DHW demands.

The primary energy saving is higher for higher DHW fractions and with the IDHP than with the MCHP. In particular, the primary energy saving obtained can reach 31 %, by using the inverter-driven heat pump with a building design load equal to 20 kW and with a total domestic hot water demand equal to 50 % of the total cooling demand.
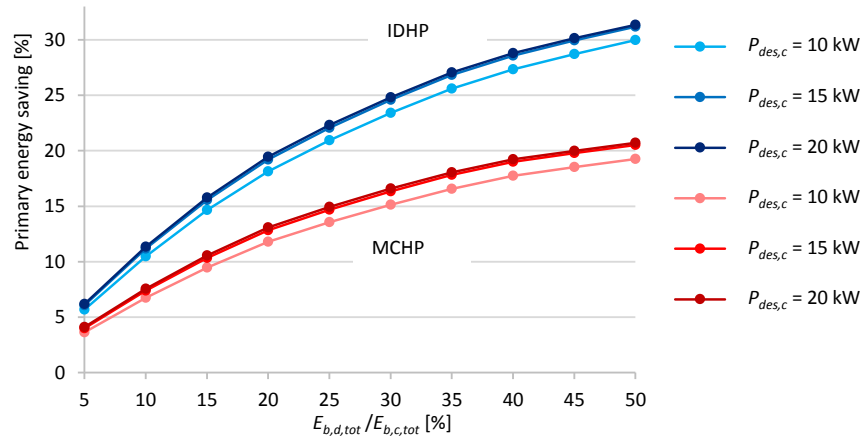
Figure 3.18: Primary energy saving, with respect to traditional system, with different building loads.

4

DYNAMIC SIMULATION CODES FOR AIR-TO-WATER HEAT PUMPS

In this chapter, numerical codes for the dynamic simulation of electric air-to-water heat pumps are presented. The codes, executable through any programming language and here implemented in MATLAB, apply to the hourly simulation of air-to-water heat pumps used for building heating, cooling and domestic hot water production, coupled with storage tanks and integrated by a gas boiler or electric heaters. The method applies both to mono-compressor on-off heat pumps and to inverter-driven ones.

Unlike the bin-method, the dynamic simulation is able to take into account the presence of a water storage tank, as it can evaluate, hour by hour, the mean temperature of the water in the storage and the corresponding energy contained.

The first section relates to the code developed for heating and DHW production during winter and presents some numerical results obtained in a test case. The second section describes the code developed for summer operation, during which the heat pump provides cooling and DHW production, with the possibility of heat recovery mode. The application of the dynamic codes to evaluate the seasonal performance of the multi-function inverter-driven heat pump used in the retrofit of a residential building is then presented.

Then, the dynamic models are validated by comparison with results obtained in simple case studies with the software TRNSYS. Finally, the hourly simulation methods for air-to-water heat pumps are compared with the bin-method.

4.1 MATLAB CODE FOR WINTER OPERATION

A numerical method for the hourly simulation of air-to-water heat pumps for heating and DHW production, written on the software MATLAB, is presented.

The studied system consists of a multi-function air-to-water heat pump, used in winter for both heating and DHW production, coupled with a storage tank for heating and a storage tank for instantaneous DHW production, and integrated by electric heaters or a gas boiler. The topics of this section are treated in Refs. [65], [66].

4.1.1 Climate implementation

To perform a dynamic simulation of an air-source heat pump, the hourly values of the external air temperature must be known. These values can be taken from local weather station recordings, being thus the effective outdoor temperature values for a selected period and location. Otherwise, the Typical Meteorological Year (TMY), like the Meteonorm TMY available on the software TRNSYS for several cities worldwide, can be used.

In Figure 4.1 the external air temperature profile, according to the Meteonorm file on TRNSYS, is plotted for the heating season in the Italian city of Bologna, while in Figure 4.2 the corresponding monthly average outdoor temperatures are compared with those of the standard UNI 10349 [25]. The heating season in Bologna is here considered from October to April, included.
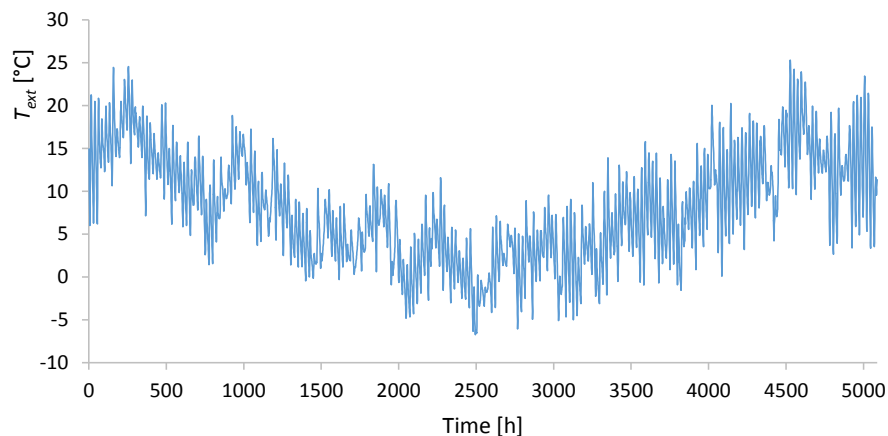
Figure 4.1: Hourly trend of the external air temperature during the heating season in Bologna (Italy) from Meteonorm TMY.
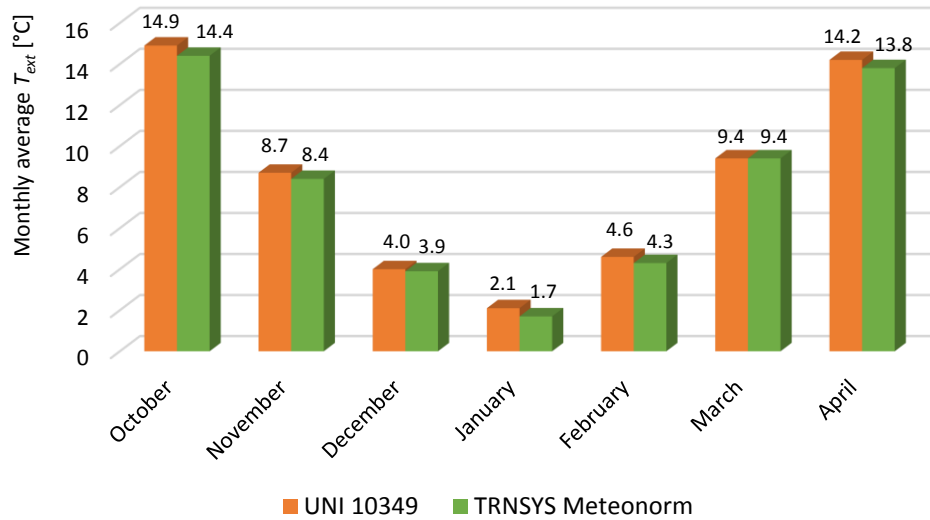
Figure 4.2: Monthly average outdoor temperatures for the heating season in Bologna (Italy).

From Figure 4.2 one can notice that, during winter, the minimum monthly average outdoor temperature (which occurs in January) is equal to 2.1 °C according to Ref. [25] and 1.7 °C according to the Meteonorm profile available on TRNSYS, while the maximum monthly average outdoor temperature (occurring in October) is equal to 14.9 °C according to Ref. [25] and 14.4 °C according to the Meteonorm profile.

4.1.2 Building hourly energy need for heating

The hourly values of the thermal energy needed by the building for heating, $E_{b,h}(i)$, are input data for the heat pump dynamic simulation code and can derive from a dynamic simulation of the building, performed by means of software like TRNSYS, EnergyPlus or ESP-r. Obviously, the hourly values of the energy required at the outlet of the generation subsystem (heat pump) must be used, which means that the hourly values of the energy properly needed by the building must be divided by the product of the distribution, emission and control efficiencies for heating.

If a dynamic simulation of the building is not available, an approximation of the hourly energy need can be obtained by using the building energy signature (BES). Once the value $T_{ext}(i)$ of the external air temperature in the i-th hour is known, the hourly value of the thermal power required by the building is, through the BES, a function of T_{ext}; the corresponding value of $E_{b,h}(i)$ is obtained by multiplying the value of the thermal power by the hour duration.

4.1.3 Building hourly energy need for domestic hot water

A residential building daily energy need for DHW production is evaluated according to Eq. (3.4) from Ref. [59]. The energy needed in correspondence of each hour, $E_{b,d}(i)$, can be obtained according to Eq. (4.1):

$$E_{b,d}(i) = \frac{E_{b,d,day}}{\eta_{em,d}\ \eta_{dis,d}}\,p_d(i)\ , \tag{4.1}$$

where $p_d(i)$ is the hourly load coefficient for DHW in residential buildings, according to the standard UNI/TS 11300-4 [11]. The value of $p_d(i)$, which gives the fraction of the daily energy demand charged to the *i*-th hour (on the basis of the daily profile for DHW provided by Ref. [11]), repeats itself every 24 hours within the selected simulation time period.

Table 4.1 provides the hourly values of the coefficient p_d defined by Ref. [11].

Table 4.1: Hourly load coefficients for domestic hot water in residential buildings.

Hour	1	2	3	4	5	6	7	8	9	10	11	12
p_d [%]	2.50	2.80	2.80	0.00	0.00	0.00	13.90	13.90	13.90	2.80	2.80	2.80
Hour	13	14	15	16	17	18	19	20	21	22	23	24
p_d [%]	2.80	0.70	0.70	0.70	0.70	13.90	13.90	2.80	2.80	2.80	0.00	0.00

Table 4.1 shows that Ref. [11] considers a peak of energy demand for DHW in residential buildings from 6:00 am to 9:00 am and from 5:00 pm to 7:00 pm.

4.1.4 Heat pump and thermal storage characterization for winter operation

To characterize the air-to-water heat pump, used in winter for heating and DHW production, the procedure described in Subsection 3.1.4 is used. Through interpolations of the manufacturer data by using second-order polynomial functions, curves of the heat pump power and *COP*, in heating mode and in DHW mode, are thus obtained as functions of the external air temperature, T_{ext}, for a fixed value of the hot water produced. In the case of inverter-driven heat pumps, a family of curves for the heat pump power and a family of curves for the heat pump *COP* are obtained, by varying the inverter frequency between the maximum and minimum value.

Combining in a single bin all the hours with the same external air temperature, the bin-method (Chapter 3) is not able to simulate a thermal storage tank, since it cannot evaluate the energy stored in a tank during a specific time, to be used later, if necessary. The

MATLAB dynamic simulation codes, on the contrary, have the possibility to consider the presence of storage tanks coupled with the heat pump.

A scheme of the studied system is reported in Figure 4.3, showing the different components of a multi-function heat pump coupled with a storage tank for heating and a storage tank for DHW (in this case integrated by electric heaters).
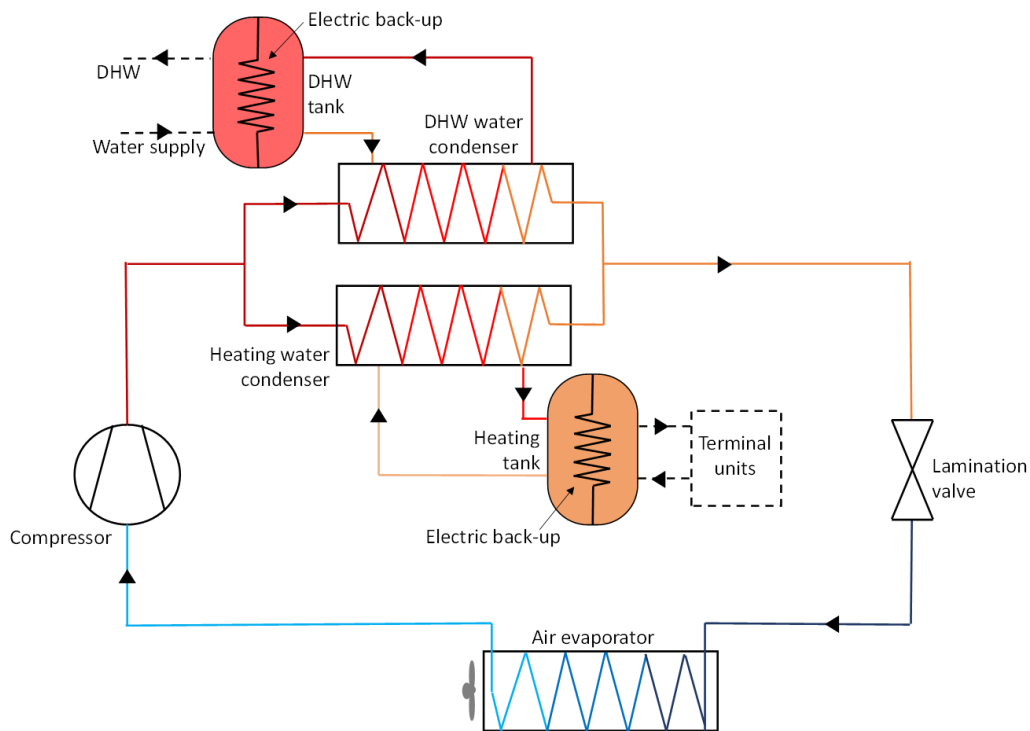
Figure 4.3: Plant scheme for winter operation.

It is important to observe that the storage tank for domestic hot water here considered is used for instantaneous DHW production, which means that the water coming from the aqueduct is heated while passing through the coil heat exchanger in the storage tank, whereas the water stored in the tank is not used as domestic hot water and, consequently, no measures against the legionella bacteria are needed.

The temperature of the water in the thermal storage tanks ($T_{s,h}$ for the heating tank and $T_{s,d}$ for the DHW one) can range from a fixed minimum to a maximum value ($T_{s,h,min}$ and $T_{s,h,max}$ for heating and $T_{s,d,min}$ and $T_{s,d,max}$ for DHW). As a consequence, the heat pump power and *COP* input data must be given for both these temperatures of the hot water produced and the procedure of Subsection 3.1.4 is repeated both fixing $T_{s,h}$ equal to $T_{s,h,min}$ and to $T_{s,h,max}$ (heating mode), or both fixing $T_{s,d}$ equal to $T_{s,d,min}$ and to $T_{s,d,max}$ (DHW mode).

To evaluate the storages heat losses, the hourly values of temperature of the storage room, $T_{s,room}(i)$, must be known. If not available, the values of $T_{s,room}(i)$ can be estimated by means of Eq. (4.2):

$$T_{s,room}(i) = T_{int} - b_u \left[T_{int} - T_{ext}(i) \right] , \tag{4.2}$$

where T_{int} is the selected internal air temperature (typically equal to 20 °C in winter for residential buildings) and b_u is the temperature reduction factor of the storage room, according to the standard EN 12831 [26]. The value of b_u can range from 0 (thermal storages placed in a heated room) to 1 (storages placed outside); b_u can be set equal to 0.5 in the case of thermal storages placed in a basement.

During each hour of the heating season, the heat pump considers priority of satisfaction of the building demand for DHW production, and, secondly, of the building demand for heating. The heating-only mode, or DHW-only mode, are obtainable by setting equal to zero the building DHW demand, or the building heating demand, respectively.

4.1.5 Hourly energy evaluations for winter operation

The input parameters of the MATLAB code for the dynamic simulation of the heat pump system in winter operation are: the hourly values $T_{ext}(i)$ of the external air temperature for the heating season; the hourly values of the building energy demand for heating, $E_{b,h}(i)$, and for DHW, $E_{b,d}(i)$; the thermal storage volumes, $V_{s,h}$ for heating and $V_{s,d}$ for DHW; the imposed minimum and maximum values of the water temperature in the thermal storages, $T_{s,h,min}$ and $T_{s,h,max}$, $T_{s,d,min}$ and $T_{s,d,max}$; the storage heat loss coefficients, $U_{s,h}$ for heating and $U_{s,d}$ for DHW; the heat pump power and *COP* data from the manufacturer; the efficiency η_{bk} of the back-up system; the hourly values of temperature of the storage room, $T_{s,room}(i)$.

Once evaluated the heat pump power and *COP* curves as functions of T_{ext} (through interpolations as described in Subsection 3.1.4), for each hour of the heating season the MATLAB code evaluates, through a *for* loop: the maximum power available from the heat pump, the energy supplied by the heat pump and by the back-up system (if any), the mean temperature of the water in the thermal storage tanks and the energy stored in the tanks, the energy lost by the storages, the energy used by the heat pump and by the back-up system. Firstly, the cut-off temperatures in heating-mode, $T_{cut-off,h}$, and in DHW-mode, $T_{cut-off,d}$, are evaluated. Let us note that the cut-off temperature is the external air temperature below which the heat pump is switched off, on the basis of the heat pump control system, and can be higher than the Temperature Operative Limit. The logic implemented in the MATLAB code turns off the heat pump, and leaves in operation only the back-up system, for the values of

T_{ext} at which the primary energy used by the heat pump becomes higher than that used by the back-up system. This situation occurs when the heat pump COP becomes lower than the ratio between $\eta_{bk,prim}$ and η_{el}. $\eta_{bk,prim}$ is the back-up efficiency, η_{bk}, in the case the back-up system is a gas boiler, whereas it is the thermodynamic efficiency of the electricity system, η_{el}, in the case the back-up system is composed by electric heaters.

In Figure 4.4, examples of curves of the heat pump COP and of the ratio between $\eta_{bk,prim}$ and η_{el} are plotted as functions of the external air temperature. Obviously, the ratio $\eta_{bk,prim} / \eta_{el}$ does not vary with the value of T_{ext} and is represented by a horizontal straight line in the plot of Figure 4.4.
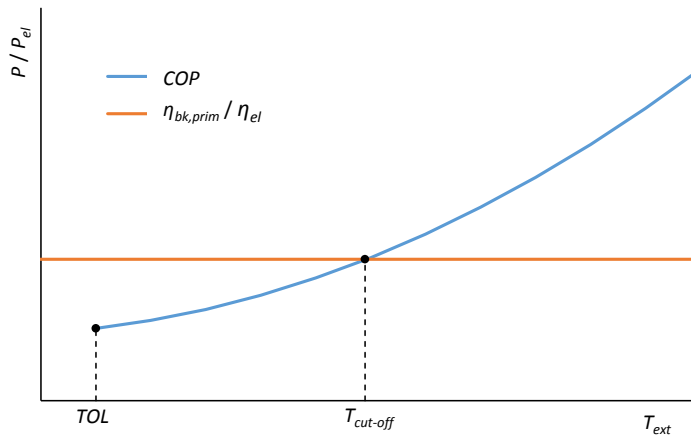
Figure 4.4: Examples of curves of the COP and of the ratio $\eta_{bk,prim} / \eta_{el}$ as functions of the external air temperature.

As put in evidence by Figure 4.4, the cut-off temperature coincides with the value of T_{ext} corresponding to the intersection between the parabolic curve of the COP and the straight line of $\eta_{bk,prim} / \eta_{el}$.

A heat pump COP depends not only on the value of T_{ext}, but also on the value of temperature of the hot water produced by the heat pump, and, for IDHPs, also on the value of the inverter frequency, parameters changing hour by hour. For the calculation of the cut-off temperature, the COP curves corresponding to $T_{s,h,max}$, in heating-mode, and to $T_{s,d,max}$, in DHW-mode, are chosen for precautionary reasons, and, for IDHPs, the maximum inverter frequency (Φ_{max}) is considered.

The cut-off temperatures in heating-mode and in DHW-mode are respectively evaluated according to Eq. (4.3) and Eq. (4.4), where the case on an IDHP is considered and the coefficient of Eq. (3.8) are recalled:

$$T_{cut-off,h} = \begin{cases} TOL_h & if\ b_{2,\Phi_{max}}^2(T_{s,h,max}) - 4\ a_{2,\Phi_{max}}(T_{s,h,max})\left[c_{2,\Phi_{max}}(T_{s,h,max}) - \dfrac{\eta_{bk,prim}}{\eta_{el}}\right] < 0 \\[3em] max\left[TOL_h;\ \dfrac{-b_{2,\Phi_{max}}(T_{s,h,max}) + \sqrt{b_{2,\Phi_{max}}^2(T_{s,h,max}) - 4\ a_{2,\Phi_{max}}(T_{s,h,max})\left[c_{2,\Phi_{max}}(T_{s,h,max}) - \dfrac{\eta_{bk,prim}}{\eta_{el}}\right]}}{2\ a_{2,\Phi_{max}}(T_{s,h,max})}\right] & else \end{cases} \tag{4.3}$$

$$T_{cut-off,d} = \begin{cases} TOL_d & if\ b_{2,\Phi_{max}}^2(T_{s,d,max}) - 4\ a_{2,\Phi_{max}}(T_{s,d,max})\left[c_{2,\Phi_{max}}(T_{s,d,max}) - \dfrac{\eta_{bk,prim}}{\eta_{el}}\right] < 0 \\[3em] max\left[TOL_d;\ \dfrac{-b_{2,\Phi_{max}}(T_{s,d,max}) + \sqrt{b_{2,\Phi_{max}}^2(T_{s,d,max}) - 4\ a_{2,\Phi_{max}}(T_{s,d,max})\left[c_{2,\Phi_{max}}(T_{s,d,max}) - \dfrac{\eta_{bk,prim}}{\eta_{el}}\right]}}{2\ a_{2,\Phi_{max}}(T_{s,d,max})}\right] & else \end{cases} \tag{4.4}$$

The water temperatures in the storages are initialized: during the first hour of the heating season, the mean temperature of the water in the heating storage tank, $T_{s,h}(1)$, is set equal to the storage room temperature, $T_{s,room}(1)$, whereas the mean temperature of the water in the DHW storage tank, $T_{s,d}(1)$, is set equal to $T_{s,d,min}$ (considering the DHW function working all year long).

The i-th values of the thermal energy stored in the tanks for heating, $E_{s,h}(i)$, and for DHW production, $E_{s,d}(i)$, are evaluated through the equations:

$$E_{s,h}(i) = \rho_w\ V_{s,h}\ c_{p,w}\left[T_{s,h}(i) - T_{s,h,min}\right], \tag{4.5}$$

$$E_{s,d}(i) = \rho_w\ V_{s,d}\ c_{p,w}\left[T_{s,d}(i) - T_{s,d,min}\right]. \tag{4.6}$$

The i-th values of the energy lost by the storages ($E_{s,lost,h}(i)$ for heating and $E_{s,lost,d}(i)$ for DHW production) are evaluated as:

$$E_{s,lost,h}(i) = t_{hour}U_{s,h}\left[T_{s,h}(i) - T_{s,room}(i)\right], \tag{4.7}$$

$$E_{s,lost,d}(i) = t_{hour}U_{s,d}\left[T_{s,d}(i) - T_{s,room}(i)\right], \tag{4.8}$$

where t_{hour} is the time duration of one hour.

The MATLAB code reads the i-th value of T_{ext} and evaluates, through linear interpolations with respect to the water temperature in the storages, the power the heat pump is able to deliver and the corresponding COP, in each operation mode (heating mode, DHW mode).

For inverter-driven heat pumps, the heat pump input data are given for at least the maximum, the minimum and an intermediate inverter frequency and the interpolation method is repeated for each frequency value, obtaining a vector for the heat pump power and a vector for the corresponding COP, in each operation mode.

The heat pump power and COP curves are stopped in correspondence of the cut-off temperature of the related operation mode ($T_{cut\text{-}off,h}$ or $T_{cut\text{-}off,d}$).

In the i-th hour, the heat pump works at its maximum capacity to satisfy the building DHW demand (if present), leaving as much time as possible to satisfy the building heating demand and, consequently, avoiding if possible the back-up activation.

The code evaluates the temperature $T'_{s,d}(i)$, which the water in the DHW storage would reach if the heat pump delivered the maximum energy, corresponding to the heat pump maximum power ($P_{HP,d,\Phi_{max}}(i)$ for IDHPs) supplied for the whole i-th hour:

$$T'_{s,d}(i) = T_{s,d}(i) + \frac{P_{HP,d,\Phi_{max}}(i)\, t_{hour} - E_{b,d}(i) - E_{s,lost,d}(i)}{V_{s,d}\rho_w c_{p,w}} \ . \tag{4.9}$$

Since the DHW storage temperature cannot exceed $T_{s,d,max}$, if $T'_{s,d}(i)$ is equal to, or lower than $T_{s,d,max}$, the energy $E_{HP,d}(i)$ supplied by the heat pump is the maximum one:

$$E_{HP,d}(i) = P_{HP,d,\Phi_{max}}(i)\, t_{hour} \ , \tag{4.10}$$

otherwise, in the i-th hour the heat pump only delivers the energy needed to satisfy the building DHW demand and the energy needed to cover the DHW tank thermal losses and to increase the water temperature to $T_{s,d,max}$:

$$E_{HP,d}(i) = E_{b,d}(i) + E_{s,lost,d}(i) + V_{s,d}\rho_w c_{p,w}[T_{s,d,max} - T_{s,d}(i)] \ . \tag{4.11}$$

The corresponding electric energy used by the heat pump in DHW mode, $E_{HP,d,us}(i)$, is evaluated dividing $E_{HP,d}(i)$ by the value of COP at maximum capacity.

The thermal energy $E_{bk,d}(i)$ delivered for DHW production by the back-up system, if needed, is obtained as:

$$E_{bk,d}(i) = E_{b,d}(i) + E_{s,lost,d}(i) - E_{s,d}(i) - E_{HP,d}(i) \ , \tag{4.12}$$

and the corresponding energy used, $E_{bk,d,us}(i)$, is equal to the ratio between $E_{bk,d}(i)$ and its efficiency, η_{bk}.

The residual time $t_{res}(i)$, available in the i-th hour for heating mode, is given by:

$$t_{res}(i) = t_{hour} - \frac{E_{HP,d}(i)}{P_{HP,d,\Phi_{max}}(i)} \quad . \tag{4.13}$$

To evaluate the energy supplied by the heat pump in heating mode in the i-th hour, the code first calculates the temperature $T'_{s,h}(i)$, which would be reached by the water in the heating storage if the heat pump delivered the maximum energy, corresponding to the heat pump maximum power ($P_{HP,h,\Phi_{max}}(i)$ for IDHPs) supplied for the whole residual time, $t_{res}(i)$:

$$T'_{s,h}(i) = T_{s,h}(i) + \frac{P_{HP,h,\Phi_{max}}(i)\, t_{res}(i) - E_{b,h}(i) - E_{s,lost,h}(i)}{V_{s,h}\rho_w c_{p,w}} \quad . \tag{4.14}$$

Since the heating storage temperature cannot exceed $T_{s,h,max}$, if $T'_{s,h}(i)$ is equal to, or lower than $T_{s,h,max}$, the energy $E_{HP,h}(i)$ supplied by the heat pump is the maximum one:

$$E_{HP,h}(i) = P_{HP,h,\Phi_{max}}(i)\, t_{res}(i) \; , \tag{4.15}$$

otherwise, in the i-th residual time, the heat pump only delivers the energy needed to satisfy the building heating demand and the energy needed to cover the heating tank thermal losses and to increase the water temperature to $T_{s,h,max}$:

$$E_{HP,h}(i) = E_{b,h}(i) + E_{s,lost,h}(i) + V_{s,h}\rho_w c_{p,w}[T_{s,h,max} - T_{s,h}(i)] \quad . \tag{4.16}$$

If $E_{HP,h}(i)$ is evaluated by means of Eq. (4.16), the energy delivered by the heat pump is lower than the maximum available and, consequently, on-off cycles are employed by ON-OFF HPs. IDHPs, on the contrary, can decrease the inverter frequency until Φ_{min}, after which on-off cycles must start.

The value of the heat pump power and of the corresponding *COP* in heating mode are known from the previous interpolations for ON-OFF HPs; for IDHPs a vector for the heat pump power and a vector for the corresponding *COP* are obtained from interpolations.

The value of the heat pump power for IDHPs, $P_{HP,h,\Phi_{eff}}(i)$, can be obtained dividing $E_{HP,h}(i)$ by $t_{res}(i)$, but if $P_{HP,h,\Phi_{eff}}(i)$ turns out lower than $P_{HP,h,\Phi_{min}}(i)$, it is set equal to $P_{HP,h,\Phi_{min}}(i)$ (situation corresponding to on-off cycles). The corresponding *COP* value, $COP_{h,\Phi_{eff}}(i)$, is then obtained by applying a second-order polynomial interpolation of the *COP* vector, as a function of the heat pump power vector.

The effective *COP* in heating mode ($COP_{h,eff}$), which takes into account the heat pump efficiency decay in the case of on-off cycles, is evaluated, according to Refs. [10], [11], multiplying the obtained *COP* value by the *COP* correction factor for on-off condition,

evaluated according to Eq. (2.1), where the capacity ratio $CR(i)$ is evaluated as the ratio between $E_{HP,h}(i)$ and the product of $P_{HP,h,\Phi_{eff}}(i)$ multiplied by $t_{res}(i)$.

The hourly value of the electric energy used by the heat pump in heating mode, $E_{HP,h,us}(i)$, is evaluated dividing $E_{HP,h}(i)$ by $COP_{h,eff}(i)$.

Eq. (4.17) evaluates the energy supplied in the i-th hour by the back-up system for heating, if the building heating demand and the heating storage thermal losses exceed the energy delivered by the heat pump and that available from the storage:

$$E_{bk,h}(i) = E_{b,h}(i) + E_{s,lost,h}(i) - E_{s,h}(i) - E_{HP,h}(i) \ . \tag{4.17}$$

The corresponding energy used by the back-up system for heating, $E_{bk,h,us}(i)$, is equal to the ratio between $E_{bk,h}(i)$ and η_{bk}.

Finally, the mean temperatures of the water in the thermal storages for the subsequent hour, $T_{s,h}(i+1)$ and $T_{s,d}(i+1)$, are determined:

$$T_{s,h}(i+1) = T_{s,h}(i) + \frac{E_{HP,h}(i) + E_{bk,h}(i) - E_{b,h}(i) - E_{s,lost,h}(i)}{\rho_w \ V_{s,h} \ c_{p,w}} \ , \tag{4.18}$$

$$T_{s,d}(i+1) = T_{s,d}(i) + \frac{E_{HP,d}(i) + E_{bk,d}(i) - E_{b,d}(i) - E_{s,lost,d}(i)}{\rho_w \ V_{s,d} \ c_{p,w}} \ . \tag{4.19}$$

By adding together the hourly energy values, the MATLAB code evaluates the energy seasonally required by the building and the energy seasonally delivered and used by the heat pump and by the back-up system.

The seasonal efficiency parameters are then obtained: the mean seasonal COP of the heat pump ($SCOP_{net}$) and of the whole system with electric heaters as back-up system ($SCOP_{on}$) are evaluated according to Eq. (3.17) and Eq. (3.18), respectively, whereas the Fuel Utilization Efficiency (FUE) is obtained by means of Eq. (4.20):

$$FUE = \frac{\sum_i E_{b,h}(i) + \sum_i E_{b,d}(i)}{\left[\dfrac{\sum_i E_{HP,h,us}(i) + \sum_i E_{HP,d,us}(i)}{\eta_{el}}\right] + \left[\sum_i E_{bk,h,prim}(i) + \sum_i E_{bk,d,prim}(i)\right]} \ . \tag{4.20}$$

The building total energy demand for heating and DHW production (satisfied by the heat pump and, if necessary, also by the back-up system) has been used as numerator in Eq. (4.20), excluding the energy delivered to cover the storage tanks thermal losses, which is not considered as an useful effect, but only as a factor of energy consumption increase.

The quantities $E_{bk,h,prim}$ and $E_{bk,d,prim}$ at the denominator of Eq. (4.20) are, as already explained for Eq. (3.19), the values of the primary energy used by the back-up system, for heating and DHW production, respectively.

The MATLAB input file and script developed for the dynamic simulation of multi-function air-to-water heat pumps in winter operation are reported in Appendix, Section 7.1.

4.1.6   Case study

As an example of application of the simulation method, the MATLAB code is used to analyze the performance of an air-source heat pump heating system located in Bologna (North-Center Italy), as a function of the bivalent temperature and of the volume of the storage tank.

The heating plant considered is composed of an electric air-to water inverter-driven heat pump, provided with a water storage tank and integrated by electric heaters as back-up system. The hourly values of the external air temperature for the heating season (October - April) are taken from the Meteonorm TMY on TRNSYS (see Figure 4.1) and the hourly values of the energy required by the building for heating are obtained starting from the building energy signature (BES). To evaluate the optimal value of the bivalent temperature, several BES are considered, by fixing T_{zl} = 16 °C and by varying the BES slope.

Several storage volumes $V_{s,h}$ are taken into account and the heat loss coefficient of the thermal storage, $U_{s,h}$, is expressed as a linear function of the storage volume:

$$U_{s,h} = a_{s,h} V_{s,h} + b_{s,h} \ .$$
(4.21)

By interpolating technical data provided by some manufacturers for storage volumes in the range 0.168 – 2.2 m^3, the following values of the coefficients of Eq. (4.21) were obtained: $a_{s,h}$ = 1.023 W/(m^3 K) and $b_{s,h}$ = 1.293 W/K. The manufacturer data and the interpolating function are illustrated in Figure 4.5. Eq. (4.21) is assumed as valid in the range of $V_{s,h}$ 0.1 – 2 m^3; if no thermal storage is employed, $U_{s,h}$ is obviously equal to 0.
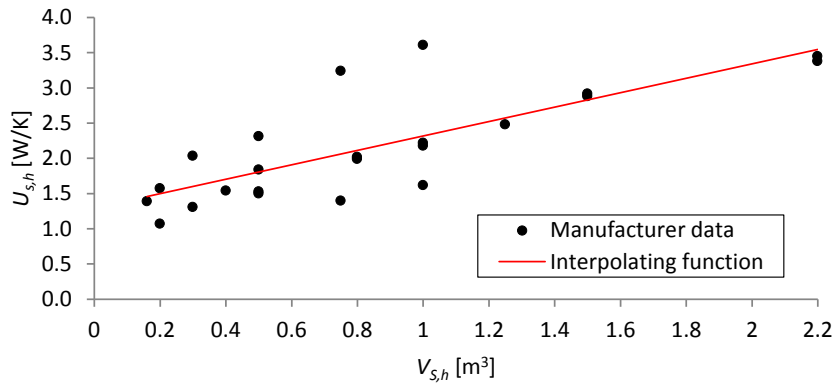
Figure 4.5: Manufacturer data and interpolating function for the heat loss coefficient of the thermal storage, versus storage volume.

The selected maximum and minimum temperatures of the water in the storage tank are, respectively, 45 °C and 35 °C. The hourly values of temperature of the storage room are evaluated through Eq. (4.2), where a temperature reduction factor of the storage room, b_u, equal to 0.5 (thermal storage placed in a basement) and a T_{int} value of 20 °C are adopted.

In Table 4.2 the data of the inverter-driven heat pump power, given by the manufacturer, are reported, for several external air temperatures, T_{ext}, and five inverter frequencies, both for the minimum and the maximum storage temperature ($T_{s,h,min}$ and $T_{s,h,max}$, respectively). In Table 4.3, the corresponding *COP* data given by the manufacturer are reported.

Table 4.2: Heat pump power [kW] at the minimum and maximum temperature of the storage.

T_{ext} [°C]	$T_{s,h,min}$					$T_{s,h,max}$				
	Frequency [Hz]					Frequency [Hz]				
	110	90	70	50	30	110	90	70	50	30
-7	8.09	6.37	4.83	3.36	2.01	7.80	6.08	4.58	3.18	1.90
2	10.60	8.45	6.41	4.49	2.69	10.14	7.98	6.05	4.22	2.53
7	12.50	9.78	7.43	5.25	3.14	11.82	9.28	6.99	4.93	2.95
12	14.30	11.30	8.66	6.07	3.66	13.69	10.82	8.18	5.75	3.44

Table 4.3: Heat pump *COP* at the minimum and maximum temperature of the storage.

T_{ext} [°C]	$T_{s,h,min}$					$T_{s,h,max}$				
	Frequency [Hz]					Frequency [Hz]				
	110	90	70	50	30	110	90	70	50	30
-7	3.01	3.13	3.17	3.08	2.78	2.47	2.54	2.57	2.51	2.29
2	3.75	3.94	4.02	3.95	3.60	2.99	3.12	3.18	3.13	2.89
7	4.33	4.52	4.63	4.61	4.21	3.39	3.54	3.60	3.58	3.32
12	4.97	5.25	5.42	5.38	4.97	3.85	4.06	4.16	4.14	3.84

The cut-off temperature, equal to the heat pump *TOL*, is -10 °C.

Figure 4.6 shows, together with one of the employed building energy signatures, the characteristic curves of the heat pump at the highest and lowest inverter frequencies, at the minimum storage temperature. In the case reported in Figure 4.6, the bivalent temperature T_{biv} turns out equal to -2 °C.
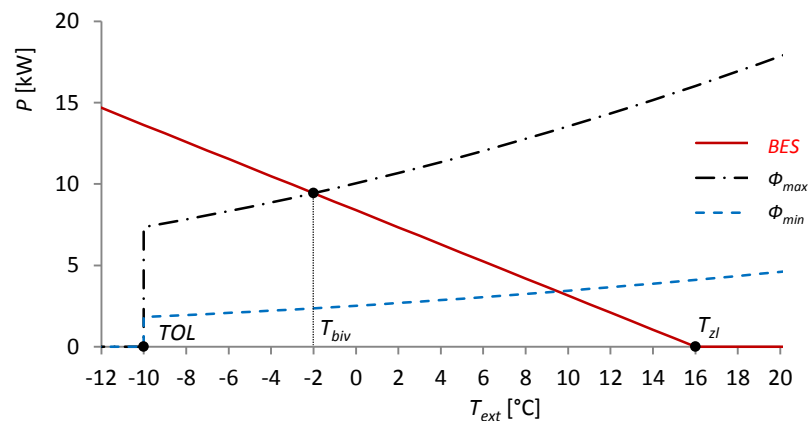
Figure 4.6: Building energy signature and heat pump power at $T_{s,h,min}$, for Φ_{max} and Φ_{min}.

Figure 4.7 shows the energy and temperature trends obtained in a cold day of the heating season, namely January 13th, for the simulation with $V_{s,h}$ = 1 m³ and T_{biv} = -2 °C. During this day the external air temperature T_{ext} oscillates around the bivalent temperature T_{biv}, which slightly varies during the day on the basis of the hourly value of the inverter frequency.
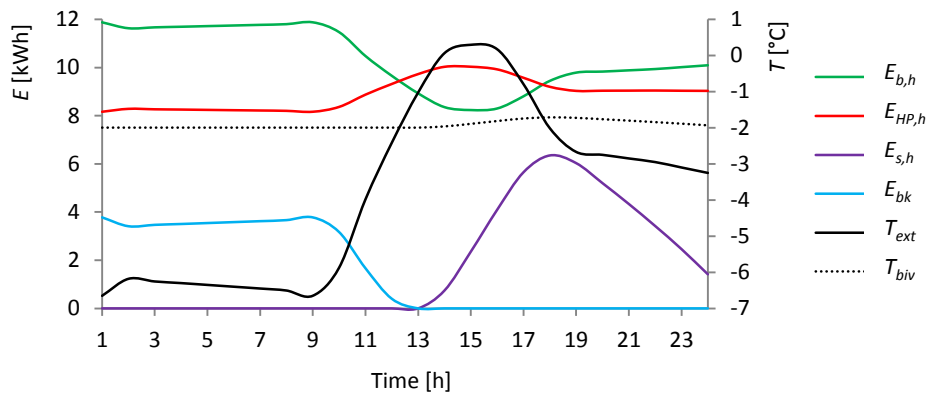
Figure 4.7: Hourly trends of T_{ext}, T_{biv}, $E_{b,h}$, $E_{HP,h}$, $E_{s,h}$, E_{bk}, for January 13th.

As can be seen in Figure 4.7, the building energy need for heating, $E_{b,h}$, decreases when T_{ext} increases, and vice versa. During the first hours of this day, the storage has no energy, but when T_{ext} becomes higher than T_{biv}, the heat pump supplies energy, $E_{HP,h}$, both to the building and to the thermal storage, whose energy, $E_{s,h}$, starts to increase. $E_{s,h}$ is then used during the last hours of the day, when T_{ext} goes back below T_{biv}. Thanks to the storage, the back-up system delivers energy, $E_{bk,h}$, only during the first hours of the day.

In order to study the effects of the bivalent temperature on the Seasonal Coefficient Of Performance of the system, several simulations are run with different slopes of the building energy signature. Also the effect of the storage volume on the $SCOP_{on}$ is analyzed, by considering values of $V_{s,h}$ between 0 and 2 m^3.

Plots of the $SCOP_{on}$ as a function of the storage volume, for several values of the bivalent temperature are reported in Figure 4.8.
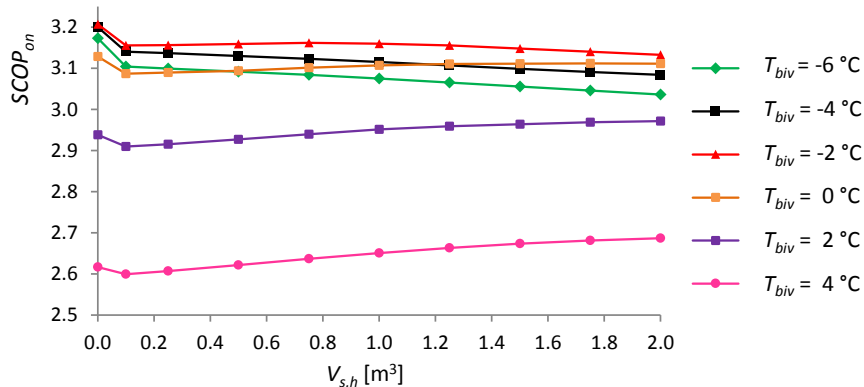
Figure 4.8: $SCOP_{on}$ as a function of $V_{s,h}$ for different values of T_{biv}, IDHP.

As highlighted by Figure 4.8, without a thermal storage the best seasonal performance is obtained by selecting values of the bivalent temperature between -6 °C and -2 °C. Despite the difference in the climate profile (TMY versus bins), this result was found also by the simulations with the bin-method of Subsection 3.3.1, where the best seasonal performance of IDHPs was obtained by adopting as bivalent temperature the design temperature (-5 °C for Bologna).

The curves of Figure 4.8 show that the effect of the storage volume on the $SCOP_{on}$ is not very significant, in agreement with the results obtained by Klein et al [27]. Regardless of $V_{s,h}$, the value of T_{biv} which gives the highest $SCOP_{on}$ is -2 °C. For T_{biv} = -2 °C, the highest seasonal performance is obtained with no storage tank ($V_{s,h}$ = 0) and is equal to 3.21.

With a bivalent temperature lower than the optimal one, i.e. with a heat pump oversized with respect to the building thermal need, an increase of the storage volume yields a slight decrease of the $SCOP_{on}$, mainly on account of larger thermal losses from the storage. On the contrary, if the bivalent temperature is much higher than the optimal one, i.e. if the heat pump is significantly undersized with respect to the building, the use of a large thermal storage volume slightly increases the seasonal performance of the system.

Whereas for a conventional heating system based on a condensing boiler the Fuel Utilization Efficiency is very close to 1, for the heat pump system here considered the FUE (Eq. (4.20)) reaches 1.48, with the optimal bivalent temperature and with no storage tank.

The analysis of the effect of the bivalent temperature and of the storage volume on the mean seasonal COP is repeated for mono-compressor on-off heat pumps: in order to evaluate the increase of $SCOP_{on}$ produced by the inverter compressor, the same heat pump is considered, constrained to operate at the maximum frequency.
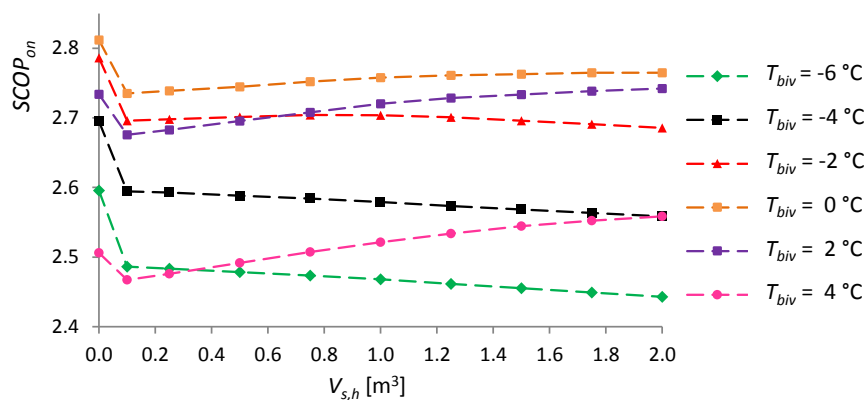
Figure 4.9: $SCOP_{on}$ as a function of $V_{s,h}$ for different values of T_{biv}, ON-OFF HP.

As shown in Figure 4.9, the value of $SCOP_{on}$ achieved by the ON-OFF HP is always lower than that obtained in the same conditions by the IDHP and the optimal bivalent temperature (0 °C) is higher than the previous case, as also observed in Subsection 3.3.1 with the simulations through the bin-method.

With the optimal bivalent temperature, the highest $SCOP_{on}$ is achieved with no storage tank, as in the previous case, but it is now equal to 2.81, i.e. more than 12 % lower.

The study performed with the mono-compressor on-off heat pump confirms that an increase of the storage volume yields a moderate decrease of the seasonal performance with low values of T_{biv}, whereas a large storage volume can slightly increase the $SCOP_{on}$ with high values of T_{biv}. The highest value of the *FUE* is 1.29, almost 13 % lower than that achieved by the inverter-driven heat pump.

4.2 MATLAB CODE FOR SUMMER OPERATION

A numerical method, implemented in MATLAB for the hourly simulation of air-to-water heat pumps for cooling and domestic hot water production, is presented.

The studied system consists of a reversible multi-function air-to-water heat pump, used in summer for both cooling and DHW production, able to work in heat recovery mode (recovery of the condensation heat to supply cooling energy and domestic hot water at the same time). The heat pump is coupled with a storage tank for air-conditioning and a storage tank for instantaneous DHW production, and is integrated by electric heaters or a gas boiler for DHW.

4.2.1   Climate implementation and building hourly energy needs

The hourly values of the external air temperature are input data for the dynamic simulation code.

In Figure 4.10 the external air temperature profile, according to the Meteonorm Typical Meteorological Year (TMY) from the software TRNSYS, is plotted for the cooling season in the Italian city of Bologna.
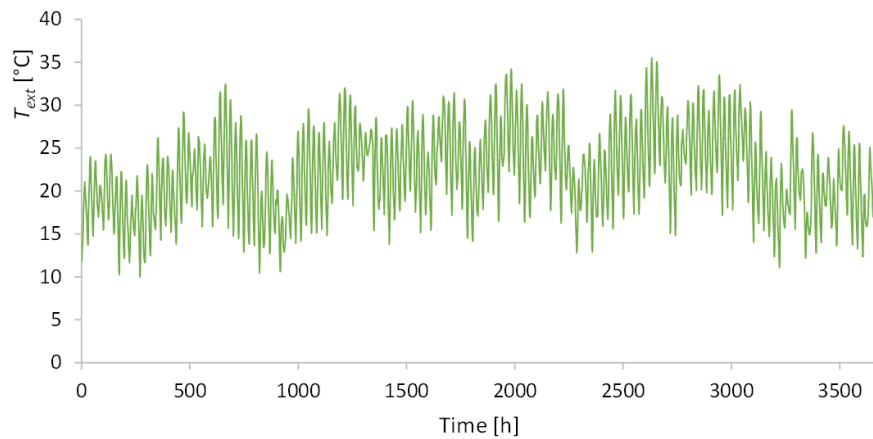
Figure 4.10: Hourly trend of the external air temperature during the cooling season in Bologna (Italy) from Meteonorm TMY.

In Figure 4.11 the monthly average outdoor temperatures obtained from the Meteonorm TMY are compared with those reported in the standard UNI 10349 [25] for the cooling season in Bologna (considered from May to September, included).
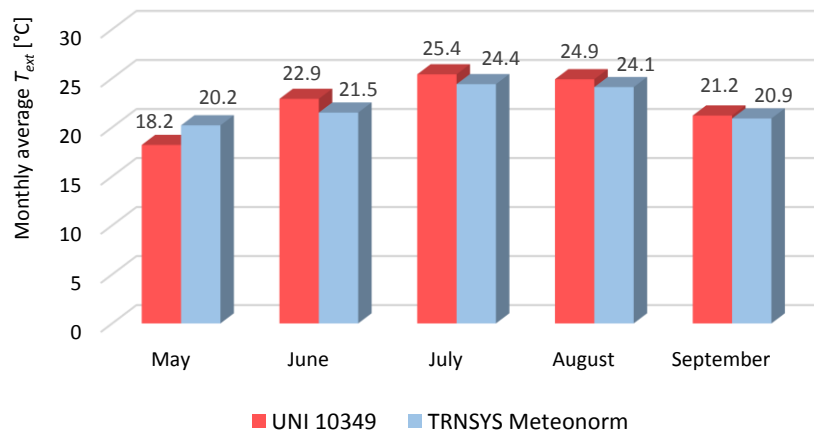
Figure 4.11: Monthly average outdoor temperatures for the cooling season in Bologna (Italy).

From Figure 4.11 one can notice that the minimum monthly average outdoor temperature in summer (which refers to May) is equal to 18.2 °C according to Ref. [25] and 20.2 °C according to the Meteonorm TMY, while the maximum monthly average outdoor temperature (occurring in July) is equal to 25.4 °C according to Ref. [25] and 24.4 °C according to the Meteonorm profile.

The hourly values $E_{b,c}(i)$ of the energy needed by the building for cooling, at the outlet of the generation subsystem (heat pump), are other input data for the MATLAB code and can derive from a dynamic simulation of the building, or can be approximately obtained by using the summer building energy signature (BES), multiplying by the hour duration (t_{hour}) the thermal power from the BES in correspondence of the outdoor temperature of the i-th hour, $T_{ext}(i)$. The hourly values $E_{b,d}(i)$ of the energy needed by the building for DHW production are obtained as explained in Subsection 4.1.3.

4.2.2 Heat pump and thermal storage characterization for summer operation

The considered reversible air-to-water heat pumps are used in summer for cooling and DHW production and can work in cooling-only, DHW-only or heat recovery mode.

Figure 4.12 shows a scheme of the reversible multi-function heat pump, coupled with a storage tank for cooling and with a storage tank for instantaneous DHW production (in this case integrated by electric heaters); the refrigerant fluid path in heat recovery mode is highlighted.
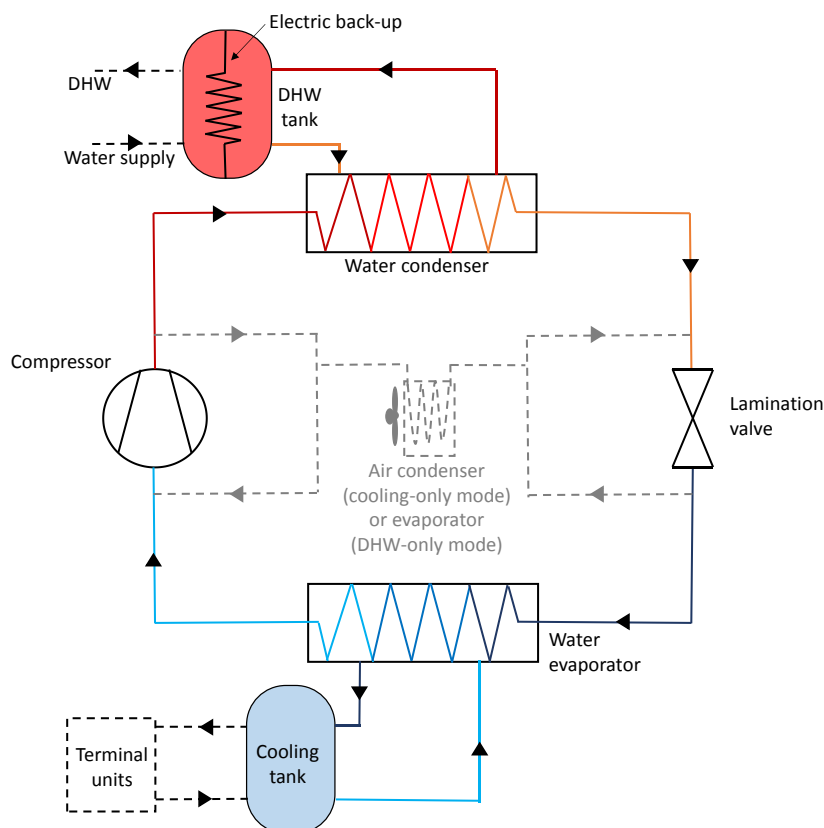
Figure 4.12: Plant scheme for summer operation.

The temperature of the water in the thermal storage tanks ($T_{s,c}$ for the cooling tank and $T_{s,d}$ for the DHW one) can range from a fixed minimum to a maximum value ($T_{s,c,min}$ and $T_{s,c,max}$ for cooling and $T_{s,d,min}$ and $T_{s,d,max}$ for DHW).

Input data of the heat pump power and *EER* in cooling-only mode are required by the dynamic code for different values of T_{ext}, and for $T_{s,c,min}$ and $T_{s,c,max}$ (and, for IDHPs, also for different values of the inverter frequency).

Similarly, input data of the heat pump power and *COP* in DHW-only mode are required for different values of T_{ext}, and for $T_{s,d,min}$ and $T_{s,d,max}$ (and, for IDHPs, also for different values of the inverter frequency).

Through interpolations of the manufacturer data as described in Subsection 3.1.4, curves of the heat pump power, *EER* and *COP*, in cooling-only mode and in DHW-only mode, are obtained as functions of T_{ext}, for a fixed temperature of the cold (or hot) water produced.

In heat recovery mode, the heat pump releases the condensation heat to a storage tank for simultaneous DHW production, working as a water-to-water heat pump, without being influenced by the hourly value of the external air temperature. Input data of the heat pump cooling power and *EER* in this mode are required for each combination of the maximum and minimum water temperature in the tanks ($T_{s,c,max}$, $T_{s,c,min}$, $T_{s,d,max}$, $T_{s,d,min}$).

The heat pump power and *EER* in heat recovery mode are expressed, through interpolations, as linear functions of the temperature of the water in the DHW storage ($T_{s,d}$), for a fixed value of temperature of the water in the cooling storage ($T_{s,c,max}$ or $T_{s,c,min}$).

For IDHPs, a family of curves for the heat pump power and a family of curves for the heat pump *EER* or *COP* are obtained, in each operation mode, by varying the inverter frequency between the maximum and minimum value.

To evaluate the thermal energy lost by the DHW storage and the thermal energy entering the cooling storage, the hourly values of temperature of the storage room, $T_{s,room}(i)$, are needed. If not available from a dynamic simulation, the values of $T_{s,room}(i)$ can be estimated through Eq. (4.2).

Simulations of a heat pump employed only for cooling, or for DHW production, are achievable by setting equal to zero the building DHW demand, or the building cooling demand, respectively.

4.2.3 Hourly energy evaluations for summer operation

The input parameters for the dynamic simulation of the heat pump in summer operation are: the hourly values $T_{ext}(i)$ of the external air temperature for the cooling season in the considered location; the hourly values of the building energy demand for cooling, $E_{b,c}(i)$, and

for DHW production, $E_{b,d}(i)$; the thermal storages volumes, $V_{s,c}$ for cooling and $V_{s,d}$ for DHW; the imposed minimum and maximum values of the water temperature in the thermal storages, $T_{s,c,min}$ and $T_{s,c,max}$, $T_{s,d,min}$ and $T_{s,d,max}$; the storages heat loss coefficients, $U_{s,c}$ for cooling and $U_{s,d}$ for DHW; the heat pump power, COP and EER data from the manufacturer in each operation mode; the efficiency η_{bk} of the back-up system for DHW; the hourly values of temperature of the storage room, $T_{s,room}(i)$.

Once evaluated the heat pump power, EER and COP curves through interpolations as previously described, the code evaluates for each hour of the cooling season, through a *for* loop, several parameters, including: the energy supplied by the heat pump for cooling, the energy recovered by the heat pump for DHW production in heat recovery mode, the energy supplied by the heat pump in DHW-only mode, the mean temperatures of the water in the thermal storage, the energy used by the heat pump and, if activated for DHW production, by the back-up system.

The water temperatures in the storages are initialized: for the first hour of the cooling season, the mean temperature of the water in the cooling storage tank, $T_{s,c}(1)$, is set equal to the storage room temperature, $T_{s,room}(1)$, whereas the mean temperature of the water in the DHW storage tank, $T_{s,d}(1)$, is set equal to $T_{s,d,min}$ (considering the DHW function working all year long).

The MATLAB code reads the *i*-th value of T_{ext}, $T_{s,c}$ and $T_{s,d}$ and evaluates, through linear interpolations, the power the heat pump is able to deliver and the corresponding EER or COP, in each operation mode (cooling-only, DHW-only and heat recovery mode).

For inverter-driven heat pumps, the heat pump input data are given for at least the maximum, the minimum and an intermediate inverter frequency and the interpolation method is repeated for each frequency value, obtaining a vector for the heat pump power and a vector for the corresponding EER or COP, in each operation mode.

For each hour, the MATLAB code determines in which operation mode the heat pump is working. First, the hourly values of the energy stored in the cold and hot water tanks, $E_{s,c}(i)$ and $E_{s,d}(i)$, respectively, are evaluated as:

$$E_{s,c}(i) = \rho_w \, V_{s,c} \, c_{p,w} \left[T_{s,c,max} - T_{s,c}(i) \right] \, , \tag{4.22}$$

$$E_{s,d}(i) = \rho_w \, V_{s,d} \, c_{p,w} \left[T_{s,d}(i) - T_{s,d,min} \right] \, . \tag{4.23}$$

Then the code evaluates the hourly values of the thermal energy entering the cold tank from the storage room, $E_{s,gain,c}(i)$, and of the thermal energy lost by the hot tank, $E_{s,lost,d}(i)$:

$$E_{s,gain,c}(i) = t_{hour} U_{s,c} \left[T_{s,room}(i) - T_{s,c}(i) \right] , \qquad (4.24)$$

$$E_{s,lost,d}(i) = t_{hour} U_{s,d} \left[T_{s,d}(i) - T_{s,room}(i) \right] . \qquad (4.25)$$

If Eq. (4.26) is satisfied, the energy stored in the cold tank in the i-th hour is enough to cover both $E_{b,c}(i)$ and $E_{s,gain,c}(i)$. Therefore, the heat pump covers the thermal energy required by the building for domestic hot water ($E_{b,d}(i)$) working in DHW-only mode.

$$E_{b,c}(i) + E_{s,gain,c}(i) \leq E_{s,c}(i) \qquad (4.26)$$

In the case in the i-th hour the heat pump works in DHW-only mode, the code evaluates, through Eq. (4.9), the temperature $T'_{s,d}(i)$, which the water in the hot tank would reach if the heat pump delivered the maximum energy, corresponding to the heat pump maximum power ($P_{HP,d,\Phi_{max}}(i)$ for IDHPs) supplied for the whole i-th hour.

If $T'_{s,d}(i)$ does not exceed $T_{s,d,max}$, the energy $E_{HP,d}(i)$ supplied by the heat pump is the maximum one (see Eq. (4.10)). Otherwise, the heat pump only delivers the energy needed to satisfy the building DHW demand and the energy needed to cover the hot tank thermal losses and to increase the water temperature to $T_{s,d,max}$ (see Eq. (4.11)); in this case, as $E_{HP,d}(i)$ is lower than the maximum energy the heat pump would be able to deliver, on-off cycles are employed by mono-compressor on-off heat pumps. Inverter-driven heat pumps, on the contrary, are able to decrease the inverter frequency and, consequently, the power delivered, until the minimum frequency is reached, after which on-off cycles must start.

The value of the heat pump power and of the corresponding *COP* in DHW-only mode are known from the previous interpolations for ON-OFF HPs; for IDHPs a vector for the heat pump power and a vector for the corresponding *COP* are obtained from interpolations.

The value of the heat pump power for IDHPs, $P_{HP,d,\Phi_{eff}}(i)$, can be obtained dividing $E_{HP,d}(i)$ by t_{hour}, but if $P_{HP,d,\Phi_{eff}}(i)$ turns out lower than $P_{HP,d,\Phi_{min}}(i)$, it is set equal to $P_{HP,d,\Phi_{min}}(i)$ (situation corresponding to on-off cycles). The corresponding *COP* value, $COP_{d,\Phi_{eff}}(i)$, is then obtained by applying a second-order polynomial interpolation of the *COP* vector, as a function of the heat pump power vector.

The effective *COP* in DHW-only mode ($COP_{d,eff}$), which takes into account the heat pump efficiency decay in the case of on-off cycles, is evaluated, according to Ref. [11], multiplying the obtained *COP* value by the *COP* correction factor for on-off condition (see Eq. (2.1)), where the capacity ratio $CR(i)$ is evaluated as the ratio between $E_{HP,d}(i)$ and the product of $P_{HP,d,\Phi_{eff}}(i)$ multiplied by t_{hour}.

The hourly value of the electric energy used by the heat pump in DHW-only mode, $E_{HP,d,us}(i)$, is evaluated dividing $E_{HP,d}(i)$ by $COP_{d,eff}(i)$.

In the case the energy supplied by the heat pump and the energy stored in the DHW tank are insufficient to cover the building demand for DHW and the hot tank thermal losses, the back-up system delivers the energy $E_{bk}(i)$, evaluated through Eq. (4.12), and the energy used by the back-up system is given by the ratio between $E_{bk}(i)$ and η_{bk}.

Finally, the temperatures of the water in the cooling tank and in the DHW tank for the subsequent hour are obtained by means of Eq. (4.27) and Eq. (4.19), respectively.

$$T_{s,c}(i+1) = T_{s,c}(i) + \frac{E_{b,c}(i) + E_{s,gain,c}(i)}{\rho_w \ V_{s,c} \ c_{p,w}} \tag{4.27}$$

In the case Eq. (4.26) is not satisfied, the heat pump has to deliver cooling energy in the i-th hour. The heat pump is also able to supply thermal energy at the same time through condensation heat recovery, if needed to cover the building DHW demand, the hot tank thermal losses and to increase the temperature of the water in the DHW tank to $T_{s,d,max}$. If Eq. (4.28) is satisfied, no thermal energy is needed and the heat pump works in cooling-only mode.

$$E_{b,d}(i) + E_{s,lost,d}(i) + [T_{s,d,max} - T_{s,d}(i)](V_{s,d}\rho_w c_{p,w}) \leq 0 \tag{4.28}$$

In the case of cooling-only mode, the code evaluates the temperature $T'_{s,c}(i)$, which the water in the cold tank would reach if the heat pump delivered the maximum energy, corresponding to the heat pump maximum power ($P_{HP,c,\Phi_{max}}(i)$ for IDHPs) supplied for the whole i-th hour:

$$T'_{s,c}(i) = T_{s,c}(i) + \frac{-P_{HP,c,\Phi_{max}}(i) \ t_{hour} + E_{b,c}(i) + E_{s,gain,c}(i)}{V_{s,c}\rho_w c_{p,w}} \ . \tag{4.29}$$

If $T'_{s,c}(i)$ is equal to or higher than $T_{s,c,min}$, the energy $E_{HP,c}(i)$ supplied by the heat pump is the maximum one:

$$E_{HP,c}(i) = P_{HP,c,\Phi_{max}}(i) \ t_{hour} \ . \tag{4.30}$$

Otherwise, the heat pump only delivers the energy needed to satisfy the building cooling demand, the energy needed to cover the heat entering the cold tank and the energy needed to decrease the water temperature to $T_{s,c,min}$:

$$E_{HP,c}(i) = E_{b,c}(i) + E_{s,gain,c}(i) + V_{s,c}\rho_w c_{p,w}[T_{s,c}(i) - T_{s,c,min}] \ . \tag{4.31}$$

The value of the power $P_{HP,c,\Phi_{eff}}(i)$ delivered by the heat pump in the i-th hour in cooling-only mode, and the value of the corresponding *EER* are obtained through the same method described for the heat pump power and *COP* in DHW-only mode.

The effective *EER* ($EER_{c,eff}$) in cooling-only mode, which takes into account the heat pump efficiency decay in the case of on-off cycles, is obtained according to Ref. [10], multiplying the obtained *EER* value by the correction factor for on-off cycles (Eq. (2.1)), where the capacity ratio *CR* (i) is evaluated as the ratio between $E_{HP,c}(i)$ and the product of $P_{HP,c,\Phi_{eff}}(i)$ multiplied by t_{hour}.

The hourly value of the electric energy used by the heat pump in cooling-only mode, $E_{HP,c,us}(i)$, is evaluated dividing $E_{HP,c}(i)$ by $EER_{c,eff}(i)$.

If the heat pump is undersized with respect to the building, the cooling energy delivered by the heat pump and stored in the cold tank can be insufficient to satisfy the building cooling demand and to cover the thermal energy entering the cold tank from the storage room. This missing energy $E_{uncov}(i)$ is:

$$E_{uncov}(i) = E_{b,c}(i) + E_{s,gain,c}(i) - E_{s,c}(i) - E_{HP,c}(i) \ . \tag{4.32}$$

The water temperatures in the cold tank and in the hot tank for the subsequent hour are then obtained:

$$T_{s,c}(i+1) = T_{s,c}(i) + \frac{E_{b,c}(i) + E_{s,gain,c}(i) - E_{HP,c}(i) - E_{uncov}(i)}{\rho_w \ V_{s,c} \ c_{p,w}} \ , \tag{4.33}$$

$$T_{s,d}(i+1) = T_{s,d}(i) + \frac{-E_{b,d}(i) - E_{s,lost,d}(i)}{\rho_w \ V_{s,d} \ c_{p,w}} \ . \tag{4.34}$$

Finally, if neither Eq. (4.26) nor Eq. (4.28) are satisfied in the i-th hour, the heat pump is required to deliver both cooling and thermal energy, working in heat recovery mode. In this case the temperature $T'_{s,c}(i)$, reached by the water in the cold tank if the heat pump delivered the maximum cooling energy, corresponding to the heat pump maximum power in heat recovery mode ($P_{HP,r,\Phi_{max}}(i)$ for IDHPs) supplied for the whole i-th hour is:

$$T'_{s,c}(i) = T_{s,c}(i) + \frac{-P_{HP,r,\Phi_{max}}(i) \ t_{hour} + E_{b,c}(i) + E_{s,gain,c}(i)}{V_{s,c} \rho_w c_{p,w}} \ . \tag{4.35}$$

If $T'_{s,c}(i)$ is equal to or higher than $T_{s,c,min}$, the energy $E_{avail,HP,r}(i)$ which the heat pump is able to deliver in heat recovery mode is the maximum one:

$$E_{avail,HP,r}(i) = P_{HP,r,\Phi_{max}}(i) \ t_{hour} \ . \tag{4.36}$$

Otherwise, the energy that the heat pump is able to deliver is lower than the maximum one and has the same expression as $E_{HP,c}(i)$ in Eq. (4.31).

The values of the corresponding cooling power, $P_{HP,r,\Phi_{eff}}(i)$, and EER, $EER_{r,\Phi_{eff}}(i)$, are obtained through the same method described in DHW-only mode.

The thermal energy $E_{avail,cond}(i)$ recoverable at the heat pump condenser for DHW production is:

$$E_{avail,cond}(i) = \frac{E_{avail,HP,r}(i)}{P_{HP,r,\Phi_{eff}}(i)}\left[P_{HP,r,\Phi_{eff}}(i) + \frac{P_{HP,r,\Phi_{eff}}(i)}{EER_{r,\Phi_{eff}}(i)}\right] .$$ (4.37)

The code evaluates the temperature $T'_{s,d}(i)$, which the water in the hot tank would reach if all the energy $E_{avail,cond}(i)$ were delivered to the hot tank:

$$T'_{s,d}(i) = T_{s,d}(i) + \frac{E_{avail,cond}(i) - E_{b,d}(i) - E_{s,lost,d}(i)}{V_{s,d}\rho_w c_{p,w}} .$$ (4.38)

If $T'_{s,d}(i)$ does not exceed $T_{s,d,max}$, the energy $E_{cond}(i)$, delivered to the DHW storage tank through condensation heat recovery, is equal to $E_{avail,cond}(i)$ and the cooling energy $E_{HP,r}(i)$ supplied by the heat pump is equal to $E_{avail,HP,r}(i)$. Otherwise, $E_{cond}(i)$ has the same expression as $E_{HP,d}(i)$ in Eq. (4.11), $E_{HP,r}(i)$ has the expression:

$$E_{HP,r}(i) = P_{HP,r,\Phi_{eff}}(i)\frac{E_{cond}(i)}{P_{HP,r,\Phi_{eff}}(i) + \frac{P_{HP,r,\Phi_{eff}}(i)}{EER_{r,\Phi_{eff}}(i)}}$$ (4.39)

and for the remaining time of the hour, $t_{res}(i)$ (Eq. (4.40)), the heat pump works in cooling-only mode, if not all the needed cooling energy has been supplied.

$$t_{res}(i) = t_{hour} - \frac{E_{cond}(i)}{P_{HP,r,\Phi_{eff}}(i) + \frac{P_{HP,r,\Phi_{eff}}(i)}{EER_{r,\Phi_{eff}}(i)}}$$ (4.40)

If $T_{s,c}(i)$ is not reduced below $T_{s,c,min}$, the energy $E_{HP,c}(i)$ delivered by the heat pump in cooling-only mode is the maximum one (product of the maximum heat pump power in cooling-only mode and $t_{res}(i)$); otherwise, $E_{HP,c}(i)$ is evaluated as:

$$E_{HP,c}(i) = E_{b,c}(i) + E_{s,gain,c}(i) + (V_{s,c}\rho_w c_{p,w})[T_{s,c}(i) - T_{s,c,min}] - E_{HP,r}(i) .$$ (4.41)

The corresponding cooling power ($P_{HP,c,\Phi_{eff}}(i)$) and EER ($EER_{c,\Phi_{eff}}(i)$) are obtained through the same method described in DHW-only mode, where $t_{res}(i)$ substitutes t_{hour}.

The effective *EER* values, $EER_{r,eff}$ in heat recovery mode and $EER_{c,eff}$ in cooling-only mode, are obtained multiplying the respective *EER* values by the correction factor for on-off cycles, where the capacity ratio is evaluated as the ratio between $E_{HP,r}(i)$ and the product of $P_{HP,r,\Phi_{eff}}(i)$ multiplied by $(t_{hour} - t_{res}(i))$ (heat recovery mode), or as the ratio between $E_{HP,c}(i)$ and the product of $P_{HP,c,\Phi_{eff}}(i)$ multiplied by $t_{res}(i)$ (cooling-only mode).

The electric energy used by the heat pump in heat recovery mode and, if needed, in cooling-only mode, respectively $E_{HP,r,us}(i)$ and $E_{HP,c,us}(i)$, are evaluated dividing $E_{HP,r}(i)$ by $EER_{r,eff}(i)$ and $E_{HP,c}(i)$ by $EER_{c,eff}(i)$, respectively.

In the case the energy recovered at the heat pump condenser and the energy stored in the DHW tank are insufficient to cover the building demand for DHW and the hot tank thermal losses, the back-up system delivers the energy $E_{bk}(i)$, evaluated through the following equation (the energy used by the back-up system equals the ratio between $E_{bk}(i)$ and η_{bk}):

$$E_{bk}(i) = E_{b,d}(i) + E_{s,lost,d}(i) - E_{s,d}(i) - E_{cond}(i) \; . \tag{4.42}$$

The uncovered cooling energy, if present, is:

$$E_{uncov}(i) = E_{b,c}(i) + E_{s,gain,c}(i) - E_{s,c}(i) - E_{HP,r}(i) - E_{HP,c}(i) \; . \tag{4.43}$$

The water temperatures in the cold and hot tanks for the subsequent hour are:

$$T_{s,c}(i+1) = T_{s,c}(i) + \frac{E_{b,c}(i) + E_{s,gain,c}(i) - E_{HP,r}(i) - E_{HP,c}(i) - E_{uncov}(i)}{\rho_w \; V_{s,c} \; c_{p,w}} \; , \tag{4.44}$$

$$T_{s,d}(i+1) = T_{s,d}(i) + \frac{E_{cond}(i) + E_{bk}(i) - E_{b,d}(i) - E_{s,lost,d}(i)}{\rho_w \; V_{s,d} \; c_{p,w}} \; . \tag{4.45}$$

The MATLAB code evaluates the total seasonal energy values by summing the corresponding hourly values.

The seasonal performance of the system is then evaluated through the *SEER* (see Eq. (3.36)) and the Fuel Utilization Efficiency (*FUE* in the following equation), which gives the ratio between the total energy delivered to the building, by the heat pump and the back-up system, for cooling and DHW production, and the corresponding total primary energy used.

$$FUE = \frac{\sum_i E_{b,c}(i) - \sum_i E_{uncov}(i) + \sum_i E_{b,d}(i)}{\left[\dfrac{\sum_i E_{HP,r,us}(i) + \sum_i E_{HP,c,us}(i) + \sum_i E_{HP,d,us}(i)}{\eta_{el}} \right] + \sum_i E_{bk,prim}(i)} \; . \tag{4.46}$$

The MATLAB input file and script developed for the dynamic simulation of multi-function air-to-water heat pumps in summer operation are reported in Appendix, Section 7.2.

4.3 Application of the codes to the energy retrofit of a residential building in the framework of the HERB project

The codes developed for the dynamic simulation of electric air-to-water heat pumps for heating, cooling and domestic hot water production have been used to evaluate the seasonal performance of the multi-function heat pump used in the energy retrofit of a residential building in the framework of the HERB project. The topic of this section is discussed in Refs. [67]-[70].

The European project HERB (Holistic Energy-efficient Retrofitting of residential Buildings), which started in October 2012, aims to develop innovative technologies for the energy retrofitting of residential buildings and to perform retrofit demonstrations in seven European Countries: United Kingdom, Italy, Portugal, Greece, Spain, Switzerland and Netherlands (Ref. [71]).

4.3.1 Building subject to retrofitting and energy retrofit intervention

In Italy, the demonstration concerns a residential building in Bologna (North-Center Italy), a detached social house with six apartments, owned by the Municipality of the city.

The house, which has a total heated floor area of 282 m^2, is composed by three floors, with two apartments each, an attic and a basement. Figure 4.13 shows street views of the house in the pre-retrofit state, while Figure 4.14 illustrates the 3-D models.

Figure 4.13: Street views of the house: Northeast side (left) and Southwest side (right).

Figure 4.14: 3-D models of the house: Northeast and Northwest sides (left), Southwest and Southeast sides (right).

From Figure 4.14 it can be noticed that the first floor is larger than the second and the third. Plans of the apartments are reported in Figure 4.15: the first floor is represented on the left, the second and the third floor (which are identical) are represented on the right.
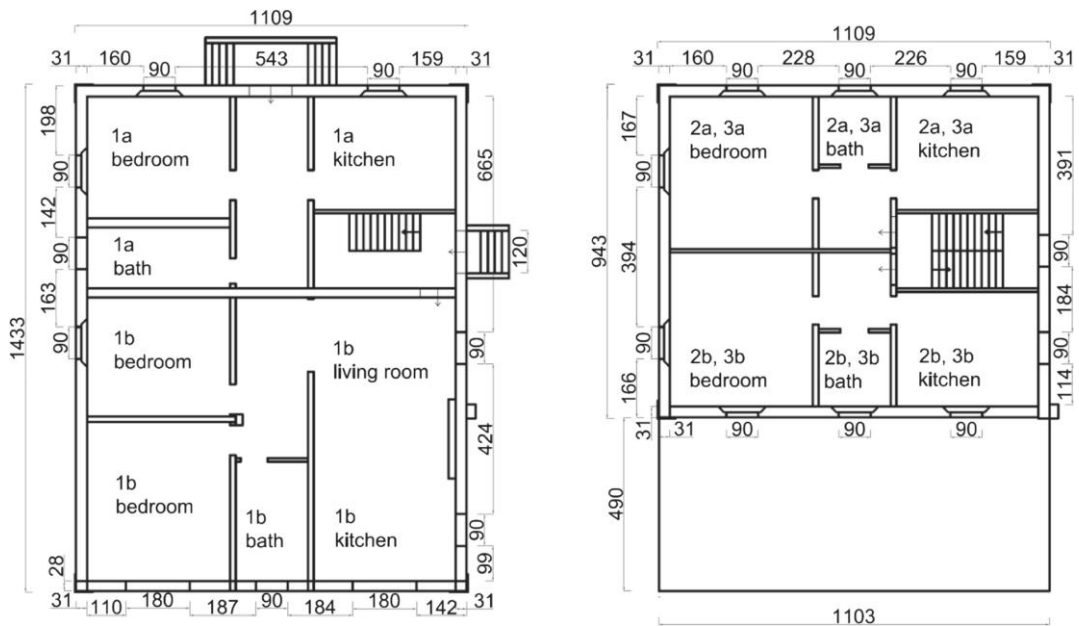
Figure 4.15: Plans of the apartments: first floor (left), second and third floor (right).

In the pre-retrofit condition the external wall, 31 cm thick, is made of solid bricks and is uninsulated, most windows are single glazed with wood frame, space heating is supplied by means of a gas boiler in the basement and radiators in the rooms, and DHW is supplied by single-apartment electric boilers (except for one apartment, which has a gas boiler). No

summer air-conditioning is present before retrofit and lighting is obtained with incandescent lamps.

With reference to the Meteonorm Typical Meteorological Year (TMY) on the software TRNSYS, the pre-retrofit annual use of primary energy for heating, DHW and lighting is 332.5 kWh/m^2. Among the efficiency targets of retrofitting prescribed by the HERB project, there are a reduction of at least 80 % in the primary energy use and an annual consumption of primary energy less than 50 kWh/m^2 (excluding appliances).

The retrofit intervention includes: thermal insulation of the external walls and floors; replacement of windows by double glazed windows with wood frame; installation of a multi-function air-to-water heat pump for heating, cooling and DHW; replacement of the old radiators by high-efficient fan coils and low temperature radiators; installation of new distribution systems for heating-cooling and DHW; LED lighting; installation on the roof of PV panels with conversion efficiency 14.5 %, area 29.25 m^2 and peak power 4.24 kW.

A reduction in the use of primary energy equal to 86.5 %, a reduction of CO_2 emission equal to 86.3 % and an annual use of primary energy equal to 44.8 kWh/m^2 (including summer cooling and dehumidifying) are expected to be reached.

Dynamic simulations of the building in the pre-retrofit and post-retrofit scenarios have been performed through TRNSYS 17; the Meteonorm TMY for Bologna available in that program has been employed. The hourly values and the mean monthly values of the external air temperature are reported in Figures 4.1, 4.10 and in Figures 4.2, 4.11, respectively.

The Meteonorm TMY has been employed also for the heat pump dynamic simulations, which have been performed by means of the two MATLAB codes described in Section 4.1 (for operation in heating and DHW production mode, with heating from October 1st to April 30th) and Section 4.2 (for operation in cooling-dehumidifying and DHW production mode, with cooling-dehumidifying from May 1st to September 30th).

The evaluation of the electric energy produced by the PV system has been performed according to the national standards UNI/TS 11300–4 [11] and UNI/TR 11328–1 [72].

4.3.2 Input data for the heat pump dynamic simulations

The dynamic simulations of the building through TRNSYS 17 allowed to determine the energy need for heating, which from 59.05 MWh/year before the retrofit becomes 16.67 MWh/year after the retrofit (set point: 20 °C), and the energy need for cooling-dehumidifying after retrofit, 8.15 MWh/year (set point: 27 °C, 50 % relative humidity).

By dividing the hourly building energy demand after retrofit by the distribution, control and emission efficiencies (each one equal to 0.98), the energy required at the outlet of the

generation subsystem (heat pump) is determined and used as input for the heat pump dynamic simulation codes.

The hourly values of the thermal power the heat pump has to supply for heating, in the Meteonorm TMY from TRNSYS 17, never exceed 11 kW.

The building thermal energy need for DHW production, which is determined by applying the national standard UNI/TS 11300–2 [59] (see Subsection 3.1.3), is equal to 5.22 MWh/year. The post-retrofit emission and distribution efficiencies for DHW can be assumed equal to 0.95 and 0.96, respectively.

In the post-retrofit scenario, a multifunction air-to-water inverter-driven heat pump (IDHP) provides heating, cooling and DHW, with the possibility of heat recovery mode for simultaneous production of cooling and DHW. The present gas boiler, installed in 2007, is kept as back-up system for heating and DHW (nominal power: 62 kW, efficiency, η_{bk}: 0.93).

The capacity of the thermal storage for DHW is 1.0 m^3 ($V_{s,d}$) and that of the thermal storage for heating/cooling is 0.2 m^3 ($V_{s,h} = V_{s,c}$); the storages heat loss coefficients are 2.3 W/K for DHW ($U_{s,d}$) and 1.1 W/K for heating/cooling ($U_{s,h} = U_{s,c}$). A b_u value of 0.5 (thermal storages placed in the basement) and a T_{int} value of 20 °C, during the heating season, and of 27 °C, during the cooling season, are adopted (see Subsection 4.1.4).

The new fan coils and radiators operate, during the heating season, with a water inlet temperature between 40 °C ($T_{s,h,max}$) and 38 °C ($T_{s,h,min}$). Table 4.4 reports the values of the thermal power supplied by the heat pump in heating mode and of the corresponding COP (COP_h), with water delivered at 40 °C and return temperature 34 °C, for several values of the external air temperature T_{ext} and of the inverter frequency Φ.

Values of the thermal power and corresponding COP in heating mode, with water delivered at 38 °C and return temperature 32 °C, for several values of the external air temperature T_{ext} and of the inverter frequency Φ, are reported in Table 4.5.

Table 4.4: Heat pump power [kW] and (COP) in heating mode; $T_{s,h}$ = 40 °C.

T_{ext} [°C]	Frequency [Hz]				
	110 (Φ_{max})	90	70	50	30 (Φ_{min})
-15 (TOL_h)	6.06 (2.29)	4.73 (2.31)	3.54 (2.25)	2.45 (2.09)	1.47 (1.77)
-7	7.63 (2.65)	6.01 (2.71)	4.53 (2.67)	3.15 (2.51)	1.89 (2.15)
2	9.99 (3.27)	7.91 (3.38)	6.01 (3.39)	4.19 (3.21)	2.51 (2.78)
7	11.70 (3.75)	9.14 (3.85)	6.95 (3.88)	4.90 (3.72)	2.93 (3.22)
12	13.50 (4.29)	10.60 (4.44)	8.09 (4.49)	5.66 (4.30)	3.41 (3.76)

Table 4.5: Heat pump power [kW] and (*COP*) in heating mode; $T_{s,h}$ = 38 °C.

T_{ext} [°C]	Frequency [Hz]				
	110 (Φ_{max})	90	70	50	30 (Φ_{min})
-15 (TOL_h)	6.10 (2.38)	4.78 (2.40)	3.56 (2.33)	2.48 (2.17)	1.48 (1.83)
-7	7.71 (2.76)	6.08 (2.82)	4.58 (2.78)	3.19 (2.61)	1.90 (2.23)
2	10.10 (3.42)	8.01 (3.55)	6.07 (3.53)	4.23 (3.35)	2.54 (2.89)
7	11.80 (3.94)	9.26 (4.05)	7.04 (4.07)	4.96 (3.90)	2.96 (3.36)
12	13.70 (4.53)	10.70 (4.68)	8.20 (4.74)	5.73 (4.52)	3.45 (3.94)

When the heat pump works for DHW production (DHW mode during the heating season, DHW-only mode during the cooling season), water is delivered with highest temperature 50 °C ($T_{s,d,max}$) and lowest temperature 48 °C ($T_{s,d,min}$); the corresponding return temperatures are 40 °C and 38 °C. Values of the heat pump power and *COP* for DHW production, with evaporator in external air and water delivered at 50 °C, for several values of the external air temperature and of the inverter frequency, are reported in Table 4.6.

Table 4.6: Heat pump power [kW] and (*COP*) in DHW mode; $T_{s,d}$ = 50 °C.

T_{ext} [°C]	Frequency [Hz]				
	110 (Φ_{max})	90	70	50	30 (Φ_{min})
-10 (TOL_d)	6.49 (2.02)	5.00 (2.03)	3.74 (1.99)	2.56 (1.85)	1.53 (1.60)
-7	7.27 (2.19)	5.67 (2.22)	4.24 (2.19)	2.94 (2.06)	1.76 (1.79)
2	9.50 (2.64)	7.42 (2.71)	5.60 (2.70)	3.90 (2.57)	2.33 (2.25)
7	11.00 (2.97)	8.62 (3.06)	6.46 (3.04)	4.56 (2.94)	2.71 (2.57)
12	12.70 (3.36)	10.00 (3.49)	7.54 (3.49)	5.29 (3.37)	3.17 (2.97)
20	15.90 (4.15)	12.60 (4.35)	9.50 (4.36)	6.67 (4.24)	3.98 (3.74)
25	18.10 (4.69)	14.30 (4.89)	10.80 (4.93)	7.51 (4.76)	4.49 (4.22)
30	20.30 (5.21)	16.00 (5.44)	12.00 (5.47)	8.38 (5.29)	4.97 (4.66)
35	22.40 (5.71)	17.60 (5.97)	13.30 (6.00)	9.24 (5.81)	5.49 (5.14)

In cooling-only mode and in heat recovery mode, cold water is delivered at maximum 7 °C ($T_{s,c,max}$) and minimum 5 °C ($T_{s,c,min}$), and returns at 12 °C or 10 °C, respectively. Values of the heat pump cooling power and *EER*, for several values of the external air temperature and of the inverter frequency, are reported in Table 4.7 ($T_{s,c,max}$) and in Table 4.8 ($T_{s,c,min}$).

Table 4.7: Heat pump power [kW] and (*EER*) in cooling-only mode; $T_{s,c}$ = 7 °C.

T_{ext} [°C]	Frequency [Hz]				
	110 (Φ_{max})	90	70	50	30 (Φ_{min})
20	11.20 (4.78)	9.13 (5.22)	7.06 (5.43)	5.06 (5.34)	3.07 (4.62)
25	10.60 (4.08)	8.68 (4.45)	6.72 (4.63)	4.81 (4.56)	2.92 (3.98)
30	10.10 (3.48)	8.22 (3.80)	6.37 (3.96)	4.56 (3.92)	2.76 (3.45)
35	9.54 (2.97)	7.76 (3.24)	6.02 (3.39)	4.30 (3.36)	2.61 (3.00)

Table 4.8: Heat pump power [kW] and (*EER*) in cooling-only mode; $T_{s,c}$ = 5 °C.

T_{ext} [°C]	Frequency [Hz]				
	110 (Φ_{max})	90	70	50	30 (Φ_{min})
20	10.60 (4.48)	8.56 (4.85)	6.64 (5.04)	4.73 (4.91)	2.87 (4.24)
25	10.00 (3.83)	8.14 (4.16)	6.29 (4.30)	4.50 (4.22)	2.73 (3.67)
30	9.48 (3.28)	7.71 (3.57)	5.96 (3.70)	4.26 (3.64)	2.58 (3.20)
35	8.93 (2.80)	7.26 (3.04)	5.63 (3.17)	4.02 (3.14)	2.43 (2.78)

Values of the heat pump power and *EER* in heat recovery mode (condensation heat supplied to DHW), either at $T_{s,c,max}$ or at $T_{s,c,min}$, are reported in Table 4.9, or Table 4.10, respectively.

Table 4.9: Heat pump power [kW] and (*EER*) in heat recovery mode; $T_{s,c}$ = 7 °C.

$T_{s,d}$ [°C]	Frequency [Hz]				
	110 (Φ_{max})	90	70	50	30 (Φ_{min})
48	8.86 (2.45)	7.11 (2.59)	5.45 (2.63)	3.84 (2.54)	2.30 (2.23)
50	8.62 (2.30)	6.92 (2.42)	5.31 (2.47)	3.74 (2.40)	2.24 (2.11)

Table 4.10: Heat pump power [kW] and (*EER*) in heat recovery mode; $T_{s,c}$ = 5 °C.

$T_{s,d}$ [°C]	Frequency [Hz]				
	110 (Φ_{max})	90	70	50	30 (Φ_{min})
48	8.25 (2.30)	6.64 (2.43)	5.07 (2.46)	3.58 (2.39)	2.14 (2.08)
50	8.03 (2.15)	6.44 (2.27)	4.93 (2.30)	3.48 (2.23)	2.07 (1.95)

4.3.3 Results of the heat pump simulations and retrofit achievements

The amount of electric energy used by the heat pump for heating and DHW from October 1st to April 30th, determined by the MATLAB hourly simulation code for winter operation described in Section 4.1, is 6536 kWh. By considering the efficiency of the electricity production system in Italy (η_{el} = 0.46 according to the Italian Regulatory Authority for Electricity, Gas and Water), one finds a corresponding use of primary energy of 14209 kWh. The primary energy used by the gas boiler, for heating and DHW integration during the heating season, is 414 kWh. Therefore, the seasonal use of primary energy for heating and DHW is 14623 kWh. The value of the *FUE* in winter operation is 1.44.

The amount of electric energy used by the heat pump for cooling-dehumidifying and DHW from May 1st to September 30th, determined by the MATLAB hourly simulation code for summer operation described in Section 4.2, is 2905 kWh, which corresponds to 6315 kWh of primary energy used. The primary energy used by the gas boiler for integration of DHW during this period is about 1 kWh. The obtained *FUE* for summer operation is therefore 1.75. The PV system provides part of the electric energy used by the heat pump and by the fan coils, and used for lighting. Table 4.11 reports the annual electric energy use of the building, the amount of electric energy produced by the PV panels, the amount of electric energy from the PV system employed for self-use and that supplied to the grid, the electric energy taken from the grid and the corresponding primary energy used. According to Refs. [11], [72], the previous electric energy balances are evaluated month by month.

Table 4.11: Annual electric energy use and corresponding primary energy consumption.

Total building	9869 kWh/year
PV	4663 kWh/year
Self-use	4251 kWh/year
To grid	413 kWh/year
From grid	5619 kWh/year
Primary	12215 kWh/year

Table 4.11 shows that the annual use of primary energy due to the use of electric energy from the grid is 12215 kWh. By adding the primary energy used by the gas boiler, 415 kWh, one obtains the total annual use of primary energy of the building, 12630 kWh, which corresponds to 44.8 kWh/m². The retrofit intervention, therefore, yields a primary energy saving with respect to the pre-retrofit scenario of 86.5 %, complying with the HERB project

efficiency targets, and providing summer cooling and dehumidifying, a service not available before the retrofit.

4.4 VALIDATION OF THE NUMERICAL CODES

At the moment of writing this Thesis, the energy retrofit described in the previous section has been started but not completed. Once finished the interventions, a post-retrofit monitoring of the building and of the plants is planned (see Section 6.2). In particular, a monitoring of the multi-function air-to-water heat pump system will be performed, in order to measure the heating and cooling energy delivered and the electric energy used by the heat pump, as well as the primary energy used by the gas boiler (back-up system).

A comparison between the obtained experimental results and the predictions of the dynamic simulation codes developed in this Thesis will then be made.

This section presents a numerical validation of the codes through the software TRNSYS, which allows to perform dynamic simulations of buildings and of several plants.

4.4.1   Inputs of the TRNSYS simulations

As described in Subsection 2.3.1, the software TRNSYS can be used to execute dynamic simulations of heat pumps; air-to-water-heat pumps, in particular, can be modelled by means of the pre-defined TRNSYS Types 917 or 941. Type 941 has been chosen for the numerical validation, as the change in humidity across the air side of the heat pump is not taken into account.

The reversible heat pump described in Section 4.3 is simulated, but constrained to operate at the maximum frequency, as the TRNSYS component is not able to simulate inverter-driven heat pumps.

A simulation of the heat pump in heating mode and a simulation in cooling-only mode are performed with TRNSYS. Figure 4.16 shows the workspace of the TRNSYS simulations, with the Type for the heat pump (Type 941), together with the other Types employed and the respective connections.
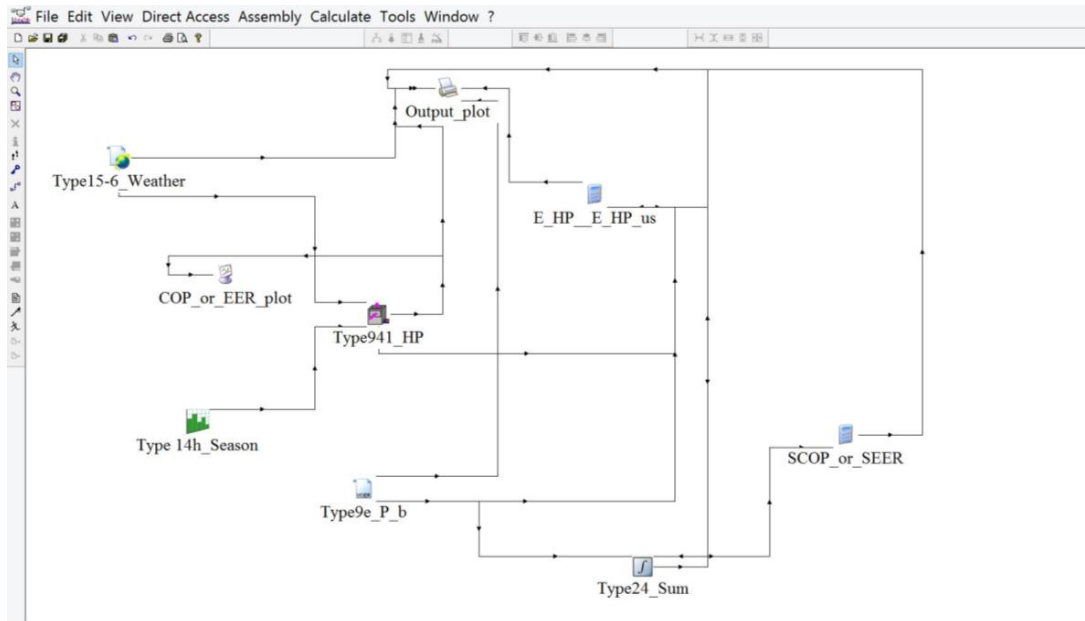
Figure 4.16: Workspace of the TRNSYS simulations.

Domestic hot water production is not considered for the validation of the codes, because, as explained in Subsection 2.3.1, Type 941 employs a different and more simplified method to produce domestic hot water.

The dynamic MATLAB codes employ second-order polynomial functions to interpolate among the manufacturer data of heat pump power and *COP*, or *EER*. On the other hand, Type 941 employs linear interpolations of the heat pump input data of power delivered, and used, at different external air temperatures (T_{ext}), without extrapolating beyond the data range provided (see Subsection 2.3.1). Consequently, if values of T_{ext} outside the heat pump data range are provided, the maximum or minimum performance values are employed by the component. Hence, in order to avoid incorrect evaluations of heat pump power, *COP* and *EER*, the file of the heat pump performance data read by Type 941 was compiled also for values of T_{ext} below and above the extreme temperatures reached in the season by the selected climate.

Tables 4.12, 4.13 report the input data of power delivered, and used, by the heat pump at different outdoor temperatures, in heating mode and in cooling-only mode, respectively. The data are expressed as fractions of the heat pump power at rated conditions, as required by Type 941.

Table 4.12: Heat pump performance inputs in heating mode for Type 941 of TRNSYS.

$T_{w,h}$ = 40 °C (inlet water temperature: $T_{w,in,h}$ = 34 °C)		
T_{ext} [°C]	$P_{HP,h}$ / ($P_{HP,h}$ at rated condition)	$P_{HP,h,us}$ / ($P_{HP,h,us}$ at rated condition)
-15	0.52	0.85
-7	0.65	0.92
2	0.85	0.98
7	1.00	1.00
12	1.15	1.01
26	1.58	1.03
$P_{HP,h}$ at rated condition = 42120 kJ/h; $P_{HP,h,us}$ at rated condition = 11232 kJ/h		

Table 4.13: Heat pump performance inputs in cooling-only mode for Type 941 of TRNSYS.

$T_{w,c}$ = 7 °C (inlet water temperature: $T_{w,in,c}$ = 12 °C)		
T_{ext} [°C]	$P_{HP,c}$ / ($P_{HP,c}$ at rated condition)	$P_{HP,c,us}$ / ($P_{HP,c,us}$ at rated condition)
10	1.11	0.82
20	1.00	1.00
25	0.94	1.11
30	0.90	1.24
35	0.85	1.37
45	0.76	1.63
$P_{HP,c}$ at rated condition = 40320 kJ/h; $P_{HP,c,us}$ at rated condition = 8424 kJ/h		

No correction factor for on-off cycles is considered in the simulations, as Type 941 has no pre-defined methodology to evaluate the associated heat pump performance decrease; manually introducing the same equations used by the MATLAB codes would obviously yield the same results.

No back-up system is considered for the comparison, because, as explained in Subsection 2.3.1, if the auxiliary heating control signal of the TRNSYS component is on, no evaluation of the needed energy is made by Type 941 and the entire capacity of the auxiliary heater is applied to the primary water stream.

Type 15-6 (see Figure 4.16) is employed in the simulations with TRNSYS to read the Meteonorm climate file of Bologna (Italy) and is linked to Type 941 to provide the hourly values of the external air temperature needed by the heat pump component.

Type 14h, which can define a time dependent forcing function, is used to provide the heating, or cooling, control signal to the heat pump Type. Heating is on from January 1st to April 30th

and from October 1st to December 31st, while cooling is on for the remaining period of the year. As described in the mathematical reference for the standard component library of the software [73], the pattern of the forcing function of the Type is established by a set of discrete data points, indicating the value of the function at various times throughout one cycle. A linear interpolation is provided in order to generate a continuous forcing function from the discrete data. In this case, the times of the data points correspond to the first hour of January 1st and of October 1st and to the last hour of April 30th and of December 31st. The value of the function for the simulation in heating mode is equal to 1 from January 1st to April 30th and from October 1st to December 31st and is equal to zero for the remaining time (the opposite values are adopted for the simulation in cooling-only mode).

The data reader Type 9e is employed to read the hourly values of the energy needed for heating and cooling by the building coupled with the heat pump; the building subject of the energy retrofit described in Section 4.3 is considered.

As the TRNSYS Type 941 does not support the building energy need as an input (see Subsection 2.3.1), an equation component is added in the TRNSYS simulations (see the Type named "E_HP__E_HP_us" in Figure 4.16) in order to determine the hourly energy supplied to the building for heating or cooling and the corresponding electric energy consumption of the heat pump. The equation component evaluates the hourly value of the energy delivered by the heat pump, $E_{HP}(i)$, as:

$$E_{HP}(i) = \min\left[\left|P_{HP}(i)\right|; \ P_b(i)\right] t_{hour} \ , \tag{4.47}$$

where the module of the heat pump power $P_{HP}(i)$ is needed as the heat pump power evaluated by Type 941 is negative in cooling mode; $P_b(i)$ is the hourly energy needed by the building for heating or cooling and t_{hour} is the hour duration.

The corresponding electric energy used by the heat pump, $E_{HP,us}(i)$, is evaluated through the equation component as:

$$E_{HP,us}(i) = \frac{E_{HP}(i)}{\left[COP(i) + 10^{-10}\right]} gt\left[COP(i); \ 10^{-10}\right] \ , \tag{4.48}$$

where $COP(i)$ is the hourly value of COP (or EER, for the summer simulation) obtained by Type 941. The term 10^{-10} at the denominator and the gt-expression at the numerator of Eq. (4.48) are added to avoid a value of $E_{HP,us}(i)$ equal to infinity for the hours without building energy needs (heat pump off, COP or EER equal to zero). The gt-expression is a TRNSYS pre-defined function, which turns out equal to 1 if the first term (the hourly value of COP or EER) is greater than or equal to the second term (10^{-10}). Therefore, if in the i-th hour the heat

pump is off, the *gt*-expression and, consequently, the value of $E_{HP,us}$ turn out equal to zero, whereas, if the heat pump is on, the *gt*-expression is equal to 1 and the heat pump electric consumption is equal to the ratio between the energy delivered and the *COP* (or *EER*) value (summing 10^{-10} practically lets the value unchanged).

The integrator Type 24 is employed and linked to Type 9e and to the equation component, in order to obtain the total (seasonal) values of energy needed by the building, supplied by the heat pump and used by the heat pump.

Finally, another equation component ("SCOP_or_SEER" in Figure 4.16) is used to evaluate the heat pump seasonal performance ($SCOP_{net}$ or *SEER*), as the ratio between the total energy supplied by the heat pump for heating (or cooling) and the total electric energy used.

4.4.2   Results and comparisons

Type 25a (printer, named "Output_plot" in Figure 4.16) is used to print the outputs of the simulations with TRNSYS. The simulation in heating mode yields a value of $SCOP_{net}$ equal to 3.39. The value of $SCOP_{net}$ derived from the same simulation performed through the dynamic MATLAB code for winter operation is 3.42. The relative discrepancy of the MATLAB code with respect to TRNSYS is thus 0.80 %. The simulation in cooling mode yields a value of *SEER* equal to 3.85 according to TRNSYS and equal to 3.87 according to the MATLAB dynamic code for summer operation. The relative discrepancy in this case is 0.38 %. The results of the comparisons are summarized in Table 4.14.

Table 4.14: Seasonal performance coefficients obtained with TRNSYS and with the MATLAB codes.

	TRNSYS	MATLAB code	Relative discrepancy
$SCOP_{net}$	3.39	3.42	0.80 %
SEER	3.85	3.87	0.38 %

Type 65d (online plotter without file, named "COP_or_EER_plot" in Figure 4.16) plots on screen the hourly values of *COP* (or *EER*) evaluated by the TRNSYS Type 941. Figure 4.17 and Figure 4.18 compare the hourly trends of *COP* and *EER* of the MATLAB codes with those of the TRNSYS simulations. As highlighted by the plots, and especially by the zoomed portions reported as examples on the right of the figures, the hourly values of *COP* and *EER* obtained with the MATLAB codes are always very similar to those obtained with TRNSYS. The maximum discrepancy observed is equal to 2.17 % and refers to the *COP*.

The very low values of relative discrepancy obtained by the comparisons allow us to conclude that the codes developed for the hourly simulation of air-to-water heat pumps are validated numerically.
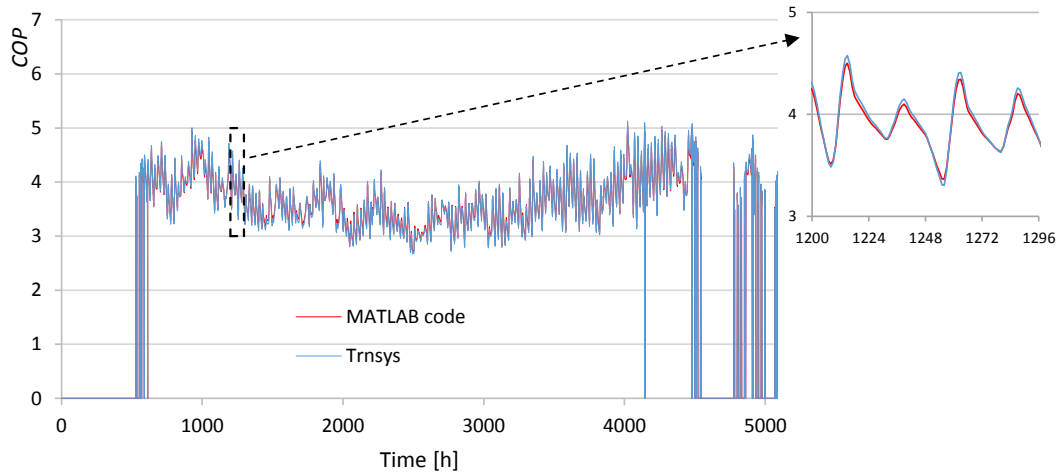
Figure 4.17: Hourly trend of *COP* according to TRNSYS and to the MATLAB codes, from October 1st to April 30th.
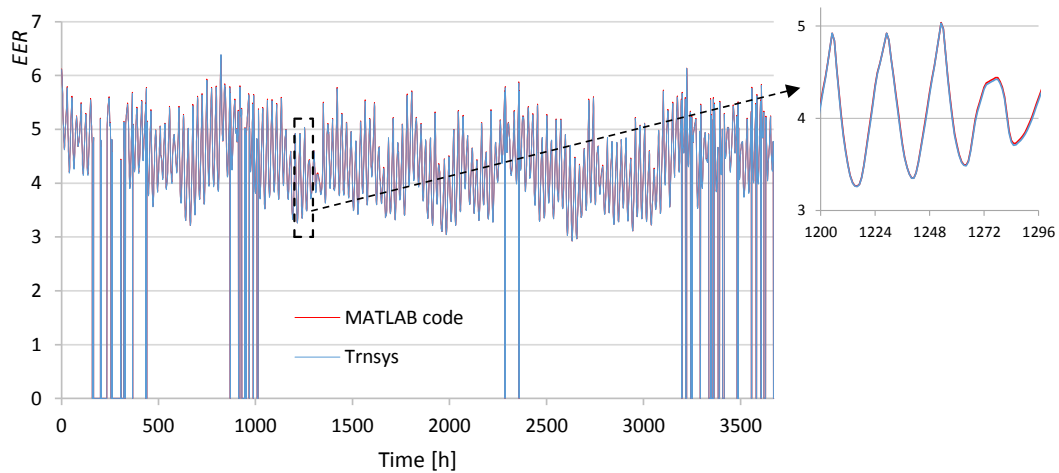
Figure 4.18: Hourly trend of *EER* according to TRNSYS and to the MATLAB codes, from May 1st to September 30th.

4.5 COMPARISON BETWEEN THE SIMULATION METHODS FOR AIR-TO-WATER HEAT PUMPS

In Sections 4.1 and 4.2 the codes implemented in MATLAB for the dynamic simulation of air-to-water heat pumps were described, while Sections 3.1 and 3.2 presented the codes for the heat pumps simulation through the bin-method, developed starting from the European standard EN 14825 [10] and the Italian standard UNI/TS 11300-4 [11].

The difference between the two methodologies, in terms of evaluation of a heat pump seasonal performance, can be negligible or significant, depending on the examined case. The aim of this section, whose topic is treated in Ref. [74], is to compare the results of the bin-method with the results deducted by using the dynamic simulation, for heat pump systems used for heating. The values of the seasonal indexes $SCOP_{net}$ and $SCOP_{on}$ obtained with the different methods, both for ON-OFF HPs and for IDHPs, integrated by electric heaters, are evaluated and compared to each other. Different buildings placed in different Italian climates are used, in order to highlight the main conditions which are responsible of the differences between the results obtained with the bin-method and with the dynamic hourly simulation.

4.5.1 Implementation of the climate, building and heat pump

In the dynamic simulation code, the hourly climate data of the Test Reference Year (TRY) defined by the Italian thermotechnical committee CTI (Comitato Termotecnico Italiano) are used, for the Italian towns of Naples (40.50 °N, 14.15 °E), Bologna (44.29 °N, 11.20 °E) and Milan (45.28 °N, 9.11 °E).

The standard UNI/TS 11300-4 [11] evaluates the bin trend of an Italian location by assuming a normal distribution of the external air temperature, T_{ext}, obtainable starting from the local values of outdoor design temperature, monthly average external air temperature and daily global solar radiation on horizontal plane. The simulations with bin-method are performed through the bin distributions for the heating season in Milan, Bologna and Naples indicated by the Italian standard and those derived from the hourly values of T_{ext} according to the TRY defined by CTI.

The conventional heating season is from October 15th to April 15th for Milan and Bologna and from November 15th to March 31st for Naples. The obtained bin profiles according to Ref. [11] are shown in Figures 4.19-4.21 (blue colour), together with the bin trends derived for the same locations from the CTI's TRY (red colour).
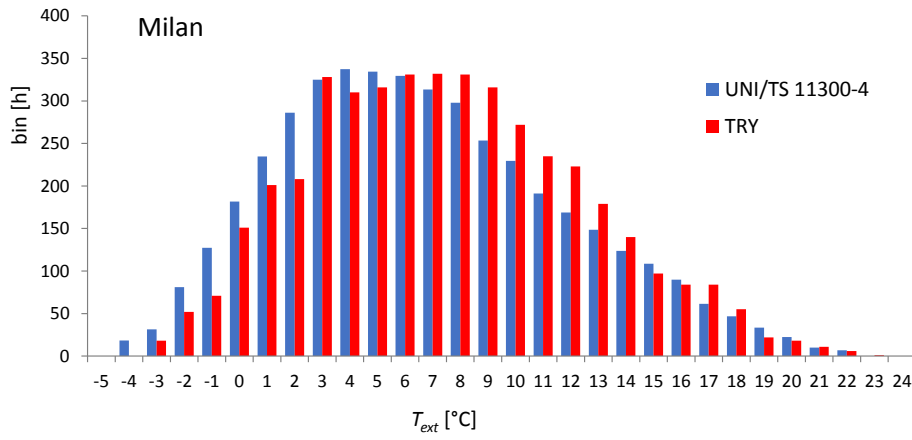
Figure 4.19: Bin profiles for Milan according to the standard UNI/TS 11300-4 and derived from the CTI's TRY.
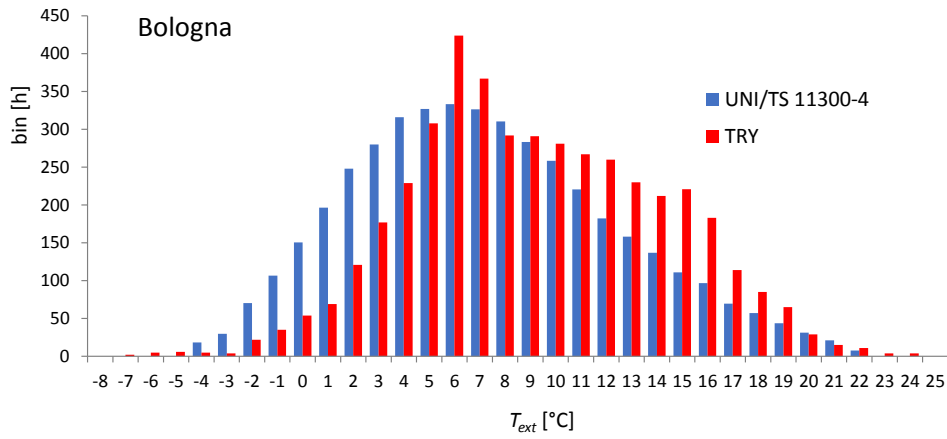
Figure 4.20: Bin profiles for Bologna according to the standard UNI/TS 11300-4 and derived from the CTI's TRY.
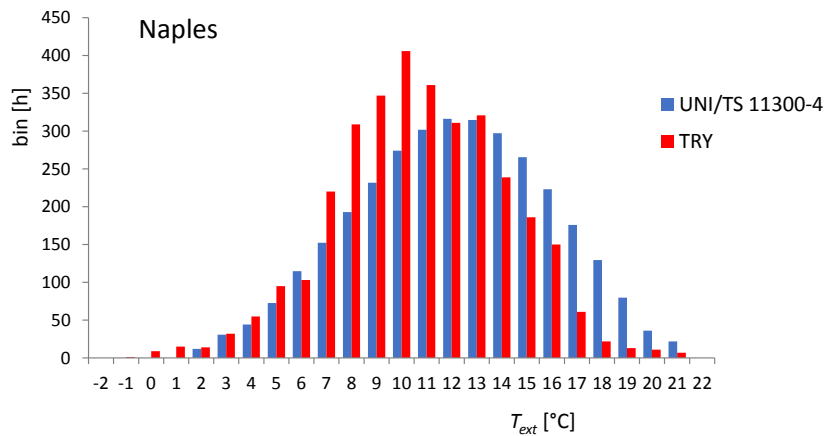
Figure 4.21: Bin profiles for Naples according to the standard UNI/TS 11300-4 and derived from the CTI's TRY.

It is evident from Figures 4.19-4.21 that the bins calculated by using the CTI's TRY and those evaluated with the method proposed by the standard UNI/TS 11300-4 [11] are different. For instance, the bin profiles evaluated according to Ref. [11] are characterized by an average temperature of 6.8 °C in Milan, 7.3 °C in Bologna and 12.1 °C in Naples, versus the values of 7.4 °C (Milan), 9.2 °C (Bologna) and 10.7 °C (Naples) obtained by using the CTI's TRY.

The thermal behavior of the building during the heating season is introduced in the simulations by using the building energy signature, BES. In order to consider different building loads and their effect on the heat pump seasonal performance, several BES lines are considered, by fixing equal to 16 °C the value of the external temperature where the building heating demand becomes zero, T_{zl}, and by varying the value of the building design load, $P_{des,h}$, in correspondence of the outdoor design temperature, $T_{des,h}$.

In order to compare the results obtained from the bin-method with those derived from the dynamic simulation, the hourly values of the energy required by the building in the dynamic simulation are calculated, in each case studied, by means of the same BES line as that used in the simulation with the bin-method.

Figure 4.22 shows the characteristic curves (P_{HP}) of the ON-OFF HP and of the IDHP (at maximum frequency) selected for the simulations. The curves are obtained by interpolation of the manufacturer data in correspondence of a temperature of the hot water produced equal to 35 °C (i.e. for radiant panels heating systems). In the same graph the corresponding curves of the electric power used by the heat pumps ($P_{HP,us}$) are also plotted. $P_{HP,us}$ is obtained as the ratio between P_{HP} and the corresponding COP.
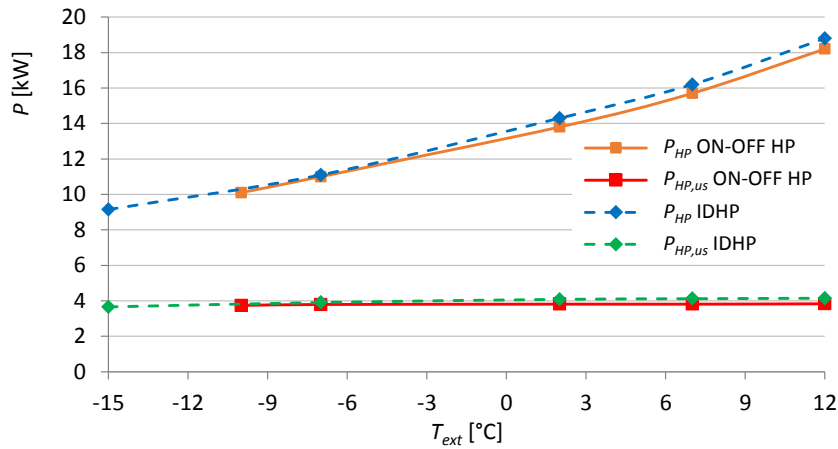
Figure 4.22: Characteristic curves of the heat pumps with corresponding electric power used.

From Figure 4.22 one can notice that the selected heat pumps are characterized by similar values of the power delivered, and used, at full load, at the same outdoor temperature conditions.

Table 4.15 shows the IDHP power and *COP* data given by the manufacturer for several inverter frequencies and external air temperatures (for a fixed hot water temperature of 35 °C).

Table 4.15: IDHP power [kW] and (*COP*) for different inverter frequencies and external air temperatures.

T_{ext} [°C]	Frequency [Hz]				
	85 (Φ_{max})	69	53	36	20 (Φ_{min})
-15 (*TOL*)	9.15 (2.50)	7.43 (2.57)	5.71 (2.56)	3.94 (2.42)	2.17 (1.98)
-7	11.10 (2.84)	9.06 (2.94)	7.00 (2.95)	4.86 (2.81)	2.67 (2.32)
2	14.30 (3.50)	11.60 (3.61)	8.93 (3.64)	6.28 (3.54)	3.42 (2.91)
7	16.20 (3.93)	13.20 (4.08)	10.30 (4.16)	7.23 (4.06)	3.94 (3.36)
12	18.80 (4.53)	15.30 (4.73)	11.90 (4.85)	8.38 (4.73)	4.60 (3.95)

By comparing to each other the data shown in Table 4.15 it is evident that, while the values of P_{HP} obviously decrease with the reduction of the inverter frequency, the values of the *COP* become higher until a frequency around half the maximum one is reached, after which they decrease.

As the bin-method cannot simulate a storage tank, no thermal storages are taken into account in the performed comparisons.

4.5.2   Results and discussion

First of all, the coherence of the bin-method with the dynamic simulation has been tested. Starting from the CTI's TRY for Milan, a comparison is made in terms of $SCOP$, by using the dynamic simulation and the bin-method in which the bins are calculated by using the same TRY data used in the dynamic simulation. The data of Figure 4.23 show the $SCOP_{on}$ and $SCOP_{net}$ obtained in Milan with the ON-OFF HP and IDHP for several buildings (several values of the bivalent temperature, T_{biv}).
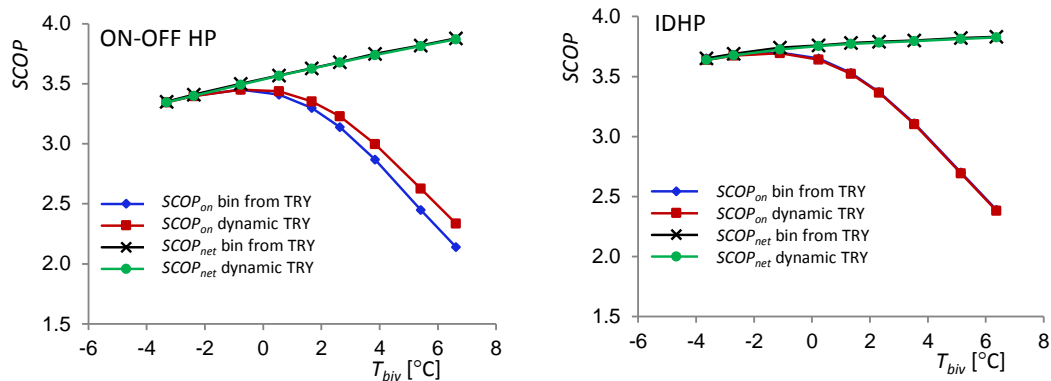
Figure 4.23: $SCOP$ as function of T_{biv} with dynamic simulation and bin simulation from CTI's TRY, ON-OFF HP (left) and IDHP (right), Milan.

As evidenced by Figure 4.23, the achieved results in terms of $SCOP$ with the two different approaches are in agreement with each other. The maximum discrepancy recorded is about 9 % and is referred to the $SCOP_{on}$ of the ON-OFF HP in the service of a building with a value of T_{biv} equal to 6.6 °C (rightmost point on the red and blue curves, graph on the left of Figure 4.23). Similar results are obtained in the climates of Bologna and Naples. This means that the bin-method is able to give a prediction of the seasonal performance coefficients of the heating plant in good agreement with the more accurate results available from the dynamic simulation of the system, if the two methods use the same climatic data as input.

The results reported in Figures 4.24-4.26, on the other hand, show the differences in the Seasonal Coefficients Of Performance, obtained by following the bin-method by UNI/TS 11300-4 [11] and the dynamic simulation based on the CTI's TRY, for buildings located in Milan, Bologna and Naples.

127
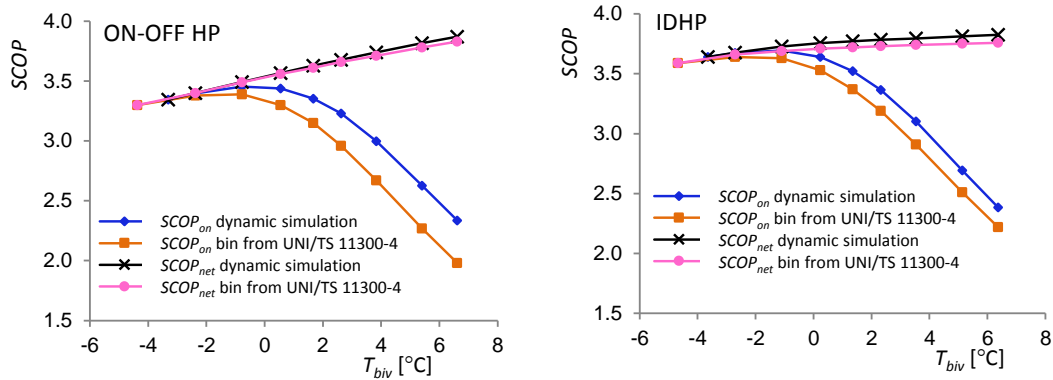
Figure 4.24: *SCOP* as function of *T*$_{biv}$ with dynamic simulation and bin simulation from UNI/TS 11300-4, ON-OFF HP (left) and IDHP (right), Milan.
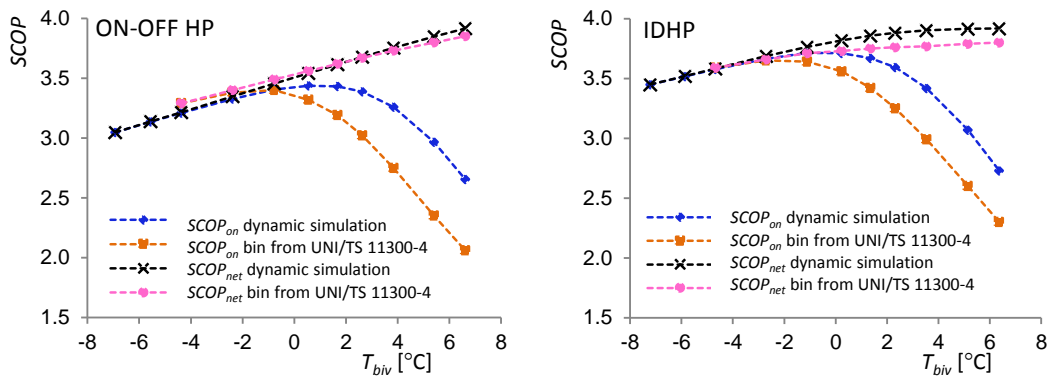
Figure 4.25: *SCOP* as function of *T*$_{biv}$ with dynamic simulation and bin simulation from UNI/TS 11300-4, ON-OFF HP (left) and IDHP (right), Bologna.
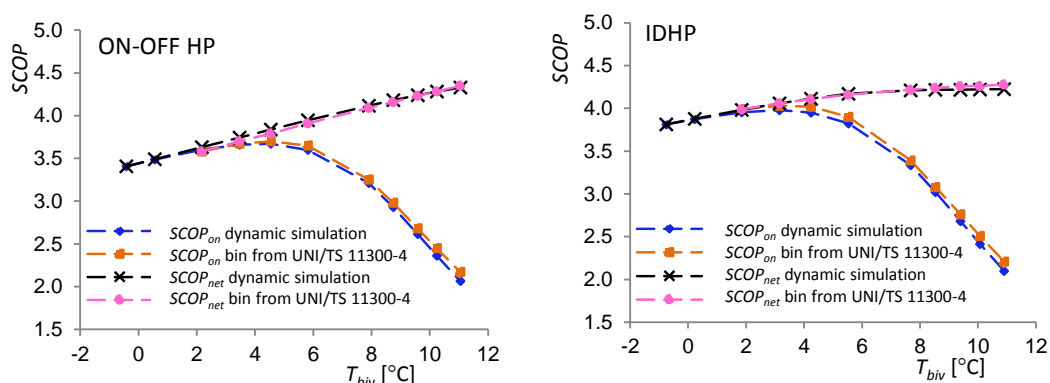
Figure 4.26: *SCOP* as function of T_{biv} with dynamic simulation and bin simulation from UNI/TS 11300-4, ON-OFF HP (left) and IDHP (right), Naples.

Since these approaches are based on climatic data not exactly coincident, Figures 4.24-4.26 evidence differences in the *SCOP* values larger than those of Figure 4.23 . More in detail, the two approaches tend to show larger differences in the values of *SCOP* in correspondence of high bivalent temperatures, i.e. with heat pumps undersized with respect to the building thermal demand. The differences in terms of $SCOP_{on}$ are mainly related to the back-up activation, which is more relevant at larger values of T_{biv} and in colder climates, conditions corresponding to a higher number of hours with T_{ext} under T_{biv} (with consequent back-up activation).

As highlighted by Figure 4.19, the bin distributions for Milan derived from the TRY and from the UNI/TS 11300-4 [11] method are very similar (the average temperature from the TRY is 0.6 °C higher than the value of the Italian standard) and the values of *SCOP* obtained with the two methods tend to be very close to each other (see Figure 4.24).

In Bologna (see Figure 4.25) higher *SCOP* are obtained with the dynamic simulation with respect to the bin-method, because of the climate differences (the CTI's TRY data present an average temperature 1.9 °C larger with respect to the bin distribution calculated through Ref. [11]).

It is evident by comparing Figure 4.24 and Figure 4.25 that in Bologna the differences in terms of $SCOP_{on}$ obtained by using the dynamic simulation and the bin-method are larger with respect to the differences obtained in Milan. In addition, for a fixed value of the bivalent temperature, the difference in terms of $SCOP_{on}$ is larger for the ON-OFF HP than for the IDHP. The difference in terms of $SCOP_{net}$ is very limited for both Milan and Bologna.

In Figure 4.26 the same evaluation is made for Naples. In this case the dynamic simulation and the bin-method give very similar values of $SCOP_{on}$ and $SCOP_{net}$, both for the ON-OFF HP

and the IDHP. When the bivalent temperature is reduced (oversized heat pump) the *SCOP* increase due to the hotter climate of Ref. [11] is reduced by the increase of the number of on-off cycles and the seasonal performance coefficients tends to become equal by using the dynamic simulation (colder outdoor temperatures, lower number of on-off cycles) and the bin-method based on the UNI/TS 11300-4 [11] distribution (hotter outdoor temperatures, higher number of on-off cycles).

Figure 4.27 shows, as function of T_{biv}, the *SCOP* difference obtained from the dynamic simulation and the bin-method. The choice of the calculation method influences especially the value of the $SCOP_{on}$, whose relative difference reaches 22.4 % (ON-OFF HP in Bologna with T_{biv} = 6.6 °C: rightmost point on the green continuous line, graph on the right of Figure 4.27), while the maximum relative difference on the $SCOP_{net}$ is very limited (3.4 % for the IDHP in Bologna with T_{biv} = 3.5 °C). These results highlight that the largest relative difference in terms of $SCOP_{on}$ is generally observed for the ON-OFF HP with high values of the bivalent temperature.
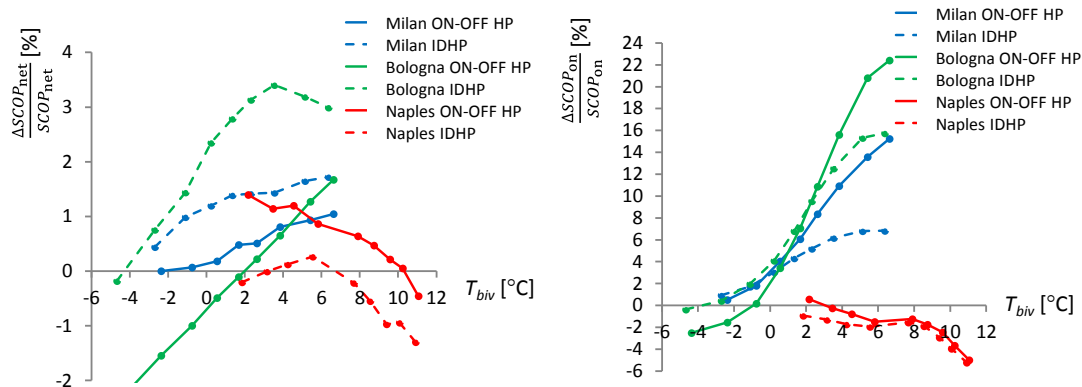
Figure 4.27: Relative differences on the seasonal coefficients as functions of the bivalent temperature.

To sum up, the obtained results put in evidence how the predictions of the bin-method are in agreement with the results of the dynamic simulation only in particular conditions. The discrepancies in the *SCOP* values between the two approaches can be higher than 20 %, varying with the climate data and with the considered type of heat pump.

5

A DYNAMIC SIMULATION CODE FOR GROUND-COUPLED HEAT PUMP SYSTEMS

In this chapter, a code for the hourly simulation of Ground-Coupled Heat Pump (GCHP) systems, based on the *g-functions* obtained in Ref. [9], is presented.

The code, executable through any programming language and here implemented in MATLAB, applies to mono-compressor on-off and inverter-driven GCHP, used for building heating and/or cooling. Both the heat pump and the coupled Borehole Heat Exchanger (BHE) field are simulated, even for several years.

The code is employed to analyze the effects of the inverter and of the total length of the BHE field on the mean seasonal *COP* and on the mean seasonal *EER* of a GCHP system designed for a residential house with dominant heating loads.

The dynamic code is validated by comparing the mean monthly temperatures of the BHE fluid obtained in a 50-year simulation by means of the proposed model and of the software Earth Energy Designer (EED).

The topics of this chapter are discussed in Ref. [75].

5.1 MATHEMATICAL MODEL

A numerical code for the hourly simulation of GCHPs for building heating and cooling, written on the software MATLAB, is presented. The studied system is composed of a brine-to-water heat pump, coupled with a borehole heat exchanger field. The simulation period can reach

several years with low computational time; several decades can be simulated with the aid of monthly simulations.

5.1.1   Building and heat pump characterization

An input of the dynamic simulation code is the vector P_b of the mean hourly loads of the building during a whole year at the outlet of the generation subsystem (heat pump) for heating or cooling. The values of P_b, which can derive from a dynamic simulation of the building, must be set as negative for the heating season and as positive for the cooling season. The corresponding hourly value $E_b(i)$ of the energy needed by the building in the i-th hour of the simulated period is evaluated as:

$$E_b(i) = t_{hour}\ P_b(i - 8760 \times [year(i) - 1])\ ,$$
(5.1)

where t_{hour} is the hour duration and $year(i)$ is the number of the year of the i-th hour within the simulated period, which can be calculated in MATLAB by using the *ceil* function (rounding to the nearest greater integer):

$$year(i) = ceil\left(\frac{i}{8760}\right).$$
(5.2)

The water(brine)-to-water heat pump is characterized by employing the same procedure as described in Subsection 3.1.4, where, in place of the external air temperature, the BHE fluid supply temperature $T_{f,out}$ (heat pump inlet temperature) is used.

The required input data in the case of mono-compressor on-off heat pumps (ON-OFF HPs) are the values, given by the manufacturer, of heat pump power, *COP* and *EER* in heating mode and in cooling mode, for a fixed value of the hot (or cool) water produced, T_w, and for different BHE fluid supply temperatures. For inverter-driven heat pumps (IDHPs), these values must be given in correspondence of the maximum, minimum and at least an additional intermediate inverter frequency.

Through interpolations of the manufacturer data by means of second-order polynomial functions, curves of the heat pump power and *COP* in heating mode and curves of the heat pump power and *EER* in cooling mode are obtained by the code as functions of $T_{f,out}$, for a fixed value of T_w. In the case of inverter-driven heat pumps, a family of curves for the heat pump power and a family of curves for the heat pump *COP* (or *EER*) are obtained, by varying the inverter frequency, Φ, between the maximum and minimum value.

The heat pump power and *COP* (or *EER*) curves are stopped in correspondence of the cut-off temperature of the related operation mode. In fact, a minimum temperature of the BHE fluid

could be admitted in winter (e.g. in order to prevent freezing, if just water is used as BHE fluid) and a maximum temperature in summer.

5.1.2 Borehole heat exchangers characterization

Regarding the borehole field, the BHE diameter (D), length (L) and thermal resistance per unit length (R_{BHE}) must be set, as well as the number of boreholes and their layout pattern and spacing. Obviously, the total length of the boreholes, L_{tot}, is equal to the number of BHEs, n_{BHEs}, multiplied by the BHE length, L.

The mean dimensionless temperature at the BHE-ground interface is evaluated by the code employing the analytical expressions of the *g-functions* obtained by Zanchini and Lazzari [9]. The polynomial coefficients of the *g-functions* taken from Ref. [9] are implemented in the code for several values of the BHE dimensionless length, $L^* = L/D$, and for several values of the dimensionless radial distance from the BHE axis, $r^* = r/D$. Tables 5.1, 5.2 report the *g-function* coefficients $a_1,..., a_6, b_1,..., b_6, x_0$ and x_1 for different r^* at $L^* = 500$ and $L^* = 700$, respectively.

Table 5.1: Values of the constants x_0, a_6, a_5, a_4, a_3, a_2, a_1, a_0, and x_1, b_6, b_5, b_4, b_3, b_2, b_1, b_0, for $L^* = 500$.

r^*	x_0	a_6	a_5	a_4	a_3	a_2	a_1	a_0
0.5	-3.826	0.000068	0.0004271	-0.0007473	-0.0061278	0.0221063	0.1477453	0.1955375
30	1.458	0.014241	-0.195288	1.079672	-3.062256	4.715197	-3.755953	1.214788
40	1.748	0.0064649	-0.0997785	0.6124448	-1.8967375	3.1285719	-2.6082876	0.8565059
60	2.184	0.0072125	-0.1248228	0.8692397	-3.1008077	5.9715622	-5.8818568	2.3078553
80	2.414	0.0103164	-0.1961421	1.5189119	-6.1234437	13.5714625	-15.709289	7.4338477
120	2.672	0.0146456	-0.3033699	2.5802257	-11.5255014	28.5308593	-37.1454893	19.8916775
170	3.116	---	---	-0.0302216	0.4490819	-2.4544879	5.8758636	-5.2151692
230	3.372	---	0.0101022	-0.2273364	2.0084646	-8.7053136	18.5362496	-15.5406194
300	3.61	---	0.0063342	-0.1563745	1.4988034	-6.9977183	15.976323	-14.317663
400	3.79	0.01092804	-0.2904565	3.18835846	-18.508177	59.95404	-102.815066	72.9655685
600	4.102	---	-0.00360603	0.07326077	-0.58416854	2.27894721	-4.32926784	3.1784414

r^*	x_1	b_6	b_5	b_4	b_3	b_2	b_1	b_0
0.5	1.35	0.0001913	-0.0034131	0.0233535	-0.0818113	0.1538121	0.0308441	0.23595
30	3.15	-0.0022582	0.0625441	-0.7084645	4.1978044	-13.7461932	23.7790033	-17.04851
40	3.6	-0.0039354	0.1105962	-1.2782469	7.775852	-26.291753	47.0563098	-34.93571
60	3.93	---	-0.0069936	0.1801604	-1.8344654	9.1972591	-22.584824	21.75163
80	4.21	---	-0.004601	0.1196875	-1.2262057	6.1549494	-15.0212218	14.2404
120	4.3	---	-0.0060394	0.1583825	-1.6424229	8.3928008	-21.0365441	20.6612
170	4.4	---	-0.0085694	0.2263958	-2.373444	12.3203117	-31.5859797	31.960534
230	4.77	---	-0.0234604	0.6284542	-6.71044	35.683985	-94.4436902	99.504275
300	4.91	---	---	-0.0100843	0.2321316	-2.0066071	7.723773	-11.134982
400	4.8	---	-0.02101006	0.56733137	-6.1109557	32.8098137	-87.7648196	93.540235
600	5.13	---	0.01326315	-0.37404103	4.21824322	-23.7816547	67.0375427	-75.595094

Table 5.2: Values of the constants x_0, a_6, a_5, a_4, a_3, a_2, a_1, a_0, and x_1, b_6, b_5, b_4, b_3, b_2, b_1, b_0, for $L^* = 700$.

r^*	x_0	a_6	a_5	a_4	a_3	a_2	a_1	a_0
0.5	-3.744	0.0000602	0.0003791	-0.000782	-0.0059429	0.0223416	0.1479999	0.1957826
30	1.404	0.012854	-0.179416	1.006941	-2.891011	4.496224	-3.611105	1.175785
40	1.718	0.012256	-0.189756	1.188060	-3.835042	6.750014	-6.167077	2.293675
60	2.198	0.009892	-0.171661	1.205961	-4.371805	8.624575	-8.783231	3.606016
80	2.428	0.005890	-0.108667	0.804090	-3.028911	6.084805	-6.113070	2.343819
120	2.77	---	---	-0.025958	0.364657	-1.860178	4.122394	-3.368229
170	3.118	---	---	-0.030379	0.458294	-2.536415	6.138353	-5.501501
230	3.358	---	---	-0.028830	0.460843	-2.713457	7.004499	-6.707967
300	3.624	---	---	-0.029577	0.494949	-3.063677	8.337908	-8.435821
400	3.852	---	---	-0.029006	0.507944	-3.301615	9.458998	-10.092800
600	4.126	---	---	-0.019533	0.363737	-2.519211	7.701607	-8.778263
r^*	x_1	b_6	b_5	b_4	b_3	b_2	b_1	b_0
0.5	1.40	---	0.000592	-0.011075	0.074007	-0.232928	0.526146	-0.0138
30	3.15	---	0.001166	-0.021041	0.133924	-0.357863	0.465240	-0.283612
40	3.6	---	-0.000555	0.021022	-0.275049	1.619706	-4.291400	4.2286
60	3.93	---	-0.004239	0.113492	-1.199785	6.226007	-15.721993	15.477299
80	4.21	---	-0.007545	0.198622	-2.074376	10.707169	-27.174483	27.11978
120	4.3	---	---	0.005540	-0.105878	0.715649	-1.933295	1.6864797
170	4.4	---	---	0.005586	-0.108992	0.759158	-2.159854	2.05198
230	4.77	---	---	0.004161	-0.081650	0.567966	-1.589673	1.422575
300	4.91	---	---	0.010411	-0.220445	1.723757	-5.867642	7.3381866
400	5.02	---	---	0.011885	-0.255941	2.044459	-7.155734	9.2577487
600	5.13	---	---	0.013103	-0.289712	2.386961	-8.671377	11.716229

The properties of the BHE heat carrier fluid (specific heat capacity at constant pressure, $c_{p,f}$, density, ρ_f, and volumetric flow rate, $\dot{V}_f$) and of the ground (thermal conductivity, k_g, thermal diffusivity, α_g, and undisturbed ground temperature, T_g) are also needed.

5.1.3 Calculation of the GCHP system seasonal performance

In order to invoke the proper *g-function* coefficients, the code calculates the BHE dimensionless length ($L^* = L/D$) and the dimensionless radial distances from the BHE axis ($r^* = r/D$) required to evaluate the mean temperature at a BHE surface through the superposition of the effects in space. As example, for the case of three in line boreholes with $L = 105$ m, $D = 0.15$ m and a distance between adjacent BHEs of 6 m, the *g-function* coefficients are needed in correspondence of L^* equal to 700 and r^* equal to 0.5 (BHE-ground interface), 40 (central BHE - lateral BHE distance) and 80 (distance between lateral BHEs distance).

If the *g-function* coefficients are not tabulated in correspondence of the required value of L^* (or r^*), the closer lower value and the closer higher value of L^* (or r^*) are considered by the code.

The dimensionless duration of one hour, t^*_{hour}, is obtained as:

$$t^*_{hour} = \frac{\alpha_g \, t_{hour}}{D^2} \quad .$$
(5.3)

At the beginning of the first hour of the simulated period, the BHE fluid is in thermal equilibrium with the surrounding ground; hence, the BHE fluid mean temperature ($T_{f,m}$) and supply temperature ($T_{f,out}$) are both initialized as equal to the undisturbed ground temperature (T_g).

For each hour of the simulated period, the MATLAB code evaluates the season to which the hour belongs:

$$season(i) = \begin{cases} -1 & if \quad 1 + 8760[year(i) - 1] \le i \le 5088 + 8760[year(i) - 1] \\ 1 & if \quad 5088 + 8760[year(i) - 1] < i \le 8760 + 8760[year(i) - 1] \end{cases} \quad .$$
(5.4)

Eq. (5.4) is written for a heating season from October to April and a cooling season from May to September, by starting the simulation on the first hour of October 1st. In Eq. (5.4), *season* (*i*) = -1 indicates the heating season (heat extracted from ground), whereas *season* (*i*) = 1 indicates the cooling season (heat supplied to the ground).

The code reads the value of $T_{f,out}$ at the beginning of the *i*-th hour and, if *season* (*i*) = -1 (1), it evaluates, through the heat pump second order polynomial functions, the heating (cooling) power that the heat pump is able to deliver and the corresponding *COP* (*EER*). For inverter-driven heat pumps, a vector for the heat pump power and a vector for the corresponding *COP* or *EER* are obtained.

If the product between the maximum heat pump capacity and t_{hour} is higher than the energy required by the building in the *i*-th hour, E_b (*i*), then the energy delivered by the heat pump, E_{HP} (*i*), is equal to E_b (*i*), otherwise it is equal to the product of the maximum heat pump capacity, t_{hour} and *season* (*i*) (*season* (*i*) is employed in order to obtain negative values of E_b (*i*) for the heating season).

For ON-OFF HPs, the values of the heat pump power and *COP* or *EER* in the *i*-th hour are known from the previous interpolations. The value of the heat pump power for IDHPs, $P_{HP,\Phi_{eff}}$ (*i*), can be obtained dividing the module of E_{HP} (*i*) by t_{hour}, but if $P_{HP,\Phi_{eff}}$ (*i*) turns out lower than $P_{HP,\Phi_{min}}$ (*i*), it is set equal to $P_{HP,\Phi_{min}}$ (*i*) (situation corresponding to on-off cycles). The corresponding *COP* or *EER*, $COP_{\Phi_{eff}}$ (*i*) or $EER_{\Phi_{eff}}$ (*i*), is then obtained by applying a second-order

polynomial interpolation of the *COP* or *EER* vector, as a function of the heat pump power vector.

The effective heat pump *COP* or *EER* (COP_{eff} or EER_{eff}), which takes into account the efficiency decay in the case of on-off cycles, is evaluated according to the standards EN 14825 [10] and UNI/TS 11300-4 [11], multiplying the obtained *COP* or *EER* value by the correction factor for on-off condition, $f_{corr}(i)$. The coefficient $f_{corr}(i)$ is calculated according to Eq. (2.1), where the capacity ratio *CR*(*i*) is evaluated as the ratio between $E_{HP}(i)$ and the product of the heat pump power and t_{hour}.

The hourly value of the electric energy used by the heat pump, $E_{HP,us}(i)$, is evaluated dividing $E_{HP}(i)$ by $COP_{eff}(i)$ (or $EER_{eff}(i)$).

To check if the GCHP is able to cover all the energy required by the building for heating and cooling, the possible uncovered energy $E_{uncov}(i)$ is calculated:

$$E_{un\text{cov}}(i) = \left|E_b(i)\right| - \left|E_{HP}(i)\right| \ . \tag{5.5}$$

The thermal energy exchanged in the *i*-th hour between the borehole heat exchangers and the ground, *Q*(*i*), is evaluated as:

$$Q(i) = E_{HP}(i)\left[1 + \frac{season(i)}{COP(i)}\right] , \tag{5.6}$$

where *COP*(*i*) is obviously substituted by *EER*(*i*) during the cooling season. *Q*(*i*) is negative if $E_{HP}(i)$ is negative, namely if heat is required by the building (extracted from the ground, during winter).

The mean value of the heat flux between BHE and ground per unit BHE length, *q*(*i*), is:

$$q(i) = \frac{Q(i)}{t_{hour}L_{tot}} , \tag{5.7}$$

The dimensionless load amplitude of the *i*-th hour, *A*(*i*), is given by the ratio between *q*(*i*) and a reference thermal load per unit length, q_0. For the evaluations of the next section, the mean value of P_b during January (which is usually the month with the highest heating demand), divided by L_{tot}, is adopted as value of q_0.

At the end of the *i*-th hour, the dimensionless temperature $T_m^*|_{r*}(i)$, averaged along the BHE length, produced at the dimensionless distance r^* from the BHE axis by a time-dependent dimensionless heat load, with steps of one hour and values given by the coefficients *A*, is:

$$T_m^*\Big|_{r^*}(i) = \sum_{k=1}^{i} A(k)\left\{g\big|_{r^*}\left[(i+1-k)t_{hour}^*\right] - g\big|_{r^*}\left[(i-k)t_{hour}^*\right]\right\} , \tag{5.8}$$

where the symbol g denotes the *g-functions*. Eq. (5.8) is derived from Eq. (2.56), by considering that T_m^* is calculated only at the end of each interval of one hour.

Eq. (5.9) explicates the evaluation of T_m^* at the end of the first three hours, as example:

$$T_m^*\big|_{r^*} (1) = A(1)\left[g\big|_{r^*} (t_{hour}^*) - g\big|_{r^*} (0) \right]$$
$$T_m^*\big|_{r^*} (2) = A(1)\left[g\big|_{r^*} (2t_{hour}^*) - g\big|_{r^*} (t_{hour}^*) \right] + A(2)\left[g\big|_{r^*} (t_{hour}^*) - g\big|_{r^*} (0) \right]$$
$$T_m^*\big|_{r^*} (3) = A(1)\left[g\big|_{r^*} (3t_{hour}^*) - g\big|_{r^*} (2t_{hour}^*) \right] + A(2)\left[g\big|_{r^*} (2t_{hour}^*) - g\big|_{r^*} (t_{hour}^*) \right] + A(3)\left[g\big|_{r^*} (t_{hour}^*) - g\big|_{r^*} (0) \right]$$

. (5.9)

By observing Eq. (5.9), one can note that, for each hour, only two new *g-functions* are needed, whereas the others are already calculated from the previous hours. Therefore, to reduce the computational time, the MATLAB code stores the *g-function* values obtained in each time step, in order to reutilize them for the following hours.

By means of Eq. (5.8), T_m^* at $r^* = 0.5$ (BHE-ground interface), and at the dimensionless distances between the BHEs, is calculated. If the *g-function* coefficients were not tabulated in correspondence of the required value of L^* (or r^*), two hourly values of T_m^* are calculated by the code, in correspondence of the lower and higher closer available values of L^* (or r^*). The actual hourly value of the dimensionless temperature is then obtained through linear interpolation as function of L^* (or r^*).

The mean dimensionless temperature at the surface of a specific borehole of the field is evaluated as the sum of the value of T_m^* produced by the specific BHE at $r^* = 0.5$, and of those produced by the other BHEs of the field at their dimensionless distances from the specific BHE axis (superposition of the effects in space).

By taking as example a BHE field with three in line boreholes, 40 diameters spaced, the mean dimensionless temperature at the surface of the central borehole is given by Eq. (5.10), that of the two lateral boreholes by Eq. (5.11) and the mean dimensionless temperature of the BHE field is evaluated according to Eq. (5.12):

$$T_{m,central\ BHE}^*(i) = T_m^*\big|_{r^*=0.5}(i) + 2\ T_m^*\big|_{r^*=40}(i) \ , \tag{5.10}$$

$$T_{m,lateral\ BHE}^*(i) = T_m^*\big|_{r^*=0.5}(i) + T_m^*\big|_{r^*=40}(i) + T_m^*\big|_{r^*=80}(i) \ , \tag{5.11}$$

$$T_{m,BHE\ field}^*(i) = \frac{T_{m,central\ BHE}^*(i) + 2\ T_{m,lateral\ BHE}^*(i)}{3} \ . \tag{5.12}$$

The definition of dimensionless temperature (see Eq. (2.29)) yields the mean temperature of the BHE field at the end of the i-th hour, $T_{m,\ BHE\ field}(i)$:

$$T_{m,BHE\ field}(i) = \frac{q_0}{k_g} T^*_{m,BHE\ field}(i) + T_g \ .$$

(5.13)

In the quasi-stationary approximation, the definition of BHE thermal resistance per unit length, R_{BHE}, yields the fluid mean temperature at the end of the i-th hour, $T_{f,m}(i)$:

$$T_{f,m}(i) = T_{m,BHE\ field}(i) + q(i)\ R_{BHE} \ ,$$

(5.14)

and the corresponding fluid supply temperature, $T_{f,out}(i)$, is obtained as:

$$T_{f,out}(i) = T_{f,m}(i) - \frac{0.5}{\dot{V}_f \rho_f c_{p,f}} \frac{Q(i)}{t_{hour} n_{BHEs}} \ .$$

(5.15)

The fluid supply temperature at the end of the i-th hour, $T_{f,out}(i)$, corresponds to that at the beginning of the subsequent ((i+1)-th) hour and is used by the MATLAB code to evaluate the heat pump performance at the subsequent hour, through a *for* cycle.

Once known the values of $T_{f,m}$ for each hour of the simulated period, the mean, minimum and maximum values of the BHE fluid temperature for each year of the simulation can be used to check the long-term sustainability of the BHE field in the case on unbalanced building loads.

The seasonal performance of the ground-coupled heat pump during a selected year can be finally evaluated. Eq. (5.16) and Eq. (5.17) calculate, respectively, the Seasonal Coefficient Of Performance and the Seasonal Energy Efficiency Ratio of the GCHP during the last year of the simulation period:

$$SCOP = \frac{\sum_{i=i_{last}-8760+1}^{i_{last}} \min[0;\ E_{HP}(i)]}{\sum_{i=i_{last}-8760+1}^{i_{last}} \min[0;\ E_{HP,us}(i)]} \ ,$$

(5.16)

$$SEER = \frac{\sum_{i=i_{last}-8760+1}^{i_{last}} \max[0;\ E_{HP}(i)]}{\sum_{i=i_{last}-8760+1}^{i_{last}} \max[0;\ E_{HP,us}(i)]} \ ,$$

(5.17)

where i_{last} is the number of the last hour of the last year. Eq. (5.16) and Eq. (5.17) are written by considering that $E_{HP}(i)$ and $E_{HP,us}(i)$ are negative during the heating season and positive during the cooling season.

In the next section, a simulation of a GCHP system is performed for several decades, by employing hourly simulations with the aid of auxiliary monthly simulations. In the case of

monthly simulation, monthly building loads are given as inputs and the same mathematical model of the hourly simulation can be used, by substituting in the equations t_{hour} with the month duration (t_{month}) and the numbers 8760 with 12 and 5088 with 7.

Since the month dimensionless duration has not a fixed value, but changes from month to month, Eq. (5.8) cannot be used to evaluate the dimensionless temperature $T_m^*|_{r*}(i)$, and must be replaced by:

$$T_m^*\Big|_{r^*}(i) = \sum_{j=1}^{i} A(j) \left\{ g\big|_{r^*} \left[\sum_{k=j}^{i} t_{month}^*(k) \right] - g\big|_{r^*} \left[\sum_{k=j+1, j<i}^{i} t_{month}^*(k) \right] \right\}. \tag{5.18}$$

Moreover, contrary to what happens in Eq. (5.9), every non-vanishing time instant at which a *g-function* is evaluated occurs only once, so that no *g-function* value can be reutilized in order to save computational time. See as example the T_m^* values at the end of the first three months:

$$T_m^*\Big|_{r^*}(1) = A(1)\left\{ g\big|_{r^*} \left[t_{month}^*(1) \right] - g\big|_{r^*}(0) \right\}$$

$$T_m^*\Big|_{r^*}(2) = A(1)\left\{ g\big|_{r^*} \left[t_{month}^*(1) + t_{month}^*(2) \right] - g\big|_{r^*} \left[t_{month}^*(2) \right] \right\} + A(2)\left\{ g\big|_{r^*} \left[t_{month}^*(2) \right] - g\big|_{r^*}(0) \right\}$$

$$T_m^*\Big|_{r^*}(3) = A(1)\left\{ g\big|_{r^*} \left[t_{month}^*(1) + t_{month}^*(2) + t_{month}^*(3) \right] - g\big|_{r^*} \left[t_{month}^*(2) + t_{month}^*(3) \right] \right\} +$$

$$+ A(2)\left\{ g\big|_{r^*} \left[t_{month}^*(2) + t_{month}^*(3) \right] - g\big|_{r^*} \left[t_{month}^*(3) \right] \right\} + A(3)\left\{ g\big|_{r^*} \left[t_{month}^*(3) \right] - g\big|_{r^*}(0) \right\} \tag{5.19}$$

Nevertheless, with the same number of simulated years, the monthly simulation (12 steps per year) is obviously much faster than the hourly simulation (8760 steps per year).

The MATLAB input file and script developed for the hourly simulation of ground-coupled heat pump systems are reported in Appendix, Section 7.3.

5.2 APPLICATION OF THE CODE

The code developed in this Thesis for the simulation of GCHPs is employed to analyze the effect of the inverter of the heat pump and the effect of the total length of the BHE field on the seasonal performance of a GCHP system designed for building heating and cooling.

5.2.1 Building characteristics

The residential building object of the HERB project (in the post-retrofit scenario) is chosen for the analysis (see Subsection 4.3.1). Figure 5.1 shows the building loads at the outlet of the generation subsystem (heat pump), as functions of time, from October 1st to September

30th. The heating season is set from October to April, included, while the cooling season from May to September, included.
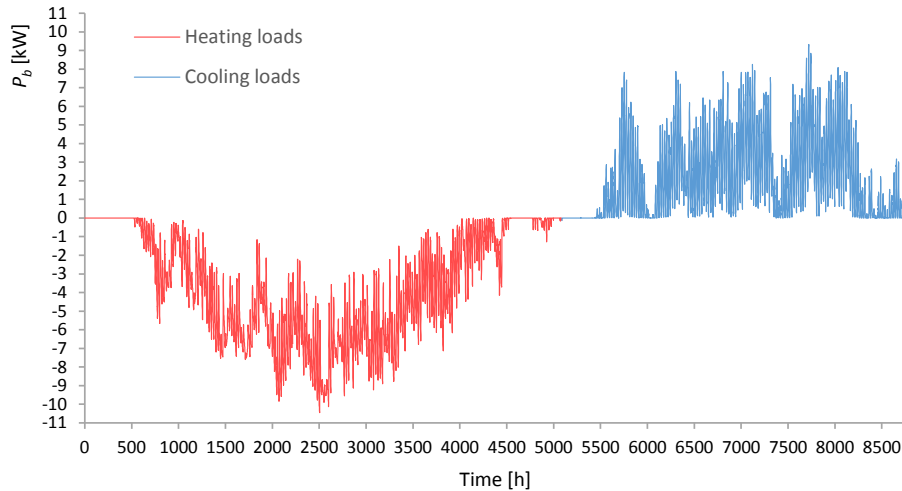
Figure 5.1: Building loads for heating and cooling-dehumidifying, from October 1st to September 30th.

In Figure 5.1 heating loads are considered negative, while cooling-dehumidifying loads are considered positive, as required by the MATLAB code. The highest magnitudes of the hourly heat load required by the building are 10.46 kW for heating and 9.32 kW for cooling.

In Figure 5.2 the corresponding monthly averaged building loads are reported.
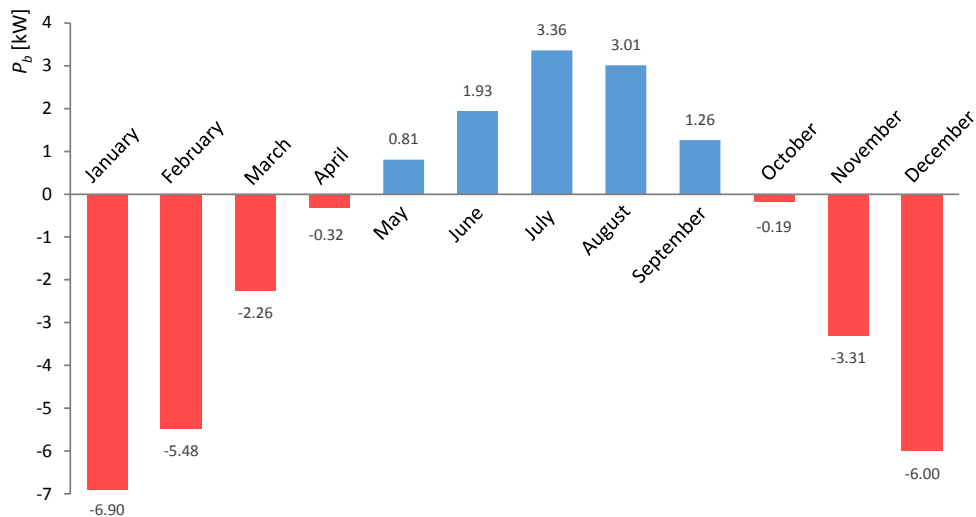
Figure 5.2: Building monthly averaged loads.

From Figure 5.2 one can note that the heating loads are dominant compared to the cooling loads.

5.2.2 Characteristics of the ground-coupled heat pump and of the borehole heat exchanger field

The selected ground-coupled heat pump, used to provide heating and cooling to the building, is an inverter-driven brine-to-water unit. Water is delivered at 40 °C (return temperature 35 °C) during winter and at 7 °C (return temperature 12 °C) during summer. The manufacturer data of heat pump power, *COP* and *EER* are shown in Tables 5.3, 5.4 for several values of the BHE fluid supply temperature, $T_{f,out}$, and of the inverter frequency, Φ.

Table 5.3: Heat pump power [kW] and (*COP*) in heating mode; $T_{w,h}$ = 40 °C.

$T_{f,out}$ [°C]	Frequency [Hz]									
	110 (Φ_{max})		90		70		50		30 (Φ_{min})	
5	12.60	(4.41)	9.91	(4.67)	7.45	(4.84)	5.19	(4.92)	3.08	(4.82)
6	13.00	(4.53)	10.20	(4.80)	7.68	(4.99)	5.34	(5.07)	3.18	(4.98)
7	13.40	(4.66)	10.50	(4.94)	7.92	(5.14)	5.51	(5.22)	3.28	(5.13)
8	13.80	(4.79)	10.80	(5.09)	8.15	(5.29)	5.67	(5.39)	3.38	(5.30)
9	14.20	(4.93)	11.10	(5.24)	8.40	(5.45)	5.85	(5.56)	3.48	(5.47)
10	14.60	(5.07)	11.50	(5.39)	8.65	(5.63)	6.02	(5.74)	3.58	(5.65)
11	15.00	(5.22)	11.80	(5.56)	8.89	(5.79)	6.20	(5.92)	3.69	(5.83)
12	15.40	(5.37)	12.10	(5.73)	9.15	(5.97)	6.38	(6.11)	3.80	(6.03)
13	15.90	(5.52)	12.50	(5.90)	9.41	(6.16)	6.57	(6.31)	3.91	(6.23)
14	16.30	(5.68)	12.80	(6.08)	9.68	(6.36)	6.76	(6.52)	4.02	(6.43)
15	16.80	(5.85)	13.20	(6.26)	9.95	(6.56)	6.95	(6.73)	4.14	(6.65)
16	17.20	(6.03)	13.60	(6.46)	10.20	(6.77)	7.14	(6.96)	4.25	(6.88)
17	17.70	(6.20)	13.90	(6.66)	10.50	(6.99)	7.34	(7.18)	4.37	(7.13)
18	18.20	(6.40)	14.30	(6.87)	10.80	(7.21)	7.54	(7.43)	4.49	(7.37)

Table 5.4: Heat pump power [kW] and (*EER*) in heating mode; $T_{w,c}$ = 7 °C.

$T_{f,out}$ [°C]	Frequency [Hz]									
	110 (Φ_{max})		90		70		50		30 (Φ_{min})	
35	12.10	(4.20)	9.61	(4.52)	7.28	(4.74)	5.08	(4.85)	3.01	(4.74)
34	12.20	(4.35)	9.73	(4.69)	7.38	(4.92)	5.15	(5.03)	3.05	(4.93)
33	12.40	(4.50)	9.84	(4.86)	7.47	(5.11)	5.21	(5.22)	3.08	(5.12)
32	12.50	(4.67)	9.96	(5.04)	7.56	(5.30)	5.28	(5.43)	3.12	(5.32)
31	12.70	(4.84)	10.10	(5.24)	7.64	(5.49)	5.34	(5.63)	3.16	(5.52)
30	12.80	(5.02)	10.20	(5.42)	7.73	(5.71)	5.40	(5.85)	3.20	(5.74)
29	12.90	(5.20)	10.30	(5.63)	7.82	(5.92)	5.46	(6.07)	3.23	(5.97)
28	13.10	(5.40)	10.40	(5.85)	7.92	(6.16)	5.52	(6.31)	3.27	(6.20)
27	13.20	(5.60)	10.50	(6.06)	7.99	(6.38)	5.59	(6.56)	3.31	(6.45)
26	13.40	(5.81)	10.70	(6.29)	8.09	(6.64)	5.65	(6.83)	3.34	(6.71)
25	13.50	(6.02)	10.80	(6.54)	8.17	(6.90)	5.71	(7.11)	3.38	(6.98)
24	13.70	(6.26)	10.90	(6.78)	8.24	(7.11)	5.73	(7.22)	3.39	(7.03)
23	13.70	(6.29)	10.90	(6.82)	8.24	(7.11)	5.73	(7.22)	3.39	(7.03)
22	13.70	(6.32)	10.90	(6.84)	8.24	(7.11)	5.73	(7.22)	3.39	(7.03)
21	13.70	(6.34)	10.90	(6.84)	8.24	(7.11)	5.73	(7.22)	3.39	(7.03)
20	13.70	(6.36)	10.90	(6.84)	8.24	(7.11)	5.73	(7.22)	3.39	(7.03)
19	13.70	(6.38)	10.90	(6.84)	8.24	(7.11)	5.73	(7.22)	3.39	(7.03)
18	13.80	(6.40)	10.90	(6.84)	8.24	(7.11)	5.73	(7.22)	3.39	(7.03)
17	13.80	(6.41)	10.90	(6.84)	8.24	(7.11)	5.73	(7.22)	3.39	(7.03)
16	13.80	(6.42)	10.90	(6.84)	8.24	(7.11)	5.73	(7.22)	3.39	(7.03)
15	13.80	(6.42)	10.90	(6.84)	8.24	(7.11)	5.73	(7.22)	3.39	(7.03)

The following ground properties are set: T_g = 14 °C, k_g = 1.8 W/(m K), α_g = 8.814 × 10^{-7} m^2/s. The BHE field coupled to the heat pump is composed of three in line double-U boreholes, 6 m spaced, with diameter D = 0.15 m and length L either 105 m or 75 m (corresponding dimensionless BHE lengths: L^* = 700 and L^* = 500, respectively).

The BHE fluid volumetric flow rate, $\dot{V}_f$, is 16 l/min. For the simulations with L = 105 m, the BHE fluid is water, whose density ρ_f is 999.25 kg/m^3 and specific heat capacity $c_{p,f}$ is 4.1896 kJ/(kg K) (properties at 14 °C). The corresponding winter cut-off temperature of the heat pump is 2 °C and the BHE thermal resistance per unit length (obtained through a numerical steady state simulation of the BHE cross section) is 0.0687 (m K)/W.

The simulations with L = 75 m would cause too low water temperatures during winter, so water is replaced by a mixture of water-glycol (monoethylenglycol 20 %), whose ρ_f is 1032 kg/m^3 and $c_{p,f}$ is 3.89 kJ/(kg K) (properties at 14 °C, from Ref. [76]). The corresponding

winter cut-off temperature of the heat pump is -8 °C and the BHE thermal resistance per unit length is 0.0732 (m K)/W.

5.2.3   Analysis of the results of the simulations

A 10-year hourly simulation of the GCHP system is performed, with the selected inverter-driven heat pump, for the case of L^* = 700.

Figure 5.3 shows the hourly values of the BHE fluid mean temperature, obtained during the last year of simulation. Each year is started on October 1st and is ended on September 30th.
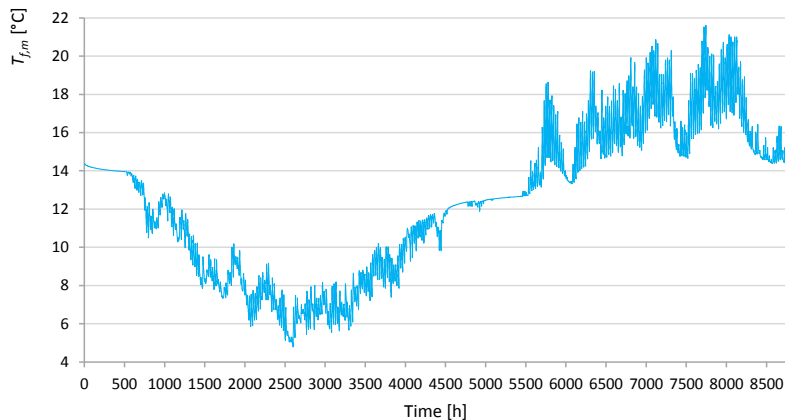
Figure 5.3: BHE fluid temperature during the 10th year, L^* = 700, inverter-driven heat pump.

In Figure 5.4 the maximum values of the mean temperature of the BHE fluid ($T_{f,m,max}$), reached in each of the 10 years, is reported, while Figure 5.5 shows the corresponding minimum values ($T_{f,m,min}$).
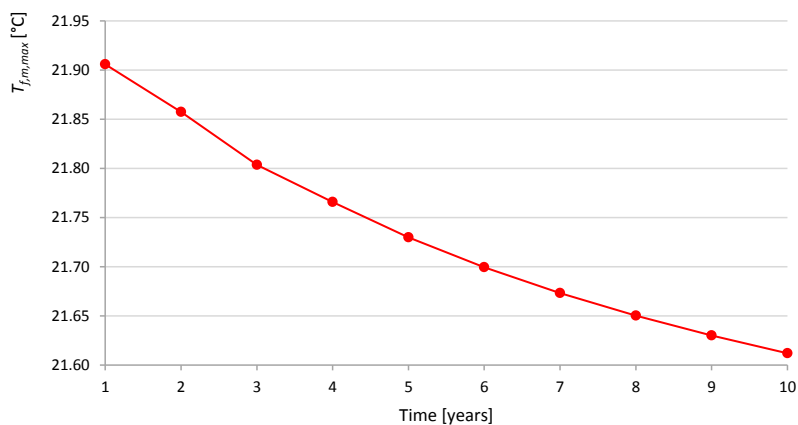
Figure 5.4: BHE fluid maximum temperatures, L^* = 700, inverter-driven heat pump.

144
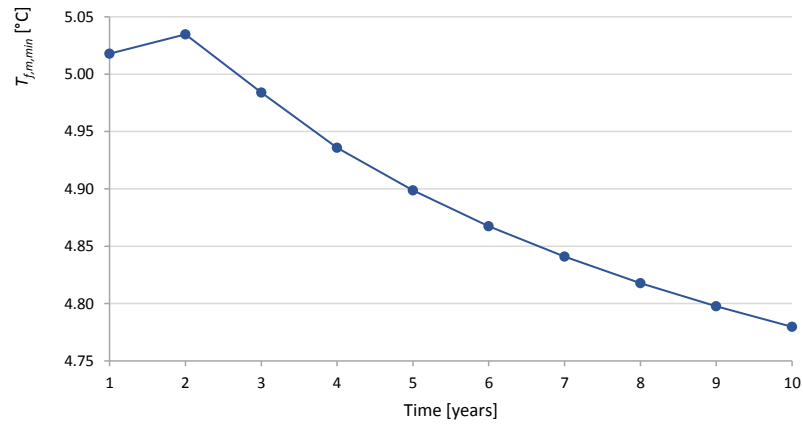
Figure 5.5: BHE fluid minimum temperatures, $L^* = 700$, inverter-driven heat pump.

From Figure 5.4 one can note that the maximum value reached by $T_{f,m}$ starts from 21.91 °C (first year) and decreases until 21.61 °C (last year).

An unexpected peak of $T_{f,m,min}$ can be seen in Figure 5.5 in correspondence of the second year of simulation. This is due to the fact that the first year starts with the heating season, which, unlike the heating seasons of all the other years, is not preceded by a cooling season (that would enhance the fluid temperature). From the second year on, an equilibrium between heat extracted from and released to the ground is obtained and $T_{f,m,min}$ has a decreasing trend (from 5.03 °C to 4.78 °C).

The values of *SCOP* and *SEER* of the GCHP during the last year of the simulation period are, respectively, 5.32 and 6.74.

The simulation is repeated considering the case of $L^* = 500$. Figure 5.6 shows the values of $T_{f,m,max}$ during the 10 simulated years and Figure 5.7 shows the values of $T_{f,m,min}$.
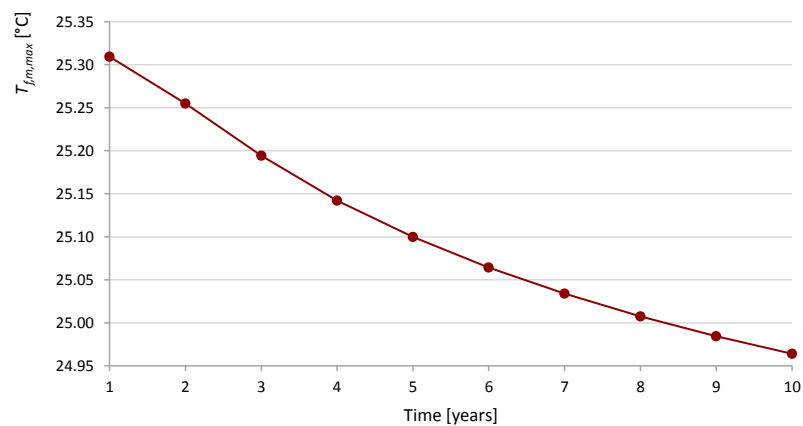
Figure 5.6: BHE fluid maximum temperatures, $L^* = 500$, inverter-driven heat pump.
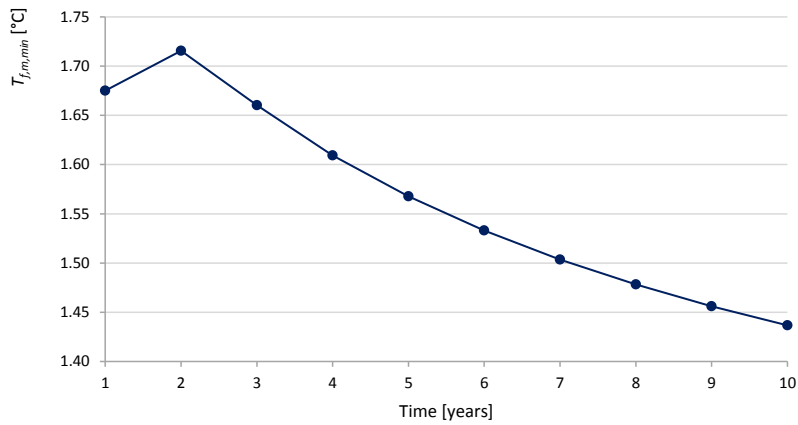
Figure 5.7: BHE fluid minimum temperatures, L^* = 500, inverter-driven heat pump.

Comparing Figure 5.6 with Figure 5.4 and Figure 5.7 with Figure 5.5, it is evident that, with L^* = 500, the BHE fluid reaches higher values of $T_{f,m,max}$ and lower values of $T_{f,m,min}$, compared to the case of L^* = 700, mainly due to higher heat loads per unit BHE length. In addition, the BHE fluid temperature difference between the first year (for $T_{f,m,max}$, or second year, for $T_{f,m,min}$) and the last year is higher than the previous case.

The value of Seasonal Coefficient Of Performance for the 10th year is 4.97 and that of Seasonal Energy Efficiency Ratio is 6.74.

To analyze the influence of the heat pump inverter on the system seasonal performance during winter and during summer, the simulations are repeated forcing the heat pump to work at its maximum frequency, as a mono-compressor on-off heat pump (ON-OFF HP). The seasonal coefficients obtained during the last year of simulation are: $SCOP$ = 4.00 and $SEER$ = 4.45, for the case with L^* = 700; $SCOP$ = 3.82 and $SEER$ = 4.42, for the case with L^* = 500.

Table 5.5 summarizes the values of $SCOP$ obtained in each of the four simulated cases, while Table 5.6 shows the corresponding values of $SEER$.

Table 5.5: $SCOP$ values with or without inverter, L^* equal to 500 or 700, 10th year.

L^*	ON-OFF HP	IDHP
500	3.82	4.97
700	4.00	5.32

Table 5.6: *SEER* values with or without inverter, L^* equal to 500 or 700, 10th year.

L^*	ON-OFF HP	IDHP
500	4.42	6.74
700	4.45	6.74

By comparing the seasonal performance values of Tables 5.5, 5.6, it can be noticed that the increase of the BHE length yields a *SCOP* enhancement of about 5 % (ON-OFF HP) – 7 % (IDHP), while the *SEER* remains nearly unchanged. The replacement of the mono-compressor on-off heat pump by an inverter-driven one yields a *SCOP* increase of about 30 % (L^* = 500) – 33 % (L^* = 700) and a *SEER* enhancement of about 51 % (L^* = 700) – 52 % (L^* = 500). Adopting both the IDHP and the higher BHE length improves the winter performance of about 39 % and the summer performance of about 52 %. The most significant improvements on the seasonal performance are obtained thanks to the inverter. The effect of the inverter, moreover, is greater on the summer efficiency (lower building loads, higher number of on-off cycles) than on the winter efficiency (higher building loads, lower number of on-off cycles).

Figure 5.8 and Figure 5.9 show, respectively, the hourly trend of $T_{f,m}$ and of the effective heat pump *COP*, obtained from November to January of the last year, with and without inverter, for the case of L^* = 700.
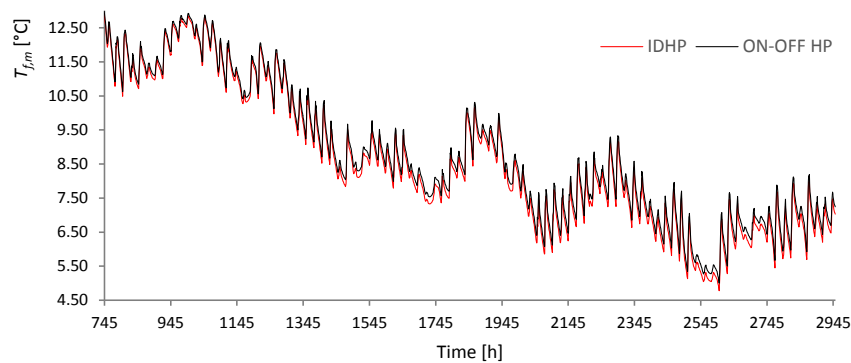
Figure 5.8: Hourly trend of $T_{f,m}$ from November to January, 10th year, L^* = 700.
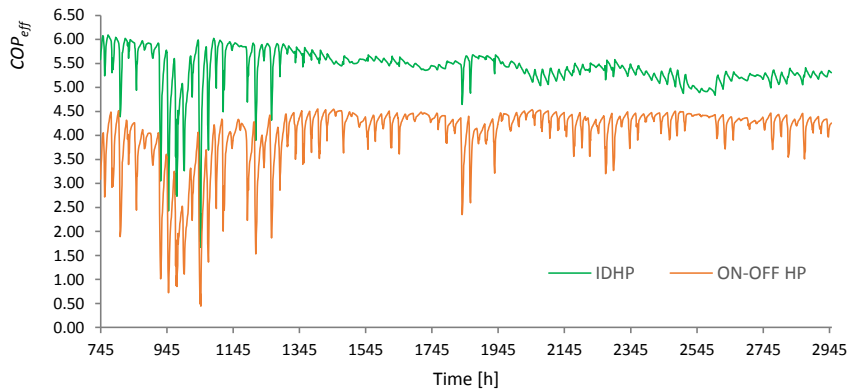
Figure 5.9: Hourly trend of COP_{eff} from November to January, 10th year, $L^* = 700$.

Figure 5.10 and Figure 5.11 show, respectively, the hourly trend of $T_{f,m}$ and of the effective heat pump *EER*, from June to August of the last year, with and without inverter, for $L^* = 700$.
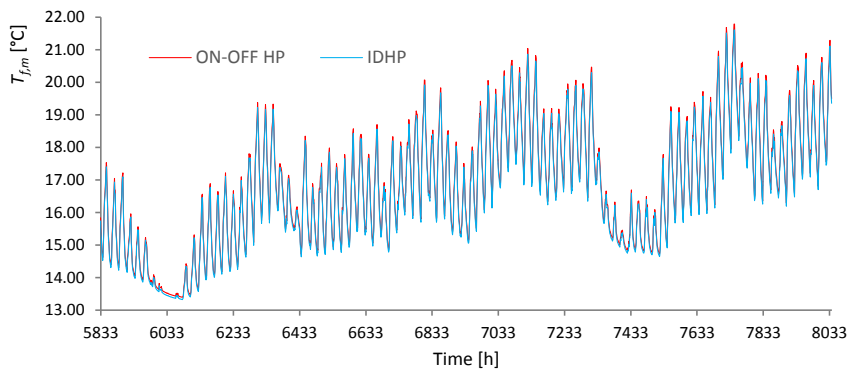
Figure 5.10: Hourly trend of $T_{f,m}$ from June to August, 10th year, $L^* = 700$.
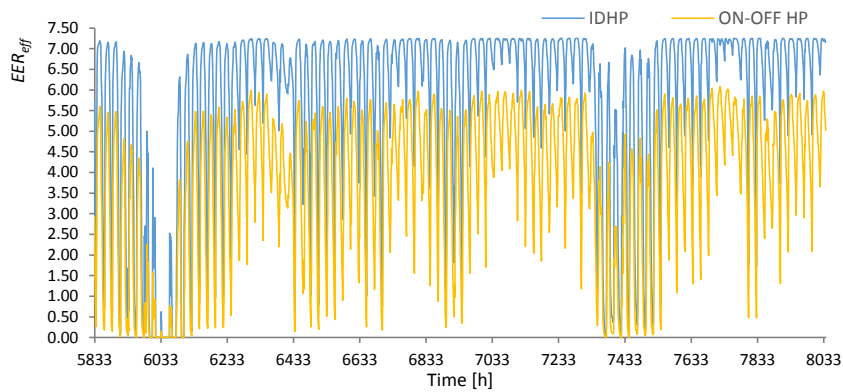
Figure 5.11: Hourly trend of EER_{eff} from June to August, 10th year, $L^* = 700$.

Figures 5.9, 5.11 highlight the better hourly efficiency of the inverter-driven heat pump with respect to the mono-compressor on-off one, thanks to the possibility of the IDHP of delaying the on-off cycles activation.

Despite the better performance of the IDHP, the hourly values of the BHE fluid mean temperature are very similar between IDHP and ON-OFF HP (see Figures 5.8, 5.10). This is due to the fact that, in the developed MATLAB code, the computation of the heat flux between borehole and ground is based on the hourly averaged power. Therefore, the on-off cycles of the heat pump do not affect the ground, but only the heat pump *COP* or *EER*. Further investigations are planned to take into account the influence of the on-off cycles on $T_{f,m}$ (see Section 6.2).

A simulation of the GCHP system is performed for 50 years by means of monthly simulations, by employing a modified version of the MATLAB code, as explained in Subsection 5.1.3.

The maximum values and the minimum values of $T_{f,m}$, reached in each of the 50 years with the IDHP and $L^* = 700$, are reported in Figure 5.12 and Figure 5.13, respectively.
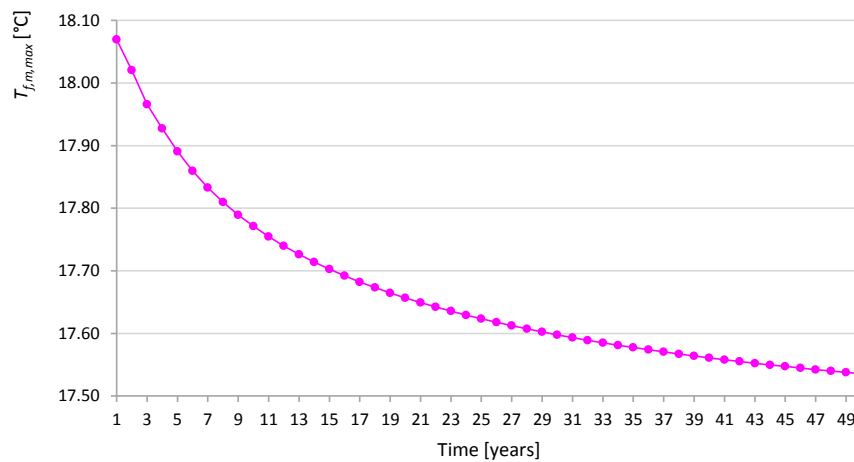
Figure 5.12: BHE fluid maximum temperatures, $L^* = 700$, IDHP, monthly simulation.
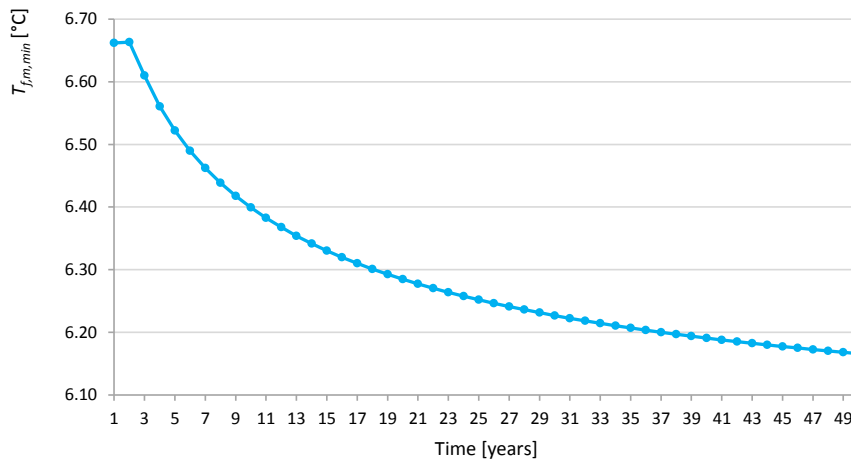
Figure 5.13: BHE fluid minimum temperatures, L^* = 700, IDHP, monthly simulation.

From Figure 5.13, it can be noticed that the minimum value of $T_{f,m}$ after 50 years is higher than 6 °C, hence, in spite of the building unbalanced heat loads, the studied GCHP system does not reveal long-term sustainability problems.

By comparing the values of $T_{f,m,max}$ and $T_{f,m,min}$ for the first 10 years of Figure 5.12 and Figure 5.13 with the corresponding values of Figure 5.4 and Figure 5.5, one can note that the BHE fluid in the monthly simulation reaches peaks of temperature less extreme than in the hourly simulation. In the monthly simulation, in fact, each calculated value of $T_{f,m}$ is a monthly averaged value, due to a monthly averaged building load. The hourly simulation, on the contrary, is able to consider the building hourly peaks of demand.

Figure 5.14 shows the trend of the difference in the values of $T_{f,m,max}$ between one year and the following one ($\Delta T_{f,m,max}$), obtained with the monthly simulation of the IDHP with L^* = 700.
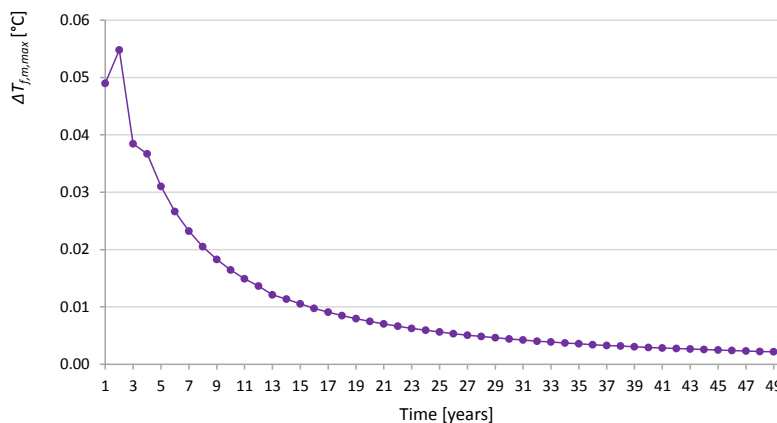
Figure 5.14: Yearly difference in the values of $T_{f,m,max}$, IDHP, L^* = 700, monthly simulation.

Figure 5.15 shows the yearly difference in the values of $T_{f,m,min}$ ($\Delta T_{f,m,min}$).
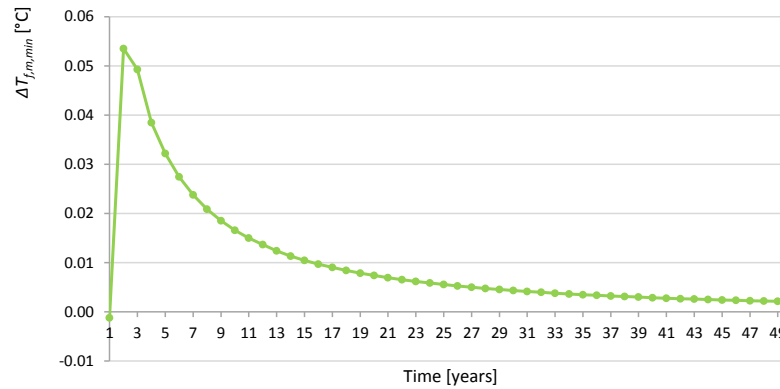
Figure 5.15: Yearly difference in the values of $T_{f,m,min}$, IDHP, $L^* = 700$, monthly simulation.

The first value of $\Delta T_{f,m,min}$ reported in Figure 5.15 is negative because, as earlier explained, the second value of $T_{f,m,min}$ is higher than the previous one.

After 50 years, the differences in the yearly values of $T_{f,m,max}$ and $T_{f,m,min}$ reach asymptotic values close to 0.

The hourly simulation of the system after 50 years can be performed by assuming that the hourly values of the BHE fluid supply temperature are equal to those obtained at the 10th year through hourly simulation, properly translated. The translation constant is the difference between the mean annual value of $T_{f,m}$ at the 10th year and that at the 50th year, obtained through monthly simulation.

The accuracy of the assumption of employing a monthly simulation is tested by comparing the difference between the mean annual value of $T_{f,m}$ at the 5th year and that at the 10th year, obtained through the monthly simulation, with the corresponding difference obtained though the hourly simulation. The relative discrepancy between the two differences never exceeds 3.3 % in the examined cases. The accuracy of the assumption of employing a mean annual value as translation constant is tested by analyzing the difference between the hourly values of $T_{f,m}$ at the 5th year and those at the 10th year, which is plotted in Figure 5.16 for the case of the IDHP with $L^* = 700$.
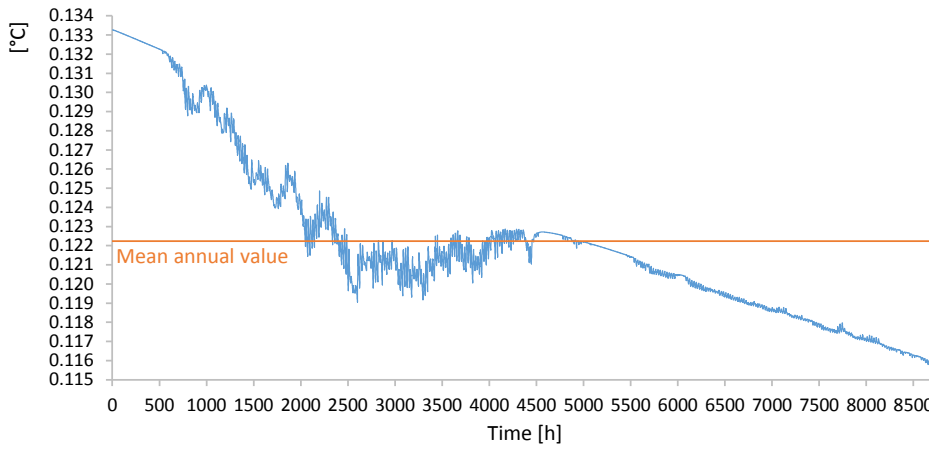
Figure 5.16: Hourly values of the difference between $T_{f,m}$ at the 5th year and $T_{f,m}$ at the 10th year, IDHP, $L^* = 700$.

The plot of Figure 5.16 shows that this difference is always very close to its mean annual value; the maximum deviation from the mean value is 0.01 °C.

The seasonal performance coefficients obtained with the hourly simulations for the 50th year are reported in Tables 5.7, 5.8.

Table 5.7: *SCOP* values with or without inverter, L^* equal to 500 or 700, 50th year.

L^*	ON-OFF HP	IDHP
500	3.81	4.93
700	3.98	5.28

Table 5.8: *SEER* values with or without inverter, L^* equal to 500 or 700, 50th year.

L^*	ON-OFF HP	IDHP
500	4.43	6.74
700	4.45	6.74

By comparing the values of Tables 5.7, 5.8 with the corresponding values of Tables 5.5, 5.6, it is clear that the heat pump seasonal efficiencies remain nearly constant between the 10th and the 50th year.

5.3   Validation of the MATLAB code with the software Earth Energy Designer (EED)

The MATLAB code developed in this Thesis for the simulation of GCHP systems is validated by comparing the values of the BHE fluid mean temperature ($T_{f,m}$) obtained in 50-year monthly simulations performed by the code and by the software Earth Energy Designer (EED). A monthly simulation of the borehole field is performed with EED, considering three double-U boreholes, with diameter D = 0.15 m and length L = 105 m, placed in line and 6 m spaced from each other.

The thermal conductivity of the grout is 1.6 W/(m K); the contact resistance pipe/filling is set equal to 0, as it is not considered by the MATLAB code; the volumetric flow rate per borehole is 16 l/min; the pipe outer diameter is 32 mm, the wall thickness 6 mm and the shank spacing 85 mm; the pipe thermal conductivity is 0.359 W/(m K).

The borehole thermal resistance fluid/ground is directly imposed in EED equal to 0.0687 (m K)/W, without taking into account the internal heat transfer.

The BHE fluid is water, with thermal conductivity 0.5875 W/(m K), specific heat capacity 4.1896 kJ/(kg K), density 999.25 kg/m^3, viscosity 0.001168 kg/(m s) and freezing point 0 °C.

The ground has a thermal conductivity of 1.8 W/(m K), a volumetric heat capacity of 2.042 MJ/(m^3 K) and an undisturbed temperature of 14 °C (obtained by typing in EED a ground surface temperature of 14 °C and a geothermal heat flux of 0).

The building peak load is set to 0.

The building base load is given in EED by means of monthly values of energy directly exchanged between BHE and ground during winter (October – April) and summer (May – September), in order to avoid the implementation of a fictitious *SPF* value (which would be constant in EED, but variable month by month in the MATLAB code). As the software EED does not simulate the heat pump (which intervenes in the calculations only with a constant performance coefficient, one for the heating season and one for the cooling season), also in the MATLAB code the monthly values of energy exchanged between BHE and ground are directly supplied as input data and kept constant year after year.

The input values of energy exchanged monthly between BHE and ground are obtained as follows. The residential building object of the HERB project in the post-retrofit scenario is considered (see Subsection 4.3.1). A 1-year monthly simulation is run with the MATLAB code, by considering the case of L^* = 700 and the inverter-driven ground-coupled heat pump described in Subsection 5.2.2. The obtained monthly values of energy exchanged between BHE and ground are employed as input for the validation.

Once detected that EED assumes for each month the same duration of 30.4167 days (365 / 12), the same simplification is implemented also in the MATLAB code.

Monthly simulations are thus performed with EED and with the MATLAB code for 50 years, setting October as first month of operation. An excerpt of the results obtained by EED is shown in Figure 5.17.

```
SPECIFIC HEAT EXTRACTION RATE [W/m]

Month              Base load      Peak heat     Peak cool
  JAN               18.21            0             0
  FEB               12.97            0             0
  MAR                5.94            0             0
  APR                0.84            0             0
  MAY               -3.01            0             0
  JUN               -6.93            0             0
  JUL              -12.41            0             0
  AUG              -11.12            0             0
  SEP               -4.51            0             0
  OCT                0.51            0             0
  NOV                8.75            0             0
  DEC               16.13            0             0

BASE LOAD: MEAN FLUID TEMPERATURES (at end of month) ['C]

Year        1          2         5         10        50
  JAN       14        6.43      6.29      6.15      5.88
  FEB       14        7.98      7.82      7.68      7.41
  MAR       14       10.46      10.3     10.16      9.89
  APR       14       12.47     12.31     12.17      11.9
  MAY       14       14.12     13.98     13.84     13.57
  JUN       14       15.86     15.73     15.59     15.33
  JUL       14       18.23      18.1     17.96      17.7
  AUG       14       18.18     18.04     17.91     17.65
  SEP       14       15.97     15.82     15.69     15.43
  OCT     13.81      14.07     13.92     13.79     13.53
  NOV     10.72      10.83     10.68     10.55      10.3
  DEC      7.67       7.69      7.54      7.41      7.16

BASE LOAD: YEAR  50
Minimum mean fluid temperature  5.88 'C at end of JAN
Maximum mean fluid temperature  17.7 'C at end of JUL
```

Figure 5.17: Extract of the EED results.

Table 5.9 shows the monthly values of $T_{f,m}$ obtained from the simulations with the MATLAB code for the 1st, the 2nd, the 5th, the 10th and the 50th year.

Table 5.9: Monthly values of $T_{f,m}$ calculated by the MATLAB code.

Month	Year				
	1	2	5	10	50
Jan	14	6.53	6.43	6.28	6.01
Feb	14	8.10	7.98	7.83	7.57
Mar	14	10.58	10.45	10.30	10.04
Apr	14	12.55	12.41	12.27	12.01
May	14	14.15	14.02	13.87	13.61
Jun	14	15.84	15.70	15.55	15.29
Jul	14	18.15	18.01	17.87	17.61
Aug	14	18.06	17.92	17.78	17.52
Sep	14	15.85	15.71	15.57	15.31
Oct	13.81	13.99	13.85	13.71	13.46
Nov	10.74	10.82	10.67	10.54	10.28
Dec	7.73	7.76	7.61	7.48	7.23

The maximum discrepancy between the two methods in the evaluation of the monthly values of the BHE fluid mean temperature is about 2.2 %.

Figure 5.18 shows the maximum and minimum annual values of the BHE fluid mean temperature, evaluated by EED for each of the 50 years.
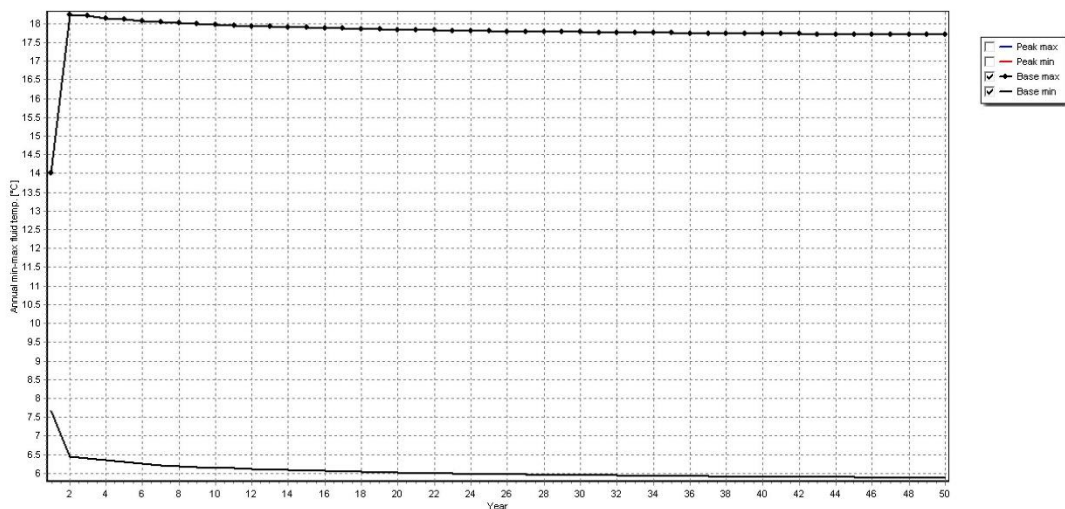
Figure 5.18: Maximum and minimum annual values of the BHE fluid mean temperature from EED.

The unexpected values of $T_{f,m,max}$ and $T_{f,m,min}$ for the first year, which appear in Figure 5.18, are due to the fact that the software defines each year starting with January and ending with December, while the first month of operation of the GCHP system is October.

Figure 5.19 compares the annual values of $T_{f,m,max}$ from the MATLAB code and from the software EED, considering for both models the year beginning in January and ending in December. Figure 5.20 compares the corresponding values of $T_{f,m,min}$.
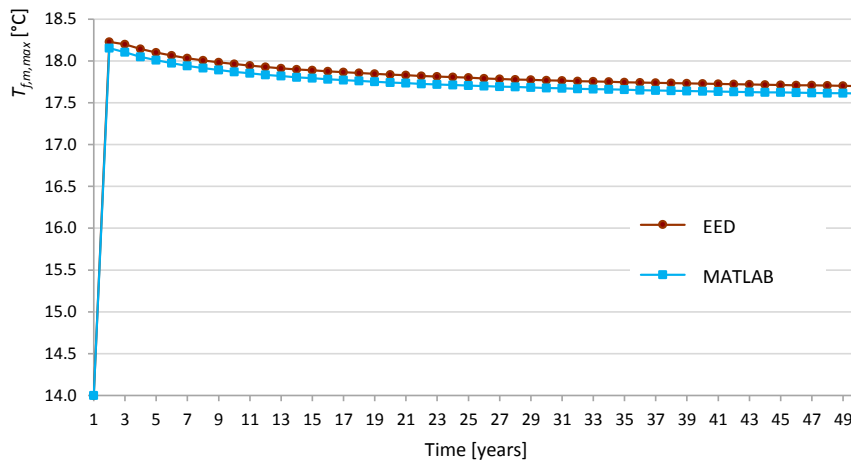
Figure 5.19: Annual values of $T_{f,m,max}$ from the MATLAB code and from EED.
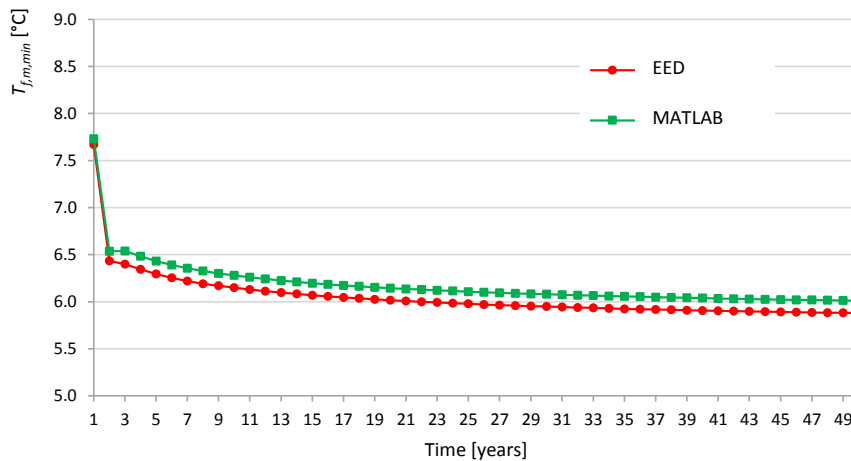
Figure 5.20: Annual values of $T_{f,m,min}$ from the MATLAB code and from EED.

Figures 5.19, 5.20 show that the plots of $T_{f,m,max}$ and of $T_{f,m,min}$ obtained through the MATLAB code are very similar to those obtained by the software EED. The maximum relative discrepancy is 2.2 %.

By considering the very low discrepancies between the results of the proposed MATLAB code and those of the software Earth Energy Designer, one can conclude that the MATLAB code is validated.

6

CONCLUSIONS AND FUTURE WORK

6.1 CONCLUSIONS

New codes have been developed in this Thesis to simulate air-to-water and ground-coupled heat pump systems for building heating, cooling and domestic hot water (DHW) production. The codes have been applied to evaluate the seasonal performance of heat pump systems in different conditions.

Mathematical models for the simulation of air-to-water heat pumps by means of the bin-method have been developed. The model for winter operation has been applied to evaluate the Seasonal Coefficient Of Performance (*SCOP*) of mono-compressor on-off heat pumps (ON-OFF HPs), multi-compressor heat pumps (MCHPs) and inverter-driven heat pumps (IDHPs), used to provide heating to several buildings, located in different Italian climates. The results have shown that the best seasonal performance of an IDHP is obtained by adopting as bivalent temperature the design temperature of the selected location, whereas for MCHPs and ON-OFF HPs the optimal bivalent temperature is higher than the design temperature. The model for summer operation has been used to evaluate the Seasonal Energy Efficiency Ratio (*SEER*) of reversible air-to-water heat pumps for building cooling and DHW production through condensation heat recovery. The results have shown that the *SEER* decreases with the increase of the building DHW demand, because of the increase of time in heat recovery mode, where the heat pump releases the condensation heat at higher temperature. In addition, worse seasonal performance has been obtained with heat pumps oversized with respect to the building cooling demand, because of the on-off cycles increase. The primary energy saving of the studied system, with respect to a traditional system in which the heat pump only provides air-conditioning and DHW is produced by a gas boiler, can be higher than 30 %.

Dynamic codes for the hourly simulation of air-to-water heat pump systems have been implemented in the software MATLAB. The code for winter operation has been used to

analyze the seasonal performance of a heat pump heating system as a function of the bivalent temperature and of the volume of the storage tank. The results have shown that the choice of the right bivalent temperature can significantly increase the system efficiency, while an increase of the storage tank volume is usually ineffective and can even reduce the performance. The dynamic codes have been employed to evaluate the primary energy consumption of the IDHP used for heating, cooling and DHW production in the retrofit of a residential building of 6 apartments in Bologna (North-Center Italy). The retrofit, which also includes external thermal insulation, replacement of windows and installation of PV panels, yields a primary energy saving of 86.5 % (from 332.5 kWh/m^2 pre-retrofit to 44.8 kWh/m^2 post-retrofit). The codes have been validated in some simple cases by means of the dynamic software TRNSYS, which has detected a maximum discrepancy of 0.80 %.

The results of the bin-method have been compared with those of the dynamic simulation, highlighting a good agreement in terms of *SCOP* for the optimal bivalent temperature or lower ones, both for ON-OFF HPs and IDHPs. For high bivalent temperatures (undersized heat pumps), the two methods give different results and the maximum observed deviation reaches 23 %.

A dynamic code for the hourly simulation of Ground-Coupled Heat Pump (GCHP) systems has been developed in this Thesis. The code, which is implemented in MATLAB, employs the *g-functions* obtained by Zanchini and Lazzari [9] and applies to GCHPs with or without inverter, used for building heating and/or cooling. Fast hourly simulations for several years (and, with the aid of auxiliary monthly simulations, even for several decades) have been performed for the whole GCHP system, composed by the heat pump and the Borehole Heat Exchanger (BHE) field. The code has been used to analyze the effects of the inverter and of the total length of the BHE field on the *SCOP* and *SEER* of a GCHP system designed for a residential house in Bologna with dominant heating loads. A BHE field with 3 boreholes has been considered, with length of each BHE either 75 m or 105 m. The results have shown that the increase of the BHE length yields a *SCOP* enhancement of about 7 %, while the *SEER* almost does not change. Employing an inverter-driven heat pump instead of an on-off one can yield a *SCOP* increase of about 30 % and a *SEER* enhancement of about 52 %. The results demonstrate the importance of employing inverter-driven heat pumps for GCHP systems. The code has been validated by comparing the mean monthly temperatures of the BHE fluid obtained in a 50-year simulation by means of the proposed model and of the software Earth Energy Designer (EED). The maximum relative discrepancy is about 2.2 %.

6.2 OPPORTUNITIES FOR FUTURE WORK

Further improvements of the research presented in this Thesis may be performed. Future developments may be oriented to the implementation of the effects of the defrost cycles into the simulation codes for air-to-water heat pumps in winter operation. Indeed, the external surface of the evaporator of an air-source heat pump placed in a cold and, especially, humid location can be subjected to the formation of frost, which decreases the area of passage of the air and acts as an insulator. Defrost may be consequently necessary and can be performed in different ways, e.g. by employing electric heaters or by reversing the heat pump cycle. Defrost cycles yield a decrease of the heat pump system performance, which should be taken into account in the evaluation of its seasonal efficiency.

An experimental monitoring of the residential building object of the HERB project is planned and will be performed as soon as the energy retrofit is completed. Comparisons of the results obtained by the codes for air-to-water heat pumps with the results derived from the monitoring of the building will be then performed.

Regarding the MATLAB code for ground-coupled heat pump systems, further investigations are planned to consider the influence of the on-off cycles not only on the hourly values of the heat pump *COP* (or *EER*), but also on the hourly values of the mean temperature of the borehole fluid.

Moreover, the code will be extended to take into account the building energy needs for domestic hot water production.

An experimental validation of the code will be performed either through the monitoring of a real plant or, more probably, by installing a heat pump coupled to a BHE in the laboratory of the Department.

An improvement of the simulation code for GCHPs, for the special case of double U-tube borehole heat exchangers, can be obtained by implementing recent analytical expressions of the *g-functions* obtained by Zanchini and Lazzari [53], which take into account the internal structure of the BHE. The new *g-functions* yield the dimensionless temperature at the interface tubes-grout and allow a more precise determination of the time evolution of the temperature of the operating fluid during hourly peak loads.

7

APPENDIX

7.1 MATLAB CODE FOR AIR-TO-WATER HEAT PUMPS IN WINTER OPERATION

MATLAB Workspace			Page 1
Name ▲	**Value**	**Min**	**Max**
b_eff	0.8700	0.8700	0.8700
bu	0.5000	0.5000	0.5000
COP_Tsmax_d	[2.2300;2.6900;3.0200;3.4100]	2.2300	3.4100
COP_Tsmax_h	*4x5 double*	2.1500	4.4900
COP_Tsmin_d	[2.3100;2.8100;3.1600;3.5800]	2.3100	3.5800
COP_Tsmin_h	*4x5 double*	2.2300	4.7400
Edhw_buil	*5088x1 double*	0	2.1788
Elost_buil	*5088x1 double*	0	10.4560
eta	0.4600	0.4600	0.4600
freq	[110 90 70 50 30]	30	110
P_Tsmax_d	[7.4100;9.6700;11.2000;12.9000]	7.4100	12.9000
P_Tsmax_h	*4x5 double*	1.8900	13.5000
P_Tsmin_d	[7.4500;9.7400;11.3000;13]	7.4500	13
P_Tsmin_h	*4x5 double*	1.9000	13.7000
Text	*5088x1 double*	-6.7500	25.3000
Text_hp	[-7 2 7 12]	-7	12
Tint	*5088x1 double*	20	20
TOL_d	-10	-10	-10
TOL_h	-15	-15	-15
Tsmax_d	50	50	50
Tsmax_h	40	40	40
Tsmin_d	48	48	48
Tsmin_h	38	38	38
U_d	0.0023	0.0023	0.0023
U_h	0.0011	0.0011	0.0011
Vs_d	1600	1600	1600
Vs_h	200	200	200

161

```matlab
% HOURLY SIMULATION OF AN ELECTRIC AIR-TO-WATER HEAT PUMP
% WINTER OPERATION: HEATING + DHW MODE

% Interpolation of the heat pump power and COP data
polyn_degree=2;

for i=1:length(freq)
    coeff1(i,:)=polyfit(Text_hp',P_Tsmin_h(:,i),polyn_degree);
    coeff2(i,:)=polyfit(Text_hp',P_Tsmax_h(:,i),polyn_degree);
    coeff3(i,:)=polyfit(Text_hp',COP_Tsmin_h(:,i),polyn_degree);
    coeff4(i,:)=polyfit(Text_hp',COP_Tsmax_h(:,i),polyn_degree);

    P_int_min_h(:,i)=polyval(coeff1(i,:),Text);
    P_int_max_h(:,i)=polyval(coeff2(i,:),Text);
    COP_int_min_h(:,i)=polyval(coeff3(i,:),Text);
    COP_int_max_h(:,i)=polyval(coeff4(i,:),Text);
end

coeff5=polyfit(Text_hp',P_Tsmin_d,polyn_degree);
coeff6=polyfit(Text_hp',P_Tsmax_d,polyn_degree);
coeff7=polyfit(Text_hp',COP_Tsmin_d,polyn_degree);
coeff8=polyfit(Text_hp',COP_Tsmax_d,polyn_degree);

P_int_min_d=polyval(coeff5,Text);
P_int_max_d=polyval(coeff6,Text);
COP_int_min_d=polyval(coeff7,Text);
COP_int_max_d=polyval(coeff8,Text);

% Determination of the heat pump cut-off temperature
COP_en_lim=b_eff/eta;
mom_h=((coeff4(1,2))^2)-4*coeff4(1,1)*(coeff4(1,3)-COP_en_lim);
mom_d=((coeff8(2))^2)-4*coeff8(1)*(coeff8(3)-COP_en_lim);

if mom_h<0
    Tcut_off_h=TOL_h
else
    Tcut_off_h=max(TOL_h,((-coeff4(1,2)+sqrt(mom_h))/(2*coeff4(1,1))))
end

if mom_d<0
    Tcut_off_d=TOL_d
else
    Tcut_off_d=max(TOL_d,((-coeff8(2)+sqrt(mom_d))/(2*coeff8(1))))
end

% Determination of the hourly values of the storage room temperature
for i=1:length(Text)
    Tsroom(i)=Tint(i)-bu*(Tint(i)-Text(i));
end

% Initialization of the storage temperature
Ts_h(1)=Tsroom(1);
Ts_d(1)=Tsmin_d;

% For-loop
```

```matlab
for i=1:length(Text)

    % Determination of the hourly values of the storage energy
    Es_h(i)=Vs_h*4.18*(Ts_h(i)-Tsmin_h)/3600;
    Es_d(i)=Vs_d*4.18*(Ts_d(i)-Tsmin_d)/3600;

    % Determination of the hourly values of the energy lost by the storage
    Elost_s_h(i)=U_h*(Ts_h(i)-Tsroom(i));
    Elost_s_d(i)=U_d*(Ts_d(i)-Tsroom(i));

    % Determination of the hourly values of the maximum heat pump power
    for r=1:length(freq)
        if Text(i)<Tcut_off_h
            P_max_hp_h(i,r)=0;
            COP_DC_h(i,r)=0;
        else
            P_max_hp_h(i,r)=P_int_min_h(i,r)+(Ts_h(i)-Tsmin_h)*(P_int_max_h(i,r)- ↙
P_int_min_h(i,r))/(Tsmax_h-Tsmin_h);
            COP_DC_h(i,r)=COP_int_min_h(i,r)+(Ts_h(i)-Tsmin_h)*(COP_int_max_h(i,r)- ↙
COP_int_min_h(i,r))/(Tsmax_h-Tsmin_h);
        end
    end

    if Text(i)<Tcut_off_d
        P_max_hp_d(i)=0;
        COP_DC_d(i)=0;
    else
        P_max_hp_d(i)=P_int_min_d(i)+(Ts_d(i)-Tsmin_d)*(P_int_max_d(i)-P_int_min_d(i)) ↙
/(Tsmax_d-Tsmin_d);
        COP_DC_d(i)=COP_int_min_d(i)+(Ts_d(i)-Tsmin_d)*(COP_int_max_d(i)-COP_int_min_d ↙
(i))/(Tsmax_d-Tsmin_d);
    end

    % Determination of the hourly values of the energy delivered by the
    % heat pump
    Tsm_d(i)=Ts_d(i)+3600/(4.18*Vs_d)*(P_max_hp_d(i)-Edhw_buil(i)-Elost_s_d(i));

    if Tsm_d(i)<=Tsmax_d
        Ehp_d(i)=P_max_hp_d(i);
        Ehp_h(i)=0;
    else
        Ehp_d(i)=Edhw_buil(i)+Elost_s_d(i)+Vs_d*4.18/3600*(Tsmax_d-Ts_d(i));
        if P_max_hp_d(i)==0
            tau_d(i)=0;
        else
            tau_d(i)=Ehp_d(i)/P_max_hp_d(i);
        end

        tau_res(i)=1-tau_d(i);
        Tsm_h(i)=Ts_h(i)+3600/(4.18*Vs_h)*(P_max_hp_h(i,1)*tau_res(i)-Elost_buil(i)- ↙
Elost_s_h(i));

        if Tsm_h(i)<=Tsmax_h
            Ehp_h(i)=P_max_hp_h(i,1)*tau_res(i);
        else
```

163

```
                Ehp_h(i)=Elost_buil(i)+Elost_s_h(i)+Vs_h*4.18/3600*(Tsmax_h-Ts_h(i));
        end
    end

    Ehp(i)=Ehp_h(i)+Ehp_d(i);

    % Determination of the hourly values of the energy delivered and used
    % by the back-up system
    Ebum_h(i)=Elost_buil(i)+Elost_s_h(i)-Es_h(i)-Ehp_h(i);
    if Ebum_h(i)>=0
        Eh(i)=Ebum_h(i);
    else
        Eh(i)=0;
    end

    Ebum_d(i)=Edhw_buil(i)+Elost_s_d(i)-Es_d(i)-Ehp_d(i);
    if Ebum_d(i)>=0
        Ed(i)=Ebum_d(i);
    else
        Ed(i)=0;
    end

    Ebackup(i)=Eh(i)+Ed(i);
    Ebackup_us(i)=Ebackup(i)/b_eff;

    % Determination of the hourly values of the COP and
    % electric energy used by the heat pump

    if Ehp_h(i)==0
        CR(i)=0;
        COP_DC_h_eff(i)=0;
        f_COP(i)=0;
        COP_h(i)=0;
        Ehp_us_h(i)=0;
    else
        if Ehp_h(i)/(P_max_hp_h(i,end)*tau_res(i))>1
            CR(i)=1;
        else
            CR(i)=Ehp_h(i)/(P_max_hp_h(i,end)*tau_res(i));
        end

        if Ehp_h(i)<(P_max_hp_h(i,end)*tau_res(i))
            COP_DC_h_eff(i)=COP_DC_h(i,end);
        elseif length(freq)==1
            COP_DC_h_eff(i)=COP_DC_h(i,end);
        else
            coeff_p_COP_h(i,:)=polyfit(P_max_hp_h(i,:),COP_DC_h(i,:),polyn_degree);
            COP_DC_h_eff(i)=polyval(coeff_p_COP_h(i,:),(Ehp_h(i)/tau_res(i)));
        end

        f_COP(i)=CR(i)/(0.1+CR(i)*0.9);
        COP_h(i)=f_COP(i)*COP_DC_h_eff(i);
        Ehp_us_h(i)=Ehp_h(i)/COP_h(i);
    end
```

```
        if Ehp_d(i)==0
            COP_d(i)=0;
            Ehp_us_d(i)=0;
        else
            COP_d(i)=COP_DC_d(i);
            Ehp_us_d(i)=Ehp_d(i)/COP_d(i);
        end

        Ehp_us(i)=Ehp_us_h(i)+Ehp_us_d(i);
        if Ehp_us(i)==0
            COP_tot(i)=0;
        else
            COP_tot(i)=Ehp(i)/Ehp_us(i);
        end

        % Storage temperature update
        Ts_h(i+1)=Ts_h(i)+3600/(Vs_h*4.18)*(Ehp_h(i)+Eh(i)-Elost_buil(i)-Elost_s_h(i));
        Ts_d(i+1)=Ts_d(i)+3600/(Vs_d*4.18)*(Ehp_d(i)+Ed(i)-Edhw_buil(i)-Elost_s_d(i));

end

% Determination of the seasonal values of the energy delivered and used
% by the heat pump and back-up system
% and of the energy required by the building
TOT_Ehp=sum(Ehp);
TOT_Ehp_us=sum(Ehp_us);
TOT_Ebackup=sum(Ebackup);
TOT_Ebackup_us=sum(Ebackup_us);
TOT_Elost_buil=sum(Elost_buil);
TOT_Edhw_buil=sum(Edhw_buil);

% Determination of SCOP, FUE, phi
SCOP=TOT_Ehp/TOT_Ehp_us
FUE=(TOT_Elost_buil+TOT_Edhw_buil)/(TOT_Ehp_us/eta+TOT_Ebackup_us)
phi=TOT_Ebackup/(TOT_Ebackup+TOT_Ehp)

% Graph of the interpolation of the heat pump power data in heating mode,
% for the maximum storage temperature, at the maximum frequency
figure(1)
x=linspace(-20,35,56);
y=polyval(coeff2(1,:),x);
plot(Text_hp,P_Tsmax_h(:,1),'b*')
hold on
plot(x,y,'b')
xlabel('Text [°C]')
ylabel('Power in heating mode, at the maximum storage temperature at the maximum ↵
frequency [kW]')
legend('Input data','Interpolating polynomial')
title('Interpolation of the heat pump power data in heating mode, for the maximum ↵
storage temperature and maximum frequency')

% Graph of the interpolation of the heat pump COP data in heating mode,
% for the maximum storage temperature, at the maximum frequency
figure(2)
yy=polyval(coeff4(1,:),x);
plot(Text_hp,COP_Tsmax_h(:,1),'r*')
hold on
plot(x,yy,'r')
xlabel('Text [°C]')
ylabel('COP in heating mode, at the maximum storage temperature at the maximum ↵
frequency')
legend('Input data','Interpolating polynomial')
title('Interpolation of the heat pump COP data in heating mode, for the maximum ↵
storage temperature and maximum frequency')
```

7.2 MATLAB CODE FOR AIR-TO-WATER HEAT PUMPS IN SUMMER OPERATION

MATLAB Workspace			Page 1
Name ▲	**Value**	**Min**	**Max**
b_eff	0.8700	0.8700	0.8700
COP_d_Tsmax_d	*4x5 double*	3.7400	6
COP_d_Tsmin_d	*4x5 double*	3.9300	6.3600
Edhw_buil	*3672x1 double*	0	2.1788
EER_cc_Tsmax_c	*4x5 double*	2.9700	5.4300
EER_cc_Tsmin_c	*4x5 double*	2.7800	5.0400
EER_cd_Tsmax_c	[2.4500 2.5900 2.6300 2.5400 2.23…	2.1100	2.6300
EER_cd_Tsmin_c	[2.3000 2.4300 2.4600 2.3900 2.08…	1.9500	2.4600
Egain_buil	*3672x1 double*	0	10.2652
eta	0.4600	0.4600	0.4600
freq	[110 90 70 50 30]	30	110
P_cc_Tsmax_c	*4x5 double*	2.6100	11.2000
P_cc_Tsmin_c	*4x5 double*	2.4300	10.6000
P_cd_Tsmax_c	[8.8600 7.1100 5.4500 3.8400 2.30…	2.2400	8.8600
P_cd_Tsmin_c	[8.2500 6.6400 5.0700 3.5800 2.14…	2.0700	8.2500
P_d_Tsmax_d	*4x5 double*	3.9800	22.4000
P_d_Tsmin_d	*4x5 double*	4.0300	22.7000
Text	*3672x1 double*	9.9500	35.5000
Text_hp	[20 25 30 35]	20	35
Tsmax_c	7	7	7
Tsmax_d	50	50	50
Tsmin_c	5	5	5
Tsmin_d	48	48	48
Tsroom	*3672x1 double*	27	27
U_c	0.0012	0.0012	0.0012
U_d	0.0033	0.0033	0.0033
Vs_c	200	200	200
Vs_d	1600	1600	1600

```matlab
% HOURLY SIMULATION OF A MULTIFUNCTION ELECTRIC AIR-TO-WATER HEAT PUMP
% SUMMER OPERATION: COOLING + DHW MODE

% Interpolation of the heat pump power, EER and COP data
for i=1:length(freq)
    coeff_d1(i,:)=polyfit(Text_hp',P_d_Tsmin_d(:,i),2);
    coeff_d2(i,:)=polyfit(Text_hp',P_d_Tsmax_d(:,i),2);
    coeff_d3(i,:)=polyfit(Text_hp',COP_d_Tsmin_d(:,i),2);
    coeff_d4(i,:)=polyfit(Text_hp',COP_d_Tsmax_d(:,i),2);

    coeff_cc1(i,:)=polyfit(Text_hp',P_cc_Tsmin_c(:,i),2);
    coeff_cc2(i,:)=polyfit(Text_hp',P_cc_Tsmax_c(:,i),2);
    coeff_cc3(i,:)=polyfit(Text_hp',EER_cc_Tsmin_c(:,i),2);
    coeff_cc4(i,:)=polyfit(Text_hp',EER_cc_Tsmax_c(:,i),2);

    coeff_cd1(i,:)=polyfit([Tsmin_d Tsmax_d]',P_cd_Tsmin_c(:,i),1);
    coeff_cd2(i,:)=polyfit([Tsmin_d Tsmax_d]',P_cd_Tsmax_c(:,i),1);
    coeff_cd3(i,:)=polyfit([Tsmin_d Tsmax_d]',EER_cd_Tsmin_c(:,i),1);
    coeff_cd4(i,:)=polyfit([Tsmin_d Tsmax_d]',EER_cd_Tsmax_c(:,i),1);

    P_int_d_min_d(:,i)=polyval(coeff_d1(i,:),Text);
    P_int_d_max_d(:,i)=polyval(coeff_d2(i,:),Text);
    COP_int_d_min_d(:,i)=polyval(coeff_d3(i,:),Text);
    COP_int_d_max_d(:,i)=polyval(coeff_d4(i,:),Text);

    P_int_cc_min_c(:,i)=polyval(coeff_cc1(i,:),Text);
    P_int_cc_max_c(:,i)=polyval(coeff_cc2(i,:),Text);
    EER_int_cc_min_c(:,i)=polyval(coeff_cc3(i,:),Text);
    EER_int_cc_max_c(:,i)=polyval(coeff_cc4(i,:),Text);
end

% Initialization of the storage temperature
Ts_c(1)=Tsmax_c;
Ts_d(1)=Tsmin_d;

% For-loop
for i=1:length(Text)
    if Text(i)<17
        Egain_buil(i)=0;
    else
        Egain_buil(i)=0.537864706*Text(i)-8.605835294;
    end

    % Interpolation of the heat pump power and EER data for cooling+DHW
    % mode
    for r=1:length(freq)
        P_int_cd_min_c(i,r)=polyval(coeff_cd1(r,:),Ts_d(i));
        P_int_cd_max_c(i,r)=polyval(coeff_cd2(r,:),Ts_d(i));
        EER_int_cd_min_c(i,r)=polyval(coeff_cd3(r,:),Ts_d(i));
        EER_int_cd_max_c(i,r)=polyval(coeff_cd4(r,:),Ts_d(i));
    end

    % Determination of the hourly values of the storage energy
    Es_c(i)=Vs_c*4.18*(Tsmax_c-Ts_c(i))/3600;
    Es_d(i)=Vs_d*4.18*(Ts_d(i)-Tsmin_d)/3600;
```

```matlab
        % Determination of the hourly values of the energy lost/gained by the
        % storages
        Egain_s_c(i)=U_c*(Tsroom(i)-Ts_c(i));
        Elost_s_d(i)=U_d*(Ts_d(i)-Tsroom(i));

        % Determination of the heat pump mode
        if (Egain_buil(i)+Egain_s_c(i))<=Es_c(i)  %-> HEAT PUMP IN DHW-only mode

            marker(i)=1;

            % Determination of the hourly values of the maximum heat pump power
            % and COP_DC in DHW-only mode
            for r=1:length(freq)
                P_max_hp(i,r)=P_int_d_min_d(i,r)+(Ts_d(i)-Tsmin_d)*(P_int_d_max_d(i,r)- ↙
    P_int_d_min_d(i,r))/(Tsmax_d-Tsmin_d);
                COP_DC(i,r)=COP_int_d_min_d(i,r)+(Ts_d(i)-Tsmin_d)*(COP_int_d_max_d(i,r)- ↙
    COP_int_d_min_d(i,r))/(Tsmax_d-Tsmin_d);
            end

            % Determination of the hourly values of the energy delivered by the
            % heat pump in DHW-only mode
            if (Ts_d(i)+3600/(4.18*Vs_d)*(P_max_hp(i,1)-Edhw_buil(i)-Elost_s_d(i))) ↙
    <=Tsmax_d
                Ehp_dd(i)=P_max_hp(i,1);
            else
                Ehp_dd(i)=Edhw_buil(i)+Elost_s_d(i)+Vs_d*4.18/3600*(Tsmax_d-Ts_d(i));
            end

            if Ehp_dd(i)<0
                disp('ERROR_1')
                break
            end

            % Determination of the hourly values of the COP and electric energy
            % used by the heat pump in DHW-only mode
            if Ehp_dd(i)==0
                CR(i)=0;
                COP_DC_eff(i)=0;
                f_COP(i)=0;
                COP(i)=0;
                Ehp_us(i)=0;
            else
                if Ehp_dd(i)/P_max_hp(i,end)>1
                    CR(i)=1;
                else
                    CR(i)=Ehp_dd(i)/P_max_hp(i,end);
                end

                if Ehp_dd(i)<P_max_hp(i,end)
                    COP_DC_eff(i)=COP_DC(i,end);
                elseif length(freq)==1
                    COP_DC_eff(i)=COP_DC(i,end);
                else
                    coeff_p_COP(i,:)=polyfit(P_max_hp(i,:),COP_DC(i,:),2);
```

```
                COP_DC_eff(i)=polyval(coeff_p_COP(i,:),Ehp_dd(i));
            end

            f_COP(i)=CR(i)/(0.1+CR(i)*0.9);
            COP(i)=f_COP(i)*COP_DC_eff(i);
            Ehp_us(i)=Ehp_dd(i)/COP(i);
        end

        % Determination of the hourly values of the energy delivered and
        % used by the back-up system in DHW-only mode
        Ebum(i)=Edhw_buil(i)+Elost_s_d(i)-Es_d(i)-Ehp_dd(i);
        if Ebum(i)>=0
            Ebackup(i)=Ebum(i);
        else
            Ebackup(i)=0;
        end

        Ebackup_us(i)=Ebackup(i)/b_eff;

        % Storage temperature update in DHW-only mode
        Ts_c(i+1)=Ts_c(i)+3600/(Vs_c*4.18)*(Egain_buil(i)+Egain_s_c(i));
        Ts_d(i+1)=Ts_d(i)+3600/(Vs_d*4.18)*(Ehp_dd(i)+Ebackup(i)-Edhw_buil(i)- ↵
Elost_s_d(i));

    else  %-> HEAT PUMP IN cooling(+DHW) mode

        % Determination of the hourly values of the maximum heat pump power
        % and EER_DC in cooling(+DHW) mode
        for r=1:length(freq)
            P_max_hp_cd(i,r)=P_int_cd_min_c(i,r)+(Ts_c(i)-Tsmin_c)*(P_int_cd_max_c(i, ↵
r)-P_int_cd_min_c(i,r))/(Tsmax_c-Tsmin_c);
            EER_DC_cd(i,r)=EER_int_cd_min_c(i,r)+(Ts_c(i)-Tsmin_c)*(EER_int_cd_max_c ↵
(i,r)-EER_int_cd_min_c(i,r))/(Tsmax_c-Tsmin_c);
            P_max_hp_cc(i,r)=P_int_cc_min_c(i,r)+(Ts_c(i)-Tsmin_c)*(P_int_cc_max_c(i, ↵
r)-P_int_cc_min_c(i,r))/(Tsmax_c-Tsmin_c);
            EER_DC_cc(i,r)=EER_int_cc_min_c(i,r)+(Ts_c(i)-Tsmin_c)*(EER_int_cc_max_c ↵
(i,r)-EER_int_cc_min_c(i,r))/(Tsmax_c-Tsmin_c);
        end

        if Edhw_buil(i)+Elost_s_d(i)+Vs_d*4.18/3600*(Tsmax_d-Ts_d(i))<=0  %-> cooling- ↵
only mode

            marker(i)=2;

            % Determination of the hourly values of the energy delivered by
            % the heat pump in cooling-only mode
            if (Ts_c(i)+3600/(4.18*Vs_c)*(-P_max_hp_cc(i,1)+Egain_buil(i)+Egain_s_c ↵
(i)))>=Tsmin_c
                Ehp(i)=P_max_hp_cc(i,1);
            else
                Ehp(i)=Egain_buil(i)+Egain_s_c(i)+Vs_c*4.18/3600*(Ts_c(i)-Tsmin_c);
            end

            if Ehp(i)<0
                disp('ERROR_2')
```

```
                break
            end

            % Determination of the hourly values of the EER and electric
            % energy used by the heat pump in cooling-only mode
            if Ehp(i)/P_max_hp_cc(i,end)>1
                CR(i)=1;
            else
                CR(i)=Ehp(i)/P_max_hp_cc(i,end);
            end

            if Ehp(i)<P_max_hp_cc(i,end)
                EER_DC_eff(i)=EER_DC_cc(i,end);
            elseif length(freq)==1
                EER_DC_eff(i)=EER_DC_cc(i,end);
            else
                coeff_p_EER(i,:)=polyfit(P_max_hp_cc(i,:),EER_DC_cc(i,:),2);
                EER_DC_eff(i)=polyval(coeff_p_EER(i,:),Ehp(i));
            end

            f_EER(i)=CR(i)/(0.1+CR(i)*0.9);
            EER(i)=f_EER(i)*EER_DC_eff(i);
            Ehp_us(i)=Ehp(i)/EER(i);

            % Determination of the uncovered cooling energy in cooling-only
            % mode
            if (Egain_buil(i)+Egain_s_c(i)-Es_c(i)-Ehp(i))<0
                Euncov(i)=0;
            else
                Euncov(i)=Egain_buil(i)+Egain_s_c(i)-Es_c(i)-Ehp(i);
            end

            % Storage temperature update in cooling-only mode
            Ts_c(i+1)=Ts_c(i)+3600/(Vs_c*4.18)*(-Ehp(i)+Egain_buil(i)+Egain_s_c(i)- ↙
Euncov(i));
            Ts_d(i+1)=Ts_d(i)+3600/(Vs_d*4.18)*(-Edhw_buil(i)-Elost_s_d(i));

        else %-> cooling+DHW mode

            marker(i)=3;

            % Determination of the hourly values of the heat pump power and
            % tau_on
            if (Ts_c(i)+3600/(4.18*Vs_c)*(-P_max_hp_cd(i,1)+Egain_buil(i)+Egain_s_c ↙
(i)))>=Tsmin_c
                Php_d(i)=P_max_hp_cd(i,1);
                tau_on(i)=1;
            else
                if Egain_buil(i)+Egain_s_c(i)+Vs_c*4.18/3600*(Ts_c(i)-Tsmin_c) ↙
<P_max_hp_cd(i,end)
                    Php_d(i)=P_max_hp_cd(i,end);
                    tau_on(i)=(Egain_buil(i)+Egain_s_c(i)+Vs_c*4.18/3600*(Ts_c(i)- ↙
Tsmin_c))/P_max_hp_cd(i,end);
                else
                    Php_d(i)=Egain_buil(i)+Egain_s_c(i)+Vs_c*4.18/3600*(Ts_c(i)- ↙
```

```matlab
                Tsmin_c);
                            tau_on(i)=1;
                    end
                end

                if (Egain_buil(i)+Egain_s_c(i)+Vs_c*4.18/3600*(Ts_c(i)-Tsmin_c))<0
                    disp('ERROR_3_1')
                    break
                end

                % Determination of the hourly values of the EER of the heat
                % pump with DHW mode on
                if Php_d(i)==P_max_hp_cd(i,end)
                    EER_DC_cd_eff(i)=EER_DC_cd(i,end);
                elseif length(freq)==1
                    EER_DC_cd_eff(i)=EER_DC_cd(i,end);
                else
                    coeff_p_EER_cd(i,:)=polyfit(P_max_hp_cd(i,:),EER_DC_cd(i,:),2);
                    EER_DC_cd_eff(i)=polyval(coeff_p_EER_cd(i,:),Php_d(i));
                end

                % Determination of the hourly values of the thermal energy
                % delivered to the DHW storage and of the time with DHW mode on
                Eavail_d(i)=tau_on(i)*(Php_d(i)+80/100*Php_d(i)/EER_DC_cd_eff(i));

                if (Ts_d(i)+3600/(4.18*Vs_d)*(Eavail_d(i)-Edhw_buil(i)-Elost_s_d(i))) ↙
        <=Tsmax_d
                    Edeliv_d(i)=Eavail_d(i);
                    tau_d(i)=tau_on(i);
                else
                    Edeliv_d(i)=Edhw_buil(i)+Elost_s_d(i)+Vs_d*4.18/3600*(Tsmax_d-Ts_d ↙
        (i));
                    tau_d(i)=Edeliv_d(i)/(Php_d(i)+80/100*Php_d(i)/EER_DC_cd_eff(i));
                end

                if Edeliv_d(i)<0
                    disp('ERROR_3_2')
                    break
                end

                % Determination of the hourly values of the cooling energy
                % delivered by the heat pump with DHW mode on
                Ehp_d(i)=Php_d(i)*tau_d(i);

                % Determination of the heat pump power values with DHW
                % mode off
                if Php_d(i)>=P_max_hp_cc(i,end)
                    tau_c(i)=tau_on(i)-tau_d(i);
                    if Php_d(i)<P_max_hp_cd(i,1)
                        Php_c(i)=Php_d(i);
                    else
                        if (Egain_buil(i)+Egain_s_c(i)+Vs_c*4.18/3600*(Ts_c(i)-Tsmin_c)- ↙
        Ehp_d(i))/(tau_on(i)-tau_d(i))<=P_max_hp_cc(i,1)
                            Php_c(i)=(Egain_buil(i)+Egain_s_c(i)+Vs_c*4.18/3600*(Ts_c(i)- ↙
        Tsmin_c)-Ehp_d(i))/(tau_on(i)-tau_d(i));
```

171

```matlab
            else
                Php_c(i)=P_max_hp_cc(i,1);
            end
        end
    else
        Php_c(i)=P_max_hp_cc(i,end);
        tau_c(i)=(Egain_buil(i)+Egain_s_c(i)+Vs_c*4.18/3600*(Ts_c(i)-Tsmin_c)- ↵
Ehp_d(i))/P_max_hp_cc(i,end);
    end

    if Php_c(i)<0
        disp('ERROR_3_3')
        break
    end

    % Determination of the hourly values of the EER of the heat
    % pump with DHW mode off
    if Php_c(i)==P_max_hp_cc(i,end)
        EER_DC_cc_eff(i)=EER_DC_cc(i,end);
    elseif length(freq)==1
        EER_DC_cc_eff(i)=EER_DC_cc(i,end);
    else
        coeff_p_EER_cc(i,:)=polyfit(P_max_hp_cc(i,:),EER_DC_cc(i,:),2);
        EER_DC_cc_eff(i)=polyval(coeff_p_EER_cc(i,:),Php_c(i));
    end

    % Determination of the hourly values of the energy delivered
    % and used by the heat pump in cooling+DHW mode
    Ehp_c(i)=Php_c(i)*tau_c(i);
    Ehp(i)=Ehp_d(i)+Ehp_c(i);
    Ehp_us(i)=(0.1+0.9*(tau_d(i)+tau_c(i)))/(tau_d(i)+tau_c(i))*(Ehp_d(i) ↵
/EER_DC_cd_eff(i)+Ehp_c(i)/EER_DC_cc_eff(i));

    % Determination of the hourly values of the energy delivered
    % and used by the back-up system in cooling+DHW mode
    Ebum(i)=Edhw_buil(i)+Elost_s_d(i)-Es_d(i)-Edeliv_d(i);

    if Ebum(i)>=0
        Ebackup(i)=Ebum(i);
    else
        Ebackup(i)=0;
    end

    Ebackup_us(i)=Ebackup(i)/b_eff;

     % Determination of the uncovered cooling energy in cooling+DHW
     % mode
    if (Egain_buil(i)+Egain_s_c(i)-Es_c(i)-Ehp(i))<0
        Euncov(i)=0;
    else
        Euncov(i)=Egain_buil(i)+Egain_s_c(i)-Es_c(i)-Ehp(i);
    end

    % Storage temperature update in cooling+DHW mode
    Ts_c(i+1)=Ts_c(i)+3600/(Vs_c*4.18)*(-Ehp(i)+Egain_buil(i)+Egain_s_c(i)- ↵
```

```matlab
            Euncov(i));
                Ts_d(i+1)=Ts_d(i)+3600/(Vs_d*4.18)*(Edeliv_d(i)+Ebackup(i)-Edhw_buil(i)- ↙
Elost_s_d(i));
            end
        end

        if marker(i)==1
            dhw_sign(i)=1;
            E_us_sign(i)=0;
        else
            dhw_sign(i)=0;
            E_us_sign(i)=Ehp_us(i);
        end
end

% Determination of the seasonal energy values
disp('Total cooling energy delivered by the heat pump')
TOT_Ehp=sum(Ehp)

disp('Total thermal energy for DHW delivered by the heat pump')
TOT_Ehp_d=sum(Ehp_d)

disp('Total electric energy used by the heat pump')
TOT_Ehp_us=sum(Ehp_us)

disp('Total thermal energy for DHW delivered by the back-up system')
TOT_Ebackup=sum(Ebackup)

disp('Total energy used by the back-up system')
TOT_Ebackup_us=sum(Ebackup_us)

disp('Total uncovered cooling energy')
TOT_Euncov=sum(Euncov)

disp('Total cooling energy demand of the building')
TOT_Egain_buil=sum(Egain_buil)

disp('Total building energy demand for DHW')
TOT_Edhw_buil=sum(Edhw_buil)

disp('Number of hours in DHW-only mode')
N_dhw_hours=sum(dhw_sign)

disp('SEER')
SEER=TOT_Ehp/sum(E_us_sign)

disp('FUE')
FUE=(TOT_Ehp+TOT_Ebackup+sum(Edeliv_d))/(TOT_Ehp_us/eta+TOT_Ebackup_us)
```

7.3   MATLAB CODE FOR GROUND-COUPLED HEAT PUMPS

MATLAB Workspace			Page 1
Name ▲	**Value**	**Min**	**Max**
a_coeff	*3x7 double*	-6.1671	6.7500
alphag	8.8140e-07	8.8140...	8.8140...
b_coeff	*3x7 double*	-27.17...	27.1198
COP_data	*14x5 double*	4.4100	7.4300
cp	4.1896	4.1896	4.1896
D	0.1500	0.1500	0.1500
EER_data	*21x5 double*	4.2000	7.2200
freq	[110 90 70 50 30]	30	110
kg	1.8000	1.8000	1.8000
L	105	105	105
num_bore	3	3	3
num_years	10	10	10
Pow_summ_data	*21x5 double*	3.0100	13.8000
Pow_wint_data	*14x5 double*	3.0800	18.2000
q0	21.8988	21.8988	21.8988
Qb_oneyear	*8760x1 double*	-10.45...	9.3176
Rb	0.0687	0.0687	0.0687
rho	999.2500	999.25...	999.25...
Tcutoff_summ	100	100	100
Tcutoff_wint	-100	-100	-100
Tfm_input_summ	*1x21 double*	15	35
Tfm_input_wint	*1x14 double*	5	18
Tg	14	14	14
V	2.6667e-04	2.6667...	2.6667...
x0	[-3.7440 1.7000 2.4280]	-3.7440	2.4280
x1	[1.4000 3.6000 4.2100]	1.4000	4.2100

```matlab
% HOURLY SIMULATION OF A GCHP SYSTEM
% 3 IN-LINE BHEs, L*=700

% Dimensionless BHE length
L_star=L/D

% Dimensionless duration of one hour
tau_h_star=alphag*3600/(D^2);

% Interpolation coefficients of the heat pump power, COP and EER data as
% functions of the fluid supply temperature
for i=1:length(freq)
    Pow_wint_coeff(i,:)=polyfit(Tfm_input_wint',Pow_wint_data(:,i),2);
    COP_coeff(i,:)=polyfit(Tfm_input_wint',COP_data(:,i),2);
    Pow_summ_coeff(i,:)=polyfit(Tfm_input_summ',Pow_summ_data(:,i),2);
    EER_coeff(i,:)=polyfit(Tfm_input_summ',EER_data(:,i),2);
end

% Graph of the heat pump heating power at the maximum frequency
figure(1)
x=linspace(-5,20);
y1=polyval(Pow_wint_coeff(1,:),x);
plot(Tfm_input_wint,Pow_wint_data(:,1),'*','markersize',15,'linewidth',2)
set(gca,'FontSize',20);
hold on
plot(x,y1,'r','linewidth',2)
set(gca,'FontSize',20);
xlabel('Tfm [°C]','FontSize',30)
ylabel('Heat pump heating power at the maximum frequency [kW]','FontSize',30)
l=legend('Input data','Interpolating polynomial');
set(l,'FontSize',30)

% Temperature initialization
Tf(1)=Tg;
Tfm(1)=Tg;
T_field(1)=Tg;

for k=1:(8760*num_years)

    % Year of the k-th hour
    year(k)=ceil(k/8760);

    % Energy required by the building
    Qb(k)=Qb_oneyear(k-8760*(year(k)-1));

    % Season determination
    if (k>=1+8760*(year(k)-1))&&(k<=5088+8760*(year(k)-1))
        seas(k)=-1;
    else
        seas(k)=1;
    end

    % Interpolation of the heat pump power and COP or EER as functions of
    % the fluid supply temperature
    if seas(k)==-1
```

175

```matlab
        for r=1:length(freq)
            if Tfm(k)<Tcutoff_wint
                Q_HP_max(k,r)=0;
                COP_EER_vect(k,r)=0;
            else
                Q_HP_max(k,r)=polyval(Pow_wint_coeff(r,:),Tfm(k));
                COP_EER_vect(k,r)=polyval(COP_coeff(r,:),Tfm(k));
            end
        end
    else
        for r=1:length(freq)
            if Tfm(k)>Tcutoff_summ
                Q_HP_max(k,r)=0;
                COP_EER_vect(k,r)=0;
            else
                Q_HP_max(k,r)=polyval(Pow_summ_coeff(r,:),Tfm(k));
                COP_EER_vect(k,r)=polyval(EER_coeff(r,:),Tfm(k));
            end
        end
    end

    % Energy delivered by the heat pump
    if abs(Qb(k))>=Q_HP_max(k,1)
        Q_HP(k)=Q_HP_max(k,1)*seas(k);
    else
        Q_HP(k)=Qb(k);
    end

    % COP or EER interpolation as a function of the compressor frequency
    if abs(Q_HP(k))<Q_HP_max(k,end)
        COP_EER(k)=COP_EER_vect(k,end);
    else
        P_COP_EER_coeff(k,:)=polyfit(Q_HP_max(k,:),COP_EER_vect(k,:),2);
        COP_EER(k)=polyval(P_COP_EER_coeff(k,:),abs(Q_HP(k)));
    end

    % Capacity Ratio
    if Q_HP_max(k,end)==0
        CR(k)=0;
    elseif abs(Q_HP(k))/Q_HP_max(k,end)>1
        CR(k)=1;
    else
        CR(k)=abs(Q_HP(k))/Q_HP_max(k,end);
    end

    % COP or EER correction factor
    f_corr(k)=CR(k)/(1-0.9+0.9*CR(k));

    % Effective COP or EER
    COP_EER_eff(k)=f_corr(k)*COP_EER(k);

    % Uncovered energy
    if (seas(k)==-1)&&(abs(Qb(k))>abs(Q_HP(k)))
        Q_BUP(k)=abs(Qb(k))-abs(Q_HP(k));
    else
```

```
            Q_BUP(k)=0;
        end

        % Thermal energy exchanged between BHE and ground
        % and electric energy used by the heat pump
        if COP_EER_eff(k)==0
            Q(k)=0;
            W(k)=0;
        else
            Q(k)=Q_HP(k)*(1+seas(k)/COP_EER(k));
            W(k)=Q_HP(k)/COP_EER_eff(k);
        end

        % Heat flux between BHE and ground per unit BHE length
        q(k)=1000*Q(k)/(num_bore*L);

        % Dimensionless load amplitude
        A(k)=q(k)/q0;

        % Evaluation of the g-functions
        zz(k)=log10(k*tau_h_star);
        ww(k)=log10((k-1)*tau_h_star);

        for j=1:num_bore
            if zz(k)<x0(j)
                g(k,j)=0;
            elseif zz(k)>=x1(j)
                g(k,j)=b_coeff(j,1)*(zz(k))^6+b_coeff(j,2)*(zz(k))^5+b_coeff(j,3)*(zz(k)) ↙
^4+b_coeff(j,4)*(zz(k))^3+b_coeff(j,5)*(zz(k))^2+b_coeff(j,6)*zz(k)+b_coeff(j,7);
            else
                g(k,j)=a_coeff(j,1)*(zz(k))^6+a_coeff(j,2)*(zz(k))^5+a_coeff(j,3)*(zz(k)) ↙
^4+a_coeff(j,4)*(zz(k))^3+a_coeff(j,5)*(zz(k))^2+a_coeff(j,6)*zz(k)+a_coeff(j,7);
            end

            if ww(k)<x0(j)
                gg(k,j)=0;
            elseif ww(k)>=x1(j)
                gg(k,j)=b_coeff(j,1)*(ww(k))^6+b_coeff(j,2)*(ww(k))^5+b_coeff(j,3)*(ww(k)) ↙
^4+b_coeff(j,4)*(ww(k))^3+b_coeff(j,5)*(ww(k))^2+b_coeff(j,6)*ww(k)+b_coeff(j,7);
            else
                gg(k,j)=a_coeff(j,1)*(ww(k))^6+a_coeff(j,2)*(ww(k))^5+a_coeff(j,3)*(ww(k)) ↙
^4+a_coeff(j,4)*(ww(k))^3+a_coeff(j,5)*(ww(k))^2+a_coeff(j,6)*ww(k)+a_coeff(j,7);
            end

            diff(k,j)=g(k,j)-gg(k,j);
        end

        T_star(k+1,:)=flip(A(1:k))*diff;

        % Evaluation of the BHE dimensionless temperature
        T_star_cent_bore(k+1)=T_star(k+1,1)+2*T_star(k+1,2);
        T_star_lat_bore(k+1)=T_star(k+1,1)+T_star(k+1,2)+T_star(k+1,3);

        % Evaluation of the BHE-field mean dimensionless temperature
        T_star_field(k+1)=1/num_bore*(T_star_cent_bore(k+1)+2*T_star_lat_bore(k+1));
```

```matlab
    % Evaluation of the BHE-field mean temperature
    T_field(k+1)=T_star_field(k+1)*q0/kg+Tg;

    % Evaluation of the BHE fluid mean temperature
    Tf(k+1)=T_field(k+1)+Rb*q(k);

    % Delta T
    deltaT(k)=((Q(k)/num_bore)/(V*rho*cp));

    % Updating of the fluid supply temperature
    Tfm(k+1)=Tf(k+1)-0.5*((Q(k)/num_bore)/(V*rho*cp));
end

% Total energy required by the building during the last year
Qb_TOT_heat=sum(min(0,Qb(end-8760+1:end)))
Qb_TOT_cool=sum(max(0,Qb(end-8760+1:end)))

% Total energy supplied by the heat pump during the last year
Q_HP_TOT_heat=sum(min(0,Q_HP(end-8760+1:end)))
Q_HP_TOT_cool=sum(max(0,Q_HP(end-8760+1:end)))

% Total energy exchanged between BHE and ground during the last year
Q_TOT_heat=sum(min(0,Q(end-8760+1:end)))
Q_TOT_cool=sum(max(0,Q(end-8760+1:end)))

% Total electric energy used by the heat pump during the last year
W_TOT_heat=sum(min(0,W(end-8760+1:end)))
W_TOT_cool=sum(max(0,W(end-8760+1:end)))

% Total uncovered energy
Q_BUP_TOT=sum(Q_BUP)

% Seasonal performance of the GCHP during the last year
SCOP_TOT=Q_HP_TOT_heat/W_TOT_heat
SEER_TOT=Q_HP_TOT_cool/W_TOT_cool
```

8

PUBLICATIONS

8.1 INTERNATIONAL JOURNALS

- C. Naldi, G.L. Morini, E. Zanchini, *A method for the choice of the optimal balance-point temperature of air-to-water heat pumps for heating*, Sustainable Cities and Society, Volume 12, 2014, pp. 85-91, http://dx.doi.org/10.1016/j.scs.2014.02.005.

- M. Dongellini, C. Naldi, G.L. Morini, *Seasonal performance evaluation of electric air-to-water heat pump systems*, Applied Thermal Engineering, Volume 90, 2015, pp. 1072-1081, http://dx.doi.org/10.1016/j.applthermaleng.2015.03.026.

- E. Zanchini, C. Naldi, S. Lazzari, G.L. Morini, *Planned energy-efficient retrofitting of a residential building in Italy*, International Journal of Future Cities and Environment, Volume 1:3, 2015, pp. 1-19, http://dx.doi.org/10.1186/s40984-015-0004-9.

- C. Naldi, M. Dongellini, G.L. Morini, *Climate influence on seasonal performances of air-to-water heat pumps for heating*, Energy Procedia, Volume 81, 2015, pp. 100-107, http://dx.doi.org/10.1016/j.egypro.2015.12.064.

- C. Naldi, M. Dongellini, G.L. Morini, *Summer performances of reversible air-to-water heat pumps with heat recovery for domestic hot water production*, Energy Procedia, Volume 78, 2015, pp. 1117-1122, http://dx.doi.org/10.1016/j.egypro.2015.11.068.

- M. Dongellini, C. Naldi, G.L. Morini, *Annual performances of reversible air source heat pumps for space conditioning*, Energy Procedia, Volume 78, 2015, pp. 1123-1128, http://dx.doi.org/10.1016/j.egypro.2015.11.070.

8.2 INTERNATIONAL CONFERENCES

- E. Zanchini, C. Naldi, S. Lazzari, S. Falcioni, G.L. Morini, *Calibration of the simulation model of the HERB building in Bologna in its present state*, Proceedings of 14th

International Conference on Sustainable Energy Technologies, Nottingham, August 25-27, 2015, E40123.

- E. Zanchini, S. Lazzari, C. Naldi, G.L. Morini, *Planning the energy retrofitting of a residential building in Bologna, Italy*, Proceedings of 13th International Conference on Sustainable Energy Technologies, Geneva, August 25-28, 2014, E40113.

8.3 NATIONAL JOURNALS AND CONFERENCES

- C. Naldi, M. Dongellini, G.L. Morini, *Effetto del clima sull'efficienza stagionale di sistemi di riscaldamento basati su pompe di calore aria-acqua*, La Termotecnica, Volume 6, July-August 2015, pp. 61-64.

- C. Naldi, M. Dongellini, G.L. Morini, E. Zanchini, *Comparison between hourly simulation and bin-method for the seasonal performance evaluation of electric air-source heat pumps for heating*, Proceedings of 2nd IBPSA-Italy Conference, Bolzano, February 4-6, 2015, pp. 255-262.

- C. Naldi, E. Zanchini, G.L. Morini, A. Loreto, *Impiego di pompe di calore elettriche ad aria per la riqualificazione energetica di alloggi ERP*, Proceedings of 32nd AiCARR National Conference, Bologna, October 23, 2014, pp. 257-275.

- C. Naldi, G.L. Morini, E. Zanchini, *Effect of the choice of the balance point on the mean seasonal COP of electric air-to-water heat pumps without inverter*, Proceedings of 31st UIT Heat Transfer Conference, Como, June 25-27, 2013, pp. 671-680.

- C. Naldi, E. Zanchini, *Hourly Simulation of a Ground-Coupled Heat Pump System*, to be presented at 34th UIT Heat Transfer Conference, Ferrara, July 4-6, 2016.

9

SOFTWARE APPLICATION

Thanks to the collaboration with a heat pump manufacturer and an ICT company, the codes for the heat pumps simulations through the bin-method, described in Chapter 3, have been implemented on a web-based software (Figure 9.1).

The software contains a database with the technical data (in terms of power, *COP* and *EER* at different conditions) of several commercial heat pumps and the climate data (of monthly average outdoor temperature and solar radiation) of different European cities.

Once the user has entered some input data, the software employs the simulation codes to evaluate automatically the heat pump seasonal performance (*SCOP*, *SEER*, *FUE*), as well as other outputs like the energy and cost savings with respect to traditional air-conditioning systems.

Figure 9.1: Heading of the web-based software.

REFERENCES

[1] US Energy Information Administration (EIA), International Energy Statistics: http://www.eia.gov/cfapps/ipdbproject/IEDIndex3.cfm#.

[2] Intergovernmental Panel on Climate Change (IPCC), Climate Change 2013: https://www.ipcc.ch/report/ar5/wg1/.

[3] European Commission portal for statistics (Eurostat): http://ec.europa.eu/eurostat/data/database.

[4] European Commission, *Energy-efficient buildings – Multi-annual roadmap for the contractual PPP under Horizon 2020*, http://www.ectp.org/cws/params/ectp/download_files/36D2981v1_Eeb_cPPP_Roadmap_under.pdf.

[5] Directive 2010/31/EU of the European Parliament and of the Council of 19 May 2010 on the energy performance of buildings (recast), L 153/13, Official Journal of the European Union, 18 June 2010.

[6] K.J. Chua, S.K. Chou, W.M. Yang, *Advances in heat pump systems: a review*, Applied Energy, Volume 87, Issue 12, 2010, pp. 3611-3624.

[7] J.W. Lund, T.L. Boyd, *Direct Utilization of Geothermal Energy 2015 Worldwide Review*, Proceedings of World Geothermal Congress 2015, Melbourne, April 19-25, 2015.

[8] Directive 2009/28/EC of the European Parliament and of the Council of 23 April 2009 on the promotion of the use of energy from renewable sources and amending and subsequently repealing Directives 2001/77/EC and 2003/30/EC, L 140/16, Official Journal of the European Union, 5 June 2009.

[9] E. Zanchini, S. Lazzari, *Temperature distribution in a field of long Borehole Heat Exchangers (BHEs) subjected to a monthly averaged heat flux*, Energy, Volume 59, 2013, pp. 570-580.

[10] European standard EN 14825, *Air conditioners, liquid chilling packages and heat pumps, with electrically driven compressors, for space heating and cooling – Testing and rating at part load conditions and calculation of seasonal performance*, 2013.

[11] Italian standard UNI/TS 11300-4, *Energy performance of buildings – Part 4: Renewable energy and other generation systems for space heating and domestic hot water production*, 2012.

[12] T. Afjei, R. Dott, *Heat pump modelling for annual performance, design and new technologies*, Proceedings of 12th Conference of International Building Performance Simulation Association, Sydney, November 14-16, 2011, pp. 2431-2438.

[13] R. Ghoubali, P. Byrne, J. Miriel, F. Bazantay, *Simulation study of a heat pump for simultaneous heating and cooling coupled to buildings*, Energy and Buildings, Volume 72, 2014, pp. 141-149.

[14] E. Bettanini, A. Gastaldello, L. Schibuola, *Simplified models to simulate part load performances of air conditioning equipments*, Proceedings of 8th International IBPSA Conference, Eindhoven, August 11-14, 2003, pp. 107-114.

[15] E. Kinab, D. Marchio, P. Rivière, A. Zoughaib, *Reversible heat pump model for seasonal performance optimization*, Energy and Buildings, Volume 42, 2010, pp. 2269-2280.

[16] European standard EN 14511-2, *Air conditioners, liquid chilling packages and heat pumps with electrically driven compressors for space heating and cooling – Part 2: Test conditions*, 2013.

[17] European standard EN 14511-3, *Air conditioners, liquid chilling packages and heat pumps with electrically driven compressors for space heating and cooling – Part 3: Test methods*, 2013.

[18] L. Cecchinato, M. Chiarello, M. Corradi, *A simplified method to evaluate the seasonal energy performance of water chillers*, International Journal of Thermal Sciences, Volume 49, 2010, pp. 1776-1786.

[19] P.W. Francisco, B. Davis, D. Baylon, L. Palmiter, *Heat pump system performance in northern climates*, ASHRAE Transactions, Volume 110, Part 1, 2004, pp. 442-451.

[20] D.E. Knebel, *Simplified energy analysis using the modified bin method*, ASHRAE, Atlanta, GA, 1983.

[21] I. Sarbu, D. Dan, C. Sebarchievici, *Performances of heat pump systems as users of renewable energy for building heating/cooling*, WSEAS Transactions on Heat and Mass Transfer, Volume 9, 2014, pp. 51-62.

[22] European standard EN 15316-4-2, *Heating systems in buildings – Method for calculation of system energy requirements and system efficiencies – Part 4-2: Space heating generation systems, heat pump systems*, 2008.

[23] European standard EN 15603, *Energy performance of buildings – Overall energy use and definition of energy ratings*, 2008.

[24] H.I. Henderson, D. Parker, Y.J. Huang, *Improving DOE-2's RESYS routine: user defined functions to provide more accurate part load energy use and humidity predictions*, Proceedings of 2000 Summer Study on Energy Efficiency in Buildings, ACEEE, Washington, August 2000.

[25] Italian standard UNI 10349, *Heating and cooling of buildings – Climatic data*, 1994.

[26] European standard EN 12831, *Heating systems in buildings – Method for calculation of the design heat load*, 2003.

[27] K. Klein, K. Huchtemann, D. Müller, *Numerical study on hybrid heat pump systems in existing buildings*, Energy and Buildings, Volume 69, 2014, pp. 193-201.

[28] F. Madonna, F. Bazzocchi, *Annual performances of reversible air-to-water heat pumps in small residential buildings*, Energy and Buildings, Volume 65, 2013, pp. 299-309.

[29] International standard ISO 13790, *Energy performance of buildings – calculation of energy use for space heating and cooling*, 2008.

[30] S.M. Al-Zahrani, F.L. Tan, F.H. Choo, *A TRNSYS simulation case study on utilization of heat pump for both heating and cooling*, Energy Science and Technology, Volume 3, n° 2, 2012, pp. 84-92.

[31] TRNSYS website: www.trnsys.com.

[32] TESSLibs 17 – Component Libraries for the TRNSYS Simulation Environment, *HVAC Library Mathematical Reference*, 2012.

[33] S.L. Do, J.S. Haberl, *A review of ground coupled heat pump models used in whole-building computer simulation programs*, Proceedings of the 17th Symposium for Improving Building Systems in Hot and Humid Climates, Austin (Texas), August 24-25, 2010.

[34] M. Philippe, M. Bernier, D. Marchio, *Validity ranges of three analytical solutions to heat transfer in the vicinity of single boreholes*, Geothermics, Volume 38, 2009, pp. 407-413.

[35] H. Yang, P. Cui, Z. Fang, *Vertical-borehole ground-coupled heat pumps: A review of models and systems*, Applied Energy, Volume 87, 2010, pp. 16-27.

[36] H.S. Carlslaw, J.C. Jaeger, *Conduction of heat in solids*, Oxford University Press, Oxford, 1959.

[37] M. Fossa, *A fast method for evaluating the performance of complex arrangements of borehole heat exchangers*, HVAC&R Research, Volume 17:6, 2011, pp. 948-958.

[38] E. Zanchini, B. Pulvirenti, *An analytical solution for the temperature field around a cylindrical surface subjected to a time dependent heat flux*, International Journal of Heat and Mass Transfer, Volume 66, 2013, pp. 906-910.

[39] S.P. Kavanaugh, K. Rafferty, *Ground-source heat pumps: design of geothermal systems for commercial and institutional buildings*, ASHRAE, Atlanta, GA, 1997.

[40] American Society of Heating, Refrigerating and Air-Conditioning Engineers, *ASHRAE Handbook – HVAC applications*, Chapter 32, ASHRAE, Atlanta, GA, 2007.

[41] P. Eskilson, *Thermal analysis of heat extraction boreholes*, PhD Thesis, Sweden: Lund University, 1987.

[42] J. Claesson, P. Eskilson, *Conductive heat extraction by a deep borehole, analytical studies*, Tech. rep. Sweden: Lund University, 1987.

[43] H. Zeng, N. Diao, Z. Fang, *A finite line-source model for boreholes in geothermal heat exchangers*, Heat Transfer – Asian Research, Volume 31 (7), 2002; pp. 558-567.

[44] T.V. Bandos, A. Montero, E. Fernandez, J.L.G. Santander, J.M. Isidro, J. Perez, P.J. Fernandez de Cordoba, J.F. Urchueguía, *Finite line-source model for borehole heat exchangers: effect of vertical temperature variations*, Geothermics, Volume 38, 2009, pp. 263-270.

[45] L. Lamarche, B. Beauchamp, *A new contribution to the finite line-source model for geothermal boreholes*, Energy and Buildings, Volume 39, 2007, pp. 188-198.

[46] M. Fossa, *The temperature penalty approach to the design of borehole heat exchangers for heat pump applications*, Energy and Buildings, Volume 43, 2011, pp. 1473-1479.

[47] C. Yavuzturk, J. Spitler, *A short time step response factor model for vertical ground loop heat exchangers*, ASHRAE Transactions, Volume 105, Part 2, 1999, pp. 475-485.

[48] G. Hellström, *Duct ground heat storage model: Manual for computer code*, Department of Mathematical Physics, Lund Institute of Technology, Lund, Sweden, 1989.

[49] G. Hellström, L. Mazzarella, D. Pahud, Duct ground heat storage model, Lund – DST – TRNSYS 13.1 version January 1996, Department of Mathematical Physics, University of Lund, Sweden, 1996.

[50] M. Fossa, F. Minchio, *The effect of borefield geometry and ground thermal load profile on hourly thermal response of geothermal heat pump systems*, Energy, Volume 51, 2013, pp. 323-329.

[51] M.A. Bernier, A. Chahla, P. Pinel, *Long-term ground-temperature changes in geoexchange systems*, ASHRAE Transactions, Volume 114, Part 2, 2008, pp. 342-350.

[52] T. Terlizzese, E. Zanchini, *Economic and exergy analysis of alternative plants for a zero carbon building complex*, Energy and Buildings, Volume 43, 2011, pp. 787-795.

[53] E. Zanchini, S. Lazzari, *New g-functions for the hourly simulation of double U-tube borehole heat exchanger fields*, Energy, Volume 70, 2014, pp. 444-455.

[54] G. Hellström, B. Sanner, T. Blomberg, J. Claesson, P. Eskilson, *EED – Earth Energy Designer, User Manual*, Version 3.2, 2015.

[55] J. Claesson, P. Eskilson, G. Hellström, *PC design model for heat extraction boreholes*, Proceedings of the 3rd WS on SAHPGCS Göteborg, CITη 1990:3, Göteborg, 1990, pp. 99-102.

[56] G. Hellström, B. Sanner, *Software for dimensioning of deep boreholes for heat extraction*, Proceedings of the Conference "Calorstock 94", Espoo - Helsinki, 1994, pp. 195-202.

[57] I. Sarbu, C. Sebarchievici, *Ground-Source Heat Pumps: Fundamentals, Experiments and Applications*, Academic Press (Elsevier Science), 2015.

[58] M. Dongellini, C. Naldi, G.L. Morini, *Seasonal performance evaluation of electric air-to-water heat pump systems*, Applied Thermal Engineering, Volume 90, 2015, pp. 1072-1081.

[59] Italian standard UNI/TS 11300-2, *Energy performance of buildings – Part 2: Evaluation of primary energy need and of system efficiencies for space heating, domestic hot water production, ventilation and lighting for non-residential buildings*, 2014.

[60] Italian draft standard prUNI/TS 11300-5, *Energy performance of buildings – Part 5: Evaluation of energy performance for the classification of building*.

[61]   C. Naldi, M. Dongellini, G.L. Morini, *Summer performances of reversible air-to-water heat pumps with heat recovery for domestic hot water production*, Energy Procedia, Volume 78, 2015, pp. 1117-1122.

[62]   C. Naldi, M. Dongellini, G.L. Morini, *Climate influence on seasonal performances of air-to-water heat pumps for heating*, Energy Procedia, Volume 81, 2015, pp. 100-107.

[63]   M. Dongellini, C. Naldi, G.L. Morini, *Annual performances of reversible air source heat pumps for space conditioning*, Energy Procedia, Volume 78, 2015, pp. 1123-1128.

[64]   C. Naldi, M. Dongellini, G.L. Morini, *Effetto del clima sull'efficienza stagionale di sistemi di riscaldamento basati su pompe di calore aria-acqua*, La Termotecnica, Volume 6, July-August 2015, pp. 61-64.

[65]   C. Naldi, G.L. Morini, E. Zanchini, *A method for the choice of the optimal balance-point temperature of air-to-water heat pumps for heating*, Sustainable Cities and Society, Volume 12, 2014, pp. 85-91.

[66]   C. Naldi, G.L. Morini, E. Zanchini, *Effect of the choice of the balance point on the mean seasonal COP of electric air-to-water heat pumps without inverter*, Proceedings of 31st UIT Heat Transfer Conference, Como, June 25-27, 2013, pp. 671-680.

[67]   E. Zanchini, C. Naldi, S. Lazzari, G.L. Morini, *Planned energy-efficient retrofitting of a residential building in Italy*, International Journal of Future Cities and Environment, Volume 1:3, 2015, pp. 1-19.

[68]   E. Zanchini, S. Lazzari, C. Naldi, G.L. Morini, *Planning the energy retrofitting of a residential building in Bologna, Italy*, Proceedings of 13th International Conference on Sustainable Energy Technologies, Geneva, August 25-28, 2014, E40113.

[69]   E. Zanchini, C. Naldi, S. Lazzari, S. Falcioni, G.L. Morini, *Calibration of the simulation model of the HERB building in Bologna in its present state*, Proceedings of 14th International Conference on Sustainable Energy Technologies, Nottingham, August 25-27, 2015, E40123.

[70]   C. Naldi, E. Zanchini, G.L. Morini, A. Loreto, *Impiego di pompe di calore elettriche ad aria per la riqualificazione energetica di alloggi ERP*, Proceedings of 32nd AiCARR National Conference, Bologna, October 23, 2014, pp. 257-275.

[71]   HERB website: www.euroretrofit.com.

[72]   Italian standard UNI/TR 11328–1, *Solar energy, Calculation of energy gains for building applications – Part 1: Evaluation of radiant received energy*, 2009.

[73]   TRNSYS 17, *Mathematical Reference for the Standard Component Library*, 2012.

[74]   C. Naldi, M. Dongellini, G.L. Morini, E. Zanchini, *Comparison between hourly simulation and bin-method for the seasonal performance evaluation of electric air-source heat pumps for heating*, Proceedings of 2nd IBPSA-Italy Conference, Bolzano, February 4-6, 2015, pp. 255-262.

[75]   C. Naldi, E. Zanchini, *Hourly Simulation of a Ground-Coupled Heat Pump System*, to be presented at 34th UIT Heat Transfer Conference, Ferrara, July 4-6, 2016.

[76]   E. Preisegger, F. Flohr, *VDI Heat Atlas – D4 - Properties of Industrial Heat Transfer Media – D4.1 - Refrigerants: Regulations*, Springer Berlin Heidelberg, Berlin, 2010.